

---

# **Keratin Dynamics and the Role of Lipids on Keratinocyte Differentiation and mRNA Stability**

**Hebah AlDehlawi**

*Submitted in partial fulfilment of the requirements for the degree of Doctor of Philosophy*

**Centre for Immunobiology and Regenerative Medicine  
Institute of Dentistry  
Barts and the London School of Medicine and Dentistry  
Queen Mary University of London**

**Primary supervisor:** Professor Ahmad Waseem

**Secondary supervisor:** Dr Anand Lalli

**This work was supported by:** King Abdulaziz University, Jeddah, Saudi Arabia

## **Statement of Originality**

I, Hebah AlDehlawi, confirm that the research included within this thesis is my own work or that where it has been carried out in collaboration with, or supported by others, that this is duly acknowledged below and my contribution indicated. Previously published material is also acknowledged below.

I attest that I have exercised reasonable care to ensure that the work is original and does not to the best of my knowledge break any UK law, infringe any third party's copyright or other Intellectual Property Right, or contain any confidential material.

I accept that the College has the right to use plagiarism detection software to check the electronic version of the thesis.

I confirm that this thesis has not been previously submitted for the award of a degree by this or any other university.

The copyright of this thesis rests with the author and no quotation from it or information derived from it may be published without the prior written consent of the author.

Signature: .....Hebah AlDehlawi.....

Date: .....

## **Abstract**

Keratin K2 is a 66 kDa type II intermediate filament protein expressed in differentiating keratinocytes of the epidermis with a very low-level expression in normal oral mucosa. In the epidermis it is expressed in the upper granular and spinous layers and is considered a marker of terminal differentiation. It is known to be upregulated in pre-cancerous lesions of the oral cavity. However, the mechanism of its induction in dysplasia and its role in oral cancer is not known. As it is only expressed *in vivo*, being down-regulated in cultured keratinocytes, there are no reported studies on the functions of this protein. Point mutations in this protein are associated with the skin condition Ichthyosis Bullosa of Siemens (IBS).

Keratin filaments are in a constant state of assembly and disassembly to maintain cell stability and support. Keratins' reorganisation and dynamics are affected mainly by their state of phosphorylation which explains the difference between health and disease and the molecular interactions between different keratin pairs as well as with other cytoplasmic proteins. Heat shock was shown to re-organises the keratin network which is mediated by phosphorylation.

A model has been developed to study keratin filaments dynamics by introducing keratin K2, into a simple epithelial cell line, MCF-7 (breast carcinoma cell line) which lacks K2 expression but expresses other keratins including K8, K18 and K19. Introduction of K2 into MCF-7 cytoplasm allows it to bind and fully integrate into the pre-existing network. To understand the mechanism of K2 integration into the pre-existing filaments, the stability of the network and its phosphorylation state using two phosphatase inhibitors, Calyculin A (CL-A) and Okadaic Acid (OA) was studied. To investigate the response of keratin cytoskeleton to stress,

the effect of heat shock on filaments reorganisation was studied using immunocytochemistry and live cell imaging.

The expression of K2 mRNA and protein was investigated in keratinocytes cell lines as well as in normal human epidermal keratinocyte (NHEK) along with other terminal differentiation keratins, K1 and K10. The absence of serum lipids (SLP) and phenol red (PR), which are generally used in culture medium, had a significant effect on the expression of these keratins at both mRNA and protein levels in NHEK. The effect was different compared to immortalised cell lines, which could be explained by immortalisation methods altering gene response. Adding back retinoic acid (ATRA) to the culture medium differentially affected the expression of these genes. Adding PR back into PR-free culture medium in NHEK did reduce the expression of K1 and K10 but not K2.

To further investigate the effect of SLP, RA and PR, the post-transcriptional stability of K2, K10 and K1 mRNAs using Actinomycin D (AD) in NHEK cells was studied. Interestingly, K2 mRNA was stabilised whereas K1 and K10 mRNAs were destabilised by ATRA. These observations explain the differential effect of ATRA on the expression of these genes previously reported in the literature. Further investigations are required to decipher the mechanism(s) regulating transcriptional changes affected by different culture conditions and by RA. The aim of this project is to study keratin dynamics and the role of lipids on keratinocyte differentiation and mRNA stability.

## **Acknowledgements**

First, I owe my deepest gratitude to God who made this thesis dream come true. I would like to thank King Abdulaziz University (Dental School) and the Ministry of Higher Education in Saudi Arabia for funding my PhD research. I would like to express my very great appreciation to my primary supervisor, Professor Ahmad Waseem. His support and guidance have no limit, he provided me with confidence and strength throughout the whole journey besides refining my research skills and knowledge. 'Thank you' will never be enough to express how grateful I feel towards all what he has done to me. I would also like to thank my second supervisor Dr Anand Lalli, for his time and support whenever I needed. Special thanks to my colleagues, Kasia, Deepa, Fatima, Saima, and Saja for making my PhD life enjoyable. I wish to acknowledge the help provided by the Dental School staff at Blizard institute (QMUL).

I would like to thank my lovely University Queen Mary University of London (Barts and the London school of Medicine and Dentistry) for giving me this opportunity and for their continuous support.

Deepest gratitude goes to my lovely husband Haitham for his unlimited support, love and patience. There are no words showing how grateful I feel towards my lovely daughters Jana, Ghina and Sarah for keeping my smile on every day, for their support and love.

Mum and Dad, your prayers made my dream come true, thank you. My lovely family, brothers (Ashraf, Aseel and Amjad), sisters (Hadeel, Afnan and Rahaf) thank you for your continuous support and lovely wishes.

Final thanks go to anyone who supported me by any means, far or near. Nothing would be possible without all this love and support.

# **Table of Contents**

<b>Statement of Originality .....</b>	<b>2</b>
<b>Abstract .....</b>	<b>3</b>
<b>Acknowledgements .....</b>	<b>5</b>
<b>Table of Contents.....</b>	<b>6</b>
<b>List of Figures .....</b>	<b>11</b>
<b>List of Tables.....</b>	<b>14</b>
<b>List of Abbreviations .....</b>	<b>15</b>
<b>1. Introduction.....</b>	<b>20</b>
1.1. Nomenclature and classification.....	22
1.2. Structure.....	25
1.3. Keratin dynamics.....	27
1.4. Keratin functions.....	30
1.4.1. Mechanical functions of keratins.....	30
1.4.2. Non-mechanical functions of keratins.....	30
1.4.3. Apoptosis and Keratins.....	32
1.5. DNA transcription, translation and post translational modifications.....	33
1.6. Keratin filament phosphorylation, regulation and stress response.....	36
1.6.1. Keratin phosphorylation.....	36
1.6.2. Stress-activated protein kinases.....	37
1.6.3. Heat Shock proteins and stress response.....	38
1.7. Keratin phosphorylation in cancer.....	38
1.8. Keratinocyte differentiation.....	39
1.9. The mechanism of keratinocyte differentiation.....	42
1.10. Factors regulating keratinocyte differentiation.....	43
1.10.1. Calcium.....	43
1.10.2. Phorbol esters.....	44
1.10.3. Steroid hormones.....	45
1.10.4. Estrogen.....	45
1.10.5. Retinoids/Retinoic acid (RA).....	46
1.10.6. High Cell Density.....	48
1.11. Keratin disorders.....	48
1.12. Keratins in cancer.....	52
1.13. Keratinocyte differentiation and cancer (Differentiation Therapy).....	54
1.14. Aim and objectives of the study.....	55

<b>2. Materials and Methods.</b> .....	<b>58</b>
2.1. Cell culture. ....	58
2.1.1. Cell Culture Media. ....	58
2.1.2. Cells used. ....	58
2.1.3. Culturing cells. ....	61
2.1.3.1. <i>Cell passaging.</i> .....	61
2.1.3.2. <i>Use of Rho-associated kinase inhibitor (ROCKi)</i> . ....	62
2.2. Cell treatments. ....	64
2.2.1. Phosphatase inhibitors. ....	64
2.2.2. Heat shock treatment. ....	64
2.2.3. Use of charcoal stripped FCS. ....	65
2.2.4. Use of phenol-red free medium. ....	66
2.2.5. All- <i>trans</i> -Retinoic acid. ....	66
2.2.6. $\beta$ - Estradiol. ....	67
2.2.7. Phenol Red. ....	67
2.2.8. Actinomycin D. ....	67
2.3. Organotypic cultures. ....	68
2.3.1. Paraffin embedding. ....	69
2.3.2. Haematoxylin and Eosin (H & E) staining. ....	70
2.4. Protein analysis techniques. ....	71
2.4.1. Western blotting (WB). ....	71
2.4.1.1. <i>Protein extraction and quantification.</i> .....	71
2.4.1.2. <i>Protein separation by SDS-PAGE, transfer on nitrocellulose and protein detection.</i> .....	72
2.4.2. Immunofluorescence (IF) staining and live cell imaging. ....	75
2.4.2.1. <i>Immunocytochemistry (ICC).</i> .....	75
2.4.2.2. <i>Immunohistochemistry (IHC).</i> .....	76
2.4.2.3. <i>Live cell imaging.</i> .....	77
2.5. Gene analysis techniques. ....	80
2.5.1. Total RNA isolation and qPCR. ....	80
2.5.2. mRNA extraction and cDNA synthesis. ....	80
2.5.3. Real-time quantitative PCR (qPCR). ....	82
2.5.4. Validation of the primers. ....	83
2.6. Cloning and gene transfer. ....	85
2.6.1. Basic techniques. ....	85
2.6.1.1. <i>Restriction digestion.</i> .....	85
2.6.1.2. <i>Agarose gel electrophoresis.</i> .....	85
2.6.1.3. <i>Ligation.</i> .....	86

2.6.1.4. Competent cells transformation and preparation of mini- and maxi DNA preps.....	87
2.6.2. Transfection and luciferase reporter assay. ....	89
2.6.2.1. Transfection. ....	89
2.6.2.2. Constructs used for luciferase reporter assay. ....	90
2.6.2.3. Luciferase reporter assay. ....	90
2.6.3. Retroviral transduction. ....	92
2.6.3.1. Retrovirus production using Phoenix A cells transfection. ....	92
2.6.3.2. Transduction of MCF7 cell lines. ....	93
2.6.3.3. Drug selection. ....	94
2.7. Statistical analysis. ....	94
<b>3. Results I. Keratin filaments dynamics, heat stress response and role of phosphorylation in live epithelial cells. ....</b>	<b>97</b>
3.1. Introduction.....	97
3.2. Integration of Keratin K2 into the pre-existing keratin network of MCF-7 cells.. ....	102
3.3. Integration of K2 into the simple epithelial keratin network did not affect normal cell physiology of MCF-7 cells. ....	106
3.3.1. Mitosis. ....	106
3.3.2. Dynamic equilibrium of keratin network. ....	107
3.4. Keratin hyperphosphorylation breaks down filaments in MCF-7 cells (use of phosphatase inhibitors). ....	109
3.5. Filament breakdown in MCF-7 expressing AcGFP-K2 or FLAG-K2 using phosphatase inhibitor CL-A: role of phosphorylation. ....	111
3.5.1. Analysis of CL-A induced keratin phosphorylation by immunostaining. ....	111
3.5.2. Analysis of CL-A induced keratin phosphorylation by western blotting. ....	116
3.5.3. Effect of K2 on migration of MCF-7 cells. ....	120
3.6. Role of heat shock stress on keratins organisation and phosphorylation. ....	122
3.6.1. Effect of heat shock on endogenous filaments network of MCF-7. ....	122
3.6.2. Stabilisation of endogenous keratin network in MCF-7 cells following heat shock. ....	124
3.6.3. Recovery of MCF-7 cytoskeleton containing AcGFP-K2 after heat shock. ....	126
3.6.4. Stabilisation of MCF-7 cytoskeleton containing AcGFP-K2 after head shock. ....	128
3.6.5. Role of heat shock protein 70 (HSP70) in keratin phosphorylation induced by heat shock in MCF-7 cells. ....	132
3.7. Discussion and conclusion. ....	135
<b>4. Results II. Expression of differentiation-specific keratins in response to serum lipids, all trans-retinoic acid and phenol red. ....</b>	<b>143</b>



4.1. Introduction.....	143
4.2. Expression of different keratins in skin. ....	149
4.3. Role of serum lipids on mRNA and protein expression of differentiation-specific keratins in Neb-1 and T103C cell lines. ....	154
4.4. Influence of serum lipids and PR on mRNA and protein expression of differentiation-specific keratins in HaCaT and N/TERT cell line. ....	156
4.5. Absence of serum lipids and PR increases mRNA and protein expression of differentiation-specific keratins in NHEK.....	160
4.6. Influence of serum lipids and PR on keratin expression in NHEK grown in 3D organotypic cultures (OTCs). ....	163
4.7. Differential effect of ATRA on mRNA and protein expression of K1, K10 and K2 in NHEK. ....	170
4.8. PR downregulates <i>KRT1</i> and <i>KRT10</i> but not <i>KRT2</i> expression in NHEK. ....	174
4.9. $\beta$ -Estradiol has no effect on K1, K10 and K2 gene expression in NHEK. ....	176
4.10. Discussion and conclusion. ....	178
<b>5. Results III. mRNA stability of differentiation-specific keratins; effect of serum lipids and ATRA. ....</b>	<b>184</b>
5.1. Introduction.....	184
5.1.1.mRNA stability. ....	187
5.1.2.Promoter activity measurements. ....	192
5.2. mRNA stability of late differentiation keratins. ....	195
5.2.1.Measuring the stability of c-Myc mRNA and 18S rRNA after Actinomycin D treatment. ....	195
5.2.2.mRNA stability of differentiation-specific keratins in the presence of Actinomycin D.....	198
5.2.3.ATRA stabilises <i>KRT2</i> but not <i>KRT1</i> and <i>KRT10</i> mRNAs. ....	200
5.3. Role of serum lipids and PR on stability of <i>KRT1</i> , <i>KRT2</i> and <i>KRT10</i> mRNA in NHEK. ....	203
5.4. Investigating the promoter activity of <i>KRT1</i> , <i>KRT2</i> and <i>KRT10</i> in response to lipids and PR in culture medium. ....	208
5.4.1.Optimisation of Keratinocytes transfection using AcGFP vector.....	208
5.4.2.Measuring AP-1, K2 and K14 promoter activities using Luciferase. ....	213
5.5. Discussion and conclusion. ....	217
<b>6. General discussion, clinical significance and future directions.....</b>	<b>225</b>
6.1. General discussion. ....	225
6.1.1.Keratin dynamics and phosphorylation. ....	225
6.1.2.Keratinocyte differentiation and serum lipids.....	231
6.1.3.mRNA stability. ....	237

6.2. Clinical significance of this study.....	241
6.2.1. Keratin phosphorylation.....	241
6.2.2. Differentiation Therapy.....	243
6.2.3. mRNA stability.....	244
6.3. Future directions of this study.....	246
<b>References.....</b>	<b>248</b>
<b>Appendix .....</b>	<b>266</b>
A.1. Supplementary results.....	266
A.2. Maps and vectors used in this study.....	272
A.3. Additional work.....	275
A.3.1. Vimentin co-localisation with other cell adhesion proteins.....	275
A.3.2. Publication.....	277
A.4. Research Presentation of this thesis.....	289
A.5. Manuscripts communicated.....	290

## **List of Figures**

Figure 1.1. Keratin classifications. ....	24
Figure 1.2. Intermediate filament structural domains. ....	26
Figure 1.3. Keratin unit length formation (ULF). ....	27
Figure 1.4. Cycle of keratin assembly and disassembly. ....	29
Figure 1.5. Steps of keratin K13 cycle in vulvar carcinoma derived A431 cell line. .....	29
Figure 1.6. Structural and regulatory functions of keratins. ....	33
Figure 1.7. Steps in transcription and translation of eukaryotic genes. ....	34
Figure 1.8. The PKC/AP-1 pathway. ....	43
Figure 1.9. Mode of action of vitamin A on keratinocytes. ....	47
Figure 1.10. Epidermolysis Bullosa Simplex. ....	50
Figure 1.11. Keratin expression in different layers of skin and oral mucosa. ....	51
Figure 1.12. Classification of oral keratin disorders. ....	52
Figure 3.1. Integration of Keratin K2 into MCF-7 keratin network. ....	104
Figure 3.2. Specificity of K2 antibody. ....	105
Figure 3.3. Reorganisation of keratin filaments during mitosis. ....	107
Figure 3.4. Time-lapse microscopy of keratin assembly and dis-assembly in the cytoplasm. ....	108
Figure 3.5. Keratin filament disruption at different concentrations of OA. ....	109
Figure 3.6. Disruption of endogenous keratin network induced by phosphatase inhibitors (OA and CL-A). ....	110
Figure 3.7. MCF-7/ FLAG-K2 and Vector control transduced MCF-7 cells treated with 2nM CL-A. ....	114
Figure 3.8. Keratins in MCF-7/ AcGFP-K2 filaments breakdown after 2nM CL-A treatment. ....	115
Figure 3.9. Western blot showing hyperphosphorylation of K8 induced by CL-A in MCF-7 transduced cells. ....	117
Figure 3.10. Western blot quantification of Figure 3.9. ....	119
Figure 3.11. Wound closure of MCF-7 cells transduced with (AcGFP-K2, FLAG- K2, AcGFP control and FLAG control). ....	122
Figure 3.12. Effect of heat shock on endogenous keratins in MCF-7 cells. ....	123
Figure 3.13. Effect of 2nM CL-A on MCF-7 keratin filaments with and without heat shock. ....	125

Figure 3.14. Time-lapse imaging of MCF-7 cells expressing AcGFP-K2 following heat shock.....	127
Figure 3.15. Time-lapse imaging of AcGFP-K2 expressing MCF-7 cells following heat shock and recovery.....	128
Figure 3.16. Treatment of AcGFP-K2 expressing MCF-7 cells with OA.....	130
Figure 3.17. Treatment of AcGFP-K2 expressing MCF-7 with OA after heat shock.....	131
Figure 3.18. Heat shock effect on keratin phosphorylation in AcGFP-K2 and AcGFP-C transduced MCF-7 cells.....	134
Figure 4.1. Haematoxylin and Eosin (H&E) staining of skin sections.....	151
Figure 4.2. Expression of differentiation specific markers in normal skin.....	153
Figure 4.3. Influence of serum lipids on mRNA and protein expression of K1, K10 and K2 in Neb-1 and T103C cell lines.....	156
Figure 4.4. Influence of serum lipids on mRNA and protein expression of K1, K10 and K2 in HaCaT cell line.....	158
Figure 4.5. Influence of serum lipids on mRNA and protein expression of K1, K10 and K2 in N/TERT cell line.....	159
Figure 4.6. Removal of serum lipids and PR affects mRNA and protein expression of K1, K10 and K2 in NHEK cells.....	162
Figure 4.7. H&E staining of NHEK OTCs.....	164
Figure 4.8. Removal of serum lipids and PR increases the protein expression of K1, K10 and K2 in 3D NHEK cultures.....	169
Figure 4.9. ATRA supresses K1 and K10 mRNA expression while K2 mRNA expression is increased.....	173
Figure 4.10. ATRA reduces protein expression of K1 in NHEK.....	173
Figure 4.11. PR supresses mRNA expression for K1 and K10 in NHEK.....	175
Figure 4.12. $\beta$ -Estradiol has no effect on the expression of <i>KRT1</i> , <i>KRT2</i> and <i>KRT10</i> genes in NHEK.....	178
Figure 5.1. Gene transcription steps.....	185
Figure 5.2. RNA transcription and translation.....	187
Figure 5.3. Main classes of methods to study RNA stability.....	189
Figure 5.4. Three main pathways controlling mRNA degradation in eukaryotes.....	192
Figure 5.5. The luciferase reporter assay.....	194

Figure 5.6. mRNA decay of 18S rRNA and c-Myc mRNA in NHEK after AD treatment.....	197
Figure 5.7. Differential stability of K1, K10, K2 and c-Myc mRNAs in NHEK. .	199
Figure 5.8. ATRA destabilises K1 and K10 but stabilises K2 mRNAs.....	202
Figure 5.9. Effect of serum lipids and PR on mRNA stability of K1, K2 and K10. .....	207
Figure 5.10. Efficiency of HaCaT transfection as measured with pLPCpuro_NAcGFP vector using different reagents.....	213
Figure 5.11. Comparison of PMA inducible AP-1 activity in HaCaT and HEK293 cells.....	214
Figure 5.12. Effect of serum lipids and PR on AP-1 reporter activity in HEK293 cells.....	215
Figure 5.13. Effect of serum lipids and PR on K2 and K14 promotor in HaCaT cell line. ....	216
Figure 5.14. 3' UTR of <i>KRT1</i> , <i>KRT2</i> and <i>KRT10</i> mRNA sequence using Ensembl genome browser 95 website. ....	218

## Appendix Figures

Figure A.1. Optimisation of CL-A treatment concentrations in MCF-7 cells.....	266
Figure A.2. Optimisation of CL-A treatment time points in AcGFP-K2/MCF-7 cells.....	267
Figure A.3. Optimisation of organotypic growth conditions.....	269
Figure A.4. Cp values of YAP and POL.....	270
Figure A.5. Map of pLPC-N-AcGFP-GS20 vector.....	271
Figure A.6. Map of pLPC-3xFLAG- GS20 vector.....	272
Figure A.7. Map of pGL4.26 vector.....	273
Figure A.8. Map of pGL4.14 vector.....	273
Figure A.9. Colocalisation of Vimentin with other proteins.....	275

## **List of Tables**

Table 1.1. Numbering of keratin categories. ....	23
Table 1.2. Nomenclature of human keratin proteins, old and new. ....	23
Table 1.3. List of human keratin disorders. ....	50
Table 2.1. Material and equipment used in cell culture. ....	62
Table 2.2. Reagents and equipment used in cell treatments. ....	68
Table 2.3. Reagents and equipment used in organotypic cultures.....	71
Table 2.4. Reagents and equipment used in protein analysis.....	74
Table 2.5. Primary antibodies used in WB, ICC and IHC.....	78
Table 2.6. Secondary antibodies used in WB, IF and IHC. ....	78
Table 2.7. Material used in immunofluorescence and live cell imaging.....	79
Table 2.8. Master mix components for cDNA synthesis.....	81
Table 2.9. qPCR master mixture.....	82
Table 2.10. Conditions used for qPCR using Roche Light Cycler LC480. ....	82
Table 2.11. Master mixture used for primer validation. ....	83
Table 2.12. List of the primers used in qPCR. ....	84
Table 2.13. Reagents and equipment used in gene analysis.....	84
Table 2.14. Reagents and equipment used for agarose gel electrophoresis. ...	86
Table 2.15. Reagents used for DNA ligation.....	87
Table 2.16. Reagents and equipment used in preparing mini and maxi DNA preps.....	89
Table 2.17. Reagents used in transfection and luciferase assay. ....	92
Table 2.18. Reagents used in retroviral transduction.....	94
Table 2.19. Reagents and equipment used in drug selection. ....	94

## List of Abbreviations

<b>AcGFP</b>	<i>Aequorea coerulea</i> green fluorescent protein
<b>AD</b>	Actinomycin D
<b>ADP</b>	Adenosine diphosphate
<b>AP-1</b>	Activator protein 1
<b>AREs</b>	AU-rich elements
<b>ATRA</b>	All- <i>Trans</i> -Retinoic acid
<b>BF</b>	Bright field
<b>Bfsp1, Bfsp2</b>	Beaded Filament Structural Protein 1,2
<b>C-t</b>	C-terminus
<b>Ca<sup>2+</sup></b>	Calcium
<b>Cp</b>	Crossing point-PCR-cycle
<b>BSA</b>	Bovine serum albumin
<b>cDNA</b>	Complementary deoxyribonucleic acid
<b>CL-A</b>	Calyculin A
<b>CMV</b>	Cytomegalovirus
<b>DAG</b>	Diacylglycerol
<b>DAPI</b>	4',6-diamidino-2-phenylindole
<b>DBS</b>	Donor bovine serum
<b>DMEM</b>	Dulbecco's Modified Eagle's medium
<b>DMF</b>	Dimethylformamide
<b>DMSO</b>	Dimethyl sulfoxide
<b>DNA</b>	Deoxyribonucleic acid
<b>dNTP</b>	deoxynucleotide triphosphate
<b>EBS</b>	Epidermolysis bullosa simplex
<b>ED</b>	Estradiol
<b>EDTA</b>	Ethylenediaminetetraacetic acid
<b>EGF</b>	Epidermal growth factor
<b>EHK</b>	Epidermolysis hyperkeratosis
<b>EMT</b>	Epithelial–mesenchymal transition
<b>ERK</b>	Extracellular signal–regulated kinases
<b>F/R (primer mix)</b>	Forward/reverse
<b>FCS</b>	Foetal calf serum
<b>FFPE</b>	Formalin-fixed paraffin-embedded
<b>GAPDH</b>	Glyceraldehyde-3-phosphate dehydrogenase
<b>gDNA</b>	Genomic deoxyribonucleic acid
<b>GFAP</b>	Glial fibrillary acidic protein
<b>GFP</b>	Green fluorescent protein
<b>Glu,E</b>	Glutamic acid
<b>GuHCL</b>	Guanidine hydrochloride
<b>GSH</b>	Glutathione

<b>GST</b>	Glutathione S-transferase
<b>h</b>	hour
<b>H<sub>2</sub>O</b>	water
<b>H&amp;E</b>	Haematoxylin and Eosin
<b>HIM</b>	Helix initiation motif
<b>HSF1</b>	Heat shock factor 1
<b>HSPs</b>	Heat shock proteins
<b>HSP70</b>	Heat shock protein 70
<b>HTM</b>	Helix termination motif
<b>OSCC</b>	Oral squamous cell carcinoma
<b>HPV (e.g. HPV16)</b>	Human papillomavirus
<b>hTERT</b>	Human telomerase reverse transcriptase
<b>ICC</b>	Immunocytochemistry
<b>IF</b>	Immunofluorescence
<b>IFN (e.g. IFN<math>\gamma</math>)</b>	Interferon
<b>IgG</b>	Immunoglobulin G
<b>IHC</b>	Immunohistochemistry
<b>IP<sub>3</sub></b>	Inositol trisphosphate
<b>IPTG</b>	Isopropyl- $\beta$ -D-thiogalactoside
<b>ISH</b>	<i>In situ</i> hybridisation
<b>JNKs</b>	c-Jun N-terminal kinases
<b>K (e.g. K1, K15)</b>	Keratin
<b>kDa</b>	kilodalton
<b>KFAPs</b>	Keratin filament associated protein
<b>KRT</b>	Keratin gene
<b>LB (medium)</b>	Lysogeny Broth, Luria-Bertani
<b>mAb</b>	Monoclonal antibody
<b>MAPK</b>	Mitogen-activated protein kinase
<b>MF</b>	Microfilament
<b>MMC</b>	Mitomycin C
<b>MT</b>	Microtubule
<b>mTOR</b>	mammalian Target of rapamycin
<b>min</b>	minute
<b>ml</b>	mililitre
<b>mM</b>	milimolar
<b>MMPs</b>	Matrix Metalloproteinase
<b>mRNA</b>	messenger ribonucleic acid
<b>N-t</b>	N-terminus
<b>NGS</b>	Normal goat serum
<b>NHEK</b>	Normal human epidermal keratinocytes
<b>nM</b>	nanomolar
<b>OA</b>	Okadaic acid



<b>OD (e.g. OD<sub>600</sub>)</b>	Optical density
<b>OT</b>	Organotypic (culture)
<b>OV</b>	Orthovanadate
<b>PBS</b>	Phosphate buffered saline
<b>PCR</b>	Polymerase chain reaction
<b>pI</b>	Isoelectric point
<b>PI</b>	Protease inhibitor
<b>PI3K</b>	Phosphoinositide 3-kinase
<b>PKC</b>	Protein kinase C
<b>PLC</b>	Phospholipase C
<b>PMA</b>	Phorbol 12-myristate 13-acetate
<b>PP</b>	Protein phosphatase
<b>PR</b>	Phenol red
<b>pRB</b>	Retinoblastoma protein
<b>PTM</b>	Posttranslational modification
<b>PV</b>	Papillomavirus
<b>qPCR</b>	quantitative real-time Polymerase chain reaction
<b>RA</b>	Retinoic acid
<b>RAR</b>	Retinoid acid receptor
<b>Rb</b>	Retinoblastoma
<b>RM+</b>	Rheinwald-Green modified (medium)
<b>RNA</b>	Ribonucleic acid
<b>RNA pol</b>	Ribonucleic acid polymerase
<b>ROCKi</b>	Rho-associated kinase inhibitor
<b>RT</b>	Room temperature
<b>RXR</b>	Retinoid X receptor
<b>S</b>	Serine
<b>SAPKs</b>	Stress activated protein kinases
<b>SEM</b>	Standard error of mean
<b>SDS</b>	Sodium dodecyl sulfate
<b>SDS-PAGE</b>	Sodium dodecyl sulfate polyacrylamide gel electrophoresis
<b>SFM</b>	Serum-free medium
<b>SLPs</b>	Serum lipids
<b>TBS</b>	Tris buffered saline
<b>TBST</b>	Tris buffered saline containing Tween 20
<b>TF</b>	Transcription factor
<b>TGM (e.g. TGM1)</b>	Transglutaminase
<b>TRADD</b>	Tumour necrosis factor receptor type 1-associated DEATH domain
<b>TX-100</b>	Triton X-100
<b>ULFs</b>	Unit length filaments
<b>UTRs</b>	Untranslated region

<b>VDR</b>	Vitamin D Receptor
<b>v/v</b>	volume/volume
<b>WB</b>	Western blotting
<b>w/v</b>	weight/volume
<b>µg</b>	microgram
<b>µl</b>	microlitre
<b>µm</b>	micrometre
<b>µM</b>	micromolar

# CHAPTER 1

## **1. Introduction.**

Epithelial cells form the outer most layer of skin and lining of internal mucosa, so they are considered to be the first line of defence against different types of every day environmental stresses. In order for the epithelial cells to perform this function as a stress barrier, they need to be stiff yet flexible at the same time. All eukaryotic cells including the epithelial cells share a protein network called the cytoskeleton, which is a complex network of tubules and filaments made of fibrous proteins distributed throughout the cytoplasm. The cytoskeleton is composed of three major components: microtubules (MT), intermediate filaments (IFs) and microfilaments (MF or stress fibers). MFs are the thinnest, 5-7 nm in diameter and are made of G-actin that assembles to form these filaments. MTs are the thickest with 20 nm thickness and are made of  $\alpha$ - and  $\beta$ -tubulin subunits. They are both polarised and highly dynamic, so mainly involved in intracellular transport and movement of particles and organelles. IFs on the other hand form 7-10 nm thick filaments, and as they are the least dynamic they are mainly involved in cell stability and mechanical stress absorption (Moll et al., 2008, Bragulla and Homberger, 2009, Gefen and Weihs, 2015). IFs represent one of the largest and most complex cytoskeletal network systems that are encoded in humans, by about 65 known genes. Some of them have the ability to bind to desmosomes and hemidesmosomes to provide strength and support of epithelial cells under different physiological conditions. Expression is cell-type-specific, so their function is also cell specific i.e. different cells express different types of IFs. Epithelial cells for example, express keratins while mesenchymal cells express vimentin and not the other way around. Keratins in epithelial cells provide support while vimentin aids in cellular migration. IFs are grouped, based on their structural

homology, into six different types, I-IV are cytoplasmic, type V is nuclear and VI is present only in the eye lens (Gefen and Weihs, 2015, Omary, 2009).

**Types I and II** Acidic and neutral to basic keratins.

**Type III** Desmin, Vimentin, GFAP (glial fibrillary acidic protein).

**Type IV** Neurofilaments.

**Type V** Nuclear lamins.

**Type VI** Bfsp1 (Filensin), Bfsp2 (Phakinin) in the lens of the eye.

IF proteins have their own features that make them different from MT and MF. They are highly insoluble proteins in normal buffers and high salt solutions but can be solubilised in chaotropic agents, such as 8 M urea or 6 M guanidine-hydrochloride (GuHCl) that weakens the hydrophobic interactions in proteins and leads to their denaturation (Herrmann et al., 2007). Keratins (Ks) are expressed in a tissue-specific manner for example, K5/14 are mostly found in the basal layer of multi-layered epithelium whereas the K1/10 pair is found in suprabasal epithelial layers. Some keratins are only expressed under certain physiological conditions, e.g. K6 and K16 are expressed during wound healing and certain hyperproliferative conditions such as psoriasis and pathological scarring and not expressed in normal epidermis (Bloor et al., 2003, Machesney et al., 1998, Omary, 2009). Likewise, K8 and K18 are not expressed in normal stratified epithelia but they are expressed in large quantities in metastatic cancer lesions (Haines and Lane, 2012, Bloor et al., 2003, Eichner et al., 1986).

## 1.1. Nomenclature and classification.

Keratins were first named and classified by Moll and co-workers in 1982, based on their isoelectric point and molecular weight as determined by 2-dimensional polyacrylamide gel electrophoresis. In this classification, the keratin family was divided into two types, type I and type II, based on their biochemical properties. Those which were acidic (isoelectric point < pH 5.5) were called type I, and those which were basic or neutral (isoelectric point > pH 6.0) were classified as type II. Keratins are usually expressed in pairs of a type I and type II partner. Type I are keratins K9-K18 while type II are K1-K8 (Table 1.1). Type I human keratins cluster is found on chromosome 17 q21.2 except K18, which is the only type I keratin found within the type II keratin locus on human chromosome 12. For type II human keratins, the cluster is found on chromosome 12q13.13 (Arin, 2009, Waseem et al., 1990). This nomenclature of Moll et al (1982) was not accommodating the newly discovered keratins when the whole human genome was sequenced, and new keratin genes were identified (Moll et al., 1982). A new nomenclature was developed which accommodated the 54 human *KRT* genes (28 type I and 27 type II) and some pseudogenes, it also gives space for *KRT* genes that are yet to be discovered as shown in (Table 1.2) (Gu and Coulombe, 2007, Schweizer et al., 2006). Keratins are not only classified according to isoelectric point (acidic and basic), they can be classified based on other criteria as shown in Figure 1.1. (Rao et al., 2014).

**Table 1.1. Numbering of keratins categories.** (Schweizer et al., 2006).

Category	Number range
Human type I epithelial keratins	9–28
Human type I hair keratins	31–40
Non-human type I epithelial and hair keratins	41–70
Human type II epithelial keratins	1–8 and 71–80
Human type II hair keratins	81–86
Non-human type II epithelial and hair keratins	87–120
Type II keratin pseudogene	121–220
Type I keratin pseudogenes	221 →

**Table 1.2. Nomenclature of human keratin proteins, old and new.** (Gu and Coulombe, 2007)

Old protein designation	New protein designation	Old protein designation	New protein designation
Type I epithelial keratins	Type I epithelial keratins	Type II epithelial keratins	Type II epithelial keratins
K9	K9	K1	K1
K10	K10	K2e	K2
K12	K12	K3	K3
K13	K13	K4	K4
K14	K14	K5	K5
K15	K15	K6a	K6a
K16	K16	K6b	K6b
K17	K17	K6e/h	K6c
K18	K18	K7	K7
K19	K19	K8	K8
K20	K20	K6irs1	K71
K23	K23	K6irs2	K72
K24	K24	K6irs3	K73
K25irs1, K10C, HIRSa1	K25	K6irs4	K74
K25irs2, K10D	K26	K6hf	K75
K25irs3, K10B, HIRSa3.1	K27	K2p	K76
K25irs4, HIRSa2	K28	K1b	K77
<b>Type I hair keratins</b>	K5b	K78	
Ha1	K31	K6l	K79
Ha2	K32	Kb20	K80
Ha3-II	K33b	<b>Type II hair keratins</b>	
Ha4	K34	Hb1, K2.9	K81
Ha5	K35	Hb2	K82
Ha6	K36	Hb3, K2.10	K83
Ha7	K37	Hb4	K84
Ha8	K38	Hb5, K2.12	K85
	K39	Hb6, K2.11	K86
	K40		

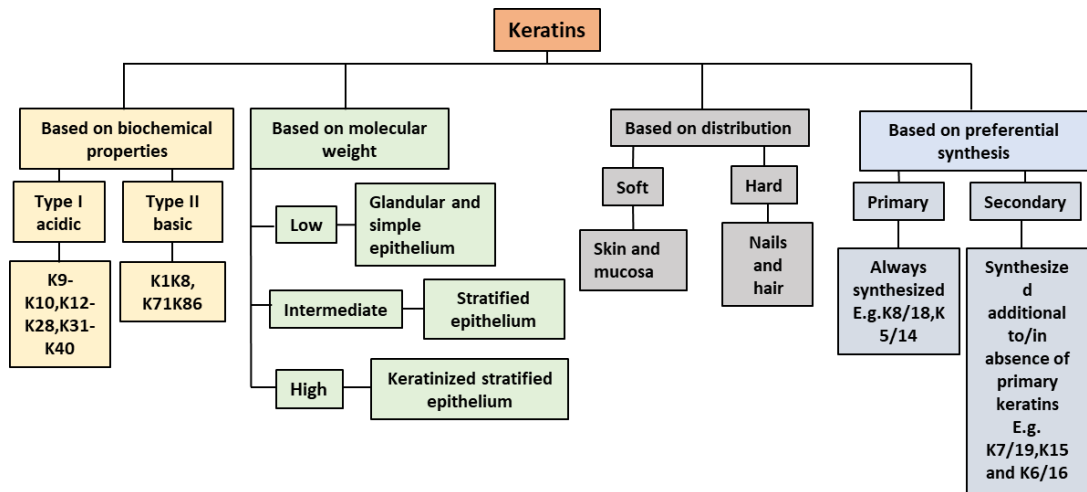


Figure 1.1. Keratin classifications. (Rao et al., 2014)



## 1.2. Structure.

All IFs share the same basic structure although their functions vary according to their expression site within the tissue as well as their PTMs. Keratin polypeptides are made of three functional domains, a central helical rod domain flanked by the N-terminal head and the C-terminal tail domains on either side. The rod domain is made up of around 300 amino acids and is highly conserved among all types of IFs whereas C- and N-terminal domains differ from one type of filament to another as shown in (Figure 1.2). The  $\alpha$ -helical coiled-coil rod domain is made up of four heptad repeat-containing regions named 1A, 1B, 2A and 2B, separated by a short, non-coiled flexible linkers, L1, L12 and L2. All vertebrate cytoplasmic IF proteins rod domains contain around 310 residues and the sizes of the individual  $\alpha$ -helical segments are absolutely conserved (Strelkov et al., 2002). Sub-domains 1B and 2B sequences are important for heterodimerisation and stabilising the coiled-coil structure of keratin IF. Local variations in the heptad repeat regions could affect IF structure assembly (Godsel et al., 2008, Wu et al., 2000, Herrmann et al., 2000). There are two main conserved regions in the coiled-coil structure, the first region is 26 residues long in the 1A segment and contains 8 residues in them that are highly conserved named the helix initiation motif (HIM). The second highly conserved sequence is located at the very end of the 2B segment and contains 32 residues in which 13 of them are extremely conserved named helix termination motif (HTM). These two motifs are common sites for human point mutations that affects dimer-dimer interactions as in various skin blistering conditions, HIM is more commonly affected than HTM (Strelkov et al., 2002, Pittenger et al., 2007). Sub-domain 2B contains a segment called “stutter” in which an additional four amino acids are inserted at the end of a heptad, interrupting the regular seven amino acids pattern of the dimer coiled-coil

domains as one of the discontinuities in this region. The conserved location of this stutter in 2B is highly important in all IFs and affects dimer stability (Strelkov et al., 2002, Herrmann and Aebi, 2016, Arslan et al., 2011). The head and tail domains are non-helical, and they are made up of short sequences of amino acids that differ from one keratin to another. Head and tail domains play an important role in keratin filaments self-assembly, lateral elongation and binding of keratins to other proteins and structural elements inside the cell (Wilson et al., 1992). Type I keratins usually have longer head and tail domains than type II. Most IFs form homodimers except keratins which form heterodimers of type I and II polypeptides arranged in register and parallel fashion. These dimers then arrange anti-parallel making the keratin filaments a non-covalently associated tetramers with no specific orientation or polarity (Deek et al., 2016). These tetramers join to form unit length filaments (ULFs) which are 60 nm long. ULFs later anneal longitudinally to form filaments that are loosely arranged and larger in size than mature filaments. The diameter of the ULF is around 16 nm that later undergoes compaction to reach the 10 nm diameter of IF as shown in Figure 1.3 (Godsel et al., 2008). This complex structure gives keratin filaments its unique rigidity and insolubility in normal cells (Moll et al., 2008, Bragulla and Homberger, 2009, Snider and Omary, 2014, Bray et al., 2015).

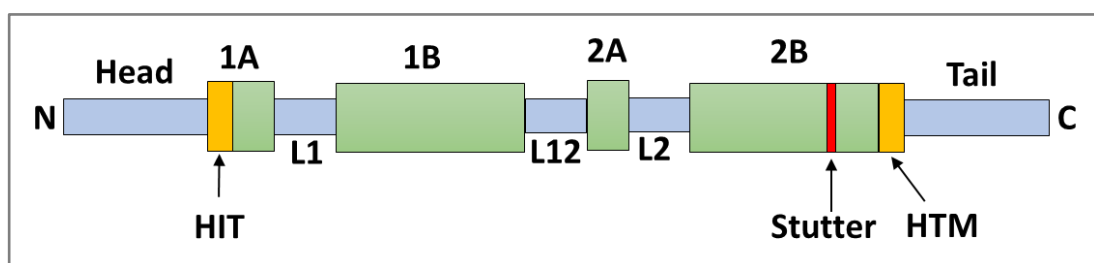


**Figure 1.2. Intermediate filament structural domains.**

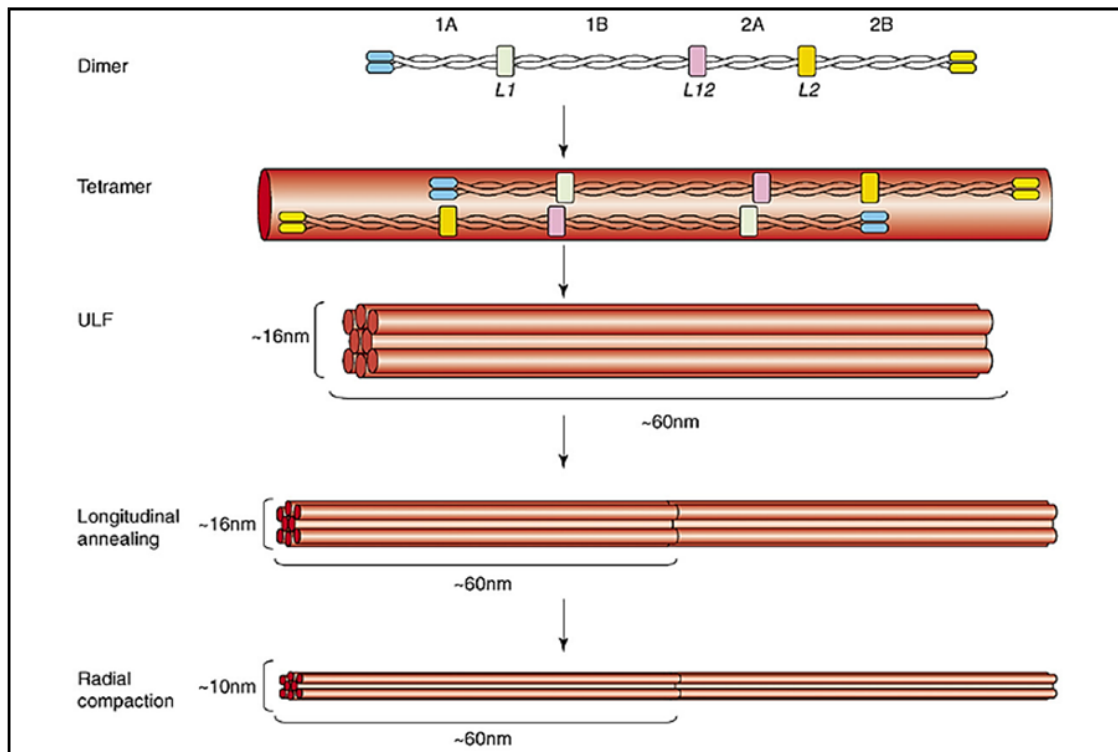


**Figure 1.3. Keratin unit length formation (ULF).** (Godsel et al., 2008).

### 1.3. Keratin dynamics.

Keratin filaments regulate several intracellular mechanisms operating during wound healing and apoptosis along with mechanical stability and stress absorption in normal conditions. These functions require that the filaments should be in a constant state of polymerisation and depolymerisation (Kolsch et al., 2010). Keratin polymerisation begins at the cell periphery at focal adhesion sites close to the cell membrane as nucleation centers, which can only be seen under super-resolution microscopy. These oligomers start to elongate as they move towards the nucleus and integrate into filamentous keratins to form bundles close to the nuclear envelope. Some filaments start to dissociate back to soluble particles and start the keratin cycle all over again (Haines and Lane, 2012, Snider and Omary, 2014, Kim et al., 2015a) (Figure 1.4 and 1.5). Keratin dynamics is a process that is highly regulated by phosphorylation. Site-specific phosphorylation

of keratins usually takes place at serine/threonine amino acids present in the head and tail domains. The localisation of a phosphate group mostly within the head or tail domain of the IF monomers is of significant importance. It has been found to alter the solubility, polymerisation and network-forming tendencies of the IF structures. Hyperphosphorylation could be correlating to complete network breakdown in some cases (Deek et al., 2016). Keratin phosphorylation is regulated by protein kinases and phosphatases. Excess phosphorylation of keratin filaments can lead to their disassembly into globules or interferes with their lateral elongation process as in Lamins IF during mitosis (Inagaki et al., 1996). Keratins are phosphorylated on serine residues more than threonine and tyrosine with serine being their main phosphorylation sites during mitosis (cell division). Phosphorylation during cell division allows keratin filaments to be reorganised and easily distributed into daughter cells. In K8, serine 73 (S73) on the head domain is the main phosphorylation site during stress (a substrate of p38  $\alpha$ -kinase), while serine 431 (S431) is mostly a phosphorylation site that is highly phosphorylated during mitosis. Point mutations in K8 and K18 major phosphorylation sites where serine is replaced by glutamic acid (Glu, E) results in shorter filaments and weaker interconnections between keratin polypeptides (Omary et al., 1998, Toivola et al., 2002). Phosphorylation plays an important role in filament elongation and assembly, as shown in hereditary keratin disorders presenting weaker easily disturbed keratin cytoskeletons (Deek et al., 2016). Phosphorylation is also critical for keratin nucleation and assembly into the existing networks because p38 mitogen activated protein kinase (MAPK) inhibition prevents the formation of keratin precursors at the cell periphery (Woll et al., 2007, Haines and Lane, 2012). Keratin dynamics and reorganisation allows newly synthesised or exogenous keratins to be smoothly introduced into the

endogenous network. When a new keratin is introduced into a cell it forms globules that are rapidly integrated into the endogenous network which reorganises to allow full integration and binding of both types (Miller et al., 1991, Miller et al., 1993b).

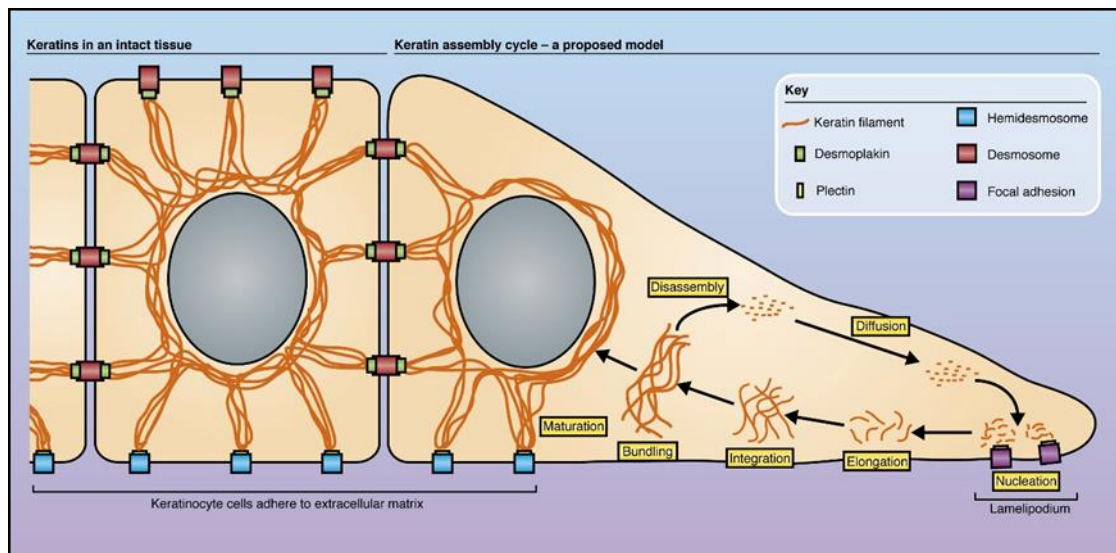


**Figure 1.4. Cycle of keratin assembly and disassembly.** (Haines and Lane, 2012).

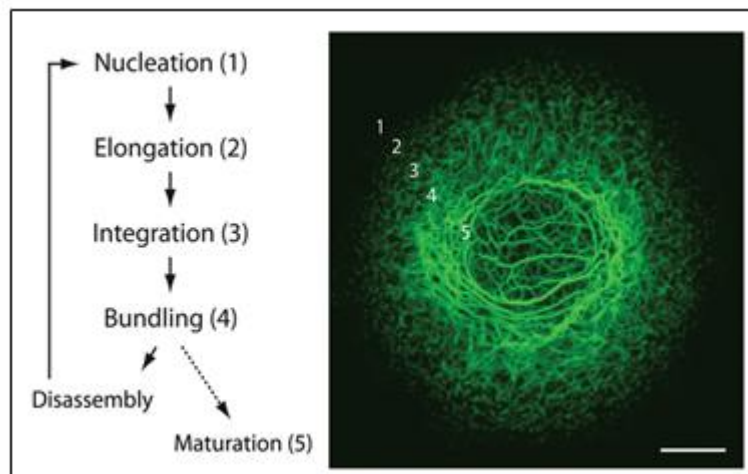


**Figure 1.5. Steps of keratin K13 cycle in vulvar carcinoma derived A431 cell line.** (Leube et al., 2011).

## **1.4. Keratin functions.**

Keratins have a broad range of intracellular functions that can be categorised into two major types, mechanical and non-mechanical functions.

### **1.4.1. Mechanical functions of keratins.**

Keratins being the most abundant cytoskeletal proteins in skin and epithelial lining, need to be able to withstand mechanical forces applied on these tissues. Despite their flexibility, keratins are described as the “bones” of keratinocytes (Magin et al., 2007). They spread all over the cytoplasm, binds to MT and MF components of the cytoskeleton and form a cage like structure around the nucleus (Haines and Lane, 2012). Keratins are also anchored to desmosomes and hemidesmosomes via desmoplakin and plectin respectively, to ensure a strong scaffold and permit stress dissipation into neighboring cells (Magin et al., 2007, Haines and Lane, 2012). In keratin mutation disorders such as Epidermolysis Bullosa Simplex (EBS) and Epidermolysis Hyperkeratosis (EHK), tissue fragility is the main issue due to loss of anchorage to desmosomes and hemidesmosomes that decreases the tissue stability and leads to epithelial sloughing (Gu and Coulombe, 2007, Pan et al., 2013).

### **1.4.2. Non-mechanical functions of keratins.**

Recently it has been discovered that keratins are much more than simply a stress barrier, as they play an important role in many cellular processes including signaling, protein transport, cell adhesion, apoptosis, growth and wound healing along with a role in cancer which will be discussed later in part (1.7). Membrane trafficking is an important keratin non-mechanical function, where melanin granules bind to the head domain of keratins and move from the cell periphery toward the nucleus in a centripetal fashion. This allows melanin pigments to

accumulate around the nucleus and protect the DNA from UV light (Gu and Coulombe, 2007). In a group of rare disorders associated with mutations in K5 and K14, the skin shows patches of hyper and hypo-pigmentation areas due to a defect in melanosome trafficking, although the exact mechanism is not fully understood (Haines and Lane, 2012). Keratin expression has an impact on epithelial cell growth and proliferation during differentiation and wound healing. The 14-3-3 $\alpha$  is an adaptor protein that binds to the head domain of keratin polypeptides and activates the protein kinase mammalian target of rapamycin (mTOR) signalling that enhances cell growth and proliferation. K17 null mice embryos show delayed wound healing and smaller cell size at the wound edges which is accompanied by reduction in mTOR kinase activity (Kim et al., 2006). During epithelial differentiation and wound healing keratin expression changes rapidly from K5/K14 to K1/K10 during differentiation or changes to K6/K16/K17 during wound healing which affects the cell size (Magin et al., 2007). During the cell cycle keratins play an important role, since mitosis is controlled by multiple cascade. During cell division, the protein kinase 2 and cyclin B (Cdc2/Cyclin B) complex undergoes phosphorylation and dephosphorylation. Its phosphorylation is activated by Cdc25 phosphatase that needs to bind to the 14-3-3 $\alpha$  protein for its activation. Phosphorylation of keratins by growth-promoting kinases attracts the 14-3-3 $\alpha$  protein out of the nucleus where it binds to the head domain and allows Cdc25 to bind and become activated. This binding allows keratins to reorganise during mitosis as K18 null mice show arrest in S/G2 phase of hepatocellular cells with 14-3-3 $\alpha$  accumulating inside the nucleus (Margolis et al., 2006, Omary et al., 2006, Magin et al., 2007).

### **1.4.3. Apoptosis and Keratins.**

Besides the mechanical and non-mechanical roles that keratins play inside the cells, they are also involved in cellular apoptosis. Apoptosis is defined as programmed cell death by which unnecessary cells are removed from a tissue and this could be part of a normal physiological process (embryogenesis) or during disease situations. Failure of apoptosis can lead to abnormal cell growth as is the case during cancer progression. Keratin proteins play an important role in cellular apoptosis. Type I keratins could bind to tumour necrosis factor receptor type 1-associated DEATH domain protein (TRADD) when phosphorylated, and down regulate the death inducing signal that is needed for apoptosis. It has been suggested that lack of a type II keratin could results in the absence of its other type I keratin pair and this could lead to activation of Fas- mediated apoptotic pathway, which would allow caspases to break down keratin filaments by proteolysis at specific site on the rod domain (Caulin et al., 1997, Kim and Coulombe, 2007). Keratins functions are summarised in Figure 1.6. (Magin et al., 2007).



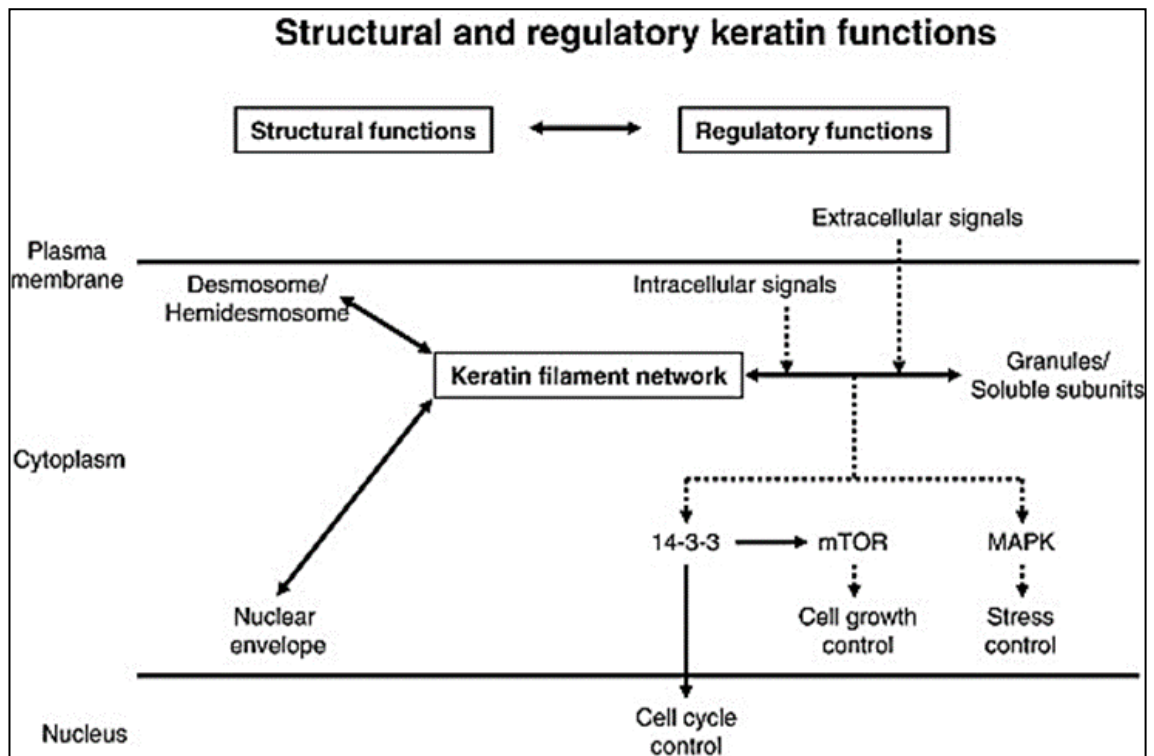
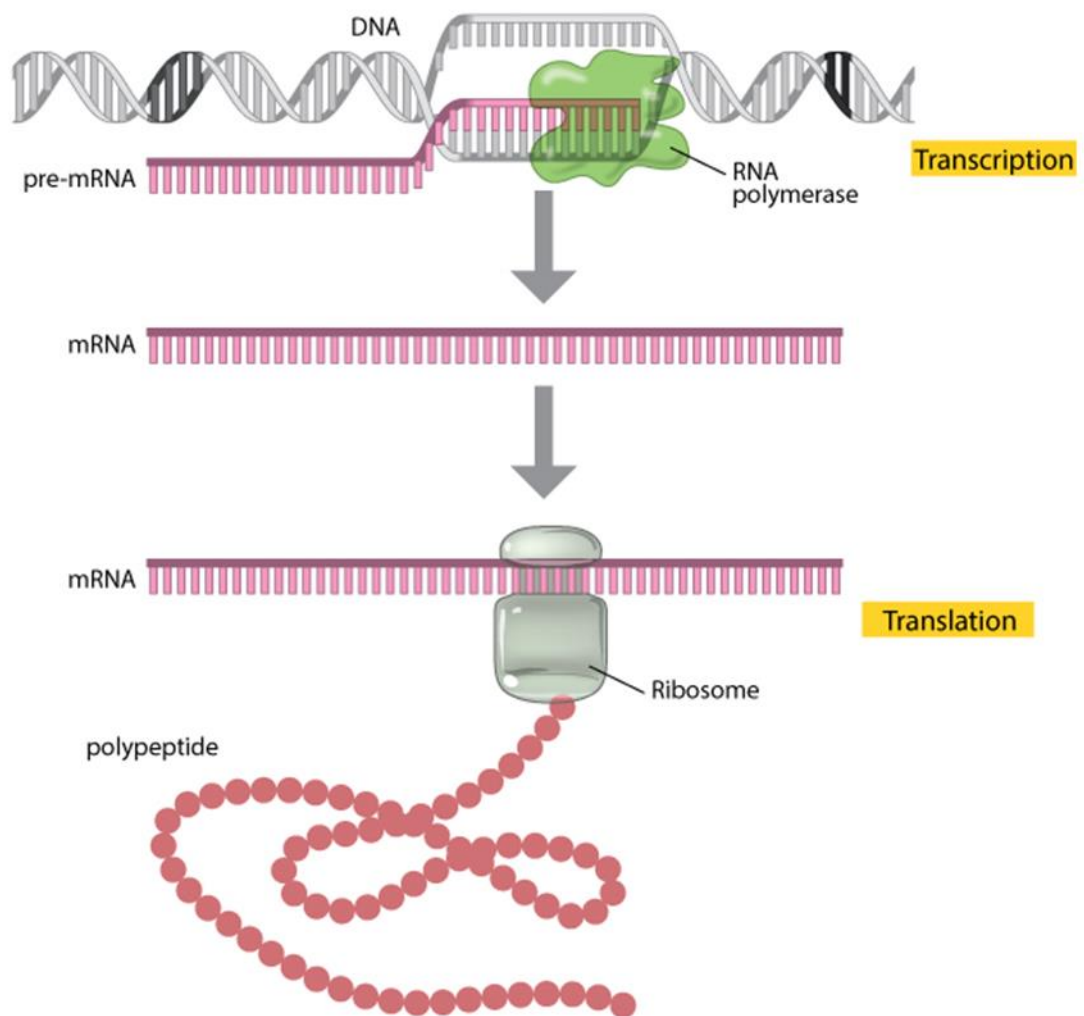


Figure 1.6. Structural and regulatory functions of keratins. (Magin et al., 2007).

## 1.5. DNA transcription, translation and post translational modifications.

DNA transcription, which is the synthesis of RNA, and the translation of messenger RNA (mRNA) into proteins is called gene regulation. Gene regulation is one of the most important steps that controls growth, differentiation and apoptosis of all cells and drive the complexity of a living organism. Transcription of a template DNA strand is carried out by a specific enzyme called RNA polymerase (RNA pol), which with transcription factors initiates the process of transcription that results in formations of transcripts (hnRNAs). These hnRNAs are modified in the nucleus before being exported into the cytoplasm as mature mRNA. Once the mRNA is in the cytoplasm, it undergoes a series of post-transcriptional modifications allowing this mRNA to be either stabilised (translated into protein) as shown in Figure 1.7, or degraded. These steps are highly

controlled and monitored by several factors and pathways that regulate this process depending on the physiological needs of each cell (Atwater et al., 1990, Guhaniyogi and Brewer, 2001, Taylor, 2006, Guo, 2014). Once the polypeptide is made and released from the ribosomes, it undergoes a series of PTMs such as phosphorylation, glycosylation etc.



**Figure 1.7. Steps in transcription and translation of eukaryotic genes.** (Nature education 2013).

PTM is a biochemical process of covalently adding a small molecule onto a selected amino acid residue after protein synthesis. This modulates and widens the range of possible functions of a particular protein inside the cell. There are more than 200 different types of PTMs that have been identified and affect a wide range of cellular functions, such as metabolism, signal transduction, and protein stability. Glycosylation, sumoylation, acetylation, ubiquitylation and phosphorylation are described in the literature as the most common types of PTMs found in natural proteins. Among these types of PTMs, phosphorylation is considered to be the main PTM found in keratin proteins. In this process, a phosphate group is added onto a specific serine, threonine or tyrosine residue in the polypeptide. These sites are mostly located at the end domains of the IF protein secondary structure including keratins (Toivola et al., 2002). Keratins can undergo phosphorylation in response to various types of stresses. In a physiological stress condition such as mitosis, phosphorylation is reversible and after reorganisation of keratin filaments into daughter cells, phosphatases take over and dephosphorylate the polypeptide, so keratins are converted back to their normal filamentous state. In case of keratin mutation, cells will be unable to withstand stress as filaments breakdown leading to loss of cellular integrity and strength (Magin et al., 2007, Snider and Omary, 2014). Phosphorylation is carried out and regulated by a group of kinases and phosphatases and they are activated in response to specific stimuli. Mechanical and chemical stresses as well as growth factors and cytokines are considered phosphorylation inducers (Inagaki et al., 1996, Kim et al., 2015b, Kim et al., 2015a). The regulation of keratin phosphorylation will be discussed in Section 1.6. Sumoylation is a type of PTM that is carried out by small ubiquitin-like modifier (SUMO) and affects IF solubility and assembly. Keratin sumoylation is carried out in hyperphosphorylated,

oxidative and apoptotic stress conditions and affects keratin dynamics. Glycosylation involves introducing  $\beta$ -N-acetyl glucosamine (GlcNAc) into Ser/Thr residues of IF proteins by O-GlcNAc transferase (OGT). It has been shown that glycosylation plays a role in activating kinases that phosphorylate keratins and therefore play a role in preserving tissue stress responses. Lysine acetylation of IFs plays a role in changing their response to metabolic alterations (Snider and Omary, 2016). There are other PTMs that are not well understood and their roles on IFs are not yet clear such as ubiquitination, transamidation and adenosine diphosphate (ADP) -ribosylation for example (Snider and Omary, 2014).

## **1.6. Keratin filaments phosphorylation, regulation and stress response.**

### **1.6.1. Keratin phosphorylation.**

PTMs regulate keratin reorganisation and their association with other proteins inside an epithelial cell (Coulombe and Omary, 2002). Phosphorylation is considered to be the key regulator compared with other modes of PTM to affect keratin properties such as solubility and structural stability (Omary et al., 2006). In general, the basal level of phosphorylation of keratins is low but if the cells are undergoing mitosis or being exposed to certain cellular stresses such as, drug-induced apoptosis, shear stress, heat stress and treatment with phosphatase inhibitors (that act on protein phosphatase 1 (PP1) and/or PP2A), the level of phosphorylation rises significantly. Okadaic acid (OA), Calyculin-A (CL-A) and Orthovanadate (OV) are the most commonly used phosphatase inhibitors in keratin dynamic studies (Yatsunami et al., 1993, Windoffer and Leube, 2004). So phosphorylation ensures keratin resiliency which is a vital need for epithelial cells

(Inagaki et al., 1996). Keratin phosphorylation mainly occurs at Ser > Thr > Tyr residues either on head or tail domains, but the number of phosphates binding to each keratin molecule is dependent on cell type, keratin involved and physiological status of the cell. Keratin phosphorylation is regulated by a balance between phosphatases and kinases activities and most keratin phosphorylation studies are performed by inducing hyperphosphorylation (Paul et al., 1997). Among different keratin phosphorylation sites, human keratin K8 phosphorylation sites are well studied and characterised. Keratin 8 is mainly phosphorylated at S23, S73, and S431 but only the S73 phosphorylation is regulated by p38 and c-jun-N-terminal kinase, both members of the MAPK family (Karantza, 2011a).

### **1.6.2. Stress-activated protein kinases.**

Stress-activated protein kinases (SAPKs) are a group of kinases that are only activated by stress, where they mediate signal transduction of an extracellular stimulus to the nucleus in order to facilitate gene transcription as a stress response. They are homologues of the p42 and p44 isoforms of MAP kinase and they play a significant role in cellular proliferation, differentiations as well as regulating keratins phosphorylation under stress (Paul et al., 1997). MAPKs are c-jun N-terminal kinases (JNKs) and p38 MAP kinase and they play a critical role in keratin reorganisation and disassembly, but they are not activated by the same type of stress. The phosphorylated p38 kinase has been shown to co-localise with phosphorylated S73 of K8 treated with OV phosphatase inhibitor *in vitro* indicating its role in filaments breakdown (Woll et al., 2007). Another study has shown the role of p38 MAP kinase in filaments breakdown by using p38 MAP kinase inhibitor prior to OV treatment. This study has shown that keratin filament breakdown was prevented by p38 MAP kinase inhibitor treatment and not by

MAPK inhibitor. This indicates the specific role of p38 kinase but not JNK, in this type of stress (Strnad et al., 2003). However, JNK have been shown to be involved in phosphorylating S73 on K8 *in vitro* in Fas-receptor mediated signalling pathway (a pro-apoptotic pathway) (He et al., 2002).

### **1.6.3. Heat Shock proteins and stress response.**

Heat shock proteins (HSPs) are a group of chaperone proteins that protect cellular proteins from damage and denaturation or misfolding induced by stress (Kregel, 2002). HSPs are associated with cellular thermotolerance (a state of being relatively unaffected by heat), they are activated when cells are exposed to sub-lethal levels of heat which induces thermotolerance. Collapse of cytoskeletal filaments and protein denaturation associated with heat shock can be prevented or minimised by the thermotolerance affect induced by HSP70 (Mizzen and Welch, 1988, Welch and Mizzen, 1988, Shyy et al., 1989). It has been shown that HSP70 can also reduce p38 kinase activity which is the main kinase affecting keratin reorganisation under stress acting as a pro-apoptotic protein. p38 kinase inhibition therefore enhances cell survival and this could be through caspase inactivation (Gabai et al., 1997, Beere, 2004).

## **1.7. Keratin phosphorylation in cancer.**

Recent studies have shown a functional role of keratins in the field of carcinogenesis beside their well-known role as a diagnostic and prognostic tool (Karantza, 2011b). Phosphorylation of IFs leads to reorganisation of keratin and vimentin filaments around the nucleus. One of the pathways that induces these filaments phosphorylation is the activation of JNK and Erk kinases by a natural

lipid Sphingosyl-phosphorylcholine (SPC). SPC has also been shown to increase cellular migration through an epithelial-mesenchymal transition (EMT)-like manner. Isolated cancer cells showed keratin re-organisation patterns similar to SPC treated cells. This has been shown in ovarian cancer patients and pancreatic cancer cells as well. It was explained by K8 and K18 phosphorylation on certain serine motifs that leads to enhanced cellular elasticity and migration (Beil et al., 2003). As a result, SPC could be used as treatment target of the migratory and invasive machinery that it provides for cancer cells as well as being a promising tool in studying keratin organisation and metastatic potential of these cells (Holle et al., 2017).

## **1.8. Keratinocyte differentiation.**

The epidermis is the first line of defence against various type of abuses to which human body is routinely exposed to. It acts as a tough barrier against environmental, mechanical and chemical insults. It is made of four different highly regulated layers. The basal layer is composed of highly proliferative cells that undergo a series of morphological and physiological changes as they move upward toward the surface. The suprabasal layers where cells start to get larger and flatter are the spinous and granular layers. The granular layer is called so due to the intracellular enclosed lamellar granules that later secrete lipids and proteins forming lamellar discs filling the intercellular spaces around corneocytes. This structure gives skin its toughness and resilience and protects against water loss. Corneocytes are enucleated cells that make the outer most layers of epidermis. They contain keratins, cross-linked proteins and transglutaminases (TGM1) (Madison, 2003). Keratinocytes undergo a process called differentiation

through their journey up to the surface. This differentiation process is guided and well regulated by a number of factors that allows a smooth transition of basal cells to supra-basal ones and ending with corneocytes that later desquamate allowing skin renewal to take place (Fuchs, 1993). Differentiation-specific keratins are found in suprabasal layers of the epithelium-associated with terminal differentiation and loss of proliferative capability of the cell. Their distribution and expression differs in normal and diseased epithelium at the level of gene and protein expression. In normal stratified epithelium, K1/K10 and K4/K13 are expressed in suprabasal layers of keratinised and non-keratinised epithelium, respectively. In oral dysplastic and squamous cell carcinoma this expression is changed. In mildly dysplastic lesions keratin expression could be more than their expression in normal tissues while in poorly differentiated lesions keratin expression is often reduced or almost not present (Kartasova et al., 1992, Bloor et al., 2000, Hansson et al., 2001). Differentiation-specific keratins play a role in physiological processes other than being markers of terminal differentiation of epithelial tissues. In epidermis, K1/K10, K2/K10 and K1/K9 are the most abundant pairs of keratins found in its suprabasal layer. K1/K10 pair is found all over the hairy skin while K2/K10 pair is at stress bearing areas such as palms and soles and the tail of mice (Fischer et al., 2016). Knocking out one of these keratins in mice leads to skin hyperkeratosis and inflammation although loss of K2/K10 leads to overexpression of K1/K9 in that area but there is still loss of normal skin structure and stratum corneum formation (Fischer et al., 2016). The loss of K2 is less severe than K1, this could be due to the fact that K1 is covering almost the entire body while K2 is more expressed in stress bearing areas. In humans, mutation in *KRT1* or *KRT10* results in EHK while ichthyosis bullosa of siemens (IBS) is the result of *KRT2* mutation (Fischer et al., 2016). Loss of K2 in



epidermis causes hyperkeratosis, water loss and inflammation with aggregations of K10 in some areas that are not partially compensated by K1. On the other hand loss of K10 aggregates K2 and it causes more severe forms of skin hyperkeratosis as K2 binds only to K10 and there is no evidence showing its binding to K9 or any other type I keratin (Fischer et al., 2014). Keratin K2 is normally expressed in the spinous and granular layers of the epidermis in most of the body parts but it is down-regulated in the case of squamous metaplasia and carcinomas, or in cultured cell lines *in vitro* (Collin et al., 1992, Bloor et al., 2003).

In normal oral epithelium, K2 has very low levels of expression in most of the oral cavity regions and complete absence in the buccal mucosa and floor of the mouth. In the case of mild dysplasia, K2 protein level is low while its mRNA is strongly expressed. Keratins K1/10 expression is induced in mild and moderately differentiated oral squamous cell carcinoma (OSCC) while all differentiation specific keratins were almost lost in poorly differentiated OSCC. Little is known about the mechanism by which the *KRT2* gene and hence mRNA is induced and its role in dysplasia (Bloor et al., 2003).

It has been shown that ectopic expression of the differentiation specific K10 (full length) into the basal layer of epidermis inhibited cell proliferation. This happens through the impaired activity of phosphoinositide 3-kinase (PI3K) preventing cell cycle progression (Santos et al., 2002). Interestingly, when K10 end domains were fused into the K14 helical rod domain (basal keratin) in the basal layer of the epidermis a totally opposite result was observed. Cells were highly proliferative and were showing high susceptibility to develop benign tumours. This demonstrates the differences between the end domains of different keratins (Chen et al., 2006).

## **1.9. The mechanism of keratinocyte differentiation.**

Keratinocyte differentiation starts when the basal cells attached to the underlying dermis/ connective tissue begin to lose their calcium activated intercellular junctions or plaques. Basal keratins comprising K5 and K14 are downregulated while a new set of differentiation-specific keratins, K1 and K10, are induced as the cell moves through the differentiation process. At the upper spinous and granular layer, K2 expression is induced, and it is considered to be a terminal differentiation marker. The induction of new keratins as the cell moves toward the surface is tissue- as well as site-specific, since in skin of palms and soles there is induction of K9 in addition to K1 and K10 in the suprabasal layers whereas K6 and K16/K17 are induced supra-basally during wound healing (Fuchs, 1993).

The process of keratinocyte differentiation is tightly regulated at the gene level by a family of regulator proteins called transcription factors. There are different transcription factors that play an important role in keratinocyte differentiation but amongst these proteins, activator proteins one (AP-1) is the most widely studied. The AP-1 transcription factor family are composed of mainly Jun and Fos proteins that form homo (Jun-Jun) or heterodimers (Jun-Fos) that bind to the AP-1 binding site on the DNA (Han et al., 2012). This binding regulates various keratinocyte key functions such as proliferation, differentiation and apoptosis (Han et al., 2012). It has been shown that TAM67 (a dominant negative form of c-Jun) suppresses some markers of terminal differentiation by binding to AP-1 binding sites (Han et al., 2012). This binding prevents or reduces AP-1 from binding to its site and therefore inactivating differentiation pathways (Han et al., 2012). One of the major signalling pathways controlling keratinocyte differentiation is the MAPK pathway. Upstream regulators of MAPK such as protein kinase C (PKC) tends to phosphorylate MAPK once a differentiation stimulus is initiated. Phosphorylated

MAPK in turns phosphorylates and activates certain transcription factors that allow them to bind to their response elements on the target gene promotor and enhance their transcription. The PKC/AP-1 pathway shown in Figure 1.8 (Eckert et al., 2013).

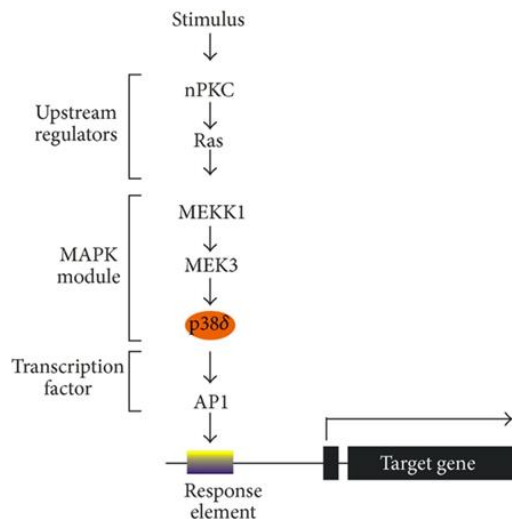


**Figure 1.8. The PKC/AP-1 pathway.** (Eckert et al., 2013).

## 1.10. Factors regulating keratinocyte differentiation.

### 1.10.1. Calcium.

Calcium is a well-known regulator of keratinocyte differentiation. It has a concentration gradient through the epidermal layers with low concentrations in the basal layer where differentiation markers are suppressed and a higher concentration as the cells move supra-basally where differentiation markers are activated specially in the granular layer. Calcium tends to play a major role as a differentiation inducer and a proliferation suppressor in keratinocytes (Boyce and Ham, 1983, Pillai et al., 1990, Eckert et al., 1997). The induction of keratinocyte differentiation by calcium could be regulated by a genomic or non-genomic

pathway (Elsholz et al., 2014). The presence of high concentration of extracellular calcium above 0.1 mM (so called “calcium switch”) rapidly activates desmosomal junction formation (non-genomic pathway) which increases the strength of cell-cell adhesion that promotes a signalling cascade for epidermal differentiation and increases the production of differentiation-specific proteins such as K1, K10, involucrin, filaggrin or TGM1 (Hennings and Holbrook, 1983, Hennings et al., 1980, Yuspa et al., 1989, Gibson et al., 1996). High calcium levels trigger phospholipase C (PLC) and PKC pathways by increasing inositol 1,4,5-triphosphate (IP<sub>3</sub>) and diacylglycerol (DAG) levels inside the cell (Karlsson et al., 2010). This in turns activates AP-1 and certain differentiation markers which is the genomic regulation pathway (Matsui et al., 1992, Elsholz et al., 2014).

### **1.10.2. Phorbol esters.**

Phorbol esters, such as phorbol 12-myristate 13-acetate (PMA, also referred to as TPA), are well-known skin tumour promoters along with being potent inducers of keratinocyte differentiation. They act as a DAG analogue and directly activate the PKC/AP-1 pathway. Phorbol esters are known not only to induce differentiation, they also inhibit cell proliferation, elevate intracellular Ca<sup>2+</sup> concentration and downregulate retinoid receptors in keratinocytes (Karlsson et al., 2010, Papp et al., 2003, Castagna et al., 1982b). While PMA treatment induces expression of late differentiation markers such as filaggrin and loricrin, it downregulates early differentiation markers, such as K1 and K10, both *in vitro* and *in vivo* (Papp et al., 2003, Bose et al., 2013, Lichti and Yuspa, 1988b, Dlugosz and Yuspa, 1993b).

### **1.10.3. Steroid hormones.**

Steroid hormones such as cortisol, oestrogen and the active form of vitamin D (1,25-dihydroxyvitamin D<sub>3</sub>) have a major effect on keratinocyte differentiation. Vitamin D is a calcium regulating hormone that activates epidermal terminal differentiation markers to stimulate the formation of the cornified skin layer (Bikle, 2012). Vitamin D<sub>3</sub> binds to its nuclear receptor VDR and directly promotes terminal differentiation, which is the most studied and well-known pathway. It could be that other indirect pathways are involved in vitamin D induced differentiation, such as PKC through activation of G protein coupled receptors pathways, that acts by inhibiting early differentiation marker expression in favour of late differentiation markers (Palazzo et al., 2017, Eckert et al., 1997). The effect of vitamin D<sub>3</sub> on differentiation is dependent on the calcium concentration and the cell density (Svendsen et al., 1997b).

### **1.10.4. Estrogen.**

Estrogen plays a major role in many age-related processes such as poor wound healing that requires proliferating keratinocytes. Estrogen replacement therapy (ERT) is known to reverse this process and allows better healing and epithelialisation. Estrogen binds to estrogen receptors (ERs), either ER- $\alpha$  or ER- $\beta$ , which are nuclear receptors that bind to DNA and have the ability to either repress or induce the target genes. In keratinocytes, oestrogen binds to ER- $\beta$  more than ER- $\alpha$  receptor. Cells stimulated with the ER- $\alpha$  agonist had similar expression of different keratins while cells treated with ER- $\beta$  agonist show lower expression of differentiation specific keratins. The expression of keratin K10 is downregulated or not expressed at all after oestrogen treatment (Sheng et al., 2008, Perzelova et al., 2016). Other genes that are not involved in the terminal

differentiation process such as *KRT19* are shown to be induced by estrogen treatment. K19 is one of the keratins believed to be important in wound healing (Choi et al., 2000).

### **1.10.5. Retinoids/Retinoic acid (RA).**

Retinoids (RA), are a group of vitamin A derivatives that play a key role in regulating cellular growth, differentiation and apoptosis *in vivo* and *in vitro*. One of the main targets of RA is the epidermal layer of skin. The mechanism of action and signalling pathways of RA were studied after the discovery of its receptors. RA receptors are ligand-activated nuclear hormone receptors and these receptors are categorised into 2 families, the retinoic acid receptors (RAR), and retinoid X receptors (RXR). Each family has different forms and multiple isotypes. In the epidermis, the major forms expressed are RXR $\alpha$ , RAR $\gamma$  and RAR $\alpha$  so the predominant heterodimer will be RAR $\gamma$ /RXR $\alpha$ . These receptors are mainly expressed in the differentiated layers of the epidermis suggesting they function mainly in keratinocyte terminal differentiation. Recent studies on RARs also indicate their role in lamellar body formation needed by differentiating keratinocytes, this suggests that any abnormality in retinoid signalling could result in an abnormal keratinocyte phenotype. It has been shown that calcium and PMA induced differentiation also play a role in the retinoid signalling (Karlsson et al., 2010). Members of the retinoid receptor subfamily can form both homo- and heterodimers, which means that two different receptors can cooperatively bind to the recognition element on the DNA (Fisher et al., 1995). These dimers bind to a specific sequence on the DNA called retinoic acid response elements (RAREs) that affect and regulate the target genes. The RA effect could be direct by binding to specific genes or indirect by modulating the effect of other transcription factors,

such as AP-1, that could affect these genes (Lee et al., 2010, Benkoussa et al., 2002, Schule et al., 1991). One of the well-studied effects of RA on epidermis is the inhibition of keratinocyte early and late stage differentiation markers. Transglutaminase I enzyme (TGMI), which is responsible for the assembly of the cornified envelope in skin, is suppressed after RA treatment as well as other terminal differentiation markers such as filaggrin and loricrin. The expression of the keratin family of genes is also regulated by RA where some genes are suppressed (*KRT1* and *KRT10*) whereas others are induced (*KRT15* and *KRT19*) (Lee et al., 2010). The mode of action of Vitamin A on keratinocytes is shown in Figure 1.9.

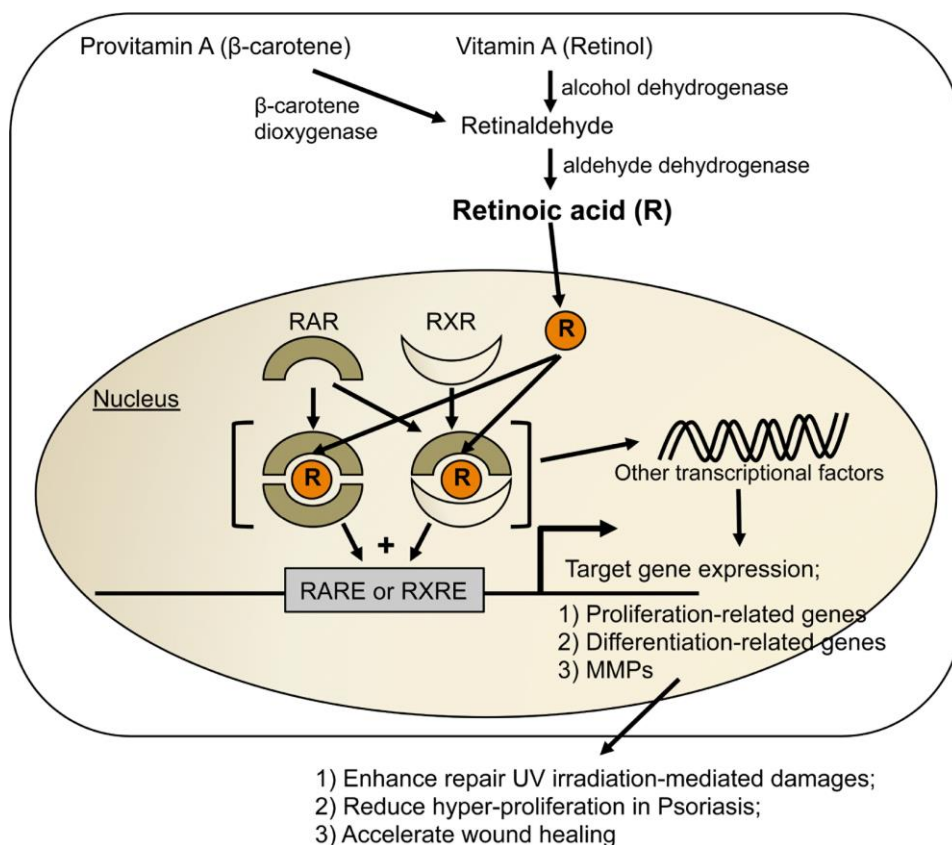


**Figure 1.9. Mode of action of vitamin A on keratinocytes.** (Park, 2015).

### **1.10.6.High Cell Density.**

High cellular density especially more than 95% confluency has also been shown to induce the expression of both early (K1, K10) and late (filaggrin, loricrin, SPRR-1) differentiation markers in keratinocytes *in vitro* even at low calcium concentrations (Poumay and Pittelkow, 1995). Cell density-mediated induction of differentiation markers has been associated with PKC activation. Recent studies have shown other factors to be involved in response to increased cell-cell contact, such as downregulation of c-Myc which is involved in cell-cycle progression as well as upregulation of Notch1 that regulates interactions between physically adjacent cells (Poumay and Pittelkow, 1995, Lee et al., 1998a, Kolly et al., 2005a, Newton, 2010a).

### **1.11. Keratin disorders.**

Keratin-associated diseases guided researchers to the importance and different functions of keratins in humans. Keratin disorders are mainly dominant negative mutations in which a mutated gene product antagonises the effect of the wild-type allele. They are rare conditions affecting the skin and some internal organs such as the liver (Strnad et al., 2008), eye lens (Haines and Lane, 2012) and intestine (Owens and Lane, 2004). Any tissue could be affected but for skin blistering disorders mutations in K5/K14 and K1/K10 are the most common. Mutations in the basal keratins K5/K14 are associated with a skin blistering condition called EBS shown in Figure 1.10 (Haines and Lane, 2012). The severity of this condition depends on the site of mutation in the polypeptide, more severe forms are associated with mutations affecting the helix initiation peptide (HIP) and helix termination peptide (HTP) of rod domain while mutations elsewhere produce



milder and more localised lesions limited to sites where mechanical stresses are applied such as palms and soles (Letai et al., 1993, Homberg et al., 2015). Epithelial cells in the basal layer are proliferative, they differentiate as they grow upward and keratin expression changes as the cells differentiate. K5/K14 are mainly in the basal layers and mutations in them lead to EBS in which blisters are formed at the basal layer (Bolling et al., 2011, Jerabkova et al., 2010). K1/K10 are found in the suprabasal layers and mutations in them cause EHK disease (Rothnagel et al., 1993). In this condition the suprabasal cells rupture and cytokines are released around the normal basal cell layer that will start to hyperproliferate causing the skin to become thick and fragile. This thick and spongy epidermis is highly susceptible to bacterial and fungal infection as well as being disfiguring and devastating for the patient (Arin, 2009, McLean and Moore, 2011). Mutation in K2, which is a late terminal differentiation keratin, leads to a skin blistering condition named IBS. It is less common than EHK and it lacks the erythroderma shown in EHK but it shows skin pigmentation in flexor areas (Moll et al., 2008, Ang-Tiu and Nicolas, 2012).

In simple epithelial keratins found in liver, pancreas and gut, K8/K18 plays a major role as stress absorbing proteins. Mutations in *KRT8* or *KRT18* lead to apoptosis and severe liver diseases in which keratins are absent or unable to perform their functions. Inflammatory bowel diseases are another example of mutated keratin disorder in the gut in which the protective barrier is lost and epithelial permeability increases resulting in inflammation. This is usually due to *KRT8* mutation as any role for K18 has not yet been shown (Arin, 2009). A list of human keratins disorders is shown in Table 1.3.

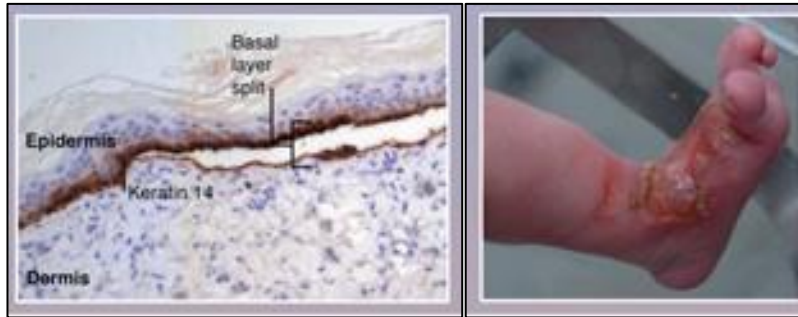


**Figure 1.10. Epidermolysis Bullosa Simplex.** In EBS, keratinocytes in the basal epithelial layer are split and separated from dermis causing blisters. (Haines and Lane, 2012).

**Table 1.3. List of human keratins disorders. (Haines and Lane, 2012).**

Keratin	Associated disease	Clinical manifestation	
<b>Type I</b>	<b>Type II</b>		
K10	K1	Bullous congenital ichthyosiform erythroderma (BCIE), epidermolytic hyperkeratosis (EHK)	Blistering in infancy; epidermolytic hyperkeratosis
K9 K10	K1	Epidermolytic palmoplantar keratoderma (EPPK)	Thickening of the upper layers of the skin on the palms and soles
	K2	Ichthyosis bullosa of Siemens (IBS)	Superficial blistering and mild epidermolytic hyperkeratosis
K14	K5	Epidermolysis bullosa simplex (EBS)	Skin blistering (splitting of the basal layer)
K14		Dermatopathia pigmentosa reticularis (DPR)	Reticulate hyperpigmentation
	K5	Dowling–Degos Disease (DDD)	Reticulate hyperpigmentation
K16 K17	K6a K6b	Pachyonychia congenita (PC)	Painful focal keratoderma on feet, thickening of the nails
K12	K3	Meesman corneal dystrophy (MCD)	Small epithelial cysts in the cornea
K13	K4	White sponge naevus	White plaques and patches of loose skin in the mouth
K18	K8	Liver disease, inflammatory bowel disease	Mutations are risk factors in various diseases
K81, K83, K86	K74	Monilethrix	Alopecia; altered structure of hair (beaded)

The maturation of the oral mucosa is slightly different than skin as the oral epithelium shows two patterns of maturation depending on the site and function in the oral cavity. Epithelium in the oral cavity could be either keratinised or non-keratinised, with maturation of the latter involving the formation of a surface layer of keratins (Figure 1.11). If the surface layer retains nuclei it will be para-keratinised but if the nuclei are absent it will be classified as an ortho-keratinised epithelium. The masticatory mucosa (including hard palate and gingiva) is

keratinised with epithelium firmly attached to the underlying tissues while the lining mucosa (including soft palate, lips, buccal and alveolar mucosa, ventral surface of the tongue and the floor of the mouth) is normally non-keratinised and supported by elastic connective tissues. The dorsum of the tongue is made of specialised mucosa, which is a combination of both keratinised and non-keratinised epithelia. Generally, lining mucosa cover 60%, masticatory mucosa 25% and the specialised mucosa 15% of the surface of the oral cavity (Collins and Dawes, 1987). Furthermore, the oral epithelium differs from the skin epithelium by its greater thickness, moist surface and relative lack of appendages (except salivary and, occasionally, sebaceous glands) (Presland and Dale, 2000, Squier and Kremer, 2001).

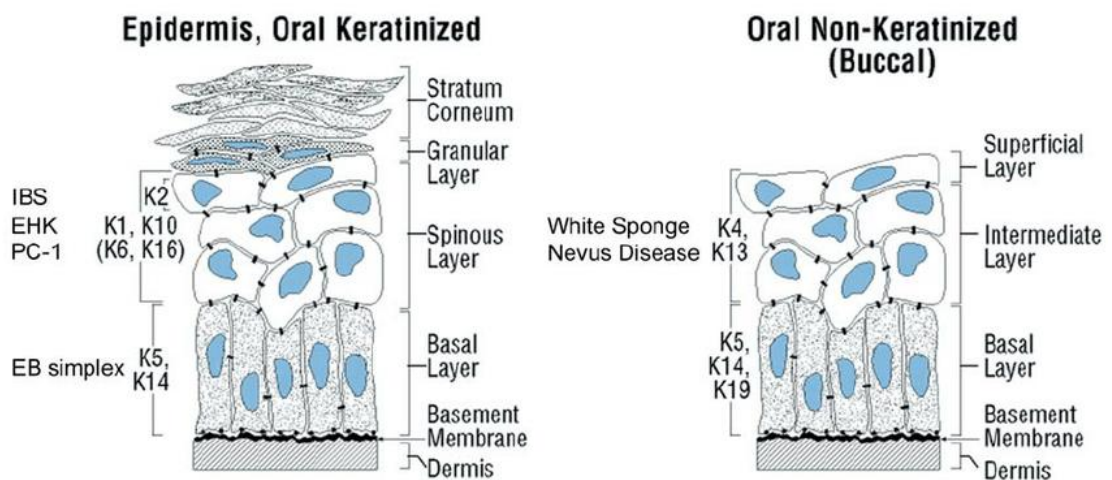


**Figure 1.11. Keratin expression in different layers of skin and oral mucosa.** (Presland and Jurevic, 2002).

Besides the well-known genetic keratin disorders, some keratin disorders could be acquired in which abnormal keratinisation takes place. Several genetic conditions in the oral cavity could be due to mutation or abnormalities in keratin filament associated proteins (KFAP) such as desmosomes. Pemphigus and

dyskeratosis congenita are two examples of these conditions. Acquired oral keratin disorders could be due to a variety of factors as infections, immune mediated lesions, neoplastic and reactive lesions like nicotine stomatitis for example. Figure 1.12 shows the classification of oral keratin disorders.

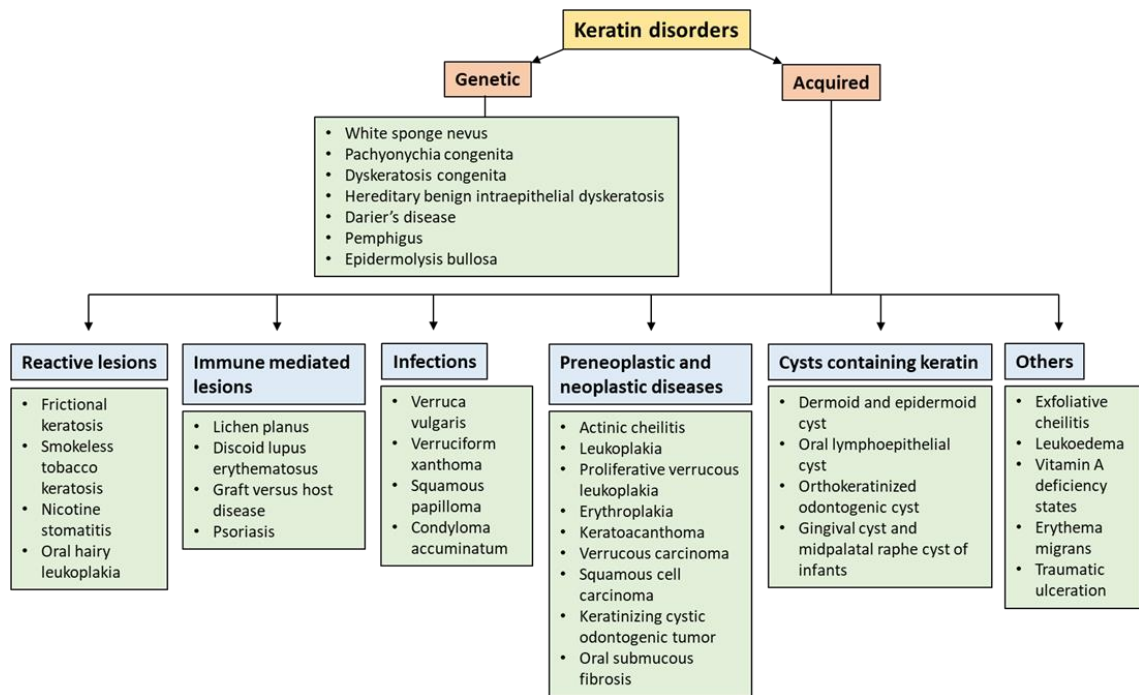


**Figure 1.12. Classification of oral keratin disorders.** (Rao et al., 2014).

## 1.12. Keratins in cancer.

Due to their tissue- and differentiation-specific expression patterns, keratins serve as excellent diagnostic markers in neoplastic as well as non-neoplastic diseases. In cancers, keratins were used as diagnostic markers, but recent studies have shown that keratin expression can also be used for prognostic purposes (Trask et al., 1990) (Harbaum et al., 2012). Keratin expression is maintained in tumor epithelial cells and this property makes it easier to identify the tumor site of origin. Knowing the origin of cancer can help to classify and later

modulate the line of treatment and this could also affect the prognosis of the case. For example, in adenocarcinoma (epithelial cancer of glandular tissues) there is expression of K8/K18/K19 while K7 and K20 expression varies. In colorectal carcinoma, K7 and K20 are expressed but their reduction is associated with highly invasive forms as it indicates EMT and metastatic spread (Karantza, 2011b, Wauters et al., 1995). Soluble keratin polypeptides circulating in the blood and bone marrow can be used to evaluate cancer progression and response to treatment. Elevated levels of K18 gives an indication of a good prognosis with less invasiveness and low metastatic potential, while reduced levels of K8/K20 in colorectal cancer indicates a poor prognosis (Magin et al., 2007, Arin, 2009). Keratin 19 and 17 are used as a diagnostic and prognostic marker in oral squamous cell carcinoma, K17 expression correlates with lymph node metastasis in which 6-fold increase in lymph node metastasis is shown when K17 is expressed. A high survival rate was shown when both keratins are downregulated (Coelho et al., 2015).

Many studies have shown the role of keratins in cell invasion and migration that contributes to tumor metastasis in distant organs. Phosphorylation of certain keratin residues leads to disassembly of keratin filaments into globules that affects the cell rigidity as well as its binding to cell anchorage proteins. These changes allow the cell to move much more freely and metastasise away from the site of origin. This mechanism is regulated by the activation of cancer promoting and EMT pathways (Karantza, 2011b, Yamaguchi et al., 2005, Kim et al., 2015a). Keratins have a protective role in epithelium that allows the cell to withstand different forms of stresses that could lead to cell death. Chemotherapy is used to kill cancer cells, which could be through activating death inducing signaling and Fas- mediated apoptosis. Cells lacking keratin expression are more sensitive to

chemotherapeutic drugs (Karantza, 2011b). In well-differentiated oral squamous cell carcinomas (OSCCs) the expression of K1/10, and K4/13 is increased. On the other hand, poorly differentiated OSCCs do not show any significant expression of these keratins but do express keratin K19. Moderate to poorly differentiated cancers that shows intermediate histology could express K8/18 and sometimes K5 and K6 which indicates a highly metastatic tumor with a low survival rate. Keratin K14 can be used to distinguish squamous cell carcinomas from mucoepidermoid carcinoma as it shows an extremely strong expression only in the former condition. In areas of metaplasia shown in both carcinomas, keratin K10 is used to distinguish between them as it shows positive staining in squamous cell carcinoma but not mucoepidermoid carcinoma. To differentiate mucoepidermoid carcinoma from other salivary gland tumors, keratin 13 expression is considered useful. K19 expression reflects differentiation and can assist in predicting the clinical outcome (Shetty and Gokul, 2012).

### **1.13. Keratinocyte differentiation and cancer (Differentiation Therapy).**

Even though significant progress has been made in the field of cancer diagnosis and therapy, cancer remains a major medical problem. Existing therapies for cancer lack ideal outcomes, mostly explained by the fact that cancer involves different genetic alterations as well as being distinct from one site of the body to another. These genetic alterations result in the loss of proliferative control of cells which is one of the defining features of cancer. The most commonly and widely used treatment options for most cancers are surgery, radiotherapy and chemotherapy and these options depends on the lesion type, site and extension.

Non-surgical treatment modalities are mainly acted by damaging cellular DNA which is a non-specific and a highly toxic mode of action. In order to reduce therapeutic complications, new treatment modalities have been introduced as adjuncts to conventional chemotherapy or radiotherapy such as differentiation therapy and angiogenesis inhibition as well as immunotherapy (Leszczyniecka et al., 2001). Cells with poorer differentiation ability are able to stimulate tissue renewal by cellular proliferation, which is of huge importance in reducing the rate of tumour growth and expansion. p53 is a gene that codes for a protein which regulates the cell cycle and therefore functions as a tumour suppressor, it induces apoptosis and cell cycle arrest. It has been shown that p53 has the ability to induce terminal differentiation in keratinocytes with no effect on apoptosis (Guinea-Viniegra et al., 2012) . It could be promising to use FOS/AP-1 inhibition, and p53 activation with TACE/NOTCH1-activating therapies in differentiation of skin SCCs. Similar approaches have been used in studies to modulate differentiation in breast cancer stem cells, so this strategy may hold great promise for future cancer treatment modalities (Guinea-Viniegra et al., 2012).

#### **1.14. Aim and objectives of the study.**

1. The main aim is to study keratin dynamics and the role of lipids on keratinocyte differentiation and mRNA stability.
2. To test whether differentiation-specific keratins can integrate into the pre-existing keratin network and whether this integration is static or dynamic.
3. To develop an *in-vitro* model to study the dynamics of differentiation-specific keratin filaments.

4. To determine keratin filaments stability, which is affected in many keratin-associated disorders, by using phosphatase inhibitors.
5. To study the effect of heat shock on keratin filament reorganisation.
6. To investigate the role of serum lipids and phenol red (PR) in the growth medium on the expression of differentiation-specific keratins.
7. To determine the mRNA stability of differentiation-specific keratins under different experimental conditions.
8. To investigate the influence of retinoic acid (RA) on the expression of differentiation-specific keratin genes.
9. To measure the promotor activity of *KRT2* and *KRT1* in normal epidermal keratinocytes under different growth conditions.



# CHAPTER 2

## **2. Materials and Methods.**

### **2.1. Cell culture.**

#### **2.1.1. Cell Culture Media.**

**DMEM.** Dulbecco's Modified Eagle Medium was supplemented with 10% foetal calf serum (FCS) (v/v), 50 IU/ml penicillin and 50 µg/ml PS (Penicillin-Streptomycin mixture) with or without Phenol-Red.

**RM<sup>+</sup> Medium.** Rheinwald-Green Modified, also called FAD medium was designed for growing primary keratinocytes and human squamous cell carcinoma cell lines (Rheinwald and Green, 1975, Rheinwald and Green, 1977). It is a 3:1 (v/v) mixture of DMEM media and Ham's F12 supplemented with 10% FCS, 50 IU/ml penicillin, 50 µg/ml streptomycin, 5 µg/ml insulin, 5 µg/ml transferrin, 0.4 µg/ml hydrocortisone,  $10^{-10}$  M cholera enterotoxin,  $2 \times 10^{-11}$  M liothyronine,  $1.8 \times 10^{-4}$  M adenine and 10 ng/ml epidermal growth factor (EGF). In this study RM<sup>+</sup> medium was used to culture HaCaT, NHEK, N/TERT, NEB-1, and T103C.

**Live cell imaging medium.** The Live Cell Imaging Solution is optically clear, used to keep cells healthy for up to 4 hours during imaging and to provide clearer images. It is a sterile solution made of (140 mM NaCl, 2.5 mM KCl, 1.8 mM CaCl<sub>2</sub>, 1.0 mM MgCl<sub>2</sub>, 20 mM HEPES). It is buffered with HEPES at pH 7.4. Agents for cell treatments were added into the pre-warmed live cell imaging medium prior to recording (Ettinger and Wittmann, 2014).

#### **2.1.2. Cells used.**

**MCF-7** is a human breast epithelial cell line that expresses three distinct keratins: K8, K18 and K19 (Taylor-Papadimitriou et al., 1989, Mackinder et al., 2012) were used in this study, grown in DMEM containing 10% FCS and 1% PS.

**NHEK** (normal human epidermal keratinocytes) were kindly provided by Professor Eric Parkinson of QMUL. They were bought commercially (Gibco, UK) and originated from expansion of keratinocytes derived from a pool of a minimum of three neonatal foreskins. Normal keratinocytes were cultured in a RM<sup>+</sup>/feeder system. In the RM<sup>+</sup>/feeder system keratinocytes were co-cultivated with 3T3 fibroblasts irradiated with the sub-lethal dosage of gamma radiation (60 Gy), cells were grown in RM<sup>+</sup> medium containing Hyclone II serum (Okazaki et al., 2003, Erdmann et al., 2017, Huang et al., 2006). This culture method supports differentiated phenotype of keratinocytes, essentially mimicking the *in vivo* features, and was first developed by Rheinwald and co-workers (Rheinwald and Green, 1977).

**HaCaT** is a keratinocyte cell line derived from histologically normal human adult skin keratinocytes spontaneously transformed by prolonged cultivation at low Ca<sup>2+</sup> concentration (0.2 mM) and moderately high temperature (38.5°C). Despite multiple chromosomal alterations, HaCaT cell line maintains a non-tumorigenic and non-invasive phenotype. HaCaT keratinocytes exhibit normal keratinocyte morphology and differentiation profile with regular distribution of differentiation-specific markers (Wilson, 2014, Deyrieux and Wilson, 2007, Fusenig and Boukamp, 1998).

**N/TERT** are human epidermal keratinocytes immortalised by ectopic expression of the telomerase catalytic subunit (hTERT) and subsequent spontaneous events leading to the loss of p16<sup>INK4a</sup> expression. N/TERT keratinocytes retain normal growth control mechanisms and have been shown to be able to initiate the program of terminal differentiation and to form a differentiated epithelium both in organotypic culture and xenografts in mice (Smits et al., 2017, van Drongelen et al., 2014).

**NEB-1** are derived from an unaffected relative of a patient suffering from the recessive form of EBS (Morley et al., 2003). This cell line was immortalised using a construct expressing HPV16 genome (lacking only the late genes) and was drug-selected with G418 (Morley et al., 2003, D'Alessandro et al., 2011). In this study, NEB-1 cells were grown without the 3T3 fibroblast feeder.

**T103C** derived from primary keratinocytes from biopsies of normal buccal and gingival tissues and were immortalised by HPV16 (Sexton et al., 1993, Bryan et al., 1995).

**Cell line used for retroviral packaging.** Phoenix A (amphotropic) is a retrovirus packaging cell line based on the 293T cells (human embryonic kidney cells expressing SV40 Large T antigen). Phoenix A cells are capable of producing gag-pol and envelope proteins for retroviruses and the resulting amphotropic retroviruses can infect most mammalian cells, including human cells (Swift et al., 2001, Lamers et al., 2006).

**Normal dermal fibroblasts** were kindly provided by Dr. Amir Sharili of QMUL and were used for organotypic co-cultures with keratinocytes.

**3T3 fibroblasts** were kindly provided by Professor Eric Parkinson of QMUL to be used as feeders for co-culturing normal skin keratinocytes. Cells were grown in DMEM with 10% donor bovine serum containing 50 IU/ml penicillin and 50 µg/ml streptomycin. These cells were irradiated to be used as feeder cells for growth and expansion of NHEK. These cells were grown to confluence before being irradiated using 60 Gy of γ radiation to stop their proliferation irreversibly (QMUL radiation facility). Irradiated cells were stored in liquid nitrogen and thawed when needed.

### **2.1.3. Culturing cells.**

All cells were routinely maintained at 37°C in a humidified atmosphere of 5% CO<sub>2</sub> + 95% air and grown in 10-cm dishes or T25, T75 and T175 flasks (as required) in the appropriate growth medium. Material and equipment used in cell culture are shown in Table 2.1.

#### **2.1.3.1. Cell passaging.**

Both normal keratinocytes and keratinocyte cell lines were routinely passaged upon reaching approximately 70 - 80% confluence to prevent them from undergoing density-dependant differentiation (Drozdoff and Pledger, 1993, Poumay and Pittelkow, 1995, Darlington, 2008, Masters and Stacey, 2007). For normal keratinocytes, KEB-11 and NEB-1 cell lines cultured in RM<sup>+</sup>/feeder system, the cells were first incubated with 0.02% (w/v) EDTA in phosphate buffered saline (PBS) and followed by vigorous pipetting of the liquid against the dish surface in order to remove the feeder fibroblasts. All keratinocyte cell lines were incubated for 5 min at 37°C with 0.02% (w/v) EDTA/PBS (to weaken cell adhesion), followed by incubation at 37°C with 0.05% (w/v) trypsin/0.01% (w/v) EDTA/PBS until the cells completely detached from the surface of culturing vessels. The trypsin was neutralised by the addition of serum-containing medium and the cell suspension was pelleted by centrifugation at 800 rpm. The supernatant was aspirated, and the cell pellet was re-suspended in fresh medium. Cells were counted using the haemocytometer and plated out for new experiments, transferred into new flasks for propagation or cryopreserved for later use. Fibroblasts and all other cell lines were passaged in a similar way as described above. However, the incubation with 0.02% (w/v) EDTA/PBS was omitted, commercial trypsin-versene mix was used instead of 0.05% (w/v)

trypsin/0.01% (w/v) EDTA/PBS and centrifugation after inactivating the trypsin was carried out at a higher speed (1000 rpm).

### **2.1.3.2. Use of Rho-associated kinase inhibitor (ROCKi).**

Prior to experimental use, NHEK maintained in the RM<sup>+</sup>/feeder system were routinely propagated in the presence of 10 µM of Y-27632, a Rho-associated kinase inhibitor (ROCKi). The addition of 5 – 10 µM ROCKi to keratinocyte culture medium, in presence of the feeder layer, has been shown to extend indefinitely but reversibly their lifespan and prevent the early onset of differentiation that limits their experimental use. This phenomenon has been described as a reversible reprogramming/immortalisation of keratinocytes that neither affects their phenotype and karyotype nor induces tumorigenicity (Chapman et al., 2010, Liu et al., 2012).

**Table 2.1. Material and equipment used in cell culture.**

<b>Cell culture reagents/equipment</b>	<b>Catalogue #</b>	<b>Supplier</b>
Adenine hemisulfate salt	A3159-25G	Sigma-Aldrich, UK
Donor bovine serum (DBS)	16030074	ThermoFisher Scientific, UK
Dulbecco's Modified Eagle's Medium 4.5g/L Glucose, w/ L-Glutamine (DMEM)	LZBE12-604F	UK supplier: SLS Ltd
	BE12-604F	Lonza, Belgium
Dulbecco's Modified Eagle's Medium 4.5g/L Glucose, w/o phenol red, w/o L-Glutamine (phenol red-free DMEM)	31053-028	Life Technologies, UK
Dimethyl sulfoxide (DMSO)	D1435	Sigma-Aldrich, UK
Epidermal growth factor (EGF)	E9644-.5MG	Sigma-Aldrich, UK
Ethylenediaminetetraaceticacid, tetrasodium salt (EDTA)	ED4SS	Sigma-Aldrich, UK
Foetal Calf Serum (FCS)	02-00-850	First Link Ltd., UK
	SH30066.03	GE Healthcare, US

HyClone™ FetalClone™ II Serum (FCII serum)		UK supplier: SLS Ltd
Ham's F-12 Medium w/L-Glutamine	BE12-615F	Lonza, Belgium
	LZBE12-615F	UK supplier: SLS Ltd
Insulin from bovine pancreas	I5500-500MG	Sigma-Aldrich, UK
Ham's F-12 Medium w/L-Glutamine without Phenol red	HFL05-500ML	Caissson Labs, USA
L-Glutamine 200 mM (100x)	25030-081	Life Technologies, UK
Penicillin-Streptomycin (Pen Strep)	15070-063	Life Technologies, UK
Phosphate Buffered Saline (Dulbecco A) (PBS)	BR0014G	Oxoid, UK
Holo-Transferrin bovine	T1283-100MG	Sigma-Aldrich, UK
Trypsin	TRL	Worthington, US
	LS003702	
Trypsin-EDTA mix (1x)	LS003703	UK supplier: Lorne Laboratories Ltd
	BE17-161E	Lonza, Belgium
Y-27632 (ROCKi)	LZBE17-161E	UK supplier: SLS Ltd
	SCM075	EMD Millipore, UK
Mitomycin C	M0503	Sigma-Aldrich, UK
Cryotubes 1.8 ml	368632	Thermo Scientific, UK
Haemocytometer Neubauer-improved	0630010	Marienfeld-Superior, DE
Heraeus™ Multifuge™ X 3R centrifuge	75004515	Thermo Scientific, UK
Phase-Contrast Microscope		Hund Wetzlar Wilovert
Mr. Frosty™ Freezing Container	5100-0001	Thermo Scientific, UK

## **2.2.Cell treatments.**

### **2.2.1. Phosphatase inhibitors.**

OA and CL-A are well known selective phosphatase inhibitors especially for serine-threonine PP1 and PP2A with CL-A being more potent on PP2A than OA (Dounay and Forsyth, 2002, Takuma et al., 1993). OA and CL-A were dissolved in DMF (N, N-Dimethylformamide) at stock concentrations of 604  $\mu$ M and 99.1  $\mu$ M, for OA and CL-A respectively, and stored at -20°C. Cells were grown in full medium (DMEM supplemented with 10% FCS and 1% PS) prior to any treatment, cells were counted and seeded in 12-well, 6-well or 35 mm cell culture dishes based on the planned experiment. After 24 h, the medium was removed and replaced with fresh medium containing the desired working concentration of each drug. The same volume of DMF was used for all experiments as vehicle control. After drug treatment, medium containing the drug was removed and cells were either fixed, lysed or live imaged in live cell imaging medium.

### **2.2.2. Heat shock treatment.**

To perform heat shock stress experiments on epithelial cells, the MCF-7 cell line was used. Cells were seeded on coverslips at a density of 10,000 cells/coverslip for immunostaining or 50,000 cells/35 mm glass bottom dishes for live cell imaging and 500,000/35 mm dishes used for collecting lysates for western blotting. The cells were cultured in full medium (DMEM supplemented with 10% FCS and 1% PS) in an atmosphere of 5% CO<sub>2</sub> + 95% air overnight, next day the cells were exposed to 43°C for 30 min over a metal rack in a pre-adjusted water bath. Prior to placing the plates in the water bath, the medium was changed with a 43°C preheated medium and the culture plates were sealed using a parafilm all around the edges and placed inside the water bath. After applying heat shock,



the dishes were removed from the water bath covered with a tin foil and placed in a 37°C incubator for recovery. The time for recovery varied from 15 min to 6 h or more. For live cell imaging experiments, the medium was replaced after recovery with the Live Cell Imaging Medium pre-warmed to 37°C containing the drug of interest (OA or CL-A) and the dishes were placed immediately on the imaging stage set at 37°C, cells with well spread keratin filaments (no granules) were selected for imaging. Three confocal z planes were chosen, videos were recorded for 3 h, and frames were taken every 30 sec for both bright field and fluorescence for AcGFP (fluorescence tag attached to K2 to make it visible under confocal microscope) (Strnad et al., 2003). For immunostaining experiments requiring heat shock, the same procedure was followed but after recovery periods the cells were fixed either immediately or after a certain time of incubation with a drug. For western blotting experiments, the same procedure was followed but after applying a drug or after a certain recovery time, cell lysates were collected and stored at -80°C until all lysates of the same experiment were collected to be processed at the same time.

### **2.2.3. Use of charcoal stripped FCS.**

It has been known for years that retinoids play an important role in cell proliferation and differentiation. RA bind to RA receptors which are transcriptional factors that could affect the gene expression of differentiation-specific keratins (Balmer and Blomhoff, 2002).

To remove serum lipid, charcoal-treated stripping of FCS was used in this study, different keratinocytes cell lines were used and compared to normal keratinocytes (Cao et al., 2009). Cells were grown in their normal culturing media containing normal FCS either in DMEM or RM<sup>+</sup>. On day of experiment, cells are trypsinised, counted and seeded in 6-well plates at a density of 200,000 cell/well

using regular FCS medium. Next day when cells are fully attached, the medium was changed to charcoal stripped FCS containing medium hereafter referred as SLP- (serum lipids free medium). Normal FCS containing medium were used on controls referred as SLP+ (serum lipids containing medium). After 72 h, the medium was removed, and the cells were lysed for mRNA extraction or WB assay. In some experiments, cells were seeded in 12- well plates using RM+ (Hyclone II serum) until attached then medium changed to SLP- and next day treatment was done.

#### **2.2.4. Use of phenol-red free medium.**

Phenol-red is used in most of tissue culture media as a pH indicator. It is known to have an estrogenic-like effect and could bind to estrogenic receptors which are transcriptional factors and affect some cellular functions and regulate genes expression (Hofland et al., 1987, Welshons et al., 1988, Glover et al., 1988). In this study, phenol-red free medium was used to grow different keratinocytes, the culture method is the same as mentioned earlier (section 2.2.3). In this set of experiments phenol-red containing medium was used as a control. Phenol-red containing and phenol-red free medium were used either with or without the charcoal stripped FCS.

#### **2.2.5. All-*trans*-Retinoic acid.**

NHEK cells were seeded in a 12 well plate, next day cells were treated with different concentrations of all-*trans*-Retinoic acid (ATRA) for 24 hours in charcoal treated RM+ medium with and without PR. ATRA was first dissolved in DMSO and diluted using ethanol, 1 $\mu$ M, 2 $\mu$ M, 3 $\mu$ M working concentrations were used in first experiment and only 1 $\mu$ M were used in later ones as 3 concentrations didn't

show any significant difference in their effect. DMSO/EtOH was used as a vehicle control (0.003%/0.03% v/v maximum).

### **2.2.6. $\beta$ - Estradiol.**

NHEK cells were seeded in 12 well plate, next day cells were treated with different concentrations of  $\beta$ - Estradiol (ED) for 24 hours in PR free RM+ medium. ED was dissolved in DMSO (stock concentration 100mM) and further diluted in culture medium to working concentrations of 10nM, 50nM, 100nM, 500nM, 1 $\mu$ M. DMSO was used as a vehicle control (0.001%).

### **2.2.7. Phenol Red.**

Phenol red (PR) was added in phenol free RM+ culture medium at concentration similar to PR concentration in commercially available normal culture medium (0.01 mg/ml). NHEK were cultured in this medium for 3 days either with or without adding 1 $\mu$ M of ATRA in the last 24h before collecting cell lysates for qPCR. For ATRA treated cells, DMSO/EtOH were used as a vehicle control (0.001%/0.01%), for PR added cells, PR free medium were used to grow cells as a control.

### **2.2.8. Actinomycin D.**

Actinomycin D (AD) was dissolved in water. NHEK with irradiated feeder fibroblasts were seeded in 12 well plates and treated next day with 2 $\mu$ g/ml AD for different time points up to 4 hours with or without prior treatment with 1 $\mu$ M ATRA for 24 hours, DMSO was used as a vehicle control (0.01%).

Reagents and equipment used in cell treatments are shown in Table 2.2.

**Table 2.2. Reagents and equipment used in cell treatments.**

Cell culture reagents/equipment	Catalogue #	Supplier
Okadaic acid (sodium salt)	19-130	Sigma-Aldrich, UK
Calyculin A	C-3987	LC Laboratories, USA
DMF (N, N-Dimethylformamide)	D4551	Sigma -Aldrich, UK
Foetal Bovine Serum, charcoal stripped	12676029	Thermo Scientific, UK
all- <i>trans</i> -Retinoic acid (ATRA)	R2625	Sigma-Aldrich, UK
$\beta$ -Estradiol	E8875	Sigma-Aldrich, UK
Phenol red	P3532	Sigma-Aldrich, UK
Actinomycin D	11805-017	Gibco, UK

### 2.3. Organotypic cultures.

Organotypic cultures (OTs) or 3D cultures are a method of culturing epithelial cells in a skin equivalent model in which cells grow in a multilayer system (stratification) allowing a much better *in vitro* tissue model. These keratinocytes grow at an air-liquid interface in which they get their nutrients from the medium underneath the collagen-fibroblast stroma only while facing air from the top (Oh et al., 2013). Structural support was provided by a simple collagen/fibroblast stroma. Fibroblasts are used to produce extracellular matrix that allow normal tissue organisation and keratinocyte differentiation (Okazaki et al., 2003). As we are looking at terminal differentiation keratins, 3D models will be an ideal model to study the effect of different factors diffused through the collagen stroma reaching keratinocytes in a way similar to the *in vivo* situation (Margulis et al., 2005). Cells used in OT cultures were cultured in their appropriate media prior to setting up the 3D model system. An insert-based method of OTs was used in this study in which inserts (pore size 0.4  $\mu\text{m}$ ) were placed in 12-well plates. Collagen solution was prepared on ice 4 mg/ml in full DMEM either with or without phenol-

red. 0.5 N NaOH was used to neutralise the solution. Primary dermal fibroblasts were trypsinised, counted and spun down. The fibroblast pellet containing the required number of 100,000 cells/insert was resuspended into the full DMEM with or without phenol-red. Re-suspended cells were added in collagen solution and mixed gently without creating bubbles. On each insert, 400 µl of collagen mix was added and plate was left in 37°C incubator for 1 h allowing collagen mix to solidify. In the meantime, keratinocytes were trypsinised, counted and a pellet containing the required number of keratinocytes (500,000 cells/insert) was re-suspended in RM+ medium (with or without phenol-red) and (with normal or charcoal stripped FCS), 300 µl/ insert. The cell suspension was slowly pipetted on top of each fibroblast-containing collagen matrix inserts. RM+ medium (2 ml) was then added underneath the inserts and the plate was returned to 37°C incubator. Next day, medium was aspirated from inside and outside of each insert and 1 ml of RM+ (with or without phenol-red) and (with normal or stripped FCS) was added underneath the inserts only. The cells were allowed to grow at an air-liquid interface for 10 days allowing stratification, the medium underneath the inserts was changed every day (Parenteau et al., 1992). Reagents and equipment used in organotypic cultures are shown in Table 2.3.

### **2.3.1. Paraffin embedding.**

OTs were harvested at day 10 and fixed in 4% (w/v) paraformaldehyde/PBS for 1 h at RT. After fixation, OTs were cut out of the inserts using a sharp blade and placed into a special cassette for paraffin processing. These cassettes were emerged in 70% ethanol until processing took place and tissues were embedded in paraffin blocks using the Tissue-Tek system available at the Centre for Cutaneous Research, QMUL. Later, paraffin blocks were cut into 5µm thick sections. Tissue sections were then stained with haematoxylin and eosin (H & E)

as described in the following section or processed for immunostaining using primary and fluorescent tagged secondary antibodies as described in section 2.4.2.2 (Canene-Adams, 2013).

### **2.3.2. Haematoxylin and Eosin (H & E) staining.**

Haematoxylin is a basic blue dye (hematein and aluminium ions) that stains basophilic cell structures, such as nucleic acids in the nucleus. On the other hand eosin is a pink acidic dye that stains acidophilic structures inside tissues such as proteins (Feldman and Wolfe, 2014). Before Haematoxylin staining, paraffin-embedded sections were first deparaffinised with xylene (paraffin solvent) by treating twice for 3 min each. These sections needed to be gradually rehydrated by immersing them into containers having decreasing strengths of ethanol (100%, 90%, and 70%), rinsed with distilled H<sub>2</sub>O and stained with haematoxylin for 3 – 5 min. Excess stain was washed off with running tap H<sub>2</sub>O and the slides were dipped 2 – 7 times in acid alcohol to differentiate nuclei and non-nuclear structures, acid alcohol was washed by immersion in running tap H<sub>2</sub>O for 5 min to oxidise the dye. The sections were then emerged in eosin to counterstain for 2 min, washed with running tap H<sub>2</sub>O. Tissues were dehydrated by emerging slides into increasing concentrations of ethanol (70%, 90% and 100%) and finally incubated with xylene. After the xylene clearing step that removes all wax residues, slides were mounted with DPX mounting medium and imaged using Leica Epi DM4000 microscope (equipped with a DFC350 digital camera and 20x/0.5 objective lenses) or using Nikon Eclipse 80i microscope (equipped with an MBF CX900 digital camera and 20x/0.75 objectives). The images were acquired by Metamorph (Leica Epi DM4000) or PictureFrame (Nikon Eclipse 80i) imaging systems using standard bright-field (BF) imaging settings and processed using the ImageJ software.

**Table 2.3. Reagents and equipment used in organotypic cultures.**

Reagents / equipment used	Catalogue #	Supplier/Company
Collagen type I, rat tail, high concentration (10.97 mg/ml)	354249	Corning, USA
		UK supplier: SLS Ltd
Paraformaldehyde GPR	294474L	(BDH) VWR, UK
Shandon™ Cryomatrix™ embedding resin	6769006	Thermo Scientific, UK
Sodium hydroxide	S8045	Sigma-Aldrich, UK
Antigen retrieval buffer 10X	S1699	DAKO, UK
Bright OTF5000 Cryostat		Jencons-PLS, USA
Leica Epi DM4000 Epi-fluorescence microscope		Leica Microsystems, UK
Leica RM2235 Rotary Mictotome		Leica Microsystems, UK
Millicell® Hanging Cell Culture Inserts	PIHT15R48	Merck Millipore, UK
Nikon Eclipse 80i microscope		Nikon, UK
S35 Feather microtome blades, stainless steel	207500000	pfm medical ag, Germany
SuperFrost® Plus Menzel-Gläser adhesion microscope slides	J1800AMNZ	Thermo Scientific, UK
Tissue embedding cassettes		Tespa
Tissue-Tek® TEC® Tissue Embedding Console System		Sakura
Tissue-Tek® VIP® Vacuum Infiltration Tissue Processor		Sakura

## 2.4. Protein analysis techniques.

### 2.4.1. Western blotting (WB).

#### 2.4.1.1. Protein extraction and quantification.

Cells were seeded in 6-well plates with the required media for each experiment. When cells became ready to be lysed, medium was removed, and cells were washed twice with cold PBS. Lysis buffer (4% (w/v) SDS, 20% (v/v) glycerol, 125 mM Tris-HCl, pH 6.8) was added (200 µl/well) on ice, cell lysates were then collected using cell scrapers into 1.5 ml Eppendorf. The lysates were either sonicated 5 seconds X 3, heated (95 – 100°C) for 5 min on a metal block to denature the proteins and spun at 15000 rpm for 10 min to remove cell debris and stored at -80°C for later use. For measuring the protein concentration in each

lysate, Lowry's assay was performed using DC Protein Assay Kit with a standard bovine serum albumin (BSA) dilution series (0 – 1.4 µg/µl). This assay is a colorimetric assay in which proteins react with an alkaline copper tartrate solution and Folin's reagent and this reaction results in a coloured compound whose absorbance is directly proportional to the amount of protein present in the cell lysate (Lowry et al., 1951, Hess et al., 1978). The BSA standards and protein lysates were mixed with protein assay reagents in a 96-well plate, incubated at RT for 15 min. By using a CLARIOstar microplate reader, the absorbance of standards and samples was measured in duplicate at 650 nm. The protein concentrations were then calculated from the BSA standard curve (BSA concentrations vs absorbance). After measuring the protein concentration, the reducing agent 2-mercaptoethanol that breaks disulphide bonds in proteins was added. A tracking dye bromophenol blue in ethanol 0.1% (w/v) were also added to the protein lysates.

#### ***2.4.1.2. Protein separation by SDS-PAGE, transfer on nitrocellulose and protein detection.***

Cell lysate samples with known protein concentrations were loaded into a pre-cast 4-12% (w/v) polyacrylamide NuPage® gels with the first well loaded with a dual-colour protein ladder. In all our WB experiments glyceraldehyde-3-phosphate dehydrogenase (GAPDH) was used as a loading control. By using a constant voltage of 80 V for the first 30 min and a 125 V for 90 min the proteins were separated electrophoretically on (SDS-PAGE) in a NuPage® MES SDS running buffer. Proteins separated on the gel were transferred electrophoretically onto nitrocellulose membranes at 30 V at RT for 90 min in a transfer apparatus filled with transfer buffer (25 mM Trizma base, 192 mM glycine and 20% (v/v) methanol). After proteins being transferred (checked by coloured molecular



weight ladder transfer), the membranes were blocked using (5% (w/v) skimmed dry milk in Tris buffered saline (TBS: 15 mM Trizma base, 137 mM NaCl, pH 7.5) containing 0.1% (v/v) Tween 20 (TBST) for 30 min at room temperature (RT) on a shaker. After blocking, the membranes were incubated with primary antibodies diluted in the blocking buffer overnight at 4°C on a roller mixer. Next day, the membranes were washed using TBST (3 x 5 min each) at RT on a shaker. Later, they were incubated with the peroxidase-conjugated secondary antibodies diluted in the blocking buffer for 1 h at RT on a roller mixer. After 3 TBST washes (5 min each) were performed on a shaker at RT, the membranes were ready for the protein detection step. ECL Prime Detection Reagent was used according to the manufacturers' instructions. The membranes were then imaged using ChemiDoc™ MP imager and Images were analysed using the ImageJ or Image Lab software. If re-probing was required, the membranes were incubated in a readymade concentrated stripping buffer for 20 min in a 37°C water bath, washed, blocked and the same WB procedure was followed. Reagents and equipment used in protein analysis (WB) are shown in Table 2.4. Primary and secondary antibodies used in WB are listed in Tables 2.5 and Table 2.6 respectively.

**Table 2.4. Reagents and equipment used in protein analysis (WB).**

Reagents/equipment	Catalogue #	Supplier/company
2-Mercaptoethanol	M3148	Sigma-Aldrich, UK
Amersham ECL Prime Western Blotting Detection Reagent	RPN2232	GE Healthcare, UK
Bromophenol blue sodium salt	B6131	Sigma-Aldrich, UK
DC™ Protein Assay Reagents package	500-0116	Bio-Rad, UK
Dried skimmed milk (99.5%)	UK FF 005M EC	Marvel, Premier International Foods, UK
Glycerol bidistilled 99.5% (w/v) AnalaR NORMAPUR	24388.260	VWR, UK
Glycine	G8790	Sigma-Aldrich, UK
Immobilon Western Chemiluminescent HRP Substrate	WBKLS0500	Merck Millipore, UK
Methanol NORMAPUR	20847.320	VWR, UK
NuPAGE® MES SDS running buffer (20X)	NP0002	Life Technologies, UK
PageRuler™ Prestained Protein Ladder, 10 to 180 kDa	26616	Thermo Fisher Scientific, UK
Precision Plus Protein™ Dual Color Standards	161-0394	Bio-Rad, UK
Protein Assay Standard II (bovine serum albumin)	500-0007	Bio-Rad, UK
Sodium chloride GPR Rectapur®	27800.360	VWR, UK
Sodium dodecyl sulfate (SDS)	161-0301	Bio-Rad, UK
SuperSignal™ West Femto Maximum Sensitivity Substrate	34094	Thermo Scientific, UK
Trizma® base	33742	Sigma-Aldrich, UK
Trizma® hydrochloride (Tris-HCl)	T3253	Sigma-Aldrich, UK
Tween® 20	P2287	Sigma-Aldrich, UK
Restore™ PLUS Western Blot Stripping Buffer	46430	Thermo Fisher Scientific, UK
ChemiDoc™ MP System	17001402	Bio-Rad, UK
Protein ladder	161-0374	Bio-Rad, UK
CLARIOstar Microplate Reader	430-0673	BMG LABTECH, UK
Nitrocellulose Membrane 0.45 µm pore size	N8392	Sigma-Aldrich, UK
NuPAGE™ 4-12% Bis-Tris Protein Gels, 1.5 mm, 15-well	NP0336BOX	Life Technologies, UK
NuPAGE™ 4-12% Bis-Tris Protein Gels, 1.5 mm, 10-well	NP0335BOX	Life Technologies, UK
NuPAGE™ 4-12% Bis-Tris Protein Gels, 1.0 mm, 12-well	NP0322BOX	
Cell scraper 25cm	734-2602	VWR, UK
PowerEase® 500 Power Supply	EI8700	Life Technologies, UK
QBT2 Block Heater		Grant
Roller Mixer SRT6		Stuart, UK
Sponge pads for Blotting	EI9052	Life Technologies, UK
XCell II™ Blot Module	EI9051	Life Technologies, UK
XCell SureLock® Mini-Cell	EI0001	Life Technologies, UK
Sonicator (SONIPREP 150)	71100-1129-06	MSE, UK

## **2.4.2. Immunofluorescence (IF) staining and live cell imaging.**

### **2.4.2.1. Immunocytochemistry (ICC).**

Cells required for ICC experiment were trypsinised, counted and 50,000 cells/coverslip seeded on top of collagen coated (10 µg/ml, 2h, 37°C) sterile round glass coverslips placed in 12-well plate. On the top of each coverslip 50-100 µl of cells were added and left in a 37°C incubator to attach. Once cells were fully attached, the coverslips are flooded with 1ml of culture medium and returned to 37°C incubator. Next day, the cells were either washed with PBS and fixed or treated with a certain drug added to a required media and incubated for certain time before washing and fixing. For fixation, 1:1 (v/v) acetone/methanol was used at RT for 10 min, coverslips were then left to air dry. Fixed cells attached to coverslips were either used for immunofluorescence (IF) straight away or left in PBS at 4°C for a few days or stored at -80°C for later use. Before incubating the coverslips with a primary antibody, the cells were blocked for 1 h at RT using (10% (v/v) normal goat serum (NGS) in washing buffer (0.1% Tween-20/PBS (v/v) to prevent non-specific binding of antibodies. For blocking, 20µl of the blocking buffer was placed as a drop on top of flat a surface covered with parafilm in which coverslips (cells facing up) were placed on top. After blocking, the cells were incubated in primary antibodies diluted in blocking buffer overnight at 4°C in a moisturised and covered metal tray. Next day, coverslips were washed (3 x 5 min each) with the washing buffer [0.1 % (v/v) Tween -20 in 1x PBS + few crystals of sodium azide] and incubated with suitable secondary antibodies diluted in the blocking buffer in the dark for 1 h at RT. All primary and secondary antibodies used in these experiments are listed in Tables 2.5 and 2.6, respectively. Following another wash with the washing buffer (2 x 5 minutes each), the cover slips were dipped in ddH<sub>2</sub>O and stained using 1 µM DAPI (4', 6-diamidino-2-phenylindole;

nuclear counterstain) in PBS for 15 min and finally mounted onto microscopic slides using a DAPI free mounting medium. On some occasion, a mounting medium with DAPI was used in which the separate DAPI staining step was omitted. Stained samples were imaged using either a Leica Epi DM5000 microscope or Leica Epi DM4000 equipped with a DFC350 FX digital camera under 20x/0.5 NA and/or 40x/0.75 NA objective lenses. The images were acquired by Metamorph imaging system and processed using the ImageJ software.

#### **2.4.2.2. Immunohistochemistry (IHC).**

Tissue sections (normal skin or OTs) bound to glass slides were first deparaffinised by treating with xylene twice for 5 min each. The sections were gradually rehydrated by emerging them into containers with decreasing strengths of ethanol (100%, 90%, and 70%), rinsed with distilled H<sub>2</sub>O and washed in PBS for 5 min. After washing, the antigen was retrieved by placing the slides in 1 X antigen retrieval buffer and boiling (95°C) for 30 min. Later, slides were left for another 30 min at RT to cool down and then washed using PBS for 10 min and later washing buffer [ 0.2% (v/v) TX-100/PBS] 2X 5 min each. The tissue sections on the slides were then encircled with a Liquid Blocker Pen and blocked using a blocking buffer [10% NGS/5% BSA/washing buffer (v/v/v)] for 1 h at RT. The tissue sections were then incubated with primary antibodies overnight at 4°C and the following day the slides were washed with the washing buffer or with PBS (3 x 5 min each) and then probed with the secondary antibodies in the dark for 1 h at RT. The primary and secondary antibodies were diluted in the blocking buffer as described for ICC (section 2.4.2.1). After washing traces of the secondary antibodies using washing buffer (3 x 5 min each), the tissue sections were quickly dipped in ddH<sub>2</sub>O, dried and stained for DAPI for 15 min at RT. Slides were then

mounted using a mounting medium, left to dry at RT for 2 h and stored at 4°C for later imaging.

#### ***2.4.2.3. Live cell imaging.***

Live cell imaging is a powerful technique allowing visualisation and tracking of intracellular tagged or stained proteins as well as monitoring their behaviour and dynamics over a chosen period of time (Ettinger and Wittmann, 2014). In this study AcGFP tagged keratin K2 was visualised in MCF-7 cells over a period of hours under different experimental conditions. Cells used for live imaging were counted and 500,000 cell/dish were seeded in glass bottomed 6-cm dishes. Next day or when cells reached between 50%-70% confluence, growth conditions for the cells were altered before imaging the cells. The medium was changed to pre-warmed clear live cell imaging medium with or without experimental treatment. Live cell imaging was carried out immediately on a confocal microscope (Nikon ECLIPSE TE2000-S) equipped with a spinning disk for recording rapid movement of particles within a live cell over a period of time. IQ Live Cell Imaging Software (Andor iQ3) was used for acquisition and visualisation. Image frames or snaps were recorded every 30 seconds and a minimum of 3 different z planes were taken for each image. Videos and montages were made using the Image J software.

Material used in immunofluorescence and live cell imaging shown in Table 2.7.

**Table 2.5. Primary antibodies used in WB, ICC and IHC.**

Antigen (clone)	Type	Host	Catalogue #, supplier	Dilution
K1	monoclonal	mouse	RCK103 Abcam, UK	IHC 1:100 WB 1:1000
K2	monoclonal	mouse	ab19122 Abcam, UK	ICC/IHC 1:20 WB 1:200-1:500
K10	monoclonal	rabbit	ab76318 Abcam, UK	IHC 1: WB 1:2000
K14 (LL001)	monoclonal	mouse	in-house	Not diluted
K15 (EPR1614Y)	monoclonal	rabbit	ab52816 Abcam, UK	IHC 1:100
K15 (LHK15)	monoclonal	mouse	in-house	IHC 1:100
K8/K18 (LE61)	monoclonal	mouse	in-house	ICC not diluted
K8/K18 (LE65)	monoclonal	mouse	in-house	ICC not diluted
K8/K18 (A4B/B3)	monoclonal	mouse	in-house	ICC not diluted
Cornifin	polyclonal	rabbit	ab123237 Abcam, UK	IHC 1:100
Loricrin	polyclonal	rabbit	ab85679 Abcam, UK	IHC 1:100
Involucrin	monoclonal	mouse	ab68 Abcam, UK	IHC 1:100
Hsp70 (5A5)	monoclonal	mouse	ab2787 Abcam, UK	WB1:1000
K8(M20)	monoclonal	mouse	ab9023 Abcam, UK	WB 1:1000
K8/p73	monoclonal	rabbit	ab32579 Abcam, UK	WB 1:4000
K8/p431	monoclonal	rabbit	ab59434, Abcam, UK	WB 1:4000
Filaggrin	polyclonal	rabbit	ab81468, Abcam, UK	IHC 1:100
Flag	monoclonal	mouse	F3165, Sigma Aldrich, UK	WB 1:2000 ICC 1:100
GAPDH	polyclonal	rabbit	ab9485, Abcam, UK	WB 1:4000

**Table 2.6. Secondary antibodies used in WB, IF and IHC.**

Antibody	Type	Host	Catalogue #, supplier	Dilution
anti-mouse IgG, peroxidase-conjugated	polyclonal	goat	AP124P, Millipore, UK	WB 1:600
anti-mouse IgG, peroxidase-conjugated	polyclonal	sheep	NA931V, Sigma Aldrich, UK	WB 1:5000
anti-rabbit IgG, peroxidase-conjugated	polyclonal	goat	AP132P, Millipore, UK	WB 1:6000
anti-mouse IgG (H+L), Alexa Fluor® 488-conjugate	polyclonal	goat	A-11029, Life Technologies, UK	ICC/IH C 1:100
anti-rabbit F(ab') <sub>2</sub> IgG (H+L), Alexa Fluor® 488-conjugate	polyclonal	goat	A-11070, Life Technologies, UK	ICC 1:100
anti-mouse IgG (H+L), Alexa Fluor® 633-conjugate	polyclonal	goat	A-21052, Life Technologies, UK	ICC 1:500
anti-mouse IgG (H+L), Alexa Fluor®569-conjugate	polyclonal	goat	A-11005, Life Technologies, UK	ICC 1:100

**Table 2.7. Material used in immunofluorescence and live cell imaging.**

<b>Reagents/ Equipment</b>	<b>Catalogue #</b>	<b>Supplier</b>
Acetone AnalaR NORMAPUR®	20066.330	VWR, UK
DAPI, dilactate	D9564	Sigma-Aldrich, UK
Normal goat serum (NGS)	ab7481	Abcam, UK
Collagen type I rat tail (100 mg/28.1ml)	08-115	Cell Signalling, UK
ProLong® Gold Antifade Mountant with DAPI	P36935	Thermo Fisher Scientific, UK
Shandon™ Immu-Mount™	9990402	Thermo Scientific, UK
VECTASHIELD Antifade Mounting Medium with DAPI	H-1200	Vector Laboratories Ltd, UK
Live cell imaging medium	A14291DJ	Thermo Fisher Scientific, UK
VECTASHIELD Antifade Mounting Medium without DAPI	H-1400	Vector Laboratories Ltd, UK
ImmuEdge™ Pen	H-4000	Vector Laboratories, UK
Antigen revival buffer 10X	S1699	DAKO, UK
Microscopic glass slides 0.8-1 mm	1156-2203	Fisherbrand, UK
Glass bottom dishes (FluoroDish™)	06062015	WPI, UK
Leica Epi DM4000 Epi-fluorescence microscope		Leica Microsystems, UK
Zeiss 710 Z2 confocal microscope		Zeiss, UK
Confocal microscope (spinning disc)	TE2000-S	Nikon, UK

## **2.5. Gene analysis techniques.**

### **2.5.1. Total RNA isolation and qPCR.**

Cells were seeded at the desired density 200,000 cells /well in 12-well plates in full RM+ medium, when cells were attached medium was changed to 4% serum containing RM+ medium either charcoal stripped or unstripped medium for overnight. In some experiments phenol free medium was also used. Next day, fresh medium was added plus treatment (AD with or without ATRA) for different time points, cells were then washed with PBS or PBS containing 0.02% EDTA to remove feeder fibroblasts before lysing the cells. RNeasy (QIAGEN, UK) was used to extract total RNA, RLT lysis buffer plus Mercaptoethanol was used to lyse the cells. Equal volume of 70% ethanol was added on the lysates and transferred into the RNA extraction columns. Cells were spun for 15 seconds maximum speed and washing buffers provided in the kit was used according to manufacturer's instructions. Once RNA was extracted, concentration was measured using NanoDrop spectrophotometer and 1µg of RNA was used for cDNA synthesis using qPCRBIO cDNA Synthesis Kit, PCR Biosystem, UK. mRNA isolation and cDNA synthesis will be discussed in the following section 2.5.2.

### **2.5.2. mRNA extraction and cDNA synthesis.**

Cells were seeded at the desired density of 200,000-500,000 cells/well in 12-well or 6-well plates, allowed to grow until they reached 60-70% confluence after which they were washed with PBS and lysed at the indicated time points after an experimental treatment or a specific media incubation. Lysates were either stored at -80 °C or subjected to mRNA extraction. Dynabeads® mRNA DIRECT™ kit was used to extract polyadenylated (polyA) mRNA according to the



manufacturer's instructions. Total RNA was added to the Dynabeads /Binding Buffer suspension, mixed thoroughly and rotated on a mixer for 10 minutes at room temperature to allow mRNA to anneal to the oligo (dT) on the beads. Tubes then were placed on a magnetic rack until the solution was clear. Supernatant was discarded and tubes were removed from the magnet and washed twice with buffers A and B. After removing the washing buffer, tubes were taken out of the magnetic rack and eluted using 20 µl elution buffer (10 mM Tris-HCl, pH 7.5). Tubes were heated to 80°C for 2 minutes and placed immediately on the magnet. Eluted mRNA was transferred to a new RNase-free tube.

The concentration of mRNA extracted was measured using a NanoDrop spectrophotometer at a setting of 40 OD at 260nm for 1µg/ml of mRNA. For cDNA synthesis, 50ng of pure mRNA was reverse transcribed using Reverse Transcriptor High Fidelity cDNA Synthesis kit with a master mix containing different components shown in the Table 2.8 or a qPCRBIO cDNA Synthesis Kit was used according to manufacturer's instructions in which all components are ready mixed and this removes the need for user optimisation of these critical factors.

**Table 2.8. Master mix components for cDNA synthesis.**

<b>Component</b>	<b>Volume [µl]</b>
mRNA (diluted with 10mM Tris-HCl, pH 8.0) (50ng)	13.0
Reaction buffer (5x)	4.0
dNTP mix (10 mM each dATP, dCTP, dGTP, dTT)	2.0
Random hexamer + oligo(dT) <sub>18</sub> primer mix	0.8
Protector RNase inhibitor	0.4
Reverse transcriptase	0.4
Total volume	20 ± 0.6

The reverse transcription reaction protocol was as follows: 42°C for 30 min, 85°C for 5 min and 4°C for 5 min. The resulting cDNA was diluted using 140 µL

nuclease-free distilled H<sub>2</sub>O (1:8) (250 ng/μL) of cDNA. Diluted cDNA can be used straightaway for qPCR gene expression analysis or stored at -20°C for later use.

### 2.5.3. Real-time quantitative PCR (qPCR).

Five or 10 μM forward and reverse (F/R) primer mixes were made by mixing equal volumes of forward and reverse primer stocks (100 μM) with suitable amount of nuclease-free H<sub>2</sub>O. For PCR amplification 384-well white plates were used with a total volume of 5 μl per well consisting of components shown in Table 2.9.

**Table 2.9. qPCR master mixture.**

Component	Volume [μl]
SYBR Green	2.5
5 or 10 μM F/R primer mix	0.5
cDNA template	2.0
Total volume	5.0

The cDNA samples were loaded into the bottom of the wells, followed by a mixture of SYBR Green and F/R primers added at the top wall of each well (in triplicates). Plates were well sealed, centrifuged and the plate was inserted into the LightCycler 480 machine for qPCR according to the protocol shown in Table 2.10.

**Table 2.10. Conditions used for qPCR using Roche Light Cycler LC480.**

Step	Function	Temperature	Duration
Denaturation	melting (hot start)	95°C	5 min
Touch-down (8 cycles)	gradual reduction of 0.6°C/cycle to maximise primer specificity	95°C	10 s
		66 – 60°C	6 s
		72°C	6 s
Amplification (55 cycles)	melting	95°C	10 s
	primer annealing	60°C	6 s
	product extension	72°C	6 s
	data acquisition	76°C	1 s
Melting analysis	melting	95°C	30 s
	cooling/annealing	65°C	30 s
	continuous data acquisition	65 – 99°C	gradual increase
Termination	cooling	40°C	5 s

The relative quantification of mRNA gene expression was measured using LightCycler® 480 software (release 1.5.0). For normalisation, *POLR2A* and *YAP1* were used as reference genes. The stability of these reference genes in a wide range of keratinocytes (normal and cell lines) and under different cellular conditions make them a good choice to be used for this purpose (Gemenetzidis et al., 2009). Data were plotted and statistically analysed using Microsoft Excel (t- test) as well as Anova.

#### **2.5.4. Validation of the primers.**

Primers used for qPCR in this study were synthesised by Sigma-Aldrich, UK and they were either custom-designed or selected from previous studies. Lyophilised oligonucleotides were resuspended in the appropriate volume of 10 mM Tris-HCl, pH 8.0 to make 100 µM stock of primers and they were stored at -20°C. Forward and reverse primers were diluted in qPCR water to a working concentration of 10 µM and stored at -20°C as well. To test the specificity of a primer set for a certain gene, a cell line that is known to express our gene of interest was used and its cDNA template was used in a qPCR reaction using a 96-well plate. Components used are shown in Table 2.11.

**Table 2.11. Master mixture used for primer validation.**

<b>Component</b>	<b>Volume [µl]</b>
SYBR Green	25.0
5 or 10 µM F/R primer mix	7.0
cDNA template	5.0
Nuclease-free H <sub>2</sub> O	15.0
Total volume	50.0 ± 2.0

Primer pairs that were giving only a single melting peak in the PCR reaction were chosen. QIAquick Gel Extraction Kit were used and the concentration of amplified

DNA was measured using the NanoDrop spectrophotometer. Based on the total number of DNA copies, the following standard dilutions of the amplified DNA were prepared with 25 µg/ml tRNA: 10<sup>11</sup>, 10<sup>9</sup>, 10<sup>7</sup>, 10<sup>6</sup>, 10<sup>5</sup>, 10<sup>4</sup>, 10<sup>3</sup> and 10<sup>2</sup> DNA copies/2 µl. Using this dilution series, a standard qPCR reaction with a total volume of 5 µl was performed to measure the efficiency of a particular primer pair using a standard curve. A value of 2.00 is considered to be an ideal efficiency, in which the amount of the target PCR product doubles with each PCR cycle (Tellmann, 2006).

All qPCR primers used in this thesis are listed in Table 2.12.

Reagents and equipment used in gene analysis are shown in Table 2.13.

**Table 2.12. List of the primers used in qPCR.**

<b>Target gene</b>	<b>Forward primer sequence (5'-3')</b>	<b>Reverse primer sequence (5'-3')</b>	<b>Amplicon Size (bp)</b>
<i>KRT1</i>	CGGAACTGAAGAACATGC AG	CATATAAGCACCATCCACAT CC	128
<i>KRT2</i>	GCCTCCTTCATTGACAAGG T	CGGGTGCCAACATTCATT	95
<i>KRT10</i>	AAACCATCGATGACCTTAA AAATC	GCGCAGAGCTACCTCATT T	134
<i>KRT14</i>	CGACCTGGAAGTGAAGAT CC	GTCCACTGTGGCTGTGAGA A	124
<i>POLR2A</i>	AGGAGTTTCGGCTCAGTG G	AGGTTCTCCAAGGGACTGC	128
<i>YAP1</i>	ACTGCTTCGGCAGGTGAG	TCGTCATTGTTCTCAATTCC TG	128
<i>cMyc</i>	CACCAGCAGCGACTCTGA	CTGTGAGGAGGTTTGCTGT G	138
<i>18sRNA</i>	GCAATTATTCCTCATGAAC G	GGCCTCACTAAACCATCCAA	123

**Table 2.13. Reagents and equipment used in gene analysis.**

<b>Reagents/ equipment</b>	<b>Catalogue #</b>	<b>Supplier</b>
Dynabeads® mRNA DIRECT™ Purification kit	61011, 61012	Life Technologies, UK
LightCycler® 480 SYBR Green I Master	04707516001	Roche, UK
qPCRBIO SyGreen Blue Mix Lo-ROX	PB20.15-20	PCR Biosystems, UK
QIAquick Gel Extraction kit	28706	QIAGEN, UK

Transcriptor High Fidelity cDNA Synthesis kit	05081955001	Roche, UK
tRNA	R8505	Sigma-Aldrich, UK
Water DNase-, RNase-, protease-free (nuclease-free H <sub>2</sub> O)	W4502	Sigma-Aldrich, UK
LightCycler <sup>®</sup> 480 Instrument		Roche, UK
LightCycler <sup>®</sup> 480 Multiwell Plate 96	04729692001	Roche, UK
LightCycler <sup>®</sup> 480 Multiwell Plate 384	04729749001	Roche, UK
Mini Plate Spinner MPS 1000 <sup>™</sup>		Labnet, USA
NanoDrop <sup>™</sup> 1000 Spectrophotometer		Thermo Scientific, UK
Veriti <sup>®</sup> 96-Well Fast Thermal Cycler		Applied Biosystems
qPCRBIO cDNA Synthesis Kit	PB30.11-10	PCR Biosystems, UK
RNeasy	74104	QIAGEN, UK

## 2.6. Cloning and gene transfer.

### 2.6.1. Basic techniques.

#### 2.6.1.1. Restriction digestion.

DNA was digested with one or two restriction enzymes in the presence of the appropriate reaction buffer. If required, bovine serum albumin (BSA) was added to prevent the adhesion of the enzymes to the walls of the reaction tubes. When the DNA digestion included two different enzymes requiring two different buffers, the insert and the vector were digested with the first enzyme, precipitated and only then digested with the second enzyme. The mixture was incubated at 37°C for several hours or overnight followed by addition of 1U of shrimp alkaline phosphatase and a further incubation of 30 min. The shrimp alkaline phosphatase treatment removed the 5' phosphate from the linearised vector end eliminating the possibility of self-ligation. This would reduce the number of false positive colonies following transformation.

#### 2.6.1.2. Agarose gel electrophoresis.

DNA fragments were separated using agarose gel electrophoresis. Briefly, 1 – 2 % (w/v) agarose (depending on the size of the DNA fragments) gels were

prepared by dissolving the appropriate amount of agarose in TBE (Tris-Borate-EDTA) buffer. Ethidium bromide (EtBr; 0.5 µg/ml) was added to the buffer for visualisation of DNA under UV light. An appropriate casting tray with a suitable comb was washed, dried and assembled. It was cooled by keeping it in a freezer for 10-15min. The casting tray was removed from the freezer and hand warm melted agarose was poured. After the gel had solidified, which took about 20 min, it was submerged in 1x TBE buffer in the gel tank containing 20µl EtBr. Samples, previously mixed with 6x DNA dye, were loaded onto the gel and run at 100 V for time required for sufficient separations of the bands. DNA ladder (1 kb or 100 bp) was used as a standard to size DNA bands. DNA fragments were then visualised under a UV transilluminator using G:BOX system and images were acquired with the Genesnap software. Reagents and equipment used for agarose gel electrophoresis shown in Table 2.14.

**Table 2.14. Reagents and equipment used for agarose gel electrophoresis.**

Reagents/equipment	Catalogue #	Supplier/company
1 kb DNA Ladder	N3232L	NEB, UK
100 bp DNA Ladder	15628-050	Invitrogen™, UK
UltraPure™ Agarose	16500-500	Invitrogen, UK
Ethidium bromide solution	E1510	Sigma-Aldrich, UK
SYBR® Safe DNA Gel Stain	S33102	Thermo Fisher Scientific, UK
TBE Buffer (10x)	A0972,5000PE	AppliChem GmbH, Germany
G: BOX		Syngene, UK

### **2.6.1.3. Ligation.**

Both the insert (cDNA of interest) and the vector were digested with the same set of restriction enzymes in appropriate reaction buffer. If needed, the target sequence was amplified by PCR using specific primers and 2 x Q5® Master Mixture containing high fidelity Q5® thermostable DNA polymerase, dNTPs, Mg<sup>2+</sup> and a proprietary broad-use buffer. In most cases the digested vector was treated

with alkaline phosphatase to dephosphorylate 5' DNA ends to prevent its re-circularisation during ligation. The digested insert and vector DNAs were run on a 1% (w/v) agarose gel/1x TBE buffer to separate the fragments of interest. Agarose gel electrophoresis was performed as described in 2.6.1.2, except that wells were wide enough to fit 50 – 100 µl of the sample. When complete separation of bands was achieved, they were visualised using a long wavelength UV lamp and excised from the gel with a scalpel. The insert/vector DNA was extracted using QIAquick Gel Extraction kit according to manufacturer's protocol. Afterward, the insert DNA was ligated into the vector DNA in the presence of the ligation buffer (50 mM Tris-HCl, 10 mM MgCl<sub>2</sub>, pH 7.5), 2 mM ATP, 10 mM DTT and 10U T4 DNA ligase. A control ligation reaction containing only the vector (with no insert) was set up alongside to determine the degree of self-ligation. Both the reaction and control ligation mixtures were incubated at RT for 4 h. The ligation mixtures were then diluted 1:3 with either H<sub>2</sub>O or 10mM Tris-HCl buffer, pH 8.0 and used for transformation of NEB Stable competent cells. Reagents used for DNA ligation shown in Table 2.15.

**Table 2.15. Reagents used for DNA ligation.**

Reagents	Catalogue #	Supplier
Antarctic Phosphatase or Shrimp alkaline phosphatase	M0289S	NEB, UK
T4 DNA ligase	M0202L	NEB, UK
QIAquick Gel Extraction Kit	28706	QIAGEN, UK

#### **2.6.1.4. Competent cells transformation and preparation of mini- and maxi DNA preps.**

*E. coli* competent cells (either NEB stable or Stl2) were thawed on ice and incubated with the diluted ligation mixtures (prepared as described in section 2.6.1.3) containing vector and insert or vector alone for 30 min, followed by a heat shock at 42°C for 25-45 sec (time depending on the *E.coli* strain). Thereafter, 500

$\mu$ l of S.O.C. medium containing high concentration of glucose was added and the *E. coli* were incubated at 30°C for 1 – 2 h under shaking (300 rpm) to allow them to recover. The transformed bacteria were then plated onto pre-warmed agar plates [1.5% (w/v) agar in Lysogeny Broth; Luria-Bertani (LB)] containing 100  $\mu$ g/ml ampicillin and these were incubated upside down overnight at 30°C. Next day, single colonies were picked with a sterile loop and suspended into 10 – 20 ml of LB medium containing 100  $\mu$ g/ml ampicillin. LB medium was prepared by dissolving 5 g yeast extract, 10 g tryptone and 10 g NaCl per litre of distilled water and sterilised by autoclaving. Tubes with colonies were incubated overnight at 30°C in an incubator shaker at 300 rpm. The following morning, tubes were centrifuged at 4000 rpm for 30 min at 4°C and the supernatants were discarded. The bacterial pellets were lysed, and DNA was purified using the isopropanol DNA precipitation method or using the QIAprep Spin Miniprep kit according to manufacturer's protocol. DNA samples were later digested with appropriate restriction enzymes and processed for DNA gel electrophoresis to identify clones carrying the correct insert. These clones were sequenced by the dideoxy method for confirmation and the correct ones were used for "maxi DNA prep", which was performed using QIAGEN Plasmid Maxi kit according to manufacturer's protocol. Reagents and equipment used in preparing mini and maxi DNA preps are shown in Table 2.16.



**Table 2.16. Reagents and equipment used in preparing mini and maxi DNA preps.**

Reagents/equipment	Catalogue #	Supplier/company
UltraPure™ Agarose	16500-500	Invitrogen, UK
Ampicillin sodium salt	A0166	Sigma-Aldrich, UK
Bacto™ Tryptone	211705	BD Biosciences, UK
BBL™ Yeast Extract	211929	BD Biosciences, UK
MAX Efficiency® Stbl2™ Competent Cells	10268-019	Invitrogen, UK
NEB Stable Competent <i>E. coli</i> (High Efficiency)	C30401	NEB, UK
QIAGEN Plasmid Maxi Kit	12163	QIAGEN, UK
QIAprep Spin Miniprep Kit	27106	QIAGEN, UK
Heraeus™ Multifuge™ 3SR+	-	Thermo Scientific, UK
Incubator shaker G25	-	New Brunswick Scientific, USA
Incubator Labheat	-	Boro Labs, UK
Sorvall® RC-5C Plus Superspeed Centrifuge	-	Beckman Coulter, US

**SOC medium preparation.** Two grams of tryptone, 0.5gm yeast extract, 50 mg NaCl, 0.5ml of 2M MgCl<sub>2</sub> and 1ml of glucose is dissolved in a total volume of 100ml of distilled water. The solution is sterilised by filtration and aliquoted in 5ml aliquots.

## 2.6.2. Transfection and luciferase reporter assay.

### 2.6.2.1. Transfection.

HaCaT keratinocytes were seeded at 150,000 cells/well in 24 well plates in full DMEM (10% FCS, 1%PS). When cells are 50-70 % confluent, the medium was changed to fresh full medium and the cells were transfected with 1, 2 and 3 µg of plasmid DNA (Plpc-puro-AcGFP) using different transfection reagents for optimisation experiments. For example, Viromer Red, X-Fect transfectin reagent, TransIT®keratinocyte reagent, DreamFect™ Gold, Helix-N and Promofectin were all used according to manufacturer's instructions (Table 2.17). In some wells, Magniffection CombiMag was used with these reagents with the aid of a magnetic plate to increase transfection efficiency. The transfection efficiency was assessed by monitoring green fluorescent protein tag (GFP) expression using

Nikon Eclipse TE2000-S microscope equipped with a camera. High and low calcium containing medium were used to see if calcium levels could affect transfection efficiency. High calcium was 1.8 mM while low calcium was 0.01-0.03 mM.

For Luciferase experiments, HaCaT cells were seeded at 100,000 cells/ well in 24- well plates in full DMEM (10% FCS and 1% PS). Next day, when cells reached 50-70% confluency, Viromer Red transfection reagent was used with total DNA used (2µg) for 48 hours before measuring the luciferase activity.

#### **2.6.2.2. Constructs used for luciferase reporter assay.**

AP-1 luciferase reporter construct and its mutant form were generated by ligation of a HPLC-purified oligonucleotide containing six copies of the AP-1 responsive element [TGA(C/G)TCA] (Angel et al., 1987) or its mutant form [TAA(C/G)TAA] (Wade et al., 1992) into *KpnI* and *BglII* sites of the pGL4.26 vector. This vector can be used in luciferase enhancer activity measurement as it contains a minimal promoter (Brown et al., 1993). To prepare K10 and K2 luciferase reporter constructs, multiple fragments of K10 and K2 promoter (F1 – F8) were amplified by PCR and cloned into *KpnI* and *HindIII* sites of pGL4.14 vector which lacks any eukaryotic promoter activity. These constructs were made by my supervisor, Prof. Ahmad Waseem, who kindly provided them for this work. Other constructs/vectors used in this study, including TAM67/pcDNA3 pUC, Renilla CMV, pGL4.14 K14, pGL.4.14, pGL4.26 were also provided by my supervisor, Prof. Ahmad Waseem.

#### **2.6.2.3. Luciferase reporter assay.**

Cellular activity of the transcription factor AP-1 and the K2 and K14 promoter were measured by luciferase reporter assay. HaCaT keratinocytes and HEK293

cells were seeded in 24-well plates at 100,000 cell/well and transfected with 2µg of AP-1 promoter in pGL4.26 vectors (expressing firefly *luc2* (*Photinus pyralis*)) or K2,K14 promoters in pGL4.14 vectors again expressing firefly activity. pRL *Renilla* Luciferase Control Reporter Vector (plasmid expressing *Renilla* luciferase) was used as an internal control to normalise the values of the experimental reporter gene (firefly) for variations that could be caused by transfection efficiency and sample handling. Viromer Red transfection reagent was used and pUC18 DNA was added to keep the total amount of transfected DNA constant in all samples. After 48 hours, the DNA-containing medium was replaced with appropriate amount of fresh culture medium (containing 10nM PMA in DMSO or 0.01% DMSO as a vehicle control) for up to 8 hours for AP-1 transfected cells before being lysed for luciferase activity measurement. Cells transfected with K2 and K14 vectors were lysed after 48 hours of transfection to measure luciferase activity. To measure luciferase activity, cells were washed with PBS, incubated with 250 µl passive lysis buffer (PLB) for 45 min on gentle shaker at RT and assayed for luciferase activity using Dual-Luciferase® Reporter Assay System. Luciferase Assay Reagent II (LARII) (50µl) was added to 10 µl lysate, previously transferred to black plates with optical bottom, and firefly luminescence was measured. Subsequently, the firefly luminescence was quenched by adding 50 µl Stop&Glo reagent in Stop&Glo buffer and *Renilla* luminescence was measured to correct for transfection variability. Lysates were also normalised for variations in protein concentration determined by DC Protein Assay Kit (section 2.4.1.1). All measurements were conducted using FLUOstar Optima Microplate Reader and analysed using Microsoft Excel 2010.

**Table 2.17. Reagents used in transfection and luciferase assay.**

Reagents/equipment	Catalogue #	Supplier
Dual-Luciferase <sup>®</sup> Reporter Assay System	E1980	Promega, UK
pRL-TK vector	E2241	Promega, UK
Viromer Red Transfection Reagent	VR-01LB-01	Lipocalyx, Promega, UK
X-Fect transfection reagent	PT5003-2	Clontech laboratories, UK
TransIT <sup>®</sup> -Keratinocytes reagent	81054927	Mirus, UK
DreamFect <sup>™</sup> Gold	DG80040	OZ Biosciences, UK
Magnitofection CombiMag	CM20025	OZ Biosciences, UK
Helix-N <sup>™</sup>	HX10030	OZ Biosciences, UK
Promofectin	PK-CT-2000-10	Promokine, UK
FLUOstar Optima Microplate Reader		BMG Labtech, UK
Microscope Nikon Eclipse	TE2000-S	Nikon
Nunc <sup>™</sup> MicroWell <sup>™</sup> 96-Well Optical-Bottom Plates	265301	Thermo Scientific, UK
Renilla CMV vector	E2261	Promega, UK
pGL4.14 vector	E6691	Promega, UK
pGL4.26 vector	E8441	Promega, UK
PMA	P1585	Sigma-Aldrich, UK

### 2.6.3. Retroviral transduction.

#### 2.6.3.1. Retrovirus production using Phoenix A cells transfection.

Twenty-four hours prior to transfection,  $1.5 - 3 \times 10^6$  of Phoenix A cells (human embryonic kidney cell line, a second generation retrovirus producer cell line) were seeded onto 10-cm collagen-coated (10 µg/ml for 1h at 37°C) dishes. Next day, a mixture of target plasmid DNA (15 µg) and transfection reagent TransIT<sup>®</sup>-LT1 (45 µg) was incubated for 15 min at RT in a total volume of 1.5 ml with PBS or DMEM. The DNA/TransIT<sup>®</sup>-LT1 complex was added dropwise into the medium covering the cells. The cells were incubated for the following 24 – 36 h and, after becoming approximately 80% confluent, they were trypsinised and seeded in collagen-coated T75 flasks. After allowing Phoenix A cells to attach, suitable antibiotic was added to the medium to select the successfully transfected cells. Phoenix A cells transfected with an empty vector and un-transfected Phoenix A

cells were used as controls. After few days of drug selection, Phoenix A cells were trypsinised and re-plated into three collagen-coated T175 flasks. When they became almost 100% confluent, remnants of the antibiotic were washed away, and the cells were incubated with 14 ml of fresh medium for exactly 24 h at 32°C. This is an optimal temperature for production of viral particles (Kotani et al., 1994, Anson, 2004). The retroviral supernatants were collected, spun down at 4300 rpm for 20 min at 4°C and snap-frozen in liquid nitrogen. Cryovials with viral supernatants were stored at -80°C until use. Medium in T175 flasks was replenished and the same cycle of collecting the supernatants was repeated two more times. The transfection efficiency was assessed by monitoring GFP expression using Nikon Eclipse TE2000-S inverted microscope equipped with a digital camera.

#### **2.6.3.2. Transduction of MCF7 cell lines.**

MCF7 cells were seeded in a 6-well plate at about  $\leq 50\%$  confluence at the time of transduction. Next day, cells were incubated with fresh medium containing 5  $\mu\text{g/ml}$  Hexadimethrine bromide (polybrene) for 10 min at 37°C. Polybrene is a polymer used to increase the efficiency of retrovirus-mediated gene transfer by enhancing adsorption of the viral particles onto the cell membranes (Davis et al., 2002, Swift et al., 2001). Polybrene-containing medium was replaced with retroviral supernatant containing the same concentration of polybrene (5  $\mu\text{g/ml}$ ). The plates were immediately centrifuged at 1000 rpm for 1 – 1 h at 32°C and incubated at 32°C for the following 24 h. Subsequently, the retroviral supernatant was replaced with fresh culture medium and the plates were further grown for 2 – 3 days at 37°C for viral integration and expression of the transduced genes. The transduced cells were trypsinised, plated in T75 flasks and cultured for few

weeks with drug selection. Reagents used in retroviral transduction are shown in Table 2.18.

**Table 2.18. Reagents used in retroviral transduction.**

Reagents	Catalogue #	Supplier
Collagen Type I, rat tail	08-115	Merck Millipore, UK
Hexadimethrine bromide (Polybrene)	107689	Sigma-Aldrich, UK
TransIT <sup>®</sup> -LT1 Transfection Reagent	MIR 2300	Mirus Bio, US
		UK supplier: Cambridge BioScience

### **2.6.3.3. Drug selection.**

Depending on the vector used for transfection/transduction, a suitable antibiotic (hygromycin, G418 or puromycin) was added into the cell culture medium for as long as necessary to select successfully transfected or transduced cells. The optimal antibiotic concentration was determined for each cell type by performing a kill curve. Briefly, cells plated in 6/12-well plates were cultured in the presence of incremental amounts of the appropriate antibiotic and their vitality was examined daily using Nikon Eclipse TE2000-S inverted microscope equipped with a camera. Reagents and equipment used in drug selection are shown in Table 2.19.

**Table 2.19. Reagents and equipment used in drug selection.**

Reagents/ Equipment	Catalogue #	Supplier
G418 disulfate salt	A1720	Sigma-Aldrich, UK
Hygromycin B solution from <i>Streptomyces hygroscopicus</i>	H0654	Sigma-Aldrich, UK
Puromycin dihydrochloride	A11138-03	Gibco <sup>®</sup> , UK
Inverted Microscope (Nikon Eclipse)	TE2000-S	Nikon, UK

## **2.7. Statistical analysis.**

Statistical analyses were performed using Microsoft Excel 2010 and Graph Pad Prism 7. All data are expressed as standard error of the means (n=3), statistical

significance was determined with unpaired Student's *t*-test or Anova (one-way or two-way) calculating p-values on raw data.

# CHAPTER 3



### **3. Results I. Keratin filament dynamics, heat stress response and role of phosphorylation in live epithelial cells.**

#### **3.1. Introduction.**

Around one third of cellular proteins undergo phosphorylation, a process in which a phosphate group is added onto a protein in order to modify its function according to the need of the cell. It is one of the PTMs that takes place after proteins are synthesised. Kinases and phosphatases are the key players in this process and they are both regulated by other enzymes that are activated by the cellular response to various stimuli (Sefton and Shenolikar, 2001). Phosphorylation of proteins can be a normal physiological event as well as happening during a disease process and its function can be to control the cell fate at the end of a cellular response. In epithelial cells, phosphorylation of keratins can change the functional and physical characteristics of the cell. For example, filaments re-organise around the nucleus in response to stress as a result of filaments phosphorylation. Phosphorylation plays a role during cell growth as well, Phosphorylation regulates cell growth by allowing the adaptor protein such as members of 14-3-3 family of proteins to bind to phosphorylated intermediate filaments, that later binds to other factors facilitating polarised cytoskeletal assembly during cell migration, changing the function from being a structural support protein to a cell migration facilitating protein (Snider and Omary, 2014). During mitosis and metastasis, phosphorylation does take place allowing the filaments to break into a soluble form giving cells the chance to split or move freely through the basal (or basement) membrane. This change in the physical properties of the epithelial cells is an example of the important role that phosphorylation plays in controlling cellular fate (Kim et al., 2015a).

Phosphorylation sites in keratins are located mostly in the head and tail domains and the addition of a phosphate group at these sites increases keratin solubility. Phosphorylation of keratins will increase the negative charges on the polypeptide, which will induce repulsive forces thereby affecting filament stability and allowing the filaments to breakdown into globules and become more soluble. These changes are needed temporarily in some cellular conditions such as during cell division, intracellular trafficking and cell migration (Yatsunami et al., 1993). This property also allows other exogenous keratins to incorporate into the network without affecting normal cell physiology and homeostasis (Windoffer et al., 2011). However, permanent breakdown of filaments could be a sign of EMT that allows the cell to move freely as in the case of cancer metastasis (Kim et al., 2015a, Snider and Omary, 2014). So, maintaining a balance between phosphorylation and dephosphorylation is necessary for the cell to maintain normal functions. Phosphatase inhibitors are well known pharmacological agents used to study protein phosphorylation. Serine and threonine phosphatase inhibitors are widely used, and this has enabled researchers to look at their effect on protein dynamics and functions. OA and CL-A are used to inhibit Ser/Thr PP1 and PP2A with CL-A being more potent on PP2A than OA (Dounay and Forsyth, 2002, Takuma et al., 1993).

Tissue homeostasis is a physiological process in which there is a balance between cellular growth and cell death. When cells are exposed to stress, this equilibrium is disturbed, and a stress response is activated leading either to cell survival (if stress can be encountered) or cell death pathways are induced. There are many different types of stresses that a cell may experience, some are intrinsic in nature that the cell faces during normal physiology such as during mitosis, for example. Stress could also be extrinsic as certain environmental changes that

could directly or indirectly affect cellular functions, and it could be physical or chemical in nature (Toivola et al., 2010). Elevated temperature, more than 5°C above normal body temperature, heavy metals, oxidants that generate free radicals, certain drugs and bacterial/viral infections are considered different forms of stresses (Fulda et al., 2010). The response of a cell towards a stress differs depending on the type and strength of the stress, the cell may move toward a protective response that stops cell death, and this is mediated through the activation of pro-survival pathways. One of the key factors playing a role in this pathway is the heat shock factor 1 (HSF1), which is a transcriptional factor distributed in the nucleus and the cytoplasm. In normal physiological conditions HSF1 exists as a monomer inactivated by binding to a constitutive form of heat shock proteins (HSPs) in the cytoplasm. When the cells are subjected to a type of stress such as heat shock, the complex of HSF1 with HSP become misfolded and start to denature and this leads to dissociation of HSF1 from its HSP counterpart to form a trimer that enters the nucleus and binds to its heat shock element on the target gene to induce transcription (Morimoto, 1993). This response is quick and takes only few minutes and leads to synthesis of heat shock proteins that play a role in cell survival. HSF1 is inactivated after returning the cell to normal physiological temperature through negative regulation by HSP. Synthesis of HSPs after the heat shock leads to thermotolerance, which is the ability of the cell to withstand severe heat shock after being subjected to a mild one. Thermotolerance is a characteristic of HSPs that bind to misfolded proteins after the heat shock to prevent aggregation. Thermotolerance starts within a few hours after the mild heat shock and lasts for a few days (Dorion and Landry, 2002).

HSPs are a large family of chaperon proteins, which under physiological conditions act as pro-survival proteins when cells are put under stress. Among the HSP family, HSP70 is a well-studied highly conserved group that is made up of four different members (HSP72, HSP73, HSP75, and HSP78) that share the same protein sequence but they are synthesised in response to different stimuli (Kregel, 2002). HSP70 is constitutively expressed inside the cell even when there is no heat shock and this form of HSP70 is named HSC70 while the inducible form is HSP72. When cells are subjected to stress, HSPs undergo post-translational modifications that change their configuration allowing HSF1 to be detached and activated. This allows synthesis of the inducible HSPs that in turn switch on the stress protective function inside the cell. Keratins are affected in response to certain types of stresses that could induce phosphorylation and affect their dynamics and organisation (Liao et al., 1997, Kim et al., 2015a). After exposure to heat shock, which is a form of stress, MAPKs are activated as the stress response and in the case of keratin filaments, p38 MAPK plays an important role in phosphorylating certain keratin residues. Keratin phosphorylation leads to formation of granules, which are associated with p38 MAPK when assayed using antibodies. Phosphorylation of K8 on S73 residue is mediated by p38 kinase, and this has been shown by using K8 phosphoserine antibody that shows co-localisation of keratin granules (formed in response to treating cells with a phosphatase inhibitor) with phosphorylated p38. Keratins 5 and 6 are also phosphorylated on S73 by p38 MAPK exactly as K8 but they are also phosphorylated on threonine residues as well (Toivola et al., 2002). Treating the cells with a p38 inhibitor showed more stable filaments that are unable to form granules when treated with phosphatase inhibitors (Liao et al., 1997).

In this chapter the role of introducing an exogenous keratin (K2) that was tagged at the N-terminus (head domain) into the pre-existing keratin network of MCF-7 cells was investigated, its integration and its effect on both filament dynamics as well as stability were studied. MCF-7 cells do express K8/K18/K19 but not K2 (Godfroid et al., 1991). K2 construct was available in the lab made by my supervisor Professor Ahmad Waseem. Besides being ready to use, K2 is an interesting keratin to be studied, as it has been shown to be downregulated after several passages in cultures of skin biopsies with no studies done on factors that might be regulating this downregulation. K2 is a terminal differentiation marker of stratified epithelium and it is upregulated in pre-cancerous hyperkeratotic oral lesions, more investigations were done on this protein starting from its integration and stability. To investigate the effect of phosphorylation, phosphatase inhibitors were used and the level of filaments breakdown among MCF-7 cells transduced with K2 were compared with empty vector control cells. Stress induces phosphorylation through activating SAPKs, and heat shock is a type of stress that our keratins face every day. The role of HSPs on keratin phosphorylation and breakdown in transduced MCF-7 cells in response to heat shock was studied. Epithelial cells generally are not very efficient in taking up DNA, so transfection could not be used to introduce K2 tagged to AcGFP or FLAG expression vectors into cells. An alternative strategy of packaging the AcGFP-K2 or FLAG-K2 (shorter tag) into recombinant retroviruses was used, which was transduction into MCF-7 cells. The transduced AcGFP-K2 MCF-7 cells produced green fluorescent keratin cytoskeleton while the FLAG-K2 transduced ones were stained using secondary antibodies that recognises anti-FLAG primary antibody.

Cells used in this chapter are MCF-7 cells, grown in DMEM with 10% FCS and 1% PS in 37°C incubator unless mentioned elsewhere. Drugs were dissolved in

DMF (0.05%), for immunostaining images a Leica DM5000B or DM4000 Epi-fluorescent upright microscope was used and Spinning disc confocal microscope was used to record live cell imaging video. More details of experimental procedures are described in Materials and Methods.

### **3.2. Integration of Keratin K2 into the pre-existing keratin network of MCF-7 cells.**

Transducing MCF-7 cells with AcGFP-K2, turned the keratin cytoskeleton in MCF-7 into green under a fluorescence microscope (Figure 3.1) suggesting that AcGFP-K2 might have integrated to the pre-existing keratin network, since K2 on its own, as any other keratin, would not form filaments (Bragulla and Homberger, 2009). To provide evidence that AcGFP-K2 had integrated into the pre-existing keratin network, the AcGFP-K2 transduced MCF-7 were immunostained with the monoclonal antibody mAb (LE65), which reacts with the endogenous keratin network containing K8 and K18/19 (Waseem et al., 1997), and counter stained the cells with AF-633-labelled rabbit anti-mouse IgG. The AF-633 staining produced a red cytoskeletal network as shown in Figure 3.1. When the AcGFP staining was merged with the AF-633 staining, the filaments overlapped perfectly, and the keratin network turned yellow in colour (Figure 3.1 d) suggesting the K2 fusion protein had integrated into the pre-existing network. AcGFP is a large protein molecule with a molecular weight of about 26kDa which would make the molecular weight of the AcGFP-K2 fusion protein to about 96kDa. To demonstrate that the presence of such a large AcGFP protein molecule at the N-terminus of K2 will not affect its integration into the pre-existing network, another fusion protein was produced in which a much smaller non-fluorescent tag 3X

FLAG was linked to K2 protein at the N-terminus. This fusion protein, termed FLAG-K2, was transduced into MCF-7 and the cells were incubated with anti-FLAG (mAb) as well as LE65 (mAb). Double labelling the cells with AF-488 and AF-633 allowed the cells to be visualised in the green for FLAG tag as well as in red channel for endogenous keratins K8/K18. As shown in (Figure 3.1 h), the FLAG-K2 and LE65 staining overlaps perfectly with the resultant staining turning into yellow suggesting that K2 had integrated into the pre-existing keratin cytoskeleton. This set of experiments shows that keratin integration is independent of the size of the tag at the N-terminus. To further demonstrate that K2 has been introduced inside the MCF-7 cells protein analysis was performed by western blotting using mouse anti-K2 that gave rise to an immunoreactive band of around 70 kDa only in cells transduced with AcGFP-K2 (>70 kDa) or FLAG-K2 (<70 kDa) as shown in Figure 3.2 (A) which also confirmed the specificity of the antibody. The specificity of the antibody was also determined using immunofluorescence staining in Figure 3.2 (B) in which MCF-7/FLAG-K2 cells only showed green filaments network compared to untransduced MCF-7 or MCF-7 transduced with an empty vector MCF-7/FLAG-C.

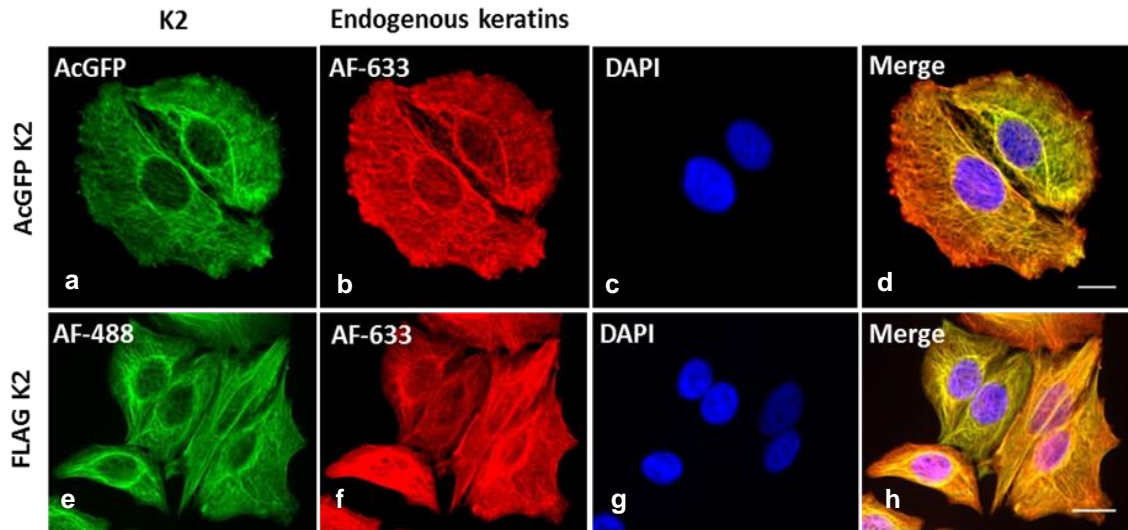


**Figure 3.1. Integration of Keratin K2 into MCF-7 keratin network.** MCF-7 cells transduced with AcGFP-K2 or FLAG-K2 were grown in full medium (DMEM, 10% FCS, 1% PS). The AcGFP tagged K2 gave green fluorescence, the FLAG tagged K2 was stained in green using anti-FLAG antibody and AF-488. The endogenous keratins were stained in red using mouse monoclonal LE65 antibody and AF-633 rabbit anti-mouse. Nuclei were stained with DAPI in blue and overlapping is shown as Merge. This figure shows full integration of K2 (green) with endogenous keratins (red) as the network is turning yellow in d and h. Leica DM5000B Epi-fluorescence microscope and DFC350 camera were used for recording images. (Scale bar = 20  $\mu$ m).



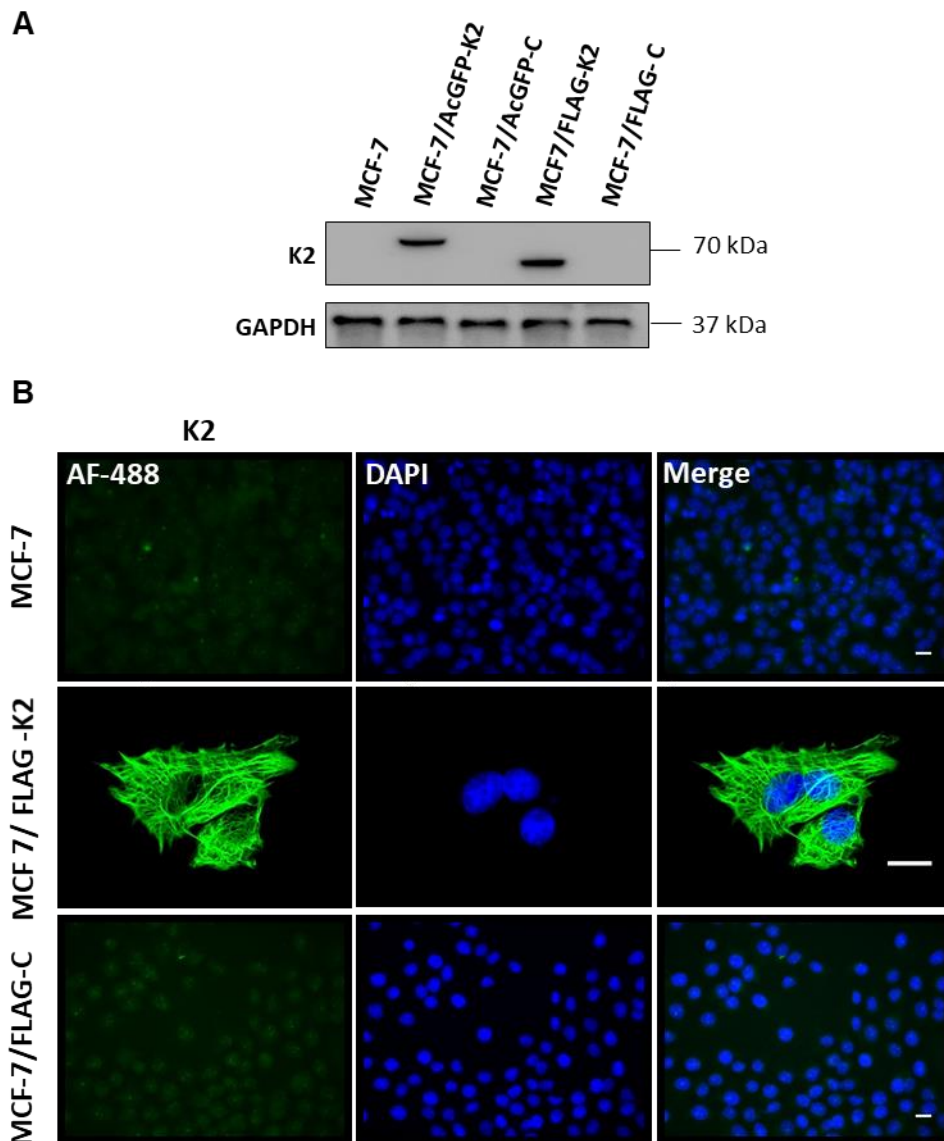


**Figure 3.2. Specificity of K2 antibody.** (A) MCF-7 cells untransduced and transduced with AcGFP-K2 or AcGFP-C, FLAG-K2 or FLAG-C were grown in full medium (DMEM, 10% FCS, 1% PS), lysed for protein analysis by western blotting using anti-K2 mouse antibody. GAPDH was used as a loading control. (B) Immunostaining of MCF-7 cells and MCF-7 transduced with FLAG-K2 or FLAG-C were stained with the same K2 antibody, AF-488 was used as secondary antibody showing green fluorescence. Nuclei were stained with DAPI in blue and overlapping is shown as Merge. This figure shows the specificity of K2 antibody as it only reacted with MCF-7/FLAG-K2 cells in WB and immunostaining. Leica DM5000B Epi-fluorescence microscope and DFC350 camera were used for recording images. (Scale bar = 20  $\mu$ m).

### **3.3. Integration of K2 into the simple epithelial keratin network did not affect normal cell physiology of MCF-7 cells.**

#### **3.3.1. Mitosis.**

The complete integration of AcGFP-K2 into MCF-7 cytoskeleton as shown in the previous section and the resultant labelling of the keratin network allowed us to monitor filament dynamics in live MCF-7 cells. The growth profile of MCF-7 cells containing the integrated AcGFP-K2 in their cytoskeleton did not change suggesting that exogenous K2 did not affect the growth characteristics. Further investigation was done to show whether integration of AcGFP-K2 into the pre-existing keratin network of MCF-7 affected their ability to undergo mitosis. MCF-7/AcGFP-K2 cells were grown in glass bottom dishes suitable for live cell imaging and replaced the medium with the clear imaging medium just before recording. Live imaging of these cells was carried out using spinning disk confocal microscope equipped with a stage that can be maintained at a constant temperature. In most cells, keratin filaments were spread across the cytoplasm reaching to the cell membrane. As a labelled cell began to undergo mitosis, the keratin cytoskeleton started to condense, and the cell started to round up. The filaments closer to the membrane started to break into globules and the cell rounding continued leading to complete disruption of filaments into globules. As the cell started to divide the keratin globules were equally distributed into the two halves just before cytokinesis. As shown in Figure 3.3 the keratin cytoskeleton started to repolymerise and extend once cells had started to spread following cytokinesis. This indicates that the integration of K2 into the endogenous network of MCF-7 cells didn't affect the normal physiological processes such as cell division.

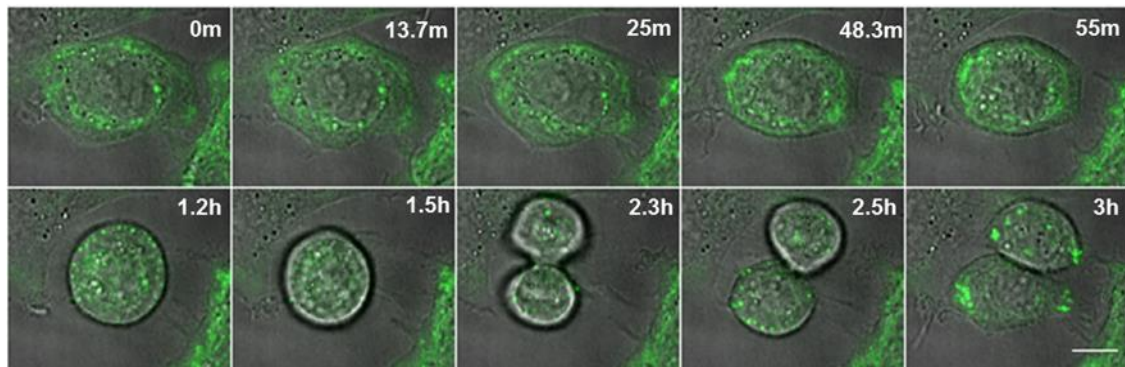


**Figure 3.3. Reorganisation of keratin filaments during mitosis.** MCF-7 cells expressing AcGFP-K2 were grown in full medium (DMEM, 10% FCS, 1% PS), in glass bottom dishes for time-lapse recording. At the beginning, the filaments were spread across the cell reaching the cell membrane (0 min), filaments start moving toward the nucleus (48.3 min), cell started to round up (55 min and 1.2 h) and filaments condensed around the nucleus, breakdown of filaments into granules at the periphery (1.2 h), granules all over the cytoplasm, soluble form (1.5 h), starts dividing, daughter cells have keratin in granular form (2.3-2.5 h), granules started to join forming squiggles at the cell periphery (3h). This figure shows stages of keratin reorganisation inside the cell during mitosis. Spinning disk confocal microscope was used for recording images. (Scale bar = 10 $\mu$ m).

### 3.3.2. Dynamic equilibrium of keratin network.

Fluorescent-labelled keratin filaments in MCF-7 expressing AcGFP-K2 cells were used to show that K2 becomes part of the normal turnover of keratin cytoskeleton and this cycle was not affected by introducing K2 into the network. In live cells, keratin filaments appear to be in a continuous dynamic state. Time-lapse microscopy showed that keratin globules exist mostly at the cell periphery where focal adhesions are located. As shown in Figure 3.4 these globules slowly merge with the existing filaments, which are constantly moving towards the nucleus and disappear. This perhaps indicates that the filaments constantly undergo disassembly near the cell periphery and undergo assembly and condensation as they move closer to the nucleus.

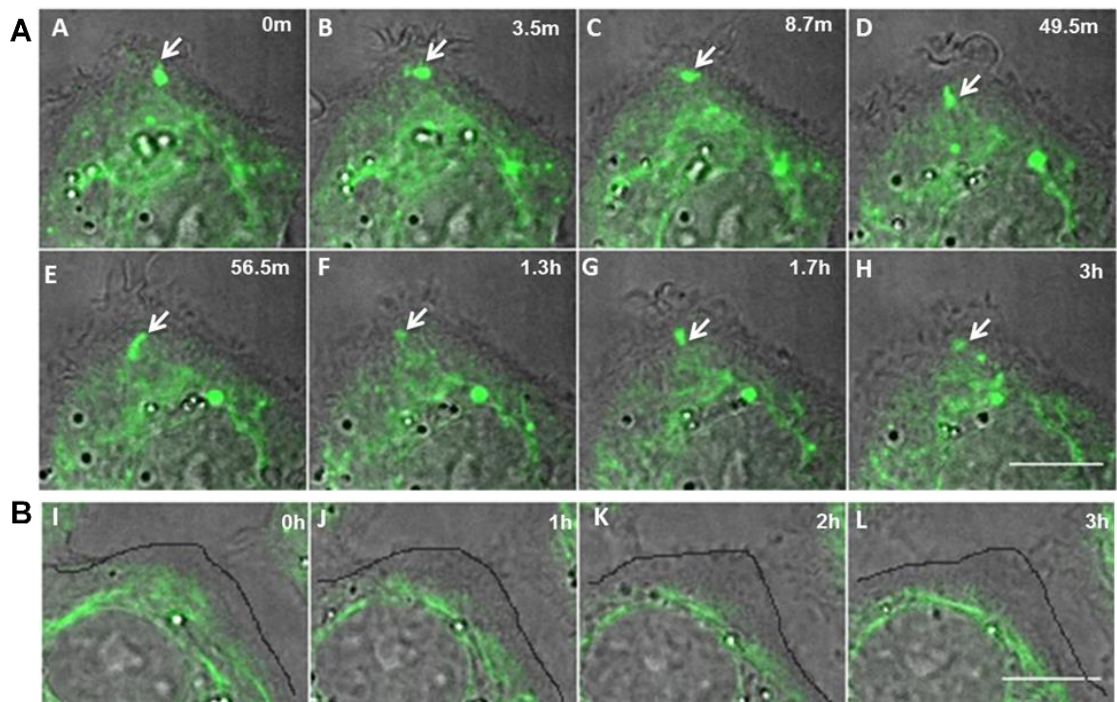


**Figure 3.4. Time-lapse microscopy of keratin assembly and dis-assembly in the cytoplasm.** (A) MCF-7 cells expressing AcGFP-K2 form globules mostly at the cell periphery. A globule is formed at 3.5 min (shown by an arrow), which slowly starts to integrate into filaments and completes the integration in 1.3 h. Another globule is shown in 1.7 h that is integrating into the network at 3h. (B) The keratin filaments that are spread across the cytoplasm constantly move towards the nucleus away from the cell periphery as a band. This band contains only filaments and could constitute the polymerisation zone for the filaments in the cytoplasm. This figure shows the integration of keratin granules into existing network and its directionality. Spinning disk confocal microscope was used for recording images. (Scale bar = 10  $\mu$ m).

### 3.4. Keratin hyperphosphorylation breaks down filaments in MCF-7 cells (use of phosphatase inhibitors).

To investigate the disruption of keratin network by phosphorylation, untransduced MCF-7 cells were treated with two inhibitors, OA and CL-A the potent inhibitors of PP1 and PP2A. The disrupted filaments were visualised by immunostaining using LE65 (mAb) and AF-488 labelled anti-mouse secondary antibody. Different concentrations of both inhibitors were tested, and images shown are for concentrations that showed breakdown of the filaments while cells were still attached. For OA the working concentration was 300 nM incubated for 3 h (Figure 3.5), while for CL-A the working concentration was 2 nM for 1h (optimisation data shown in Figure A.1 in appendix), suggesting a more potent effect of CL-A compared to OA. Filaments breakdown as a result of phosphatase inhibitors treatment is shown in Figure 3.6.

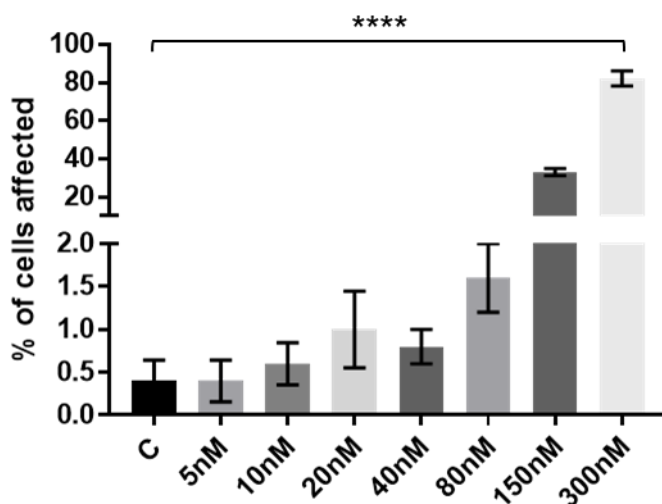


**Figure 3.5. Keratin filament disruption at different concentrations of OA.** MCF-7 cells were grown in full medium (DMEM, 10% FCS, 1% PS), treated with different concentration of OA for 3 h. The Number of cells with disrupted keratin network were converted into percentage and plotted against OA concentrations. The criteria used for OA effect was when filaments started to breakdown and show fluorescent granules in the cytoplasm. Around 500 cells were counted and investigated for filament disruption at each concentration. STAT: n=3, Error bars=SEM, one-way ANOVA= \*\*\*\* significance, p-value ( $p \leq 0.0001 = ****$ ).

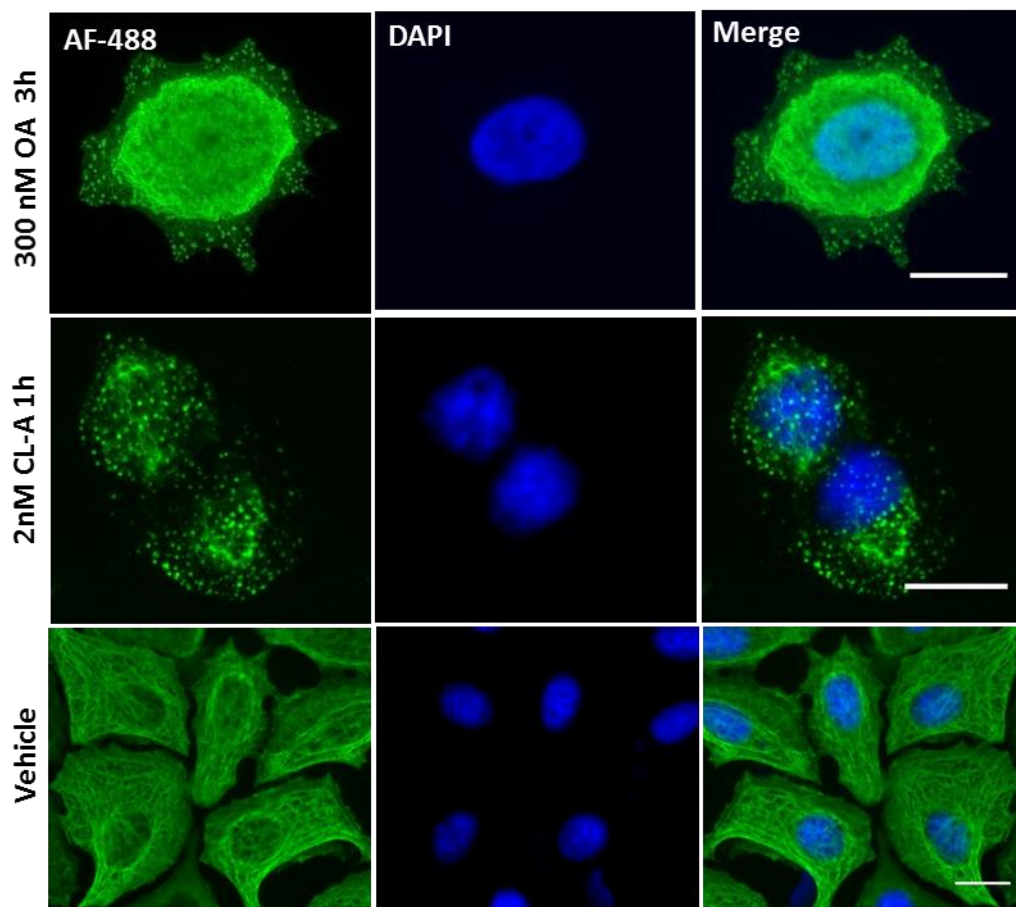


**Figure 3.6. Disruption of endogenous keratin network induced by phosphatase inhibitors (OA and CL-A).** MCF-7 cells grown in full medium (DMEM, 10% FCS, 1% PS), treated with 300 nM OA for 3 h showed breakdown of filaments into granules starting at the cell periphery. A more extensive breakdown was shown using 2 nM of CL-A for one hour. DMF treated cells for up to 3 hours are shown as a vehicle control. All cells were immunostained with mAb LE65 and AF-488-labelled anti-mouse secondary antibody. Nuclei are stained with DAPI in blue and overlapping of immunostaining with DAPI is shown as Merge. This figure shows that CL-A is more potent than OA in breaking down keratin filaments. Leica DM5000B Epi-fluorescence microscope and DFC350 camera were used for recording images. (Scale bar = 20  $\mu$ m).

### **3.5. Filament breakdown in MCF-7 cells expressing AcGFP-K2 or FLAG-K2 using phosphatase inhibitor CL-A: role of phosphorylation.**

#### **3.5.1. Analysis of CL-A induced keratin phosphorylation by immunostaining.**

To study the effect of phosphatase inhibitors on MCF-7 cells expressing AcGFP-K2 or FLAG-K2, 2nM CL-A inhibitor for only 30 min was used (not 1h as used for untransduced cells) as at this time point filaments were already breaking down in AcGFP-K2 transduced cells (1h in AcGFP-K2 was rounding up and lysing some cells as shown in Figure A.2 in appendix). In FLAG-K2 transduced cells the same time point was used for comparison. The cellular cytoskeleton was labelled with 3x FLAG without (Figure 3.7A) or with the attached K2 using retroviral transduction (Figure 3.7B). The transduced cells were treated with 2nM CL-A in DMF for 30 min (d, e, f and m, n, o) or 0.05% DMF as vehicle control (g, h, I and p, q, r) or without any treatment (a, b, c and j, k, l). The MCF-7 cells expressing only the FLAG tag (Figure 3.7A, a-i) will not label the cytoskeleton as the construct does not contain keratin cDNA. These cells were immunostained with mouse LE65 (mAb) followed by AF-488 anti-mouse secondary antibody to visualise the endogenous cytoskeleton (Figure 3.7A, a-i). On the other hand, the keratin cytoskeleton of MCF-7 cells transduced with FLAG-K2 should label the cytoskeleton as the K2 protein will integrate into the pre-existing keratin network and will label the cytoskeleton with anti-FLAG antibody followed by AF-488 labelled anti-mouse secondary antibody (Figure 3.7B, j-r). As shown in Figure 3.7B the keratin cytoskeleton in all panels appeared identical to those transduced with only FLAG vector control (Figure 3.7A) suggesting that the presence of K2 did not alter the organisation in MCF-7 keratin network. Furthermore, the keratin

network organisation in MCF-7 cells treated with 2nM CL-A for 30min remained identical to those untreated or treated with DMF as vehicle control. These observations suggest that 2nM CL-A does not induce enough phosphorylation to cause disruption of keratin filament network. To investigate if increasing the size of the tag would amplify the effect of CL-A, 3x FLAG was replaced with AcGFP, which is about 10 times larger than the former. Cells transduced with vector control virus and expressing only AcGFP were stained with LE65 mouse mAb and AF-488 to visualise the endogenous keratin network. AcGFP-K2 cells did not require any further immunostaining as K2 was integrated into the pre-existing keratin network which was lighting up green on the fluorescence microscope. The MCF-7 cells transduced with AcGFP-C or AcGFP-K2 were treated with 2nM CL-A in DMF for 30 min (d, e, f and m, n, o) or 0.05% DMF as vehicle control (g, h, i and p, q, r) or without any treatment (a, b, c and j, k, l). Immunofluorescence analysis showed filament breakdown in AcGFP-K2 cells after treating these cells with 2nM CL-A in about 30 min compared to AcGFP-C (Figure 3.8A; compare d, e and f with m, n and o). On the other hand, filaments in untreated or vehicle treated controls were intact. Comparing the data presented in Figure 3.7(m, n, o) with Figure 3.8 (m, n, o) clearly show that 2nM CL-A did not influence the filaments when a smaller tag, 3x FLAG was used. However, the same treatment disrupted the filaments when a much larger tag, AcGFP was used at the N-terminus. These observations suggest that integration of keratin polypeptides into pre-existing filaments is not dependent on the size of tag since both 3x FLAG and AcGFP tagged K2 polypeptides were integrated into the pre-existing filaments. However, the size of the tag does determine the stability of the integrated cytoskeleton, smaller tagged keratins do not influence stability whereas larger sized tags appear to destabilise the cytoskeleton (Figure 3.7 and 3.8). The



mechanism of destabilisation could involve change in the protein conformation due to integration of a bigger tag (AcGFP, 26 kDa) plus ( $\approx 70$  kDa) K2 of keratins into the cytoskeleton, perhaps exposing more phosphorylation sites that can be phosphorylated by the action of CL-A. Hyperphosphorylation of the exposed Ser/Thr sites due to AcGFP-K2 integration would collapse the endogenous cytoskeleton. This hypothesis is supported by the observation presented in section 3.4 that untagged MCF-7 cells required a much longer treatment with CL-A to breakdown filaments compared to tagged cells.

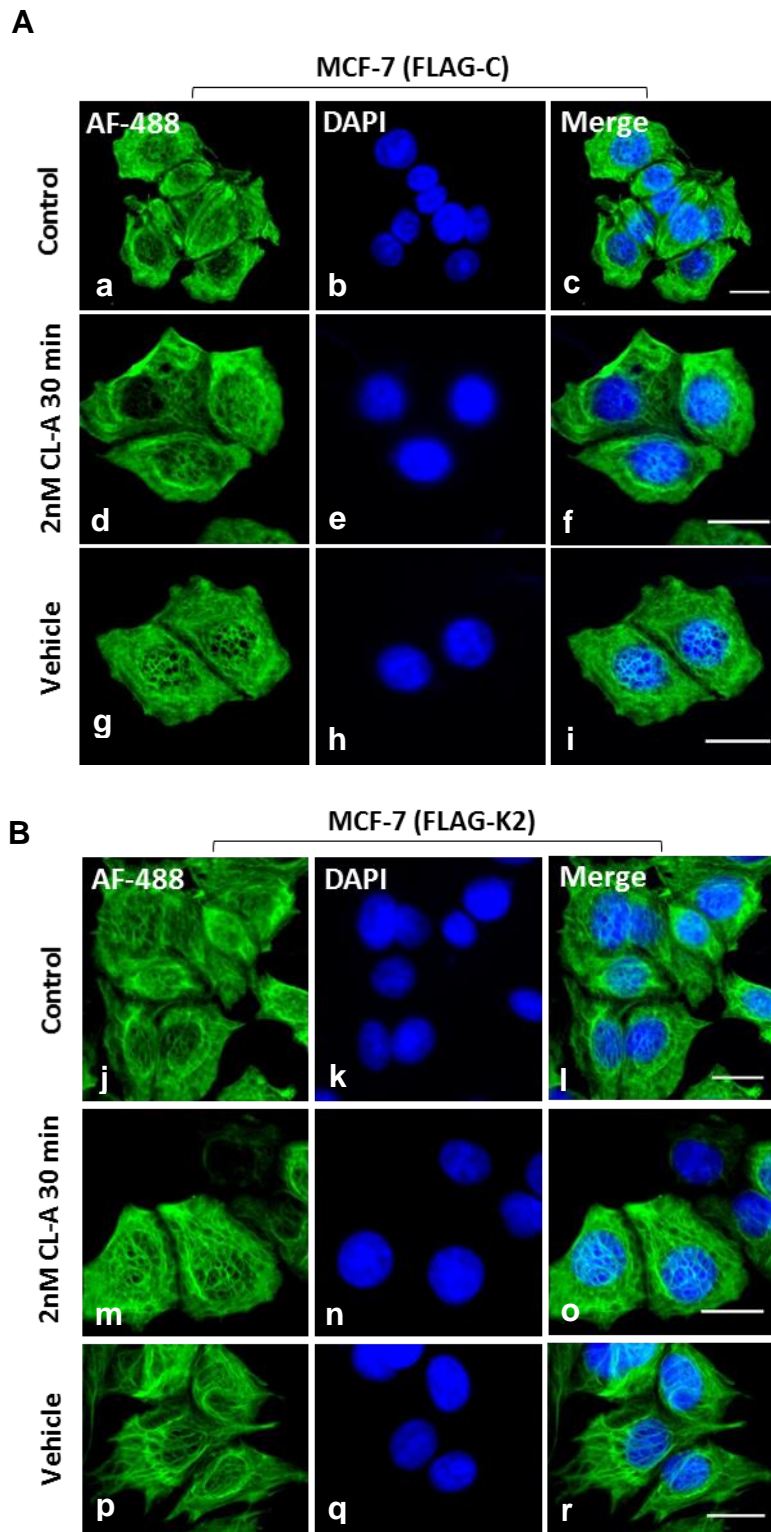


**Figure 3.7. MCF-7/ FLAG-K2 and Vector control transduced MCF-7 cells treated with 2nM CL-A.** Cells were grown in full medium (DMEM 10% FCS and 1%PS). Later medium was replaced by 2 nM CL-A containing medium for 30 min. No filaments breakdown was seen in these two types of transduced cells. Cells expressing Flag control vector were fixed and stained with LE65. Anti-FLAG mAb was used to stain FLAG-K2 cells. AF-488 labelled anti-mouse was used as a secondary antibody for LE65 and anti-Flag antibodies. Nuclei were stained with DAPI in blue, overlapping of DAPI and green shown as Merge. Control is untreated cells and vehicle control is DMF treated cell. This figure shows that the presence of FLAG tag didn't affect filaments stability. Leica DM5000B Epi-fluorescence microscope model and DFC350 camera were used for recording images (Scale bar=20  $\mu$ m).

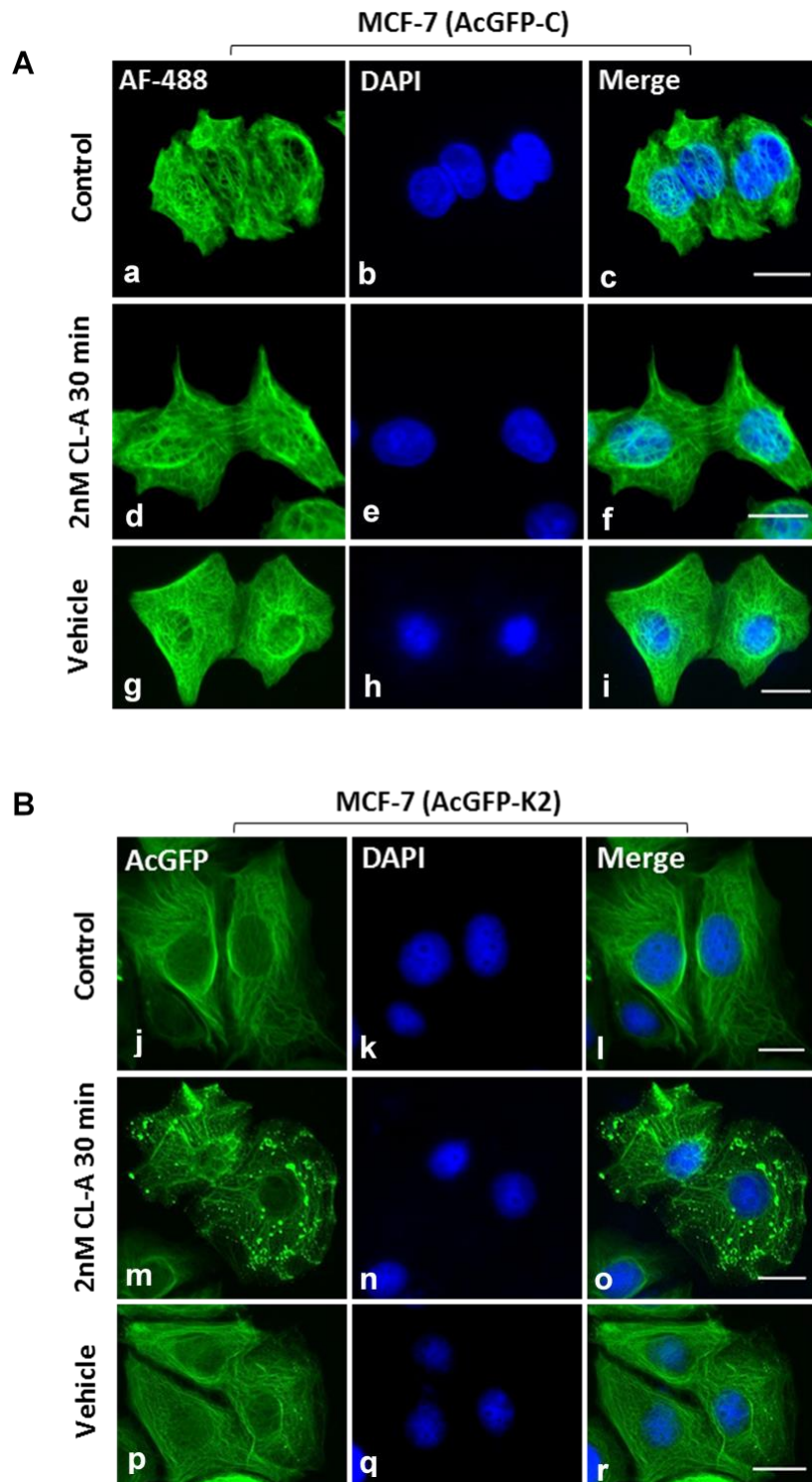


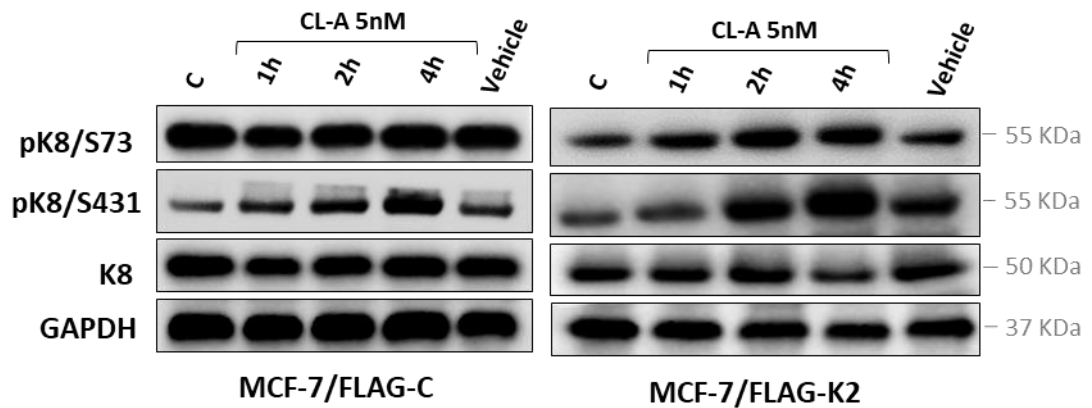
**Figure 3.8. Keratins in MCF-7/ AcGFP-K2 filaments breakdown after 2nM CL-A treatment.** Cells were grown in full medium (DMEM 10% FCS and 1%PS). Later medium was replaced by 2 nM CL-A containing medium for 30 min. AcGFP-K2 expressing cells shows filaments breakdown compared to AcGFP-C and (FLAG-K2 and FLAG-C) in Figure 3.7. Cells were fixed and stained with LE65 for those expressing AcGFP as control while those expressing AcGFP-K2 were showing green fluorescence due to integration of K2 into the pre-existing keratin network. AF-488 was used as a secondary antibody for LE65. Nuclei were stained with DAPI in blue, overlapping of DAPI and green shown as Merge. Control is untreated cells and vehicle control is DMF treated cell. This figure shows that the presence of AcGFP tag did affect filaments stability. Leica DM5000B Epi-fluorescence microscope equipped with DFC350 camera was used for image recording images. (Scale bar=20  $\mu$ m).

### **3.5.2. Analysis of CL-A induced keratin phosphorylation by western blotting.**

To further investigate the role of the tag in inducing hyperphosphorylation using CL-A phosphatase inhibitor, the transduced cells of Figure 3.7 and 3.8 were used and treated them with 5nM CL-A for increasing times, 1h, 2h and 4h before collecting lysates for protein analysis by western blotting. Keratin 8, an endogenous keratin of MCF-7 cytoskeleton, is known to be phosphorylated on residue S73 in response to stress (Toivola et al., 2002), which was discussed in detail in section 3.1. To monitor endogenous CL-A induced keratin phosphorylation K8 phosphorylation was used as detected by mAb targeting these phosphorylation sites in western blotting to investigate different phosphorylation levels induced by CL-A.

Both MCF-7/AcGFP-K2 and MCF-7/FLAG-K2 cells showed increased phosphorylation of S73 and S431 sites compared to their control cells at 2h and 4h of treatment each compared to vehicle or untreated controls (Figure 3.9 A, B). Quantification of WB in Figure 3.10 showed no statistical significance in the level of phosphorylation of S73 and S431 on both MCF-7/AcGFP-K2 and MCF-7/FLAG-K2 cells using Two-way ANOVA. These data indicate that the size of the tag did not affect the level of phosphorylation and the breakdown that was seen in Figure (3.7B, m-o) was not a result of higher levels of phosphorylation.

**A**



**B**

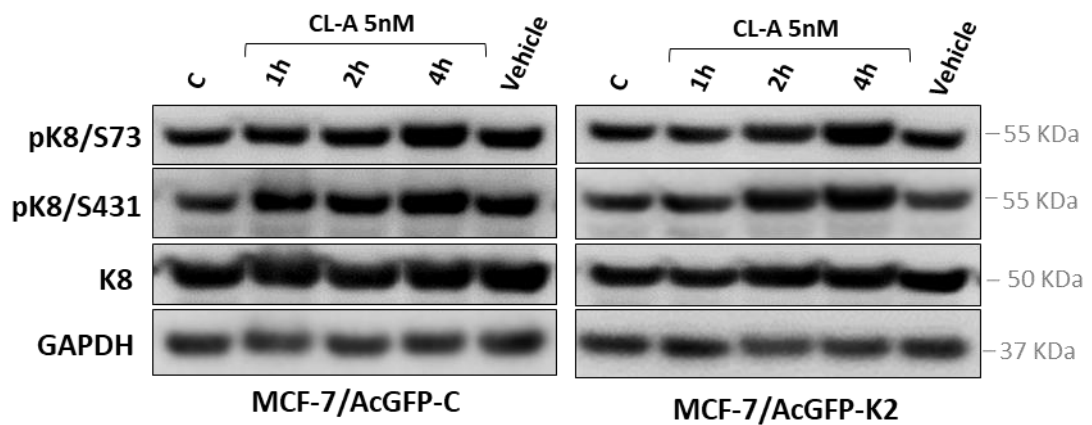
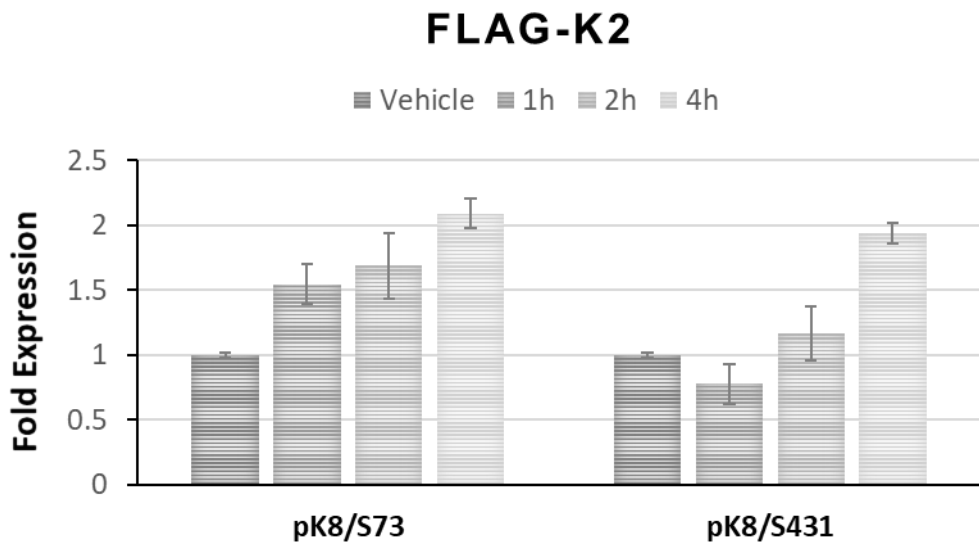
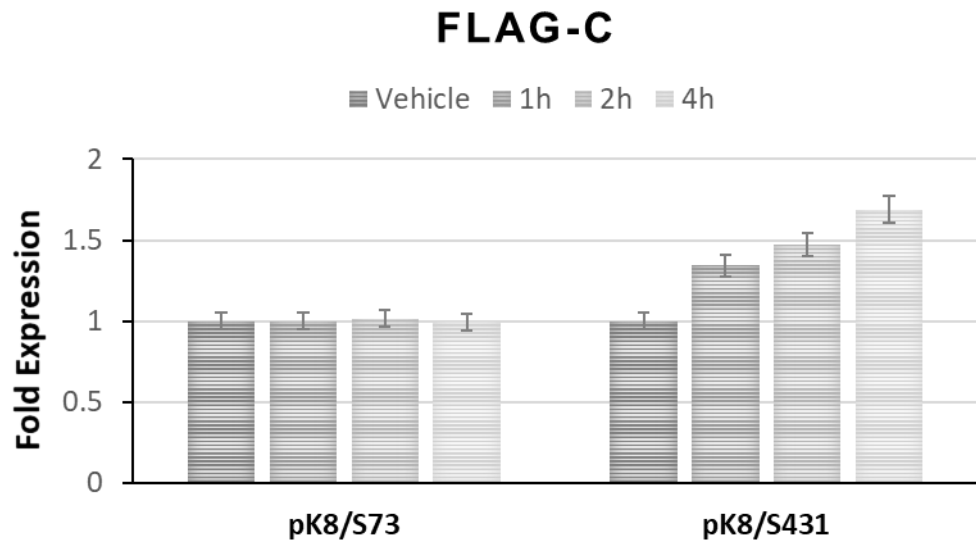


**Figure 3.9. Western blot showing hyperphosphorylation of K8 induced by CL-A in MCF-7 transduced cells.** Cells were grown in full medium (DMEM, 10%FCS,1% PS), treated with 5nM CL-A for different time points (1h, 2h, 4h). Control is untreated cells; vehicle are cells treated with 0.05% DMF. FLAG-K2 cells show more phosphorylation of pK8/S73 and pK8/S431 compared with FLAG-C (A). Similarly, AcGFP-K2 cells shows stronger phosphorylation of pK8/S73 and pK8/S431 compared with AcGFP-C after 4h treatment (B). GAPDH was used as loading control. This figure shows that filaments breakdown seen earlier is not due to hyperphosphorylation. ChemiDoc™Biorad imaging system was used for protein detection.

A



B

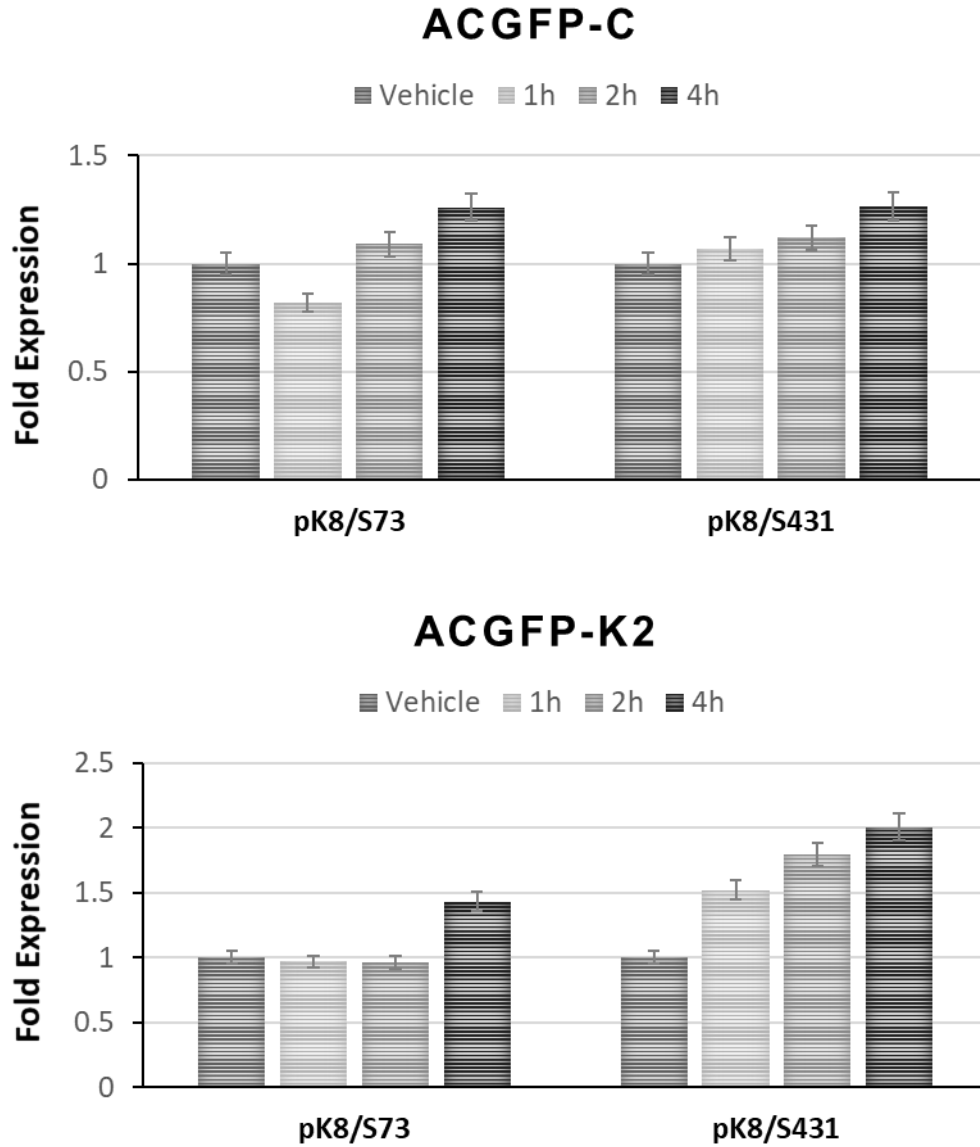


**Figure 3.10. Western blot quantification of Figure 3.9.** Quantification of WBs shown in Figure 3.9 after normalisation to loading control and later to Vehicle control values. Data for untreated control was taken arbitrarily as 1, other treated values (5nM CL-A up to 4h) are shown as fold expression. (A) FLAG-K2 and FLAG-C and (B) AcGFP-K2 and AcGFP-C.

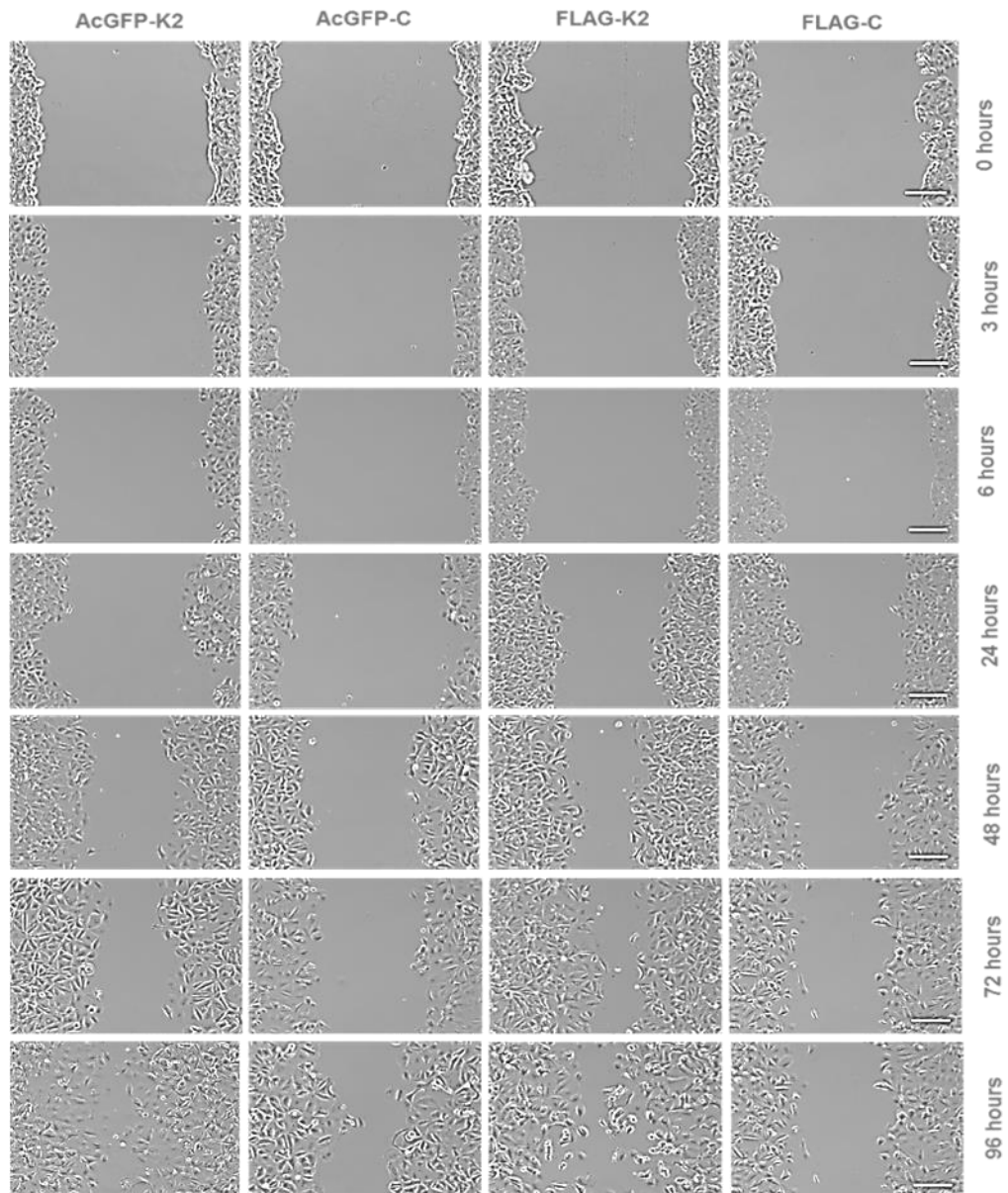
### 3.5.3. Effect of K2 on migration of MCF-7 cells.

The effect of introducing K2 into MCF-7 cells with both tags (FLAG vs AcGFP) on cell migration using the scratch assay was investigated. As hyperphosphorylation breaks down filaments into globules that allow the cell to be less rigid and more flexible and easy to move (a phenomenon seen during EMT), a hypothesis was made that having a high molecular weight protein (K2) tagged either to AcGFP or FLAG that allows more phosphorylation to take place compared to vector control cells as shown in Figure 3.7 – 3.9 will allow cells to move faster. This was based on the fact that keratin nucleation takes place at the focal adhesion sites and that globules can bind to some focal adhesion components such as integrin and may play a role in cell migration (Windoffer et al., 2011). Transduced MCF-7 cells were plated to about 100% confluence and treated with 40 µg/ml Mitomycin C to inhibit proliferation. A scratch was made in the middle of the plate using a pipette tip and first set of images were recorded immediately and that was taken as 0 h recording (Figure 3.11 A). The scratch was imaged at regular intervals and several time points were taken up to a maximum of 96 h. From the images taken the surface area unoccupied by migrating cells was calculated using the image J software. The surface area of 0 h for all cells were calculated using the surface area measuring tool in image J and converted into 100%. Other time points areas were subtracted from the 0 h time area and converted into percentage. This percentage was used to measure wound closure over time as shown in (Figure 3.11,B) It is clear that cells expressing K2 showed faster movement compared with cells transduced with the empty vector. FLAG-K2 transduced MCF-7 cells were showing higher percentage of wound closure, and therefore faster migration, compared to AcGFP-K2 which could probably be explained by being easier to bind to focal adhesion component than a bigger tag. Further



experiments are required on co-localisation with focal adhesion components and the role of different size tags in binding to focal adhesion proteins.

**A**



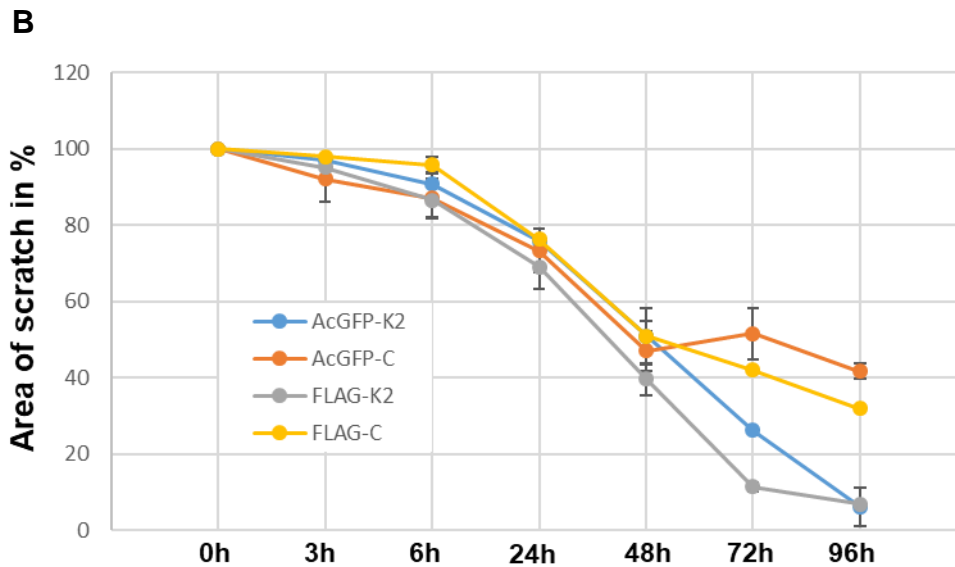


**Figure 3.11. Wound closure of MCF-7 cells transduced with (AcGFP-K2, FLAG-K2, AcGFP control and FLAG control).** (A) MCF-7 cells stably expressing different constructs were plated in 12 well plates until 100% confluent. Scratch was made in the middle of the well after inhibiting proliferation using 40µg/ml mitomycin C, images were recorded at different time intervals. Nikon Eclipse TE 2000-S microscope was used (scale bar=200µm). (B) Graph showing wound closure in term of percentage of scratch area in 4 different transduced MCF-7 culture samples used in this experiment. This figure shows that FLAG-K2 cells migrate faster than other cells. STAT: n=3, Error bars=SEM, Two -way ANOVA was used between each group and its control and between AcGFP-K2/FLAG-K2, p-values ( $p \leq 0.001 = **$ ,  $p \leq 0.0001 = ****$ ).

AcGFP-K2/AcGFP-C ( $p \leq 0.001 = **$ ), FLAG-K2/FLAG-C ( $p \leq 0.0001 = ****$ ),

AcGFP-K2/FLAG-K2 ( $p \leq 0.0001 = ****$ ).

### 3.6. Role of heat shock stress on keratins organisation and phosphorylation.

#### 3.6.1. Effect of heat shock on endogenous filaments network of MCF-7.

MCF-7 cells were grown in full medium (DMEM, 10% FCS, 1% PS) in a 37°C incubator and next day the medium was changed to 43°C pre-warmed medium and cells were incubated in a 43°C water bath for 30 min and later transferred to 37°C incubator for 15 min recovery as described in section 2.2.2 in materials and methods section. Cells were fixed with acetone/methanol and stained with LE65 mAb detecting K8/K18 (endogenous keratins) and AF-488 as a secondary antibody. As shown in Figure 3.12, in MCF-7 cells that were heat shocked the

filaments were more condensed around the nucleus compared to spread-out network before the heat shock.

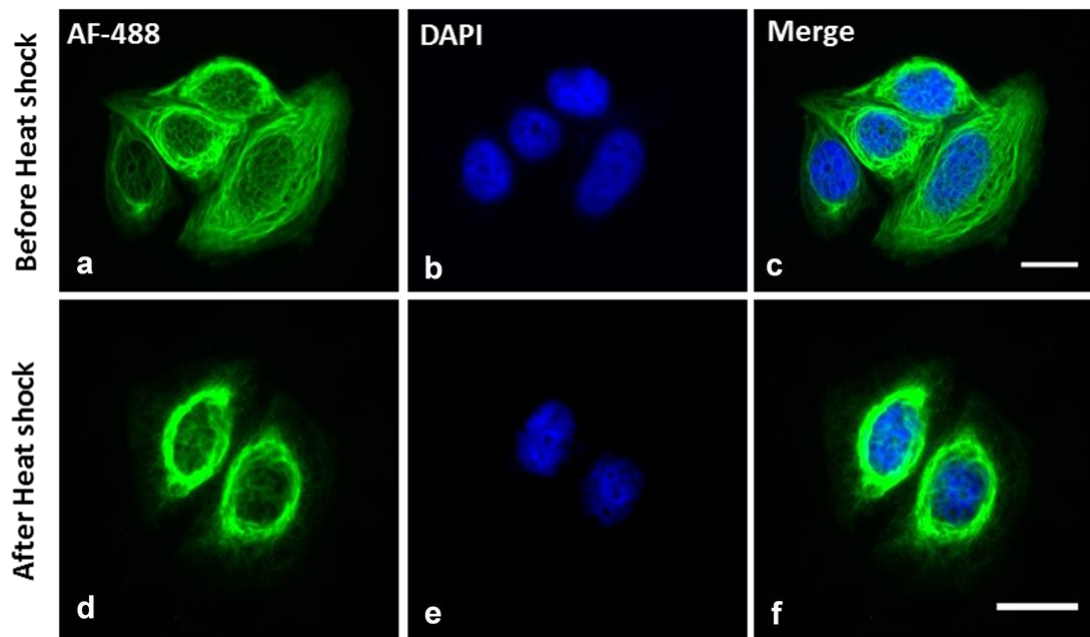


**Figure 3.12. Effect of heat shock on endogenous keratins in MCF-7 cells.** MCF-7 cells grown in full medium (DMEM + 10%FCS + 1%PS) on collagen coated glass coverslips were given a heat shock of 43°C for 30 min followed by a 15 min recovery at 37°C. MCF-7 cells before heat shock were used as control. The endogenous keratin network was stained using LE65 mAb and AF-488 (Green), Nuclei were stained with DAPI in blue and overlapping was shown as Merge. This figure shows that heat shock allowed keratin filaments to move and condense around the nucleus. Leica DM5000B Epi-fluorescence microscope and DFC350 camera were used for recording. (Scale bar =20  $\mu$ m).

### **3.6.2. Stabilisation of endogenous keratin network in MCF-7 cells following heat shock.**

As phosphatase inhibitors were used to induce phosphorylation of keratin polypeptides in our experiments, different concentrations of CL-A were tested on MCF-7 endogenous keratins over different time intervals and 2 nM for 1 h was used as it breaks down the filaments without affecting cell viability as mentioned in section 3.3 and shown in Figure 3.6. In this set of experiments, two sets of MCF-7 cells were used. One set was treated with 2nM CL-A while the other set was given a heat shock for 30 min at 43°C then allowed to recover for 15 min at 37°C followed by treatment with 2 nM CL-A for 1 h. As shown in Figure 3.13 (a, b, c) treating MCF-7 cells with 2 nM CL-A for 30min caused almost complete collapse of filaments into globules. However, when these cells were given a prior heat shock followed by 2 nM CL-A treatment (HS + 2nM CL-A) the filaments were still spread and no sign of filament breakdown into globules was observed (sign of phosphorylation) suggesting that heat shocking the cells before CL-A treatment protected the cytoskeleton against phosphorylation induced filament breakdown, which could be explained by thermotolerance (the ability of cells to withstand another stress after being subjected to a former heat shock), which is explained in more details in section 3.1.

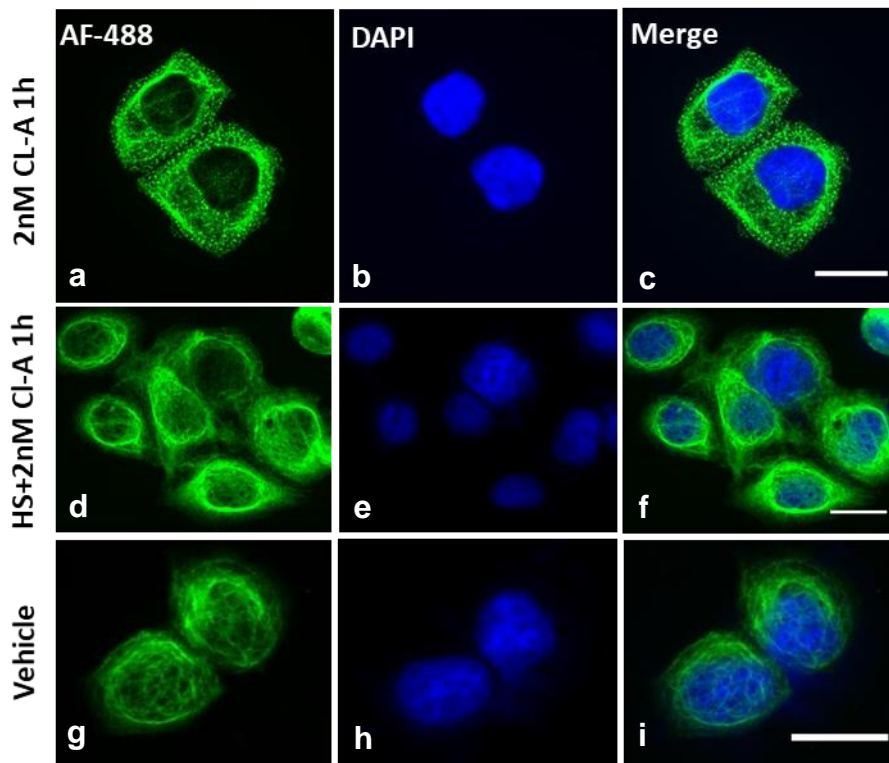


**Figure 3.13. Effect of 2nM CL-A on MCF-7 keratin filaments with and without heat shock.** MCF-7 cells were grown in full medium (DMEM + 10% FCS + 1% PS) on collagen coated glass coverslips, cells were treated with 2nM CL-A for 1 h and shows breakdown of filaments into smaller globules (a, b, c). Another group of cells were heat-shocked at 43°C for 30 min with 15 min recovery at 37°C then treated with 2nM CL-A 1h (d, e, f). DMF treated cells for 1 h was used as control (g, h, i). All cells were fixed using acetone/methanol (1:1) and immunostained using LE65 mouse mAb detecting the endogenous keratins and AF-488 was used as a secondary antibody. DAPI stained in blue and overlapping is shown as 'Merge'. This figure shows that heat shock protect or delay filaments breakdown caused by CL-A. Leica DM5000B Epi-fluorescence microscope and DFC350 camera were used for recording. (Scale bar =20 µm).

### **3.6.3. Recovery of MCF-7 cytoskeleton containing AcGFP-K2 after heat shock.**

The effect of heat shock on the endogenous network of untransduced MCF-7 cells was investigated in (section 3.6.1) but to be able to track the changes and dynamics of keratin filaments after heat shock, AcGFP-K2 tagged MCF-7 cells were used, which labelled the cytoskeleton with a green fluorescent tag (AcGFP) to allow us to visualise and live track any changes as shown in section 3.3. Cells were grown in full DMEM medium on glass bottom live imaging plates. Next day, the medium was changed to 43°C pre-warmed medium and incubated in a water bath set at 43°C for 30 min for the heat shock (same procedure as used for untransduced MCF-7 cells, sections 3.6.1 and 3.6.2). After the heat shock, plates were moved immediately to a spinning disk confocal microscopic stage maintained at 37°C and started the recording. In Figure 3.14 images were taken every 10 min to track the changes. The bright field imaging was used to show that cells were normally spread out and not affected by heat shock up to 30 min. The overlapping images clearly show that keratin filaments (green) have moved toward the nucleus and condensed around it but it slightly started to move back toward the periphery as pointed by a white arrow at 10 min. This could be part of the recovery phase after the shock as the spinning disk temperature was maintained at 37°C. Therefore, to track the recovery of the filaments and their spreading to the cell periphery a longer time was needed. The same cells (MCF-7 expressing AcGFP-K2) were used under the same conditions but the cells were left to recover for 15 min in a 37°C incubator before starting the recording (Figure 3.15). The bright field imaging showed no change in cell membrane periphery overtime, but the filaments were moving toward the periphery of the cell as shown

by yellow arrow pointing at the cell membrane that at 0 min there was no filament reaching that point but after 30 min the filaments spreads back reaching to the cell membrane.

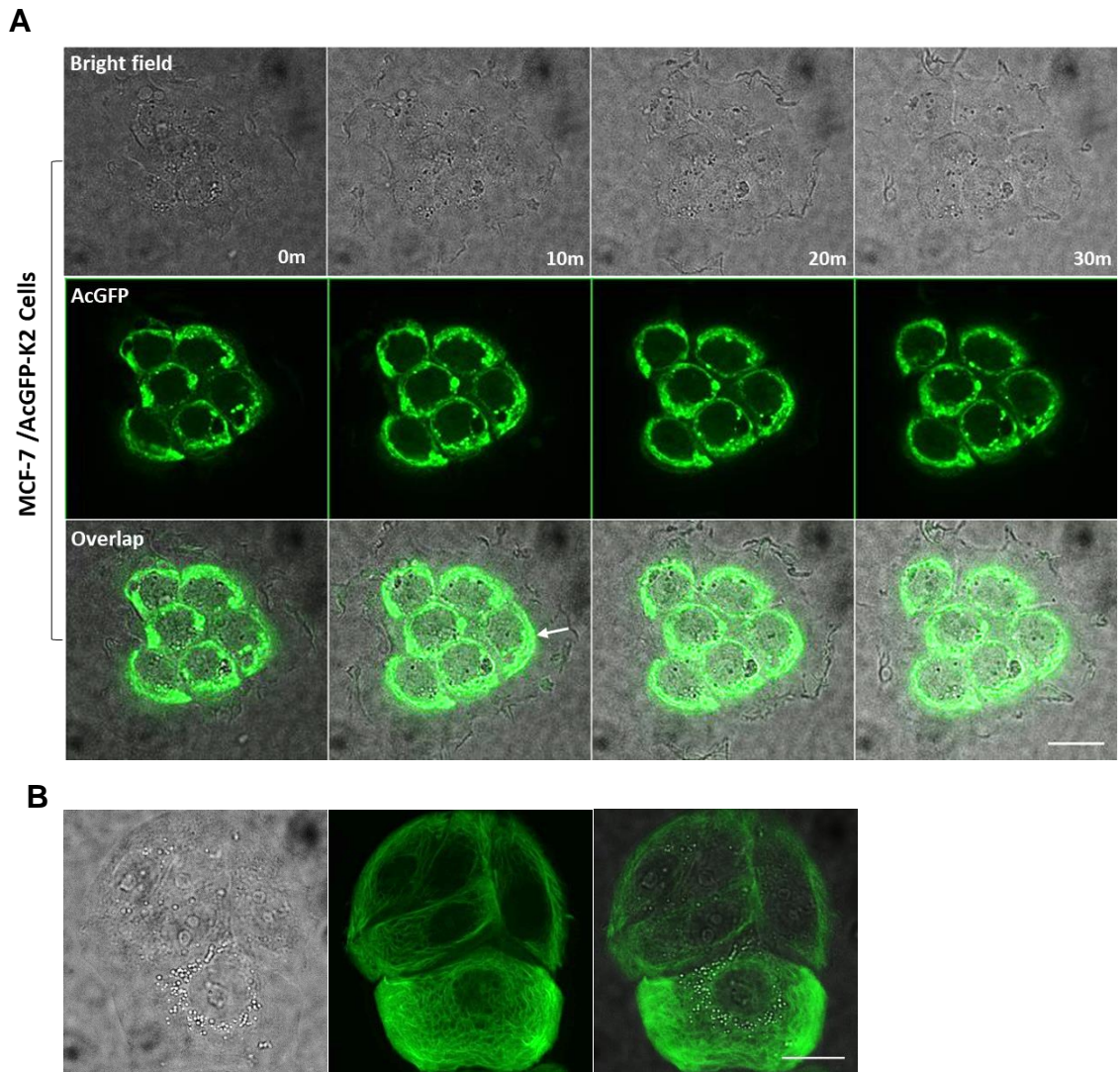


**Figure 3.14. Time-lapse imaging of MCF-7 cells expressing AcGFP-K2 following heat shock.** MCF-7 cells stably expressing AcGFP-K2 were grown in full medium (DMEM + 10% FCS + 1% PS) for 48 h at 37°C then subjected to a heat shock at 43°C for 30 min without any recovery period. Recording started immediately after the shock and snaps at 10 min intervals were taken. Bright field snaps are shown in the top set. AcGFP fluorescent cells shown in the second and composite of bright field and AcGFP sets are shown as overlap (A). Compared to cells before heat shock (B) reorganisation of filaments around the nucleus away from the cell periphery as a response to the heat shock was clear. This figure shows that keratin filaments move toward the nucleus after heat shock. Spinning disk confocal microscope was used for recording. (Scale bar =20µm).

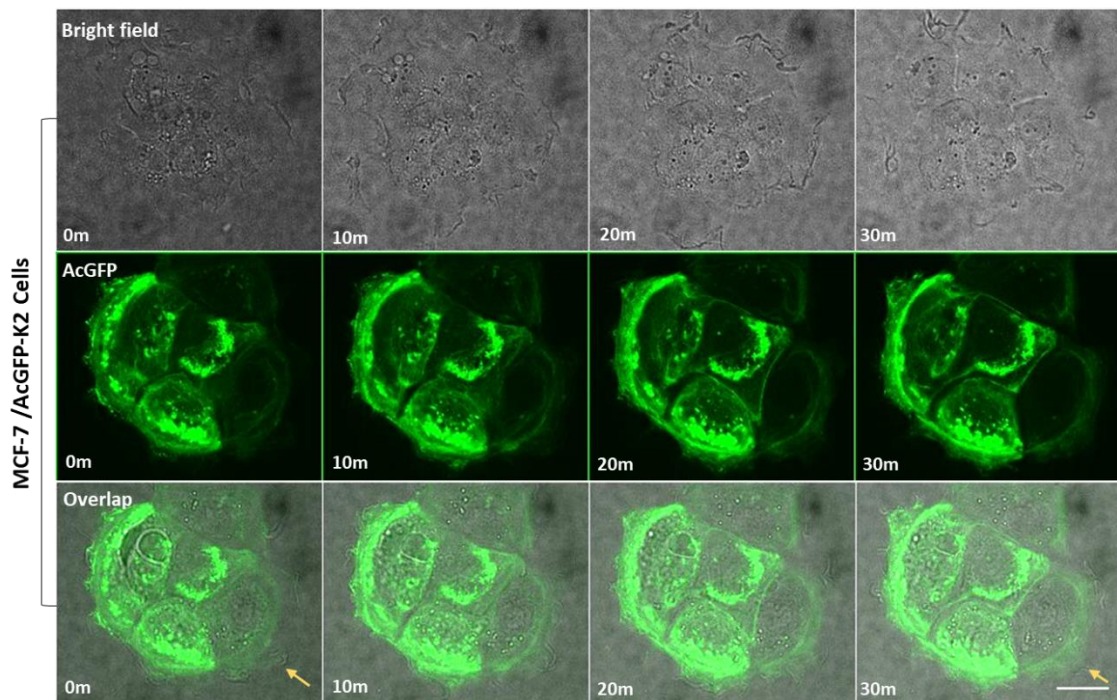


**Figure 3.15. Time-lapse imaging of AcGFP-K2 expressing MCF-7 cells following heat shock and recovery.** MCF-7 cells stably expressing AcGFP-K2 were grown in full medium (DMEM + 10% FCS + 1% PS) for 48 h at 37°C then subjected to a heat shock at 43°C for 30 min and 15 min recovery at 37°C. Recording started after the recovery period and snaps were taken at 10 min intervals, bright field snaps are shown in the top set. AcGFP fluorescent cells shown in second and composite of bright field and AcGFP are shown as overlap. Compared to cells in Figure 3.14 reorganisation of filaments back toward the cell periphery during recovery can be seen. This figure shows that recovery time after heat shock allows keratin filaments to spread out to cell periphery. Spinning disk confocal microscope was used for recording. (Scale bar =20µm).

### 3.6.4. Stabilisation of MCF-7 cytoskeleton containing AcGFP-K2 after heat shock.

In this set of experiments, MCF-7 cells expressing AcGFP-K2 were seeded on glass bottom dishes for live imaging and after 48 h the culture medium was replaced with live cell imaging clear medium containing 300 nM OA and plates were placed under the spinning disc microscope to start recording. The live cell imaging of keratin filaments showed that the filaments started to breakdown into globules at around 7 min after drug application and the breakdown continued in other cells as well and increased overtime until the whole keratin network was



turned into globules after 3 h (Figure 3.16). AcGFP-K2 transduced MCF-7 cells treated with OA were compared to another group of cells that was heat shocked for 30 min 43°C followed by 15 min recovery at 37°C prior to OA treatment. In both Figures 3.16 and 3.17 the same time frames were selected for better comparison so, it can be seen in Figure 3.17 that only after one hour of drug treatment, filaments started to break down but on later time points breakdown looks similar in heat treated and untreated cells. These observations support the data shown in Figure 3.13 in which heat shocked MCF-7 cells treated with 2 nM CL-A showed no breakdown in the first hour. A hypothesis that something was delaying the breakdown of filaments was made and this could be by inhibiting phosphorylation pathways (breakdown of filaments) and as the type of stress that was applied is heat, heat shock proteins (HSPs) were predicted to be playing a role and this was investigated in the next set of experiments. As mentioned in section 3.4 that CL-A is more potent and takes less time to breakdown filaments compared to OA but in this set of experiments ,tracking changes slowly overtime was needed as well as more time for HSPs was allowed to be activated, as a result OA was used.

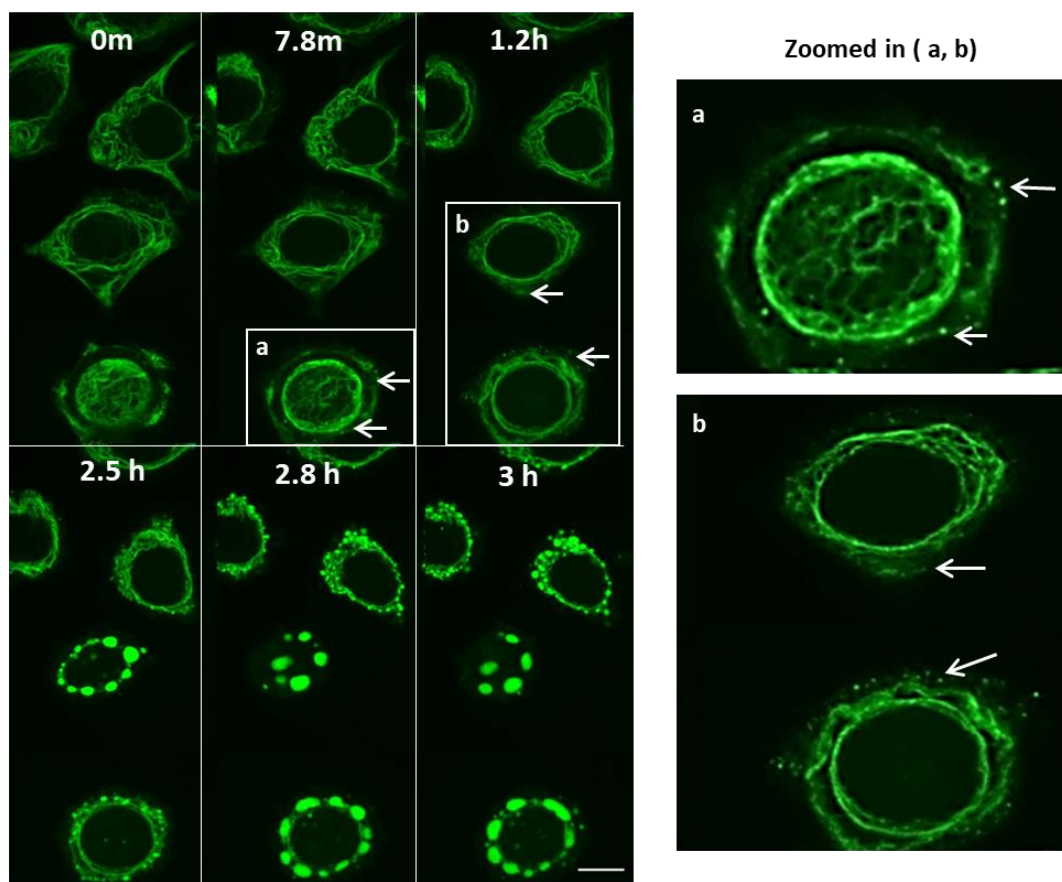


**Figure 3.16. Treatment of AcGFP-K2 expressing MCF-7 cells with OA.** AcGFP-K2 transduced MCF-7 cells were grown in full medium (DMEM +10% FCS +1% PS) at 37°C on glass bottom dishes suitable for live imaging and after 48 h medium was replaced with live cell imaging medium containing 300nM OA and recording started immediately for 3 h. Frames were selected at different time intervals in which changes were pronounced. Filaments spread with no breakdown in 0 min, after around 7.8 min filaments started to break into small globule at cell periphery. More cells are involved, and more breakdown of filaments are seen over time up to 3h (arrows in zoomed in images of a and b are showing keratins granules or breakdown). This figure shows breakdown of filaments due to OA treatment. Spinning disk confocal microscope was used for recording. (Scale bar =20  $\mu$ m).

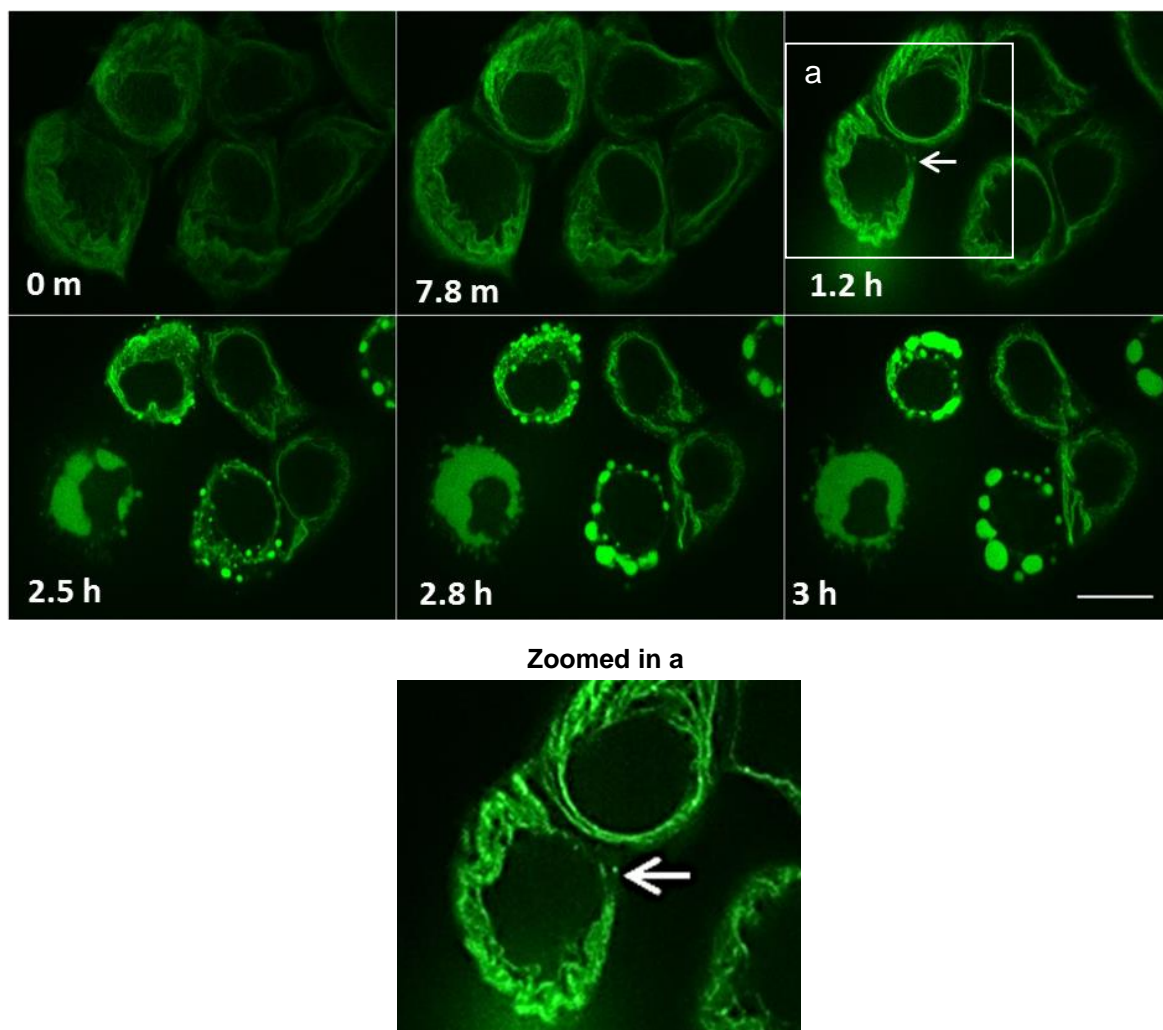


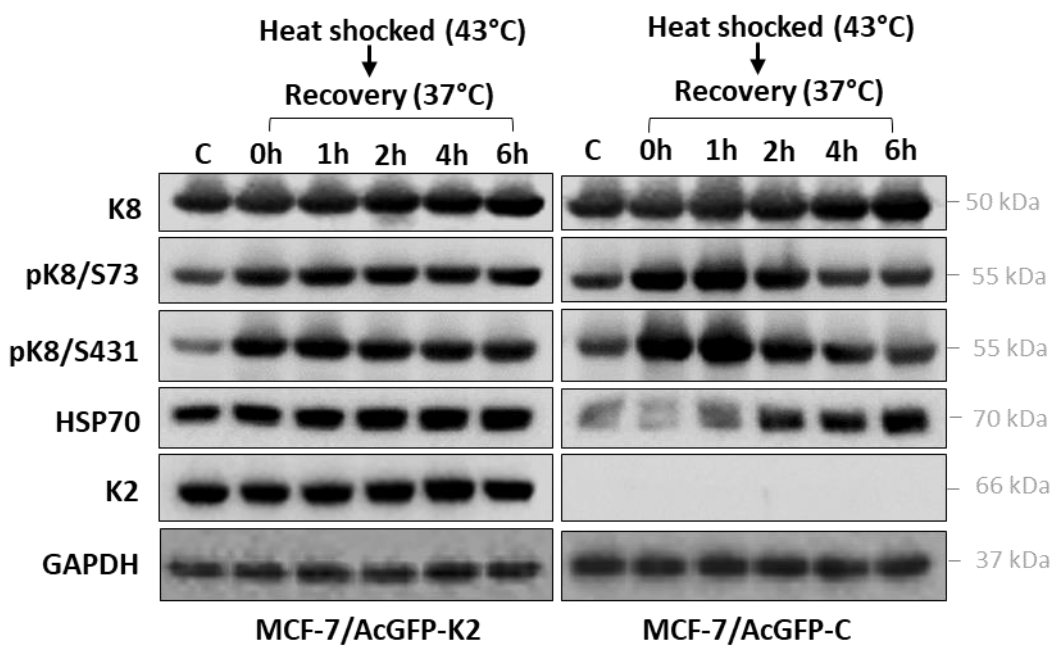
**Figure 3.17. Treatment of AcGFP-K2 expressing MCF-7 with OA after heat shock.** AcGFP-K2 expressing MCF-7 cells were grown in full medium (DMEM + 10% FCS + 1% PS) at 37°C incubator on glass bottom dishes suitable for live imaging and after 48 h the medium was replaced by 43°C warmed medium and cells were heat shocked at 43°C for 30 min followed by 15 min recovery at 37°C. After the heat shock the medium was replaced with live cell imaging medium containing 300nM OA and recording started immediately for 3 h. Frames were selected with the same time intervals as in Figure 3.16 for comparison. No filament breakdown was seen before 1.2 h. At 1.2 h breakdown started as shown by an arrow (arrow in zoomed in image a is showing keratins granules or breakdown). More cells were involved, and more breakdown of filaments was observed over time. This figure shows that heat shock delayed filaments breakdown caused by OA treatment. Spinning disk confocal microscope was used for recording. (Scale bar =20  $\mu$ m).

### **3.6.5. Role of heat shock protein 70 (HSP70) in keratin phosphorylation induced by heat shock in MCF-7 cells.**

As shown in sections 3.6.2 and 3.6.4 that heat treatment either delays or inhibits breakdown of filaments when phosphorylation is induced by OA or CL-A phosphatase inhibitors and a hypothesis was made that HSP may be playing a role in this phenomenon. So, MCF-7 cells were grown in full medium (DMEM + 10% FCS + 1% PS) at 37°C. Next day, medium was replaced by 43°C pre-warmed medium and cells were heat shocked for 30 min in a 43°C water bath. Recovery periods varied from 0h to 6h and this was done by replacing the medium with pre-warmed medium at 37°C and incubating for different time intervals. At each time point, the cells were washed twice with PBS and lysates were collected. Cells prior to heat shock were used as a negative control. WB analysis was performed using SDS gel electrophoresis and pK8/S73, pK8/S431, K8, K2 and HSP70 primary antibodies were used to detect the level of phosphorylation and the level of these proteins in transduced MCF-7 cells after heat shock followed by recovery. Figure 3.18 (A, B) shows K8 phosphorylation in transduced MCF-7 cells, in AcGFP-K2 cells there is an increase in pK8/S431 compared to pK8/S73 after heat shock and up to 1h recovery time. Later pK8/S431 showed a lower yet stable pattern up to 6 hours of recovery. pK8/S73 showed same pattern as pK8/S431 in these cells with less protein expression. HSP70 showed higher expression after heat shock and a stable expression throughout recovery time. In comparison AcGFP-C/MCF-7 cells were showing high expression of pK8/S73 and pK8/S431 after heat shock and 1h recovery time while HSP70 was showing low expression. At 2 h recovery and up to 6 h, pK8/S73 and pK8/S431 were showing gradual decrease in protein expression with pronounced increase in HSP70. This indicates that HSP70 could affect phosphorylation thereby making

the filaments more stable and less prone to break down. In the case of AcGFP-K2 a stable pattern of HSP70 expression was observed with very slight reduction of pK8/S431 which indicates a role of K2 itself in changing the cytoskeletal conformation that could affect the availability of different phosphorylation sites. In conclusion, pK8/S431 is more phosphorylated compared to pK8/S73 after heat shock. Phosphorylation of both sites is reduced after 2 h recovery and up to 6 h and this reduction is more prominent in AcGFP-C cells. K8 antibody (M20) was used to detect total K8 in both cell types while K2 antibody was used to show cells expressing K2.

**A**



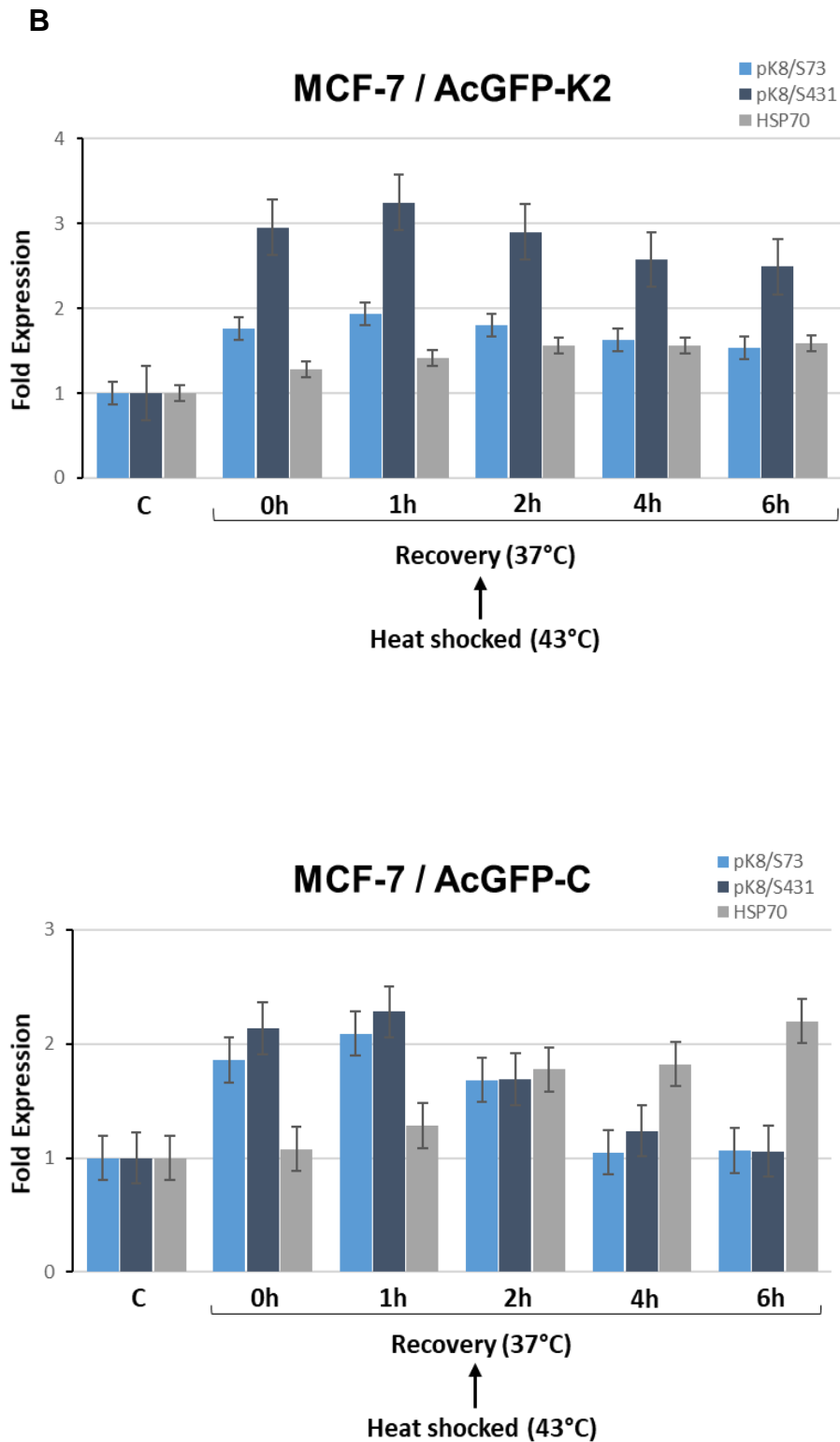


**Figure 3.18. Heat shock effect on keratin phosphorylation in AcGFP-K2 and AcGFP-C transduced MCF-7 cells.** AcGFP-K2 and AcGFP-C cells were grown in full medium (DMEM + 10% FCS +1% PS) at 37°C, after 48 h medium was replaced by 43°C pre-warmed medium for 30 min followed by 1h, 2h, 4h, and 6h recovery at 37°C. Lysates were collected for WB analysis using K8, pK8/S73, pK8/431, HSP70 and K2 primary antibodies to detect the level of these proteins after heat shock and recovery (A). Quantification of the blots in A are shown as fold expression in (B). GAPDH is used as a loading control. This figure shows that as heat shock increases, phosphorylation on S73 and S431 decreases. ChemiDoc™ Biorad imaging system was used for protein detection.

### **3.7. Discussion and conclusion.**

Keratins are dynamic and that means they are in an ongoing cycle of assembly and disassembly which gives them the ability to perform their wide range of functions within epithelial cells. During cell division, apoptosis, membrane trafficking, migration and wound healing keratin reorganisation is needed, and they are considered the major stabilising protein of the cytoskeleton (Strnad et al., 2001). This dynamic behaviour allows new keratin proteins to be introduced and integrated into an existing endogenous network without affecting cell stability (Windoffer et al., 2011). In normal human epidermis, changes in keratin gene expression take place as cells migrate from the basal layer that expresses K5/K14 upward during stratification. Keratins K5/K14 downregulates and a new set of suprabasal keratins, K1/K10, start to be activated and integrate into the existing network. In this process, new keratins are introduced and start to replace the existing ones (Waseem et al., 1999). This phenomenon was used to introduce a new keratin K2 into an existing network of K8/K18/K19 in MCF-7 allowing K2 to integrate into the network to be able to study the dynamics of this keratin in this cell-based model. Full integration of AcGFP and FLAG tagged K2 into MCF-7 was shown using retroviral transduction that allowed us to use this cell line as a model to study keratin filaments dynamics.

The cycle of assembly and disassembly of keratin polypeptides in cytoskeleton is basically a process of phosphorylation and dephosphorylation. This has been shown in previous studies in which phosphatase inhibitors were used to induce phosphorylation (Paramio, 1999, Toivola et al., 1997). Reorganisation of filaments during mitosis (physiological condition) in AcGFP-K2 MCF-7 cells were shown by live cell imaging using spinning disk confocal microscopy. During mitosis, filaments start to dis-assemble into small globules that allows the cell to

be more flexible for mitosis. After the cell division, the globules start to join at the periphery of the cell forming short filaments that later elongate while moving toward the nucleus forming a cage like structure (Figure 3.3 and 3.4) (Windoffer and Leube, 2004). When MCF-7 were treated with PP1A and PP2A phosphatase inhibitors OA and CL-A, keratin filaments show breakdown into granular structures while controls showed regular spread of filamentous keratin structure as shown in Figure 3.6. This is consistent with previous studies where keratin phosphorylation had been reported to be induced by OA treatment in keratinocytes (Yatsunami et al., 1993).

The state of phosphorylation of keratins inside the cell has to be balanced in order for the cell to function normally. This is regulated by kinases and phosphatases activities that stabilises the keratin network. If this balance is lost, deregulation of these enzymes occur as in the case of cancer, cells start to behave differently as their migration, proliferation and differentiation are affected (Bononi et al., 2011). Using phosphatase inhibitors does induce hyperphosphorylation that leads to filament breakdown and a weaker network inside the cell as shown in Figure 3.6, 3.13 and 3.16. In toxic liver disease, Mallory bodies are seen due to hyperphosphorylation and this has been shown primarily due to p38 kinase pathway activation which also play a role in other intermediate filaments aggregations that are seen in various diseases, including cardiac myopathy and numerous neurodegenerative disorders (Schutte et al., 2004, Woll et al., 2007). p38 is considered to be the major filament regulating signalling pathway involved in keratin phosphorylation and organisation in various physiological and stress or disease induced situations. S73 in the head domain of K8 is considered a major phosphorylation site by p38 kinase and it could also be phosphorylated through other pathways such as Jun kinases (JNKs). In K8 , S23 and S431 are also well



known phosphorylated sites they are activated under basal conditions or by SAPKs (JNKs and MAPK), respectively, while p38 phosphorylates only S73 (Woll et al., 2007). Phosphorylation of K8/S73 (on head domain) which is highly conserved among type II keratins and K8/S431 (on tail domain) as being well-known phosphorylation sites on K8 were investigated. MCF-7 cell line that expresses K8 was used, so antibodies against these well-known phosphorylation sites were used to study phosphorylation in our cell model (Toivola et al., 2002).

Although integration of a big protein (K2) that is around 70kDa into the cell tagged to a big tag such as AcGFP did not affect the normal cell division process or the directionality of the filaments moving inside the cell nor the globules integration into the network, it did affect the stability of the network. Using CL-A to induce phosphorylation that breakdown filaments into globules required less time in cells expressing AcGFP-K2 compared to cells expressing a smaller tag FLAG-K2 as well as the empty vector control tag AcGFP-C or FLAG-C. This could be explained by having a big protein tag that may change the conformation of the existing network allowing more phosphorylation sites to be exposed to the drug allowing more breakdown of the filaments (Figure 3.8). As in phosphorylation, there is an increase in negative charge either on head or tail that prevent the interaction of these parts with the negatively charged rod domain opening the protein structure. Seemingly, these changes could allow disassembly of the filaments and break them up into globules which is believed to be happening in wider scale in AcGFP-K2 tagged cells (Omary et al., 2006). However, there is an alternative explanation for the deleterious effect of the tag at the N-terminus of K2 on filament stability. In the filament assembly model, the rod domain of heterotypic keratins first associate as heterodimers followed by anti-parallel association into tetramers. In this model it has been shown that the head domains

fold back and interact with the rod domains. Although it has been shown to occur in vimentin (Aziz et al., 2010), a similar situation is likely to happen in other intermediate filaments due to highly conserved structure of these polypeptides (Bray et al., 2015). In such a situation when rod domains are packing tightly into filaments the size of head domain will be critical. Small tags such as 3x FLAG will be tolerated whereas large tags such as AcGFP will still be allowed to assemble into filaments, but they are likely to affect inter-rod domain association causing the filaments to destabilise which will be more obvious when filaments are hyperphosphorylated (Bray et al., 2015, Aziz et al., 2010). So introducing a large protein as K2 into the network attached to AcGFP did allow more breakdown of filaments compared to a smaller tag (FLAG) but according to data shown from WB (Figure 3.9 and 3.10) , phosphorylation is not the main cause of filaments disassembly as phosphorylated S73 and S431 of K8 didn't show any significant difference between cells transduced with different sized vectors. The folding of heads domain back into the rod domain with a bigger tag that interfere with inter-rod binding is the most reasonable explanation of the weaker filament of AcGFP tagged K2 cells. This need more investigations and transduction of the same cell line with different parts of K2 constructs. Immunostaining was performed on a fixed time point (30 min) that was clear to show breakdown of AcGFP-K2 expressing cells but not to other cells, indicating that FLAG-K2 expressing cells as well as vector control cells requires a longer treatment time presumably 1h treatment as needed by un-transduced MCF-7 showed in Figure 3.6.

A different type of stress that also activates stress kinases and phosphorylates the main phosphorylation sites on K8 was also studied. MAPK is a group of stress kinases that phosphorylates other proteins in response to different types of stresses (Paul et al., 1997). As our focus was on heat shock type of stress which

also leads to activation of the MAPK pathway (Rouse et al., 1994) MCF-7 cells subjected to a sub-lethal heat shock of 43°C for 30 mi. It was shown using immunostaining and time-lapse confocal microscopy that keratin filaments started to reorganise and move toward the nucleus and condense around it in response to heat shock. This reorganisation requires phosphorylation of keratin filaments that is later balanced during recovery by phosphatases and the filaments started to spread back toward the cell periphery as in Figure 3.12 and 3.15 (Shyy et al., 1989). In EBS, an inherited keratin mutation disorder, keratins form aggregates when subjected to heat stress and it takes longer time to re-spreads after removing the insult compared to normal keratin containing cells. This delay in keratin remodelling gives more time for cytolysis if subjected to any other type of stress during this time (Morley et al., 1995).

HSF1 heat shock transcription factor is activated after stress by hyper phosphorylation and its activation leads to synthesise of HSPs (Guettouche et al., 2005). HSPs are considered pro-survival proteins that protect the cell from lysis induced by stress-induced phosphorylation (Lanneau et al., 2008). If MCF-7 cells were exposed to heat shock before inducing phosphorylation by phosphatase inhibitors, breakdown of filaments by phosphorylation is delayed or inhibited (Figures 3.13 and 3.17). This could be due to the effect of HSPs that act as inhibitors of the pro-apoptotic pathway regulated by MAPKs (Gabai et al., 1997). Protein expression of HSP70 was measured in transduced MCF-7 cells subjected to heat shock and recovery for different time intervals. At the same time the protein level of pK8/S73 and pK8/S431 which are the main phosphorylation sites affected by p38 stress activated MAPK were checked (Toivola et al., 2002) and it shows that phosphorylation levels were either stabilised or reduced after 2 h of recovery from heat shock while the level of HSP70 was stabilised or

increased overtime. This supports the hypothesis that HSP70 could be blocking or inhibiting the action of MAPK phosphorylating S73 and S431 on K8 (Gabai et al., 1997) and this phenomenon is most likely to induce thermotolerance in which a first heat shock taken by the cell produce a series of cascades that aim to protect the cell from a second stress (which is phosphatase inhibitor treatment in our case) that lasts for few days only (Landry et al., 1982, Dorion and Landry, 2002). These findings must be confirmed by treating the cells with SB203580 a p38 MAPK inhibitor to determine the protective effect as shown by heat shock prior to phosphorylation induction. This has been done on epidermal keratinocytes, in which light was used on these cells before treating with OV tyrosine phosphatase inhibitor (Strnad et al., 2003, Woll et al., 2007). Light gives a form of protection against phosphorylation and breakdown of keratin filaments that can be used as a therapeutic approach in skin fragility disorders caused by keratin mutations.

**In conclusion**, this chapter compares the phosphorylation of endogenous keratin network in MCF-7 cells (K8/K18/K19) with keratin network of MCF-7 cells after transduction with a differentiation specific type II keratin K2.

- AcGFP-K2 transduced cells showed breakdown at lower doses and less incubation time with phosphatase inhibitors compared with untransduced cells or FLAG-K2 and vectors controls in immunostaining. MCF-7 cells transduced with AcGFP-K2 or FLAG-K2 were compared to their empty vector transduced cells (control) in which all cells show almost same level of phosphorylation at S73 and S431 on K8 protein compared to their control, shown by WB in Figure 3.9.

- Heat stressed MCF-7 untransduced or AcGFP-K2 transduced cells did show delayed breakdown of their filaments after inducing phosphorylation by OA or CL-A treatment shown by live cell imaging, immunostaining and WB.
- In wound closure experiment, MCF-7/FLAG-K2 cells were migrating faster than its control and faster than MCF-7/AcGFP-K2 cells.

# CHAPTER 4

## **4. Results II. Expression of differentiation-specific keratins in response to serum lipids, all trans-retinoic acid and phenol red.**

### **4.1. Introduction.**

Skin is a core barrier between the inner body and the outer environment, it absorbs the effects of environmental stresses including UV light, chemicals and microbes as well as protecting against water body loss (Madison, 2003). It is a multi-layered organ that is made up of two main compartments, the epidermis and the dermis. Each compartment plays a unique role, as the epidermis is the uppermost layer, it directly faces different environmental insults and it primarily functions as a barrier. On the other hand, the dermis lies underneath and it is rich in blood vessels, nerves and fibroblasts so it provides support to the epidermis which runs the biological functions of the skin (Park, 2015). The epidermis is made up of stratified epithelial cells (keratinocytes), arranged in a multi-layered fashion in which the basal layer is the deepest and the only mitotically active layer. Cells move upward as they divide until they become shed off on the skin surface through a process called epithelial differentiation (Bragulla and Homberger, 2009). In keratinocytes, keratin intermediate filaments account for about 80% of the epithelial cellular content (Pekny and Lane, 2007). Keratins play different roles inside the cell from acting as resilient stress absorber to playing a critical role in the progression of cancer and other diseases (Magin et al., 2007, Karantza, 2011b). As keratin expression is tightly regulated, different layers express different types of keratins. In skin, the basal keratins constitute the K5 and K14 pair, when basal keratinocytes which are attached to the underlying connective tissue containing dermis begin to lose their calcium activated intercellular junctions or plaques, differentiation starts to take place and keratin

expression changes. Cells start to flatten and a new set of differentiation-specific keratins, K1 and K10, are induced as the cells move up to begin the programme of differentiation. At the upper spinous and granular layers, another keratin K2 is synthesised and is classified as one of the terminal differentiation markers (Wang et al., 2016). The synthesis of new keratins as the cells move toward the surface is a tissue-specific as well as a physiological process. For example, in the skin of palms and soles (Palmoplantar) there is induction of K9 in addition to K1 and K10 in the suprabasal layers while K6 and K16 are induced supra-basally during wound healing (Fuchs, 1993, Moll et al., 2008).

The differentiation process is tightly regulated at the level of genes by a family of transcription factors. Transcription of genomic DNA to RNA, which means turning on certain genes is a key process in gene expression that identifies cells from each other and give each cell its unique identity (Guo, 2014). The synthesised mRNA is then translated into proteins which are the functional products of the genes. In keratinocyte, differentiation-specific genes produce differentiation-specific proteins such as involucrin, loricrin, cornifin and a set of differentiation-specific keratins which can be used to identify these cells from their undifferentiated counterparts (Lee et al., 1998b). There are several factors that affect the process of keratinocyte differentiation that will be discussed in detail in this chapter.

**Retinoids /Retinoic acid (RA)**, a group of vitamin A derivatives that play a key role in regulating cellular growth, differentiation and apoptosis of several cell types *in vivo* and *in vitro*. One of the main targets of RA is the epidermal compartment of skin (Torma, 2011). It is a widely used therapeutic drug for different skin conditions as it is known to induce proliferation and modulate keratinocyte differentiation, although its suppressive effect on certain genes



differs *in vivo* and *in vitro* (Gendimenico and Mezick, 1993). The mechanism of action and signalling pathways involving RA have been studied after the discovery of RA receptors, which are ligand-activated nuclear hormone receptors. These receptors are categorised into 2 families, the retinoic acid receptors (RAR), and retinoid X receptors (RXR). Each family has 3 different forms which can form functional homo and heterodimers ( $\alpha$ ,  $\beta$ ,  $\gamma$ ). These receptors have different ligand specificities. Normal RAR ligands include both all-trans RA (ATRA) and 9-cis RA (9cRA). On the other hand, RXR interact with 9cRA, but not ATRA. Both RAR and RXR bind to RARE located in gene promoters as heterodimers (RAR·RXR) mainly (RAR $\alpha$ /RXR $\gamma$ ) or RXR homodimers (RXR/RXR). These receptors are mainly expressed in the differentiated layers of the epidermis proposing to have their role in terminal differentiation (Di et al., 1998, Lefebvre et al., 2005, Jho et al., 2005). The latest studies on RARs are also indicating their role in lamellar body formation needed by differentiating keratinocytes, suggesting that any abnormality in retinoid signalling pathways could result in forming abnormal keratinocytes phenotype. Retinoid signalling is greatly altered upon keratinocyte differentiation and the effects depend on how cellular differentiation is commenced. Calcium treatment increases RAR $\gamma$  and RXR $\alpha$  expression while PMA treatment reduced protein and mRNA expression of RAR $\gamma$  and RXR $\alpha$  suggesting that the effect of PMA on retinoid receptors is either translational or post-translational (Karlsson et al., 2010). The RA effect could be either direct by binding to specific genes or indirect by modulating the effect of some other transcription factors that in turn affect the target genes (Lee et al., 2009). One of the well-studied effects of RA in epidermis is the inhibition of both early and late stage differentiation markers (Fuchs and Green, 1981, Eichner et al., 1992). Transglutaminase 1 (TGM1) enzyme, which

is responsible for the assembly of the cornified envelope in skin, is suppressed after RA treatment as well as other terminal differentiation markers such as filaggrin and loricrin (Marvin et al., 1992, Hohl et al., 1991). Keratin family of genes are also regulated by RA in which some genes such as *KRT1* and *KRT10* are suppressed whereas other genes *KRT13*, *KRT15* and *KRT19* are induced (Lee et al., 2009). The effect of RA on the expression of late differentiation keratins in culture of human skin keratinocyte compared to skin samples is highly variable. For example, *KRT1* was shown to be downregulated, or in some cases unaffected, in skin samples treated with topical application of RA cream while its protein expression was unchanged. A similar expression pattern was shown by K10 with mRNA downregulation on skin samples treated with RA but immunostaining showing either no change or downregulation of protein. K2 mRNA levels were also reduced with no change or undetectable protein levels following RA treatment (Torma, 2011, Rosenthal et al., 1992, Virtanen et al., 2000, Rosenthal et al., 1990). In human epidermal keratinocyte cultures, the expression profile of these keratins exhibited a wide range of variations depending on the culture conditions, RA concentrations, cell line used and keratin protein detection method. K1 and K10 were expressed in a similar manner in which using high concentrations of RA (1 $\mu$ M) was downregulating mRNA and protein expression profile when serum free medium or low serum containing medium were used. The expression of keratin K2 was not detectable at the protein level, mRNA for K2 was upregulated at early time points and downregulated at late time points of adding low concentrations of RA to low serum containing or serum free culture medium. K2 also revealed higher levels of downregulation when treated with Tazarotene (a member of the acetylenic class of retinoids, sold as topical cream or gel) compared to other retinoids which

presented almost no difference (Torma, 2011, Karlsson et al., 2010, Kopan et al., 1987, Lee et al., 2009, Fuchs, 1993, Hsia et al., 2008). In the literature, there were many variables used in growing cells or taking biopsies and analysing them that ended up with these controversies about the effect of RA on different keratin expression.

**Calcium** is a well-known regulator of keratinocyte differentiation. It has a concentration gradient through the epidermal layers with low concentrations at the basal layer where differentiation markers are suppressed. Higher concentration is shown as we move supra-basally where differentiation markers are activated specially at the spinous and granular layers. Calcium tends to play a major role as a differentiation inducer and a proliferation suppressor in keratinocytes (Boyce and Ham, 1983, Eckert et al., 1997, Pillai et al., 1990).

**Phorbol ester**, such as phorbol 12-myristate 13-acetate (PMA, also referred to as TPA), is a well-known skin tumour promoter along with being a potent inducer of keratinocyte differentiation. They act as a diacyl glycerol (DAG) analogue and directly activate PKC/AP-1 pathway. Phorbol esters are known not only to induce differentiation, they inhibit cell proliferation, elevate intracellular  $Ca^{2+}$  and downregulate retinoid receptors in keratinocytes (Castagna et al., 1982a, Papp et al., 2003, Karlsson et al., 2010). While PMA treatment induces expression of late differentiation markers such as filaggrin and loricrin, it downregulates early differentiation markers, such as K1 and K10, both *in vitro* and *in vivo* (Lichti and Yuspa, 1988a, Dlugosz and Yuspa, 1993a, Papp et al., 2003, Bose et al., 2012).

**Steroid hormones** as cortisol and the active form of vitamin D (1,25-dihydroxyvitamin  $D_3$ ) have major effects on keratinocyte differentiation. The active form of vitamin D is a calcium regulating hormone, it activates epidermal

terminal differentiation markers and stimulate the formation of the cornified skin layer. Vitamin D<sub>3</sub> binds to its nuclear receptor, VDR, and directly promotes terminal differentiation, this is the most considered and well-known pathway. It could be that other pathways are involved in vitamin D induced differentiation such as PKC and G protein pathways as well (Bikle, 2011, Eckert et al., 1997). The effect of vitamin D<sub>3</sub> on differentiation is dependent on the calcium concentration and the cell density (Svendsen et al., 1997a).

**Estrogen** plays a major role in many age-related processes. Wound healing is one example that requires proliferating keratinocytes and is highly affected by low estrogen levels. Estrogen replacement therapy is known to reverse this process and allows better healing and epithelialisation. Estrogen binds to estrogen receptors either ER- $\alpha$  or ER- $\beta$  which are nuclear receptors that binds to DNA and has the ability to either repress or induce target genes (Perzelova et al., 2016, Merlo et al., 2009). In keratinocytes, estrogen binds to ER- $\beta$  more than ER- $\alpha$ , cells stimulated with the ER- $\alpha$  agonist had similar expression of different keratins while cells treated with ER- $\beta$  agonist show lower expression of differentiation-specific keratins. The direct effect of estrogen on keratin expression is not yet clear with some evidence suggesting upregulation of *KRT2*, *KRT14* and *KRT19* genes in human scalp skin after  $\beta$ -Estradiol treatment (Ramot et al., 2009, Choi et al., 2000).

**High cellular density** especially 100% confluency has also been shown to induce the expression of both early (K1, K10) and late (Filaggrin, loricrin, SPRR-1) differentiation markers in keratinocytes *in vitro*. Cell density-mediated induction of differentiation markers has been associated with PKC activation. Recent studies have shown other factors to be involved in response to increased cell-cell contact, as downregulation of c-Myc which is involved in cell-cycle progression

as well as upregulation of Notch1 that regulates interactions between physically adjacent cells (Lee et al., 1998b, Poumay and Pittelkow, 1995, Kolly et al., 2005b, Newton, 2010b).

To attain more detailed knowledge on the role of lipids especially SLP, ATRA and estrogen on the expression of differentiation-specific keratins K1, K2 and K10, different types of keratinocytes cultured in different conditions of lipid-free or phenol-free medium were used. To study the effect of these different conditions, qPCR and protein analyses using WB and immunofluorescence staining of 3D cultures of NHEK were used. To specifically study the effect of the main active lipid ingredient in the FCS ATRA was added back to the charcoal treated serum at different concentrations and the effect was measured using qPCR and WB. The effect of PR removal was performed based on some studies that reveal an estrogenic like activity of PR that could play a role in keratin gene expression (Ramot et al., 2009, Merlo et al., 2009, Choi et al., 2000, Sheng et al., 2008, Perzelova et al., 2016, Welshons et al., 1988).

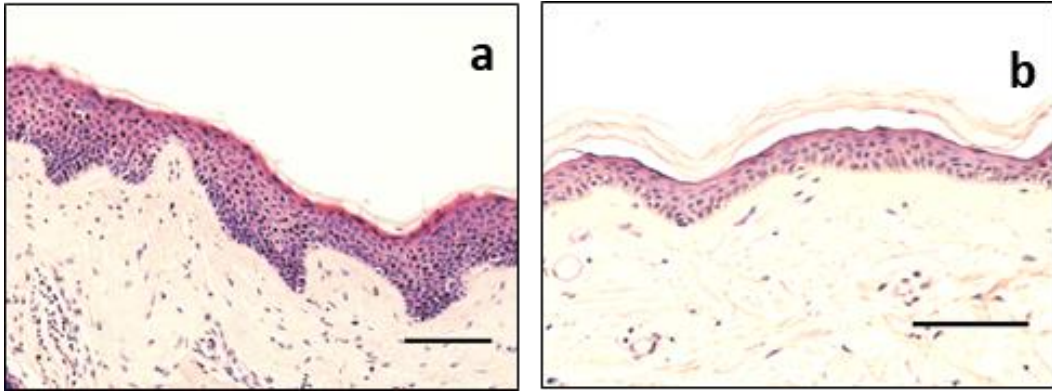
In this chapter, different keratinocyte cell lines and NHEK were used and grown in RM<sup>+</sup> medium under different conditions containing normal or charcoal stripped serum with and without PR. These studies were complemented by growing NHEK cells in charcoal stripped serum with and without ATRA. The expression of different keratins was analysed in 2- and 3- dimensional cultures using WB, qPCR and immunostaining.

## **4.2. Expression of different keratins in skin.**

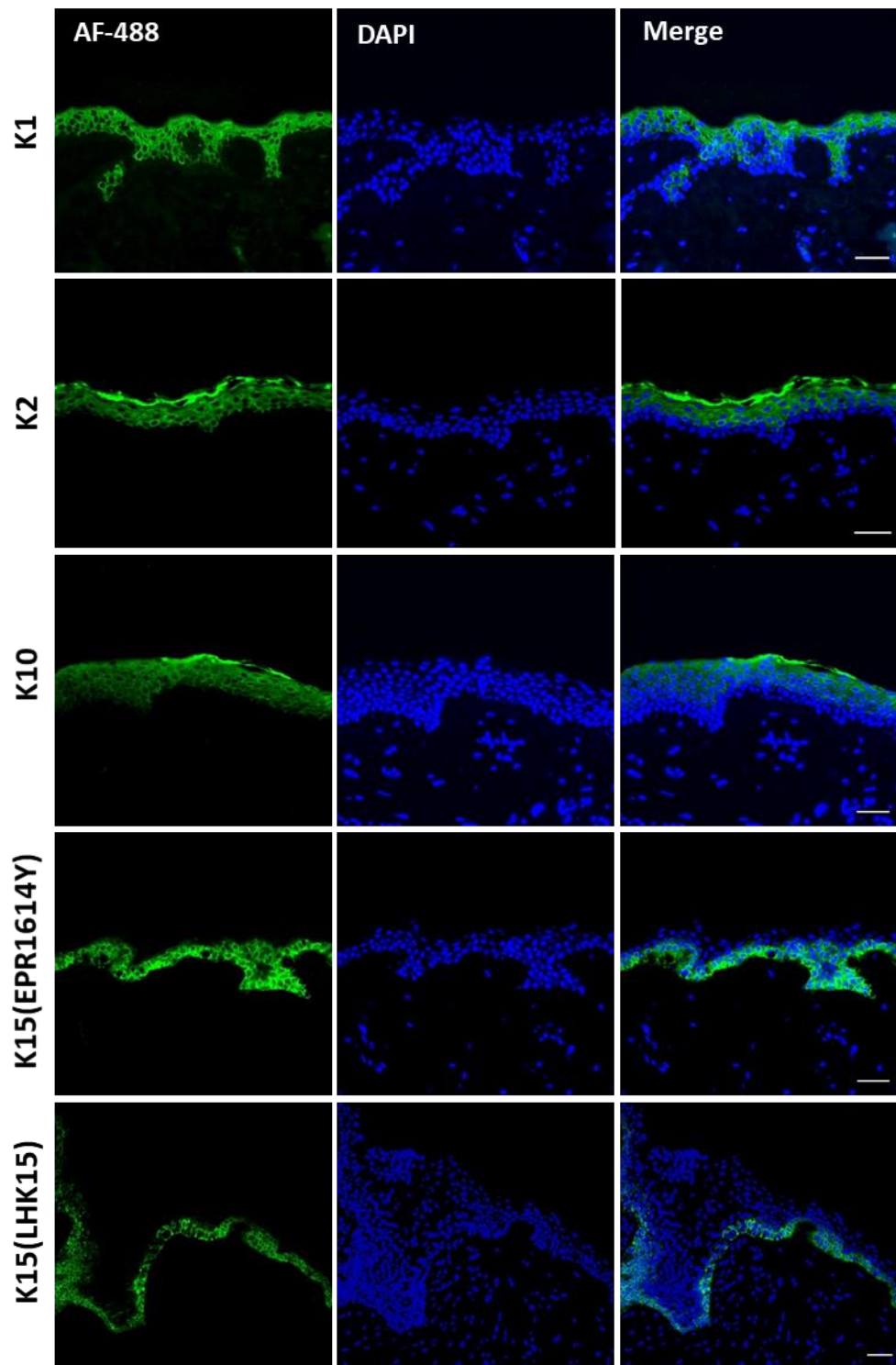
In this set of experiments, the pattern of expression of the main keratin proteins as well as late differentiation markers in the human epidermis was investigated. Normal skin samples were obtained from discarded tissue during facial lift and

tummy reduction surgeries. Informed consents were obtained from all patients for collection of skin samples and the procedure was reviewed and approved by the NRES Committee London- City and East (REC ref. 09/H0704/69) and all methods were performed in accordance with the relevant guidelines and regulations. The samples were fixed in 4% (w/v) paraformaldehyde, dehydrated with increasing concentrations of ethanol and paraffin embedded using the facility available in the Centre for Cutaneous Research (Blizard Institute). The paraffin embedded blocks were stored at RT for later use. Tissue sample containing blocks were incubated at low temperature before cutting into 5 µm thick sections using a Leica Rotary Microtome. The sections were de-waxed with xylene followed by rehydration with decreasing concentrations of ethanol until they were completely rehydrated in PBS. The sections were then stained with (H&E) in order to visualise and differentiate dermis from epidermal layers as shown in Figure 4.1.

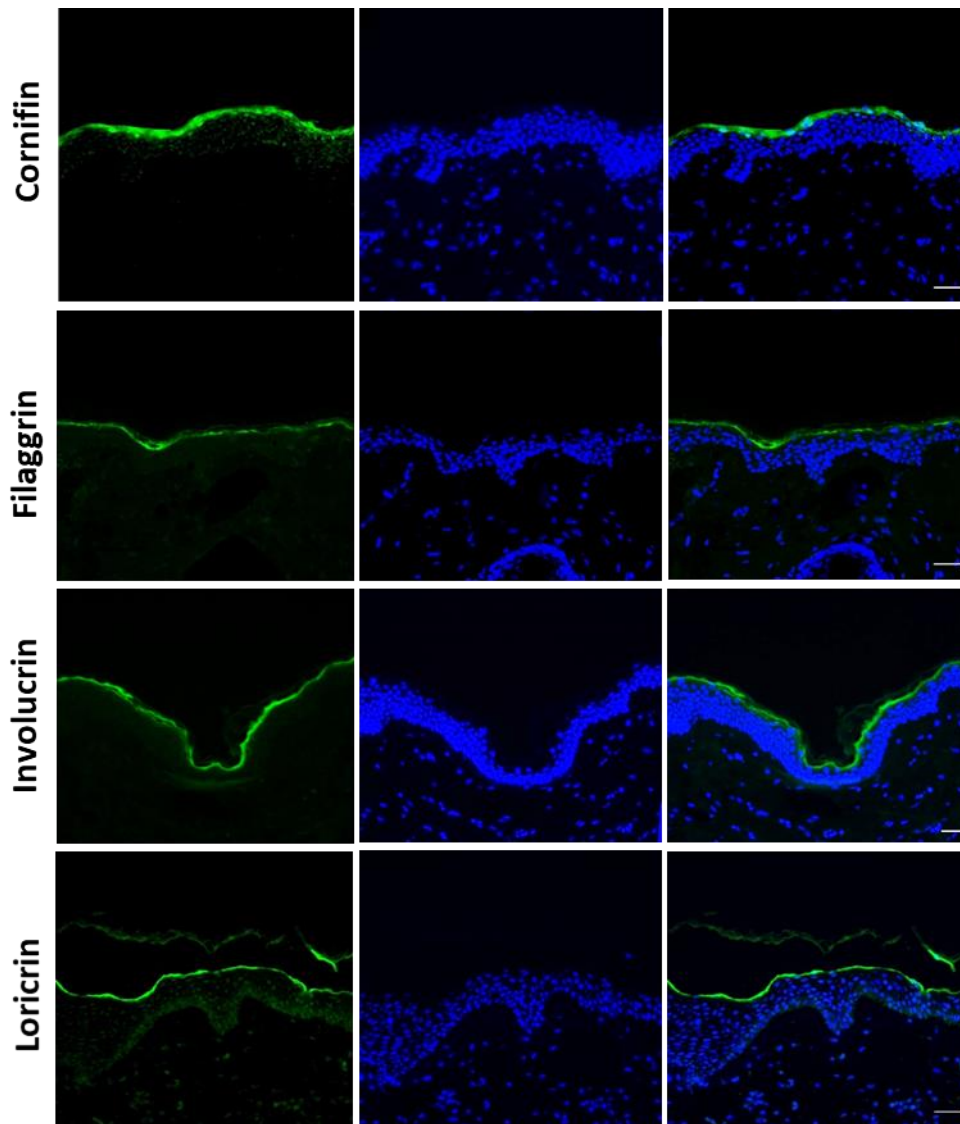
To detect the antigen expression, the tissue sections were incubated with the primary antibodies against specific antigens and then stained with corresponding secondary antibodies. The expression of keratins K1, K2 and K10 was primarily detected in the suprabasal layers of the epidermis. The tissue section were also immunostained with two different antibodies for keratin K15 (LHK15 and EPR1614Y) showing staining of the basal layer of the epithelium. The LHK15 staining gave discontinuous staining whereas EPR1614Y gave us a continuous staining (See Figure 4.2). Antibodies against several non-keratin differentiation markers including cornifin, filaggrin, loricrin and involucrin were used and it was found that all of them were staining only the uppermost layer of the epidermis plus the cornified layer as shown in Figure 4.2.



**Figure 4.1. Haematoxylin and Eosin (H&E) staining of skin sections.** Skin was given from facial lift surgery (a), abdominal skin (b), fixed using 4% paraformaldehyde and processed, paraffin embedded and sectioned into 5  $\mu\text{m}$  thick sections. Re-hydrated tissue sections were stained, de-hydrated and mounted using DPX mounting medium. Nikon Eclipse 80i Stereology Microscope was used for recording. (Scale bar =100  $\mu\text{m}$ ).



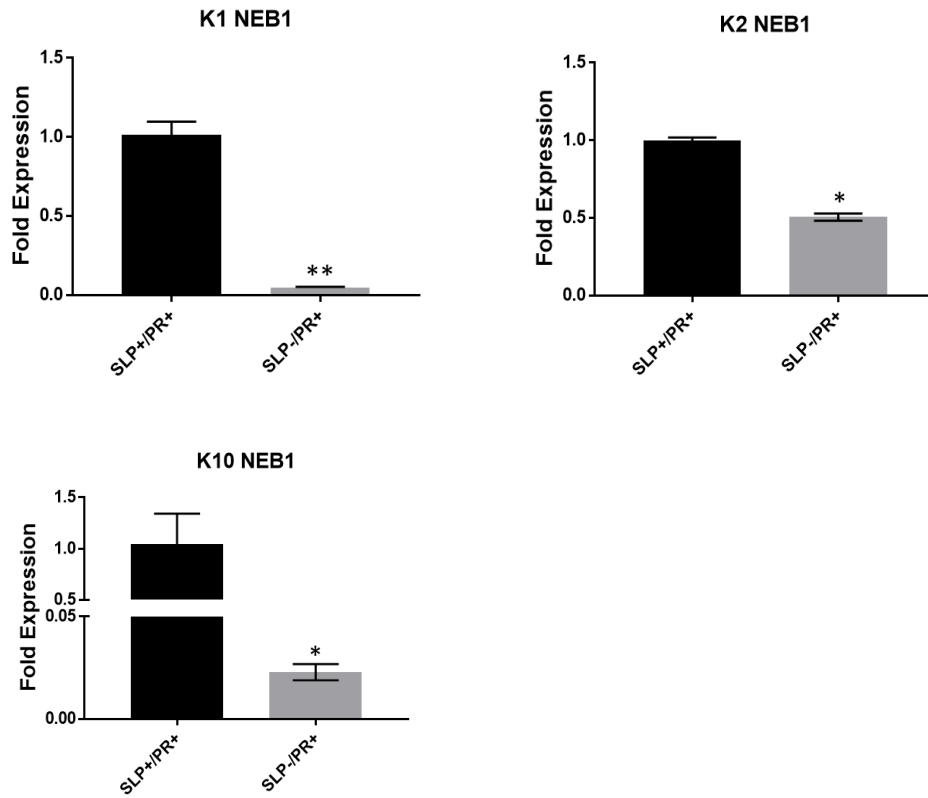
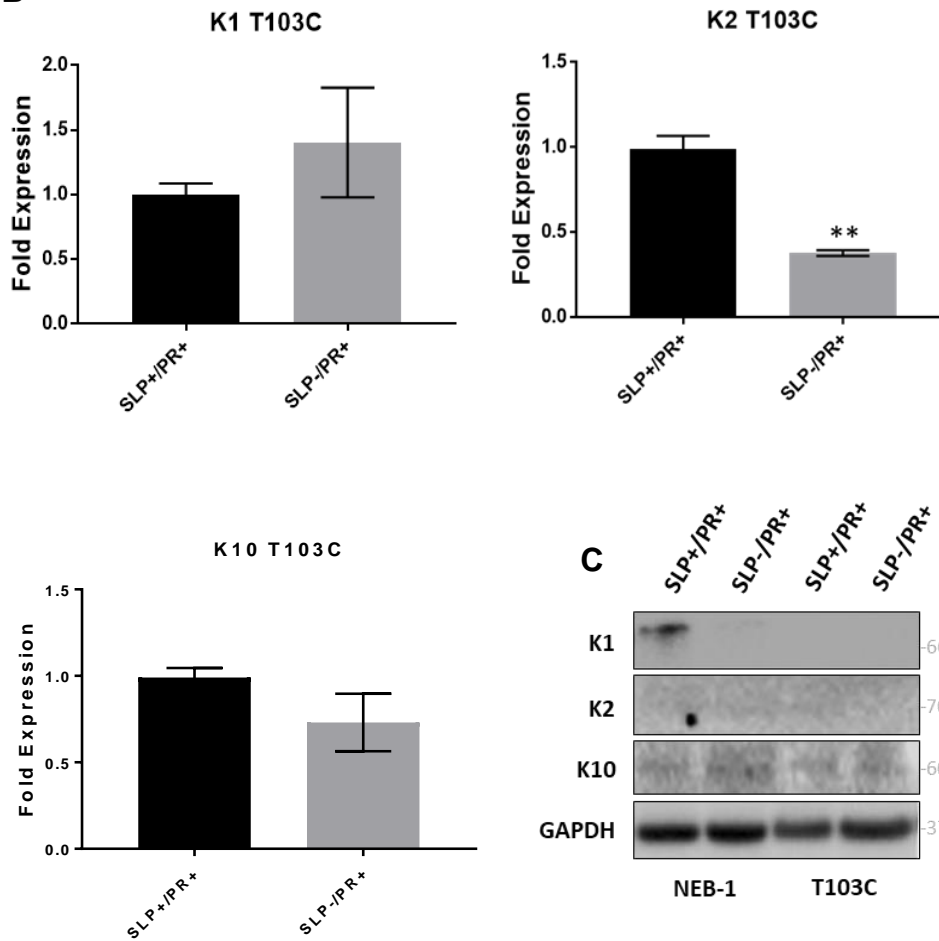
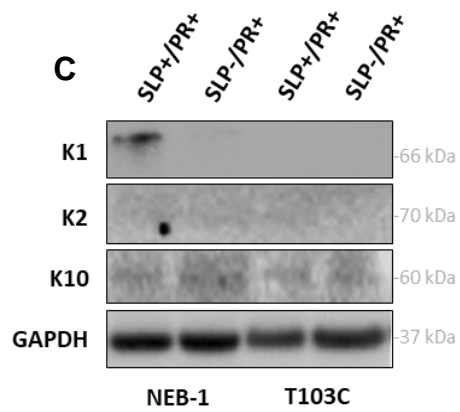




**Figure 4.2. Expression of differentiation specific markers in normal skin.** Skin was made available following facial lift surgery, fixed and processed, cut into 5  $\mu\text{m}$  thick sections, antigen retrieval was performed as described in the Methods and Materials. Sections were immunostained with primary mAb and AF- 488 labelled secondary antibodies. Leica DM4000 Epi-fluorescence microscope with DFC350 FX digital camera was used for recording. (scale bar= 20  $\mu\text{m}$ ).

### **4.3. Role of serum lipids on mRNA and protein expression of differentiation-specific keratins in Neb-1 and T103C cell lines.**

In this set of experiments, the role of SLP was investigated as being one of the main ingredients of serum used in tissue culture and well known to affect cellular proliferation and differentiation. Two cell lines sharing the same immortalisation method originated from different tissues were used. Neb-1 is a skin keratinocyte cell line while T103C is an oral keratinocyte cell line (Dickson et al., 2000, Bryan et al., 1995). Charcoal treated FCS in RM+ medium was used to grow cells for 3 days before collecting lysates for qPCR mRNA and WB protein analyses. Data were compared to cells grown in normal FCS in RM+ medium. As shown in Figure 4.3, Neb-1 cells were showing a significant downregulation of *KRT1*, *KRT2* and *KRT10* when serum was stripped with charcoal (SLP-/PR+), T103C cells showed either downregulation of *KRT2* and *KRT10* or a non-significant upregulation of *KRT1*. Protein expression was not detectable except for Neb-1 K1 that showed clear downregulation of the protein expression when stripped serum was used as shown in Figure 4.3 B.

**A****B****C**

**Figure 4.3. Influence of serum lipids on mRNA and protein expression of K1, K10 and K2 in Neb-1 and T103C cell lines.** Cells were grown for 3 days in RM+ media either containing normal FCS (SLP+/PR+) or RM+ with charcoal stripped FCS (SLP-/PR+), lysates were collected and analysed using qPCR (A, B) and western blotting (C). Data are shown as fold expression normalised to the expression of the two housekeeping genes, POL2A and YAP1 under different growth conditions. STAT: n=3, Error bars= SEM, Student's t-test was performed, p-values (ns=p>0.05, \*=p<0.05, \*\*=p<0.01). In WB analysis of the proteins in keratinocyte lysates using antibodies against K1, K10 and K2. GAPDH was used as a loading control.

#### **4.4. Influence of serum lipids and PR on mRNA and protein expression of differentiation-specific keratins in HaCaT and N/TERT cell line.**

In this set of experiments, the influence of SLP on the expression of three differentiation-specific keratins K1, K2 and K10 in two keratinocytes cell lines was investigated, HaCaT and N/TERT that are known to be the closest cell lines to normal keratinocytes and not immortalised by HPV16 as Neb-1 and T103C (Smits et al., 2017). Charcoal treated stripped FCS was used, which would remove most of the SLPs from our RM+ culture medium. PR free medium was also used to investigate its effect on keratin expression in conjunction with SLPs. HaCaT and N-TERT cell lines were grown in four different conditions of RM+ medium for three days before determining specific mRNA levels for *KRT1*, *KRT2* and *KRT10* by qPCR and protein expression by western blotting. As shown in Figure 4.4 K1 mRNA expression was upregulated in HaCaT cells grown in lipid free with or without PR containing medium (SLP-/PR+, SLP-/PR-) by about 2.5 folds. This suggests that PR does not show any significant effect on K1 expression in the presence or absence of SLPs (Figure 4.4 A, K1). Compared with K1, the K10 mRNA expression was much more sensitive to SLPs, much higher K10 mRNA expression was observed in charcoal stripped serum conditions compared with the unstripped serum. It was 25- and 35- fold higher for K10 mRNA in (SLP-/PR+) and (SLP-/PR-), respectively, with a significant

difference between them suggesting that K10 mRNA was highly affected by PR. In the absence of PR and the full lipid containing serum (SLP+/PR-) K10 mRNA showed more than 10 folds increase compared with PR containing full lipid serum medium (SLP+/PR+) (see Figure 4.4 A, K10). Interestingly, keratin K2, which is also expressed in the suprabasal epidermal keratinocytes, showed a reverse pattern of gene expression in which the absence of PR and SLP together (SLP-/PR-) reduced the expression while having full lipid serum in PR free medium increased the expression significantly (Figure 4.4 A, K2). Removal of SLP in PR containing medium did not show any significant difference in K2 mRNA expression. As expected, the mRNA expression pattern was mimicked at the protein level with both K1 and K10 showing higher protein expression in both SLP-/PR+ and SLP-/PR- conditions compared to SLP+/PR+ and SLP+/PR- conditions, respectively (Figure 4.4 B). Under these conditions K2 protein was not detectable in HaCaT cells.

In N-TERT keratinocytes, the effect of SLPs and PR on mRNA expression of K1, K2 and K10 is very different compared with that observed in HaCaT cells. For K1, K2 and K10 mRNA, removal of PR in the presence of serum lipids (SLP+/PR-) showed about 3 fold increase compared to serum lipid and PR containing medium (SLP+/PR+) indicating a more significant role of PR in this cell line (Figure 4.5 A).

The WB data showed strong protein expression of K1 and K10 on SLP+/PR- condition compared with other conditions (Figure 4.5 B). K2 didn't show any protein expression under these condition in N-Tert-1 cells.

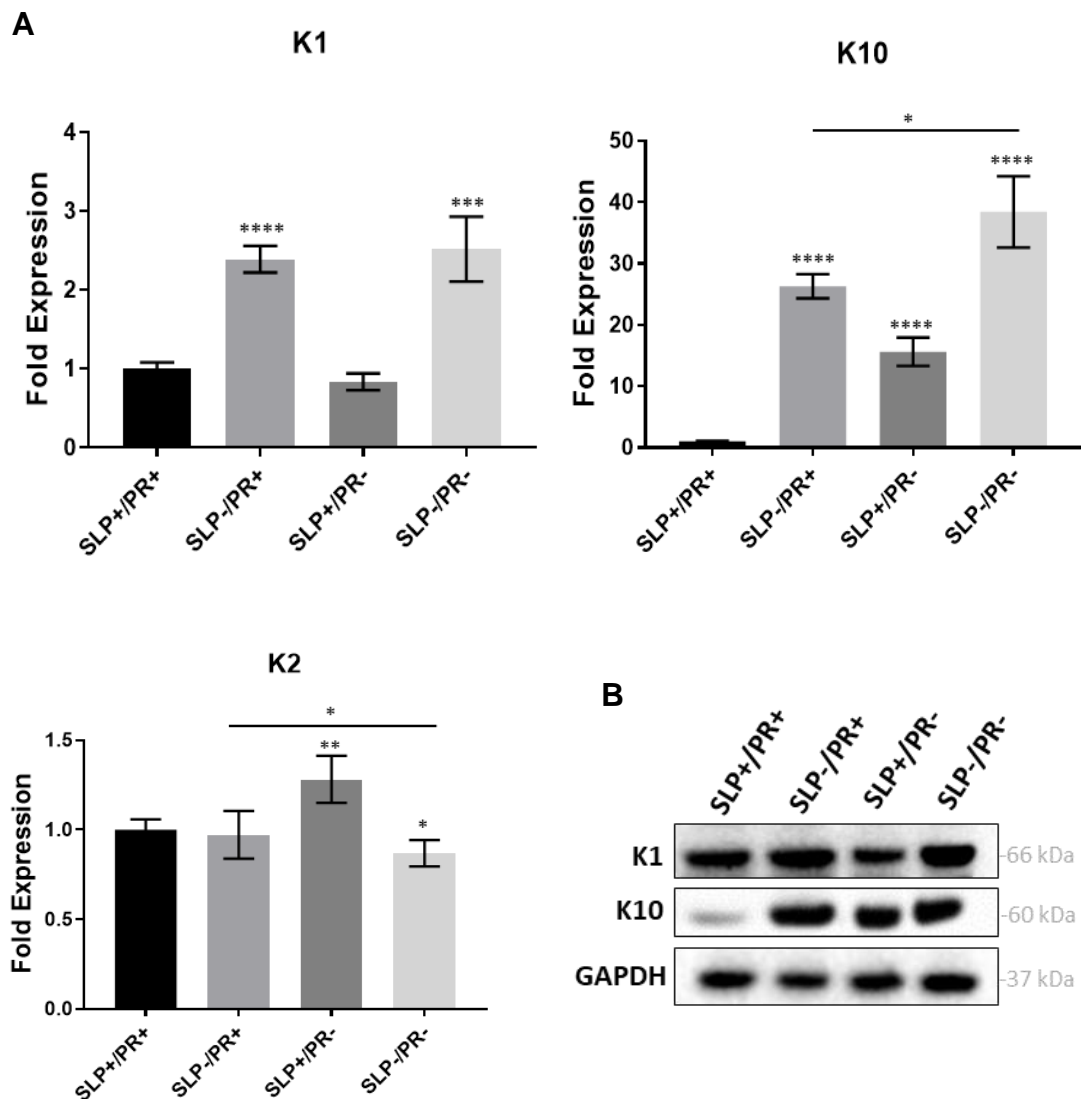


**Figure 4.4. Influence of serum lipids on mRNA and protein expression of K1, K10 and K2 in HaCaT cell line.** HaCaT cells were grown for 3 days in four different RM+ media conditions, lipid containing FCS was added in RM+ with or without PR (SLP+/PR+, SLP+/PR-), charcoal stripped FCS was added with or without PR (SLP-/PR+, SLP-/PR-). Lysates were collected and analysed using qPCR and western blotting. (A) Data are shown as fold expression normalised to the expression of the two housekeeping genes, POL2A and YAP1 under different growth conditions. STAT: n=3, Error bars= SEM, Student's t-test was performed, p-values (ns=p>0.05, \*=p<0.05, \*\*=p<0.01, \*\*\*=p<0.001 and \*\*\*\*=p<0.0001). (B) WB analysis showed, absence of lipids and PR increases protein expression of K1 and K10 in HaCaT, using antibodies against K1, K10 and K2. GAPDH was used as a loading control.

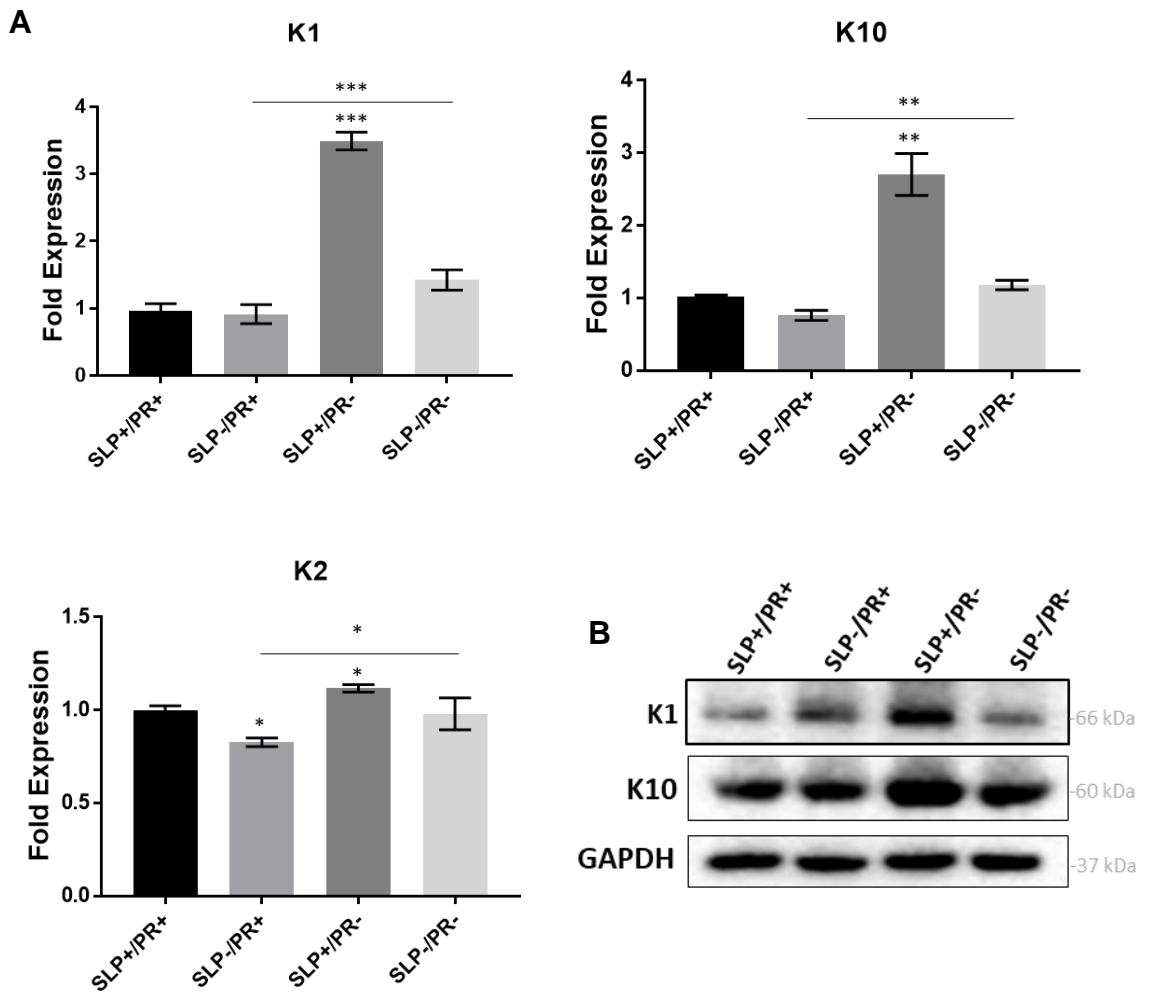


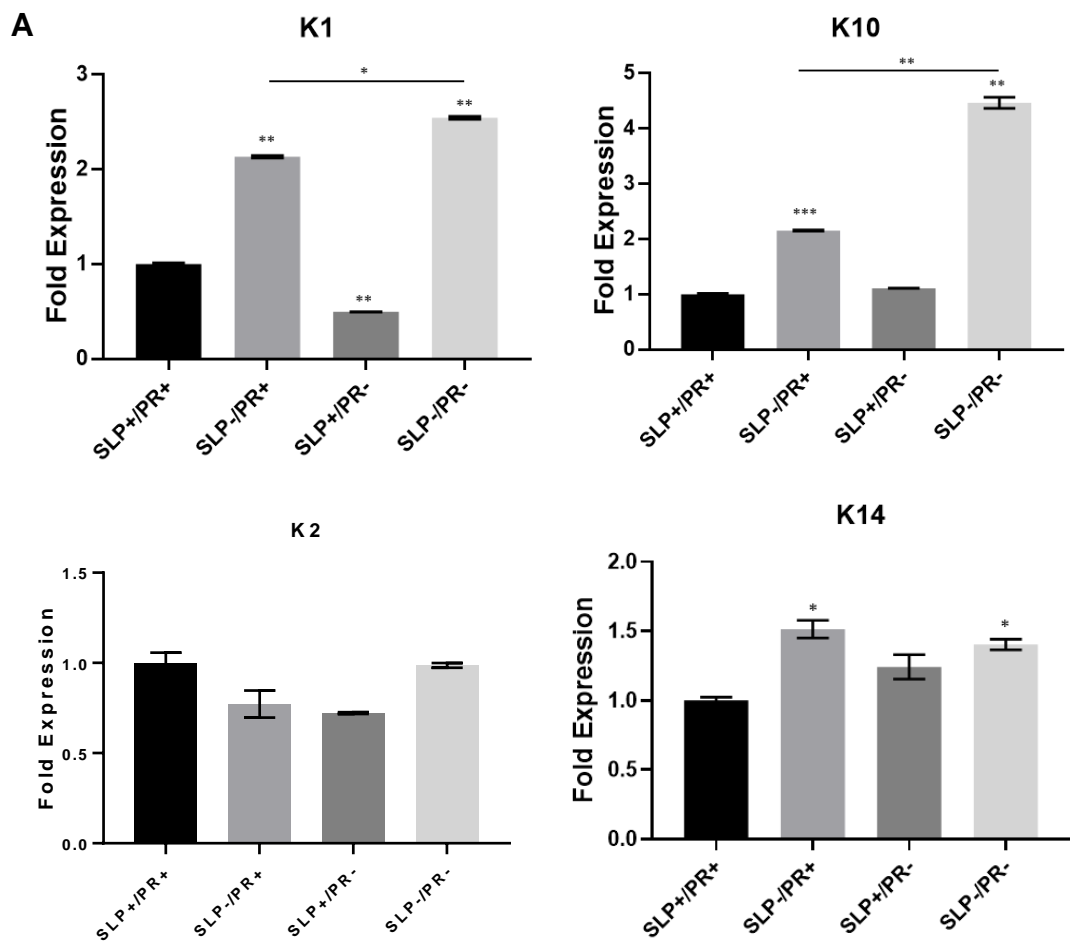
**Figure 4.5. Influence of serum lipids on mRNA and protein expression of K1, K10 and K2 in N/TERT cell line.** N/TERT cells were grown for 3 days in four different RM+ media conditions, lipid containing FCS was added in RM+ with or without PR (SLP+/PR+, SLP+/PR-), charcoal stripped FCS was added with or without PR (SLP-/PR+, SLP-/PR-). Lysates were collected and analysed using qPCR and western blotting. (A) Data are shown as fold expression normalised to the expression of two housekeeping genes, POL2A and YAP1 under different growth conditions. STAT: n=3, Error bars= SEM, Student's t-test was performed, p-values (ns=p>0.05, \*=p<0.05, \*\*=p<0.01 and \*\*\*=p<0.001). (B) WB analysis of the proteins in keratinocyte lysates using antibodies against K1, K10 and K2 showed increased expression of K1 and K10 protein in the absence of phenol red. GAPDH was used as a loading control

#### **4.5. Absence of serum lipids and PR increases mRNA and protein expression of differentiation-specific keratins in NHEK.**

To explain the variations observed in HaCaT and N/TERT cell line that could be due to the procedure used to immortalise these cells, normal epidermal keratinocytes were substituted for the cell lines in future experiments. NHEK cells were co-cultured with 3T3 fibroblasts irradiated with sub-lethal dosage of gamma-radiation to be used as feeder cells in RM+ medium with the same conditions mentioned in section 4.4 for HaCaT and N-TERT cell lines. Around 2-fold increase in expression of K1 mRNA was observed in SLP-/PR+ and SLP-/PR- conditions compared to the SLP+/PR+ control, lipid removal did allow more expression of K1 mRNA in the presence or absence of PR with the latter being more pronounced. K10 showed similar pattern with 2- and 4-folds increase in SLP-/PR+ and SLP-/PR-, respectively. In K1 and K10, the highest mRNA expression was observed when PR was removed in the absence of SLP suggesting their expression is sensitive to the presence of PR. On the other hand, expression of K2 mRNA was not altered significantly by changes in growth conditions by either removing SLP or PR or both. These data were compared to K14, a keratin which is proliferation specific, a significant increase was observed in its mRNA expression in presence of charcoal stripped serum but was insensitive to PR (Figure 4.6 A). At protein level, the WB data showed a pattern similar to mRNA expression in which K1 and K10 showing highest expression in (SLP-/PR-). Removing SLP and PR (SLP-/PR-) had a synergistic effect on K1 and K10 protein expression in which the removal of both at the same time showed much stronger effect than removing either of them. K2 protein expression



increased in SLP-/PR+ which further increased in SLP-/PR- condition again similar to K1 and K10 (Figure 4.6 B).



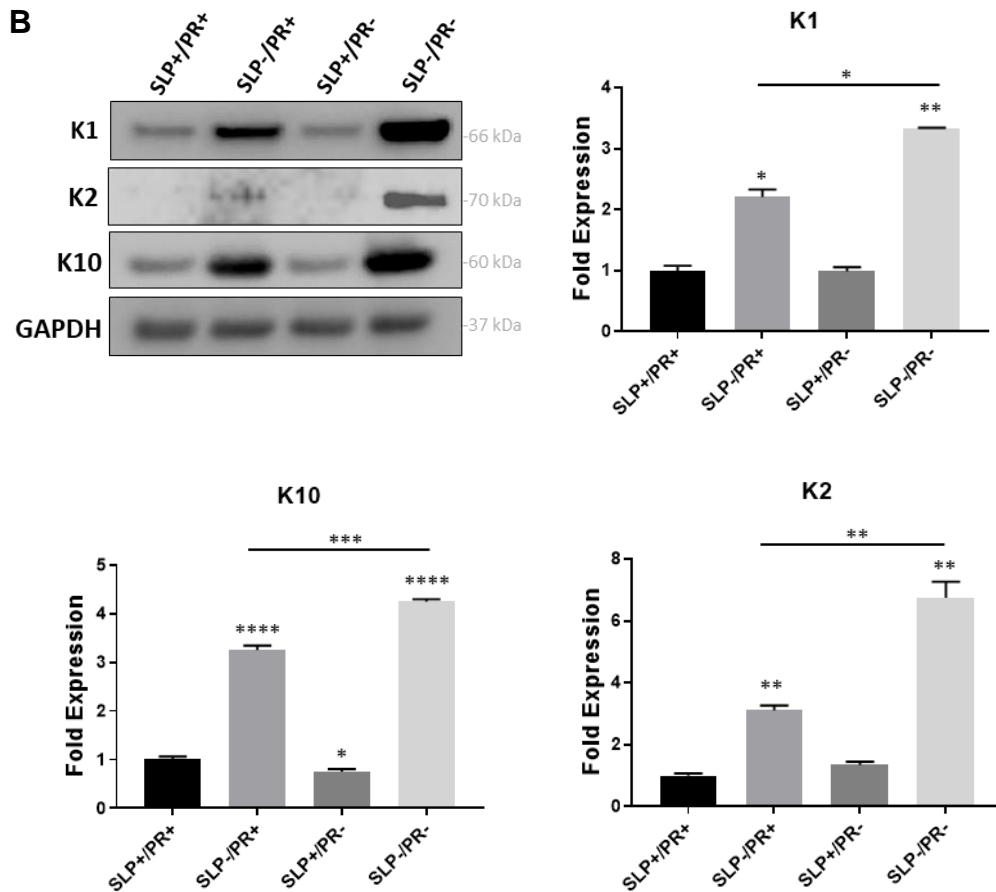


**Figure 4.6. Removal of serum lipids and PR affects mRNA and protein expression of K1, K10 and K2 in NHEK cells.** NHEK cells were grown with irradiated 3T3 feeder cells for 3 days in four different RM<sup>+</sup> media conditions, lipid containing FCS in RM<sup>+</sup> with or without PR (SLP<sup>+</sup>/PR<sup>+</sup>, SLP<sup>+</sup>/PR<sup>-</sup>), charcoal stripped FCS in RM<sup>+</sup> with or without PR (SLP<sup>-</sup>/PR<sup>+</sup>, SLP<sup>-</sup>/PR<sup>-</sup>). Lysates were collected and analysed using qPCR and WB. (A) Data are shown as fold expression normalised to the expression of two housekeeping genes, POL2A and YAP1 under different growth conditions. STAT: n=3, Error bars= SEM, Student's t-test was performed, p-values (ns=p>0.05, \*=p<0.05, \*\*=p<0.01, \*\*\*=p<0.001 and \*\*\*\*=p<0.0001). (B) WB analysis of the proteins present in keratinocyte lysates using antibodies against K1, K10 and K2. GAPDH was used as a loading control.

## **4.6. Influence of serum lipids and PR on keratin expression in NHEK grown in 3D organotypic cultures (OTCs).**

To study keratin protein expression in a 3D culture system, which mimics an *in vivo* situation of human skin expressing differentiation-specific markers in a way resembling normal skin, NHEK cells were grown in an organotypic model at an air-liquid interface for 10 days. Cells were grown in RM<sup>+</sup> medium with and without charcoal stripped serum either in the presence or absence of PR. The OTCs plugs were removed and fixed using 4% (w/v) paraformaldehyde, dehydrated using increasing concentrations of ethanol and paraffin embedded. Later, 5 µm sections were cut, de-waxed, antigen retrieved and immunostained using mAbs specific for the keratin proteins of our interest. More detailed procedure on fixation, waxing and de-waxing is described in the Material and Methods section 2.3. H & E staining were used to show the stratification and cornification of keratinocytes and to show the differences between the superficial layer and the deep fibroblast containing collagen layer shown in Figure 4.7. From the immunofluorescence staining shown in Figure 4.8 (A, B, C, D), the expression of K1, K2 and K10 showed the strongest staining when cultured in PR free RM<sup>+</sup> medium with charcoal stripped serum (SLP-/PR-) supporting the previous mRNA and WB data shown in Figure 4.6. K14 and K15 did not show any significant changes in expression when the culturing conditions were altered. In Figure 4.8 (E) a summary of the effect of different conditions on the expression of K1, K2 and K10 was shown in one figure to make it easy to compare.

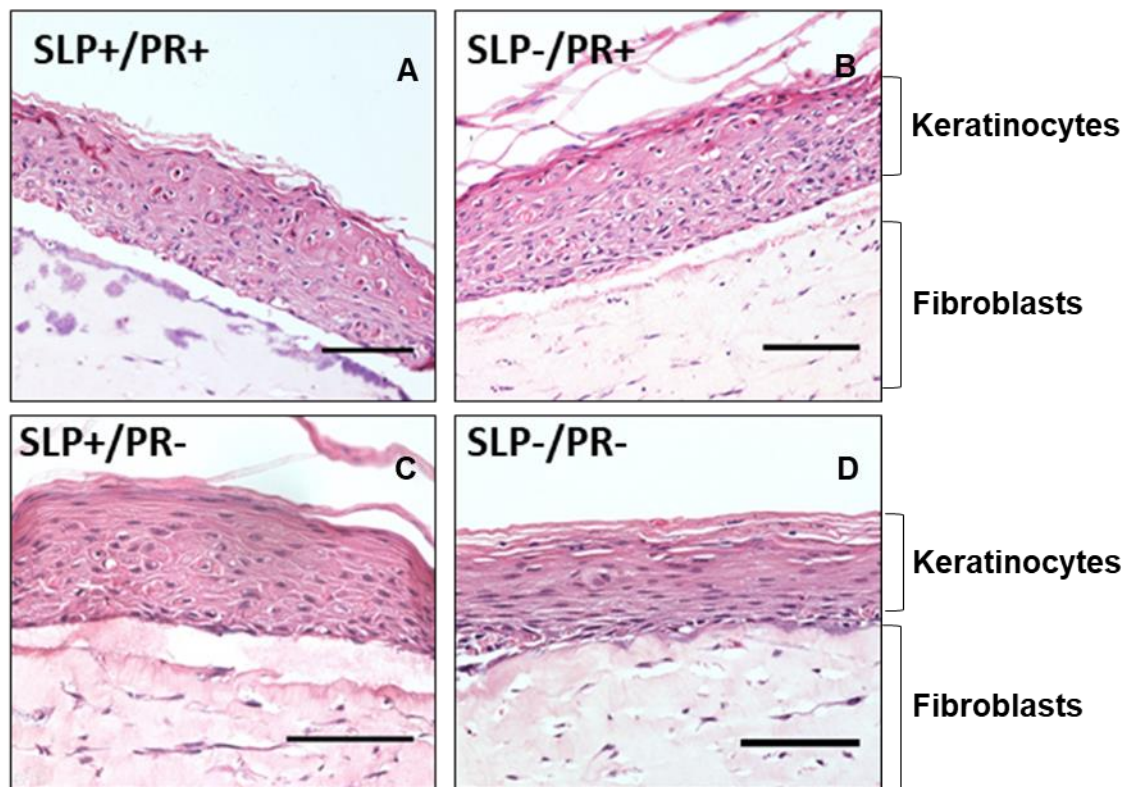
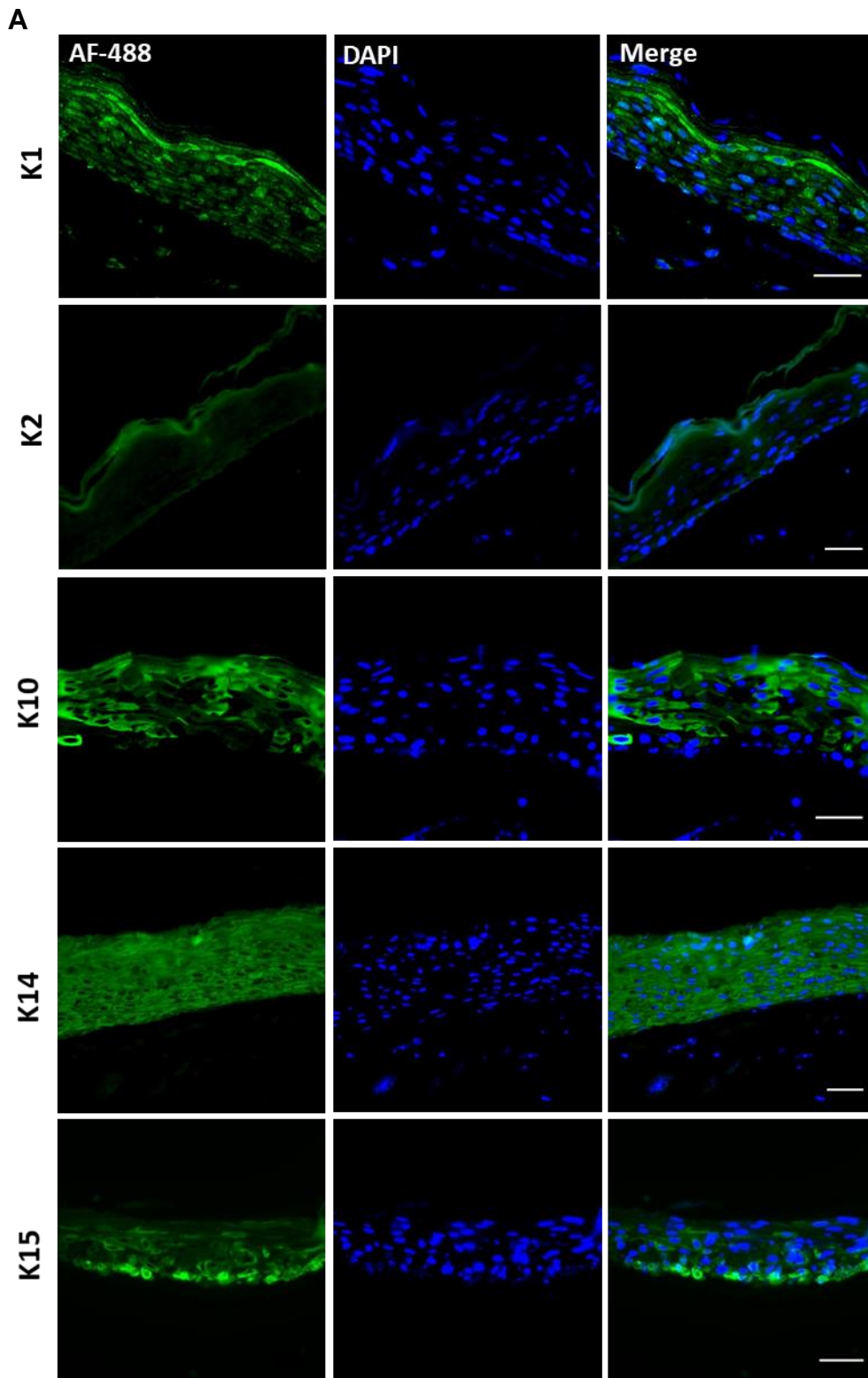


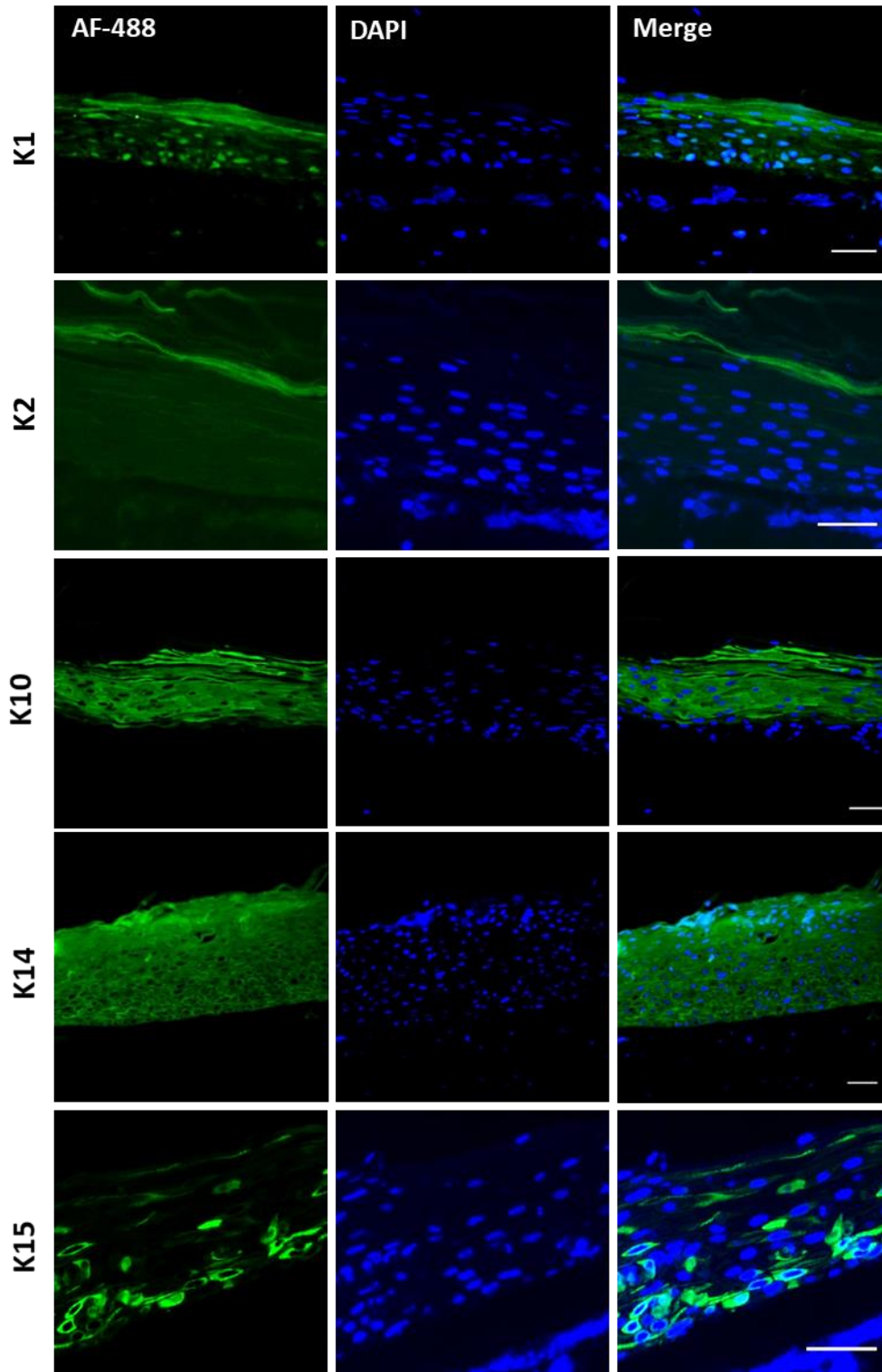
**Figure 4.7. H&E staining of NHEK OTCs.** NHEK were grown in OTCs in an insert (pore size 0.4  $\mu\text{m}$ ) based method. Primary dermal fibroblasts were used in collagen matrix to support the growth of NHEKs. The cells were grown at air-liquid interface for 10 days with 4 different media conditions (A:SLP+/PR+, B:SLP-/PR+, C:SLP+/PR- and D:SLP-/PR-),fixed in 4% (w/v) paraformaldehyde/PBS and paraffin embedded. Sections of 5  $\mu\text{m}$  thickness were cut, de-waxed, re-hydrated, stained, de-hydrated and mounted using DPX mounting medium. Nikon Eclipse 80i Stereology Microscope was used for recording. (Scale bar =100  $\mu\text{m}$ ).

SLP+/PR+

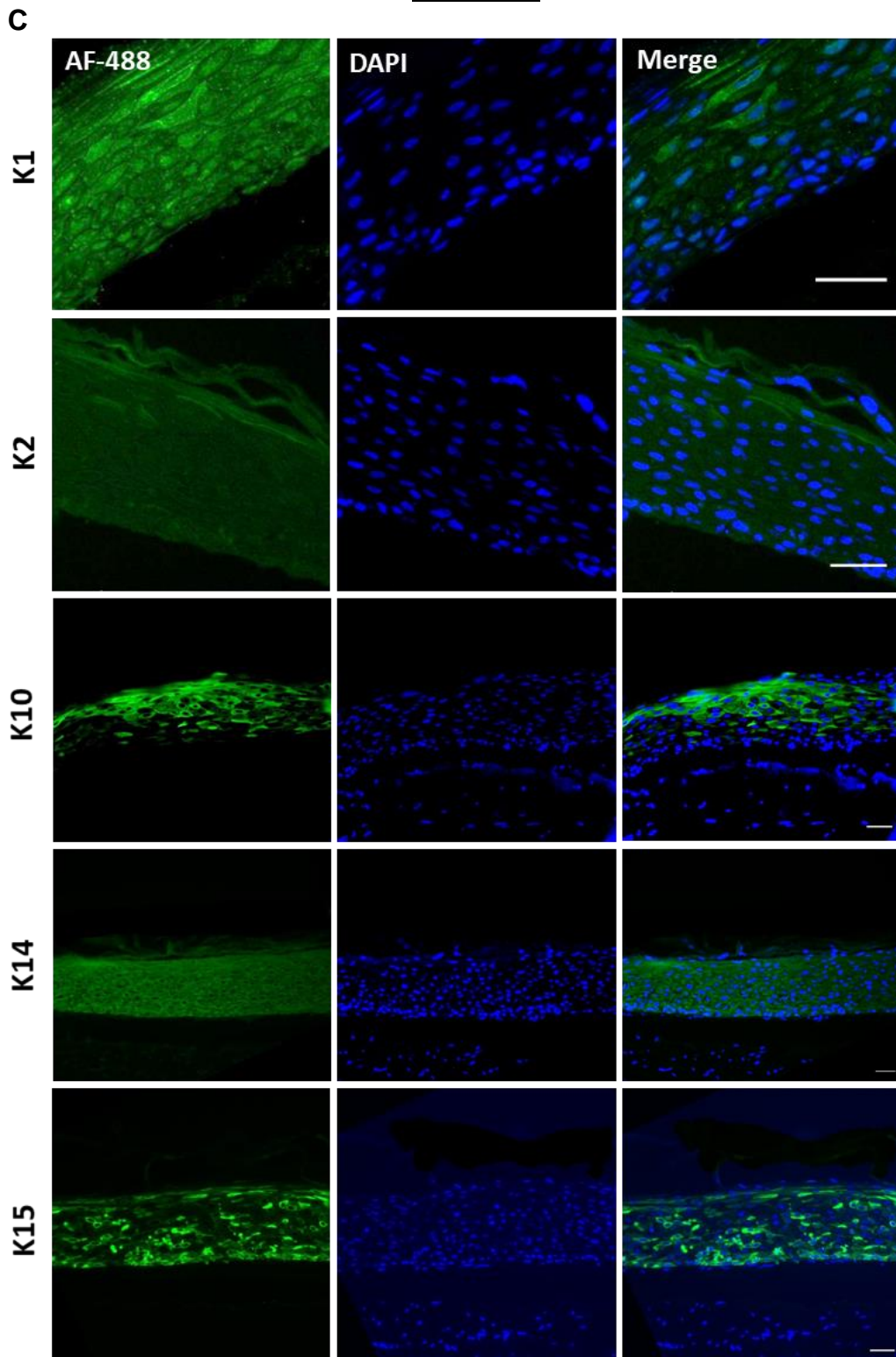


SLP-/PR+

B

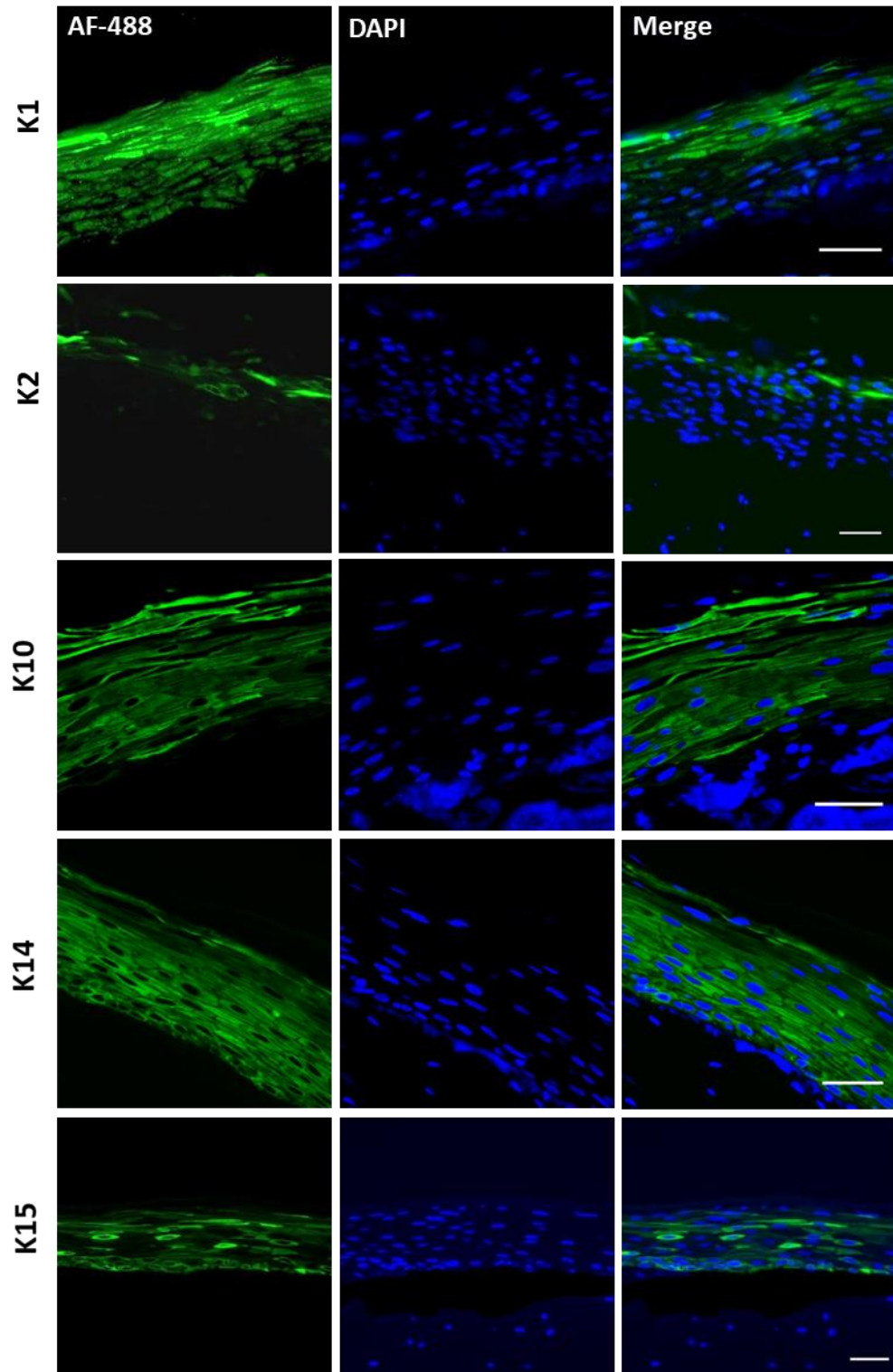


SLP+/PR-



SLP-/PR-

D





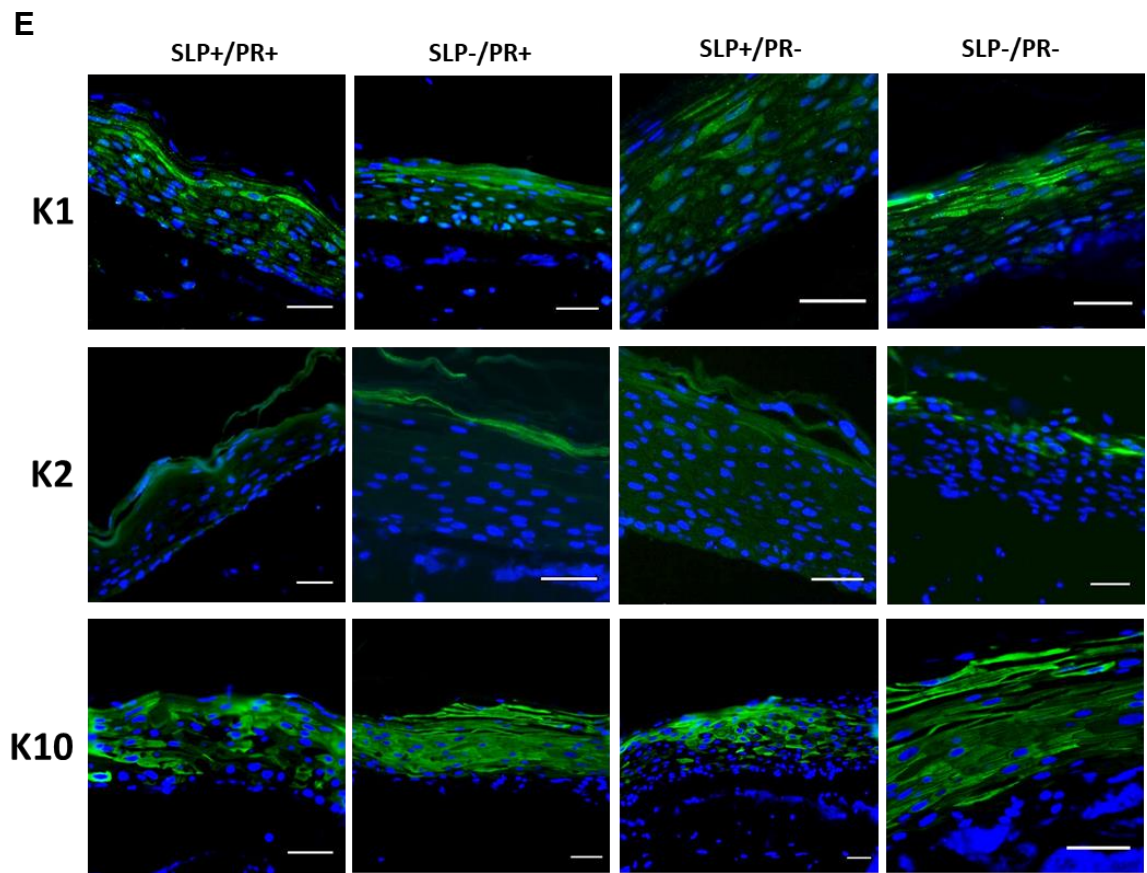


**Figure 4.8. Removal of serum lipids and PR increases the protein expression of K1, K10 and K2 in 3D NHEK cultures.** NHEK were grown in OTCs in an insert (pore size 0.4  $\mu\text{m}$ ) based method. Primary dermal fibroblasts were used in collagen matrix to support the growth of NHEKs. The cells were grown at air-liquid interface for 10 days with 4 different media conditions (A: SLP+/PR+, B: SLP-/PR+, C: SLP+/PR-, D: SLP-/PR-), fixed in 4% (w/v) paraformaldehyde/PBS and paraffin embedded. Sections of 5  $\mu\text{m}$  thickness were cut, antigen retrieved, followed by immunostaining with antibodies against K1, K2, K10, K14 and K15, the nuclei were counterstained with DAPI in blue, overlapping is shown as merged images. Leica DM4000B Epifluorescence microscope and DFC350 camera was used for recording. (scale bar = 20  $\mu\text{m}$ ). In E a summary of the effect of different culture conditions on the expression of keratins K1, K2 and K10 is shown.

## **4.7. Differential effect of ATRA on mRNA and protein expression of K1, K10 and K2 in NHEK.**

In our previous set of experiments, the role of SLPs and PR on mRNA expression of late differentiation markers was investigated. Although SLPs contain fatty acids as well as RA and their metabolites, RA has been known for its role in keratinocyte differentiation and has been used for years by dermatologists targeting various skin conditions. Based on the RA role and its importance in keratinocyte differentiation, the effect of adding ATRA on the expression of differentiation-specific keratins K1, K2 and K10 in NHEK has been studied. Cells were grown with irradiated feeder fibroblasts in RM+ medium containing charcoal stripped FCS (de-lipidised serum) either in the presence (PR+) or absence of PR (PR-) as shown in Figure 4.9. ATRA stocks were dissolved in DMSO for long term storage and further diluted in pure ethanol before use. Working concentrations of 1  $\mu$ M, 2  $\mu$ M, 3  $\mu$ M were used for 24 h to investigate the effect of ATRA in charcoal treated serum containing medium (Lee et al., 2009). After 24 h of treatment, cells were lysed for K1, K10 and K2 mRNA quantification using qPCR, DMSO/EtOH (0.003%/0.03%,v/v) was used as a vehicle control. The expression of both K1 and K10 mRNAs were reduced by 0.5 folds with or without PR in the growth medium at all three ATRA concentrations (Figure 4.9 A, B). There was no significant difference between the 3 different concentrations as measured using One-way ANOVA. The K2 mRNA expression pattern was starkly different, with ATRA showing no effect on K2 expression in the presence of PR but showing significant (2 fold) increase in the absence of PR (Figure 4.9 C), supporting previous data (see Figure 4.6 A) showing opposite effect when lipids and PR were removed. To further investigate the effect of ATRA on the protein level, NHEK were grown with irradiated 3T3 fibroblasts as feeder in charcoal treated

stripped serum containing RM+ medium in presence and absence of PR. Next day, 1 $\mu$ M ATRA was added to these cells for 24 h and DMSO/EtOH (0.001%/0.01%, v/v) was used as a vehicle control. Cells were washed and lysed for WB analysis, K1, K10 and K2 mAbs were used to measure the protein expression after treatment and GAPDH was used as a loading control. In PR containing medium, K1 and K10 did not show any significant change in protein expression after ATRA treatment (Figure 4.10 A). On the other hand, treatment with ATRA for 24 h in the absence of PR did show 0.5-fold reduction in K1 expression with no change in K10 expression (Figure 4.10 B). These data correlate well with the mRNA expression data shown in Figure 4.9 (A, B) in which K1 expression was showing a much more significant reduction compared with K10. This indicates that ATRA is reducing the expression of K1 and K10 on mRNA and protein levels in NHEK and this effect is more pronounced in the absence of PR. K2 did not show any protein expression and this could be due to the fact that K2 is a late differentiation marker and growing the cells for less than 3 days may not be enough to have a detectable protein level of K2.

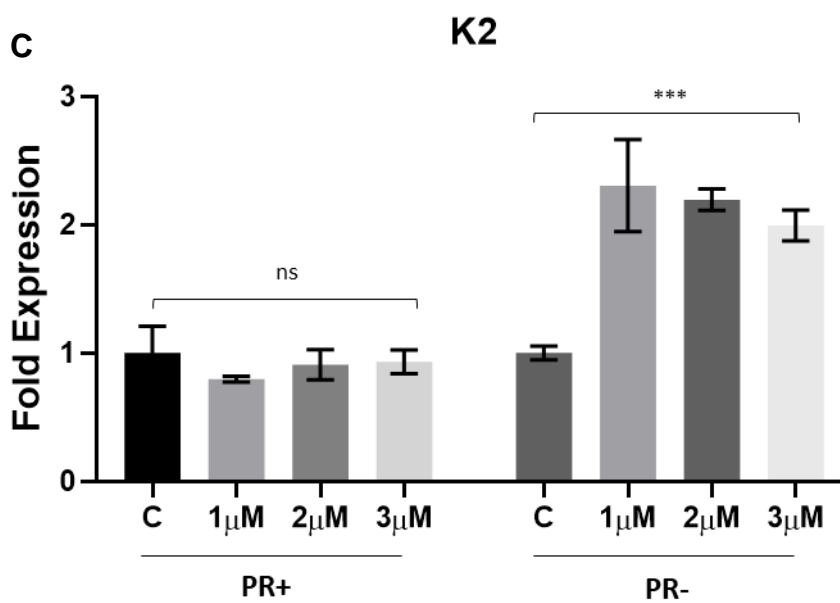
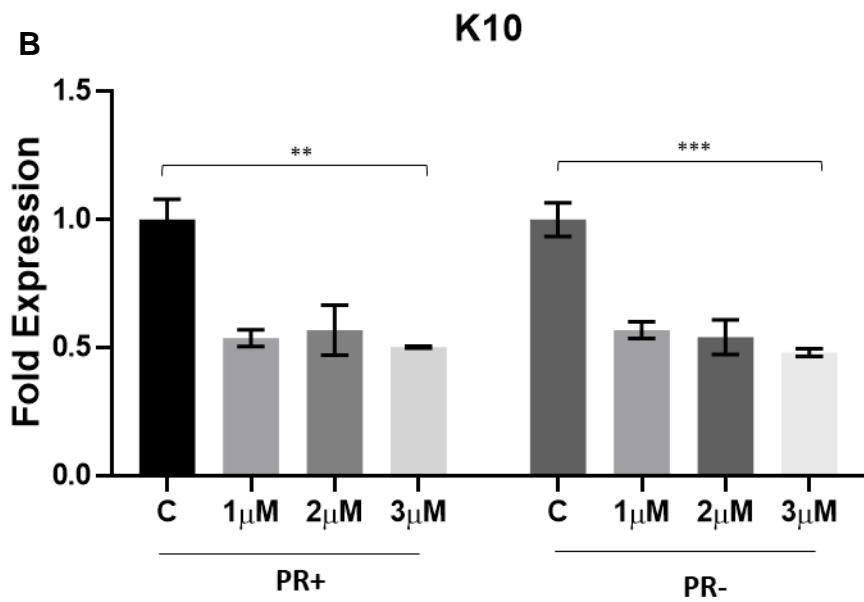
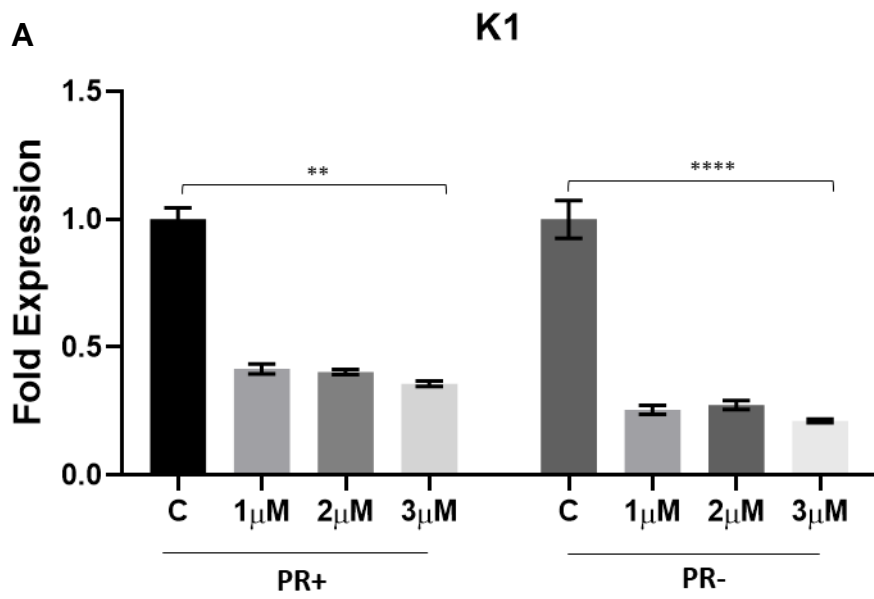


**Figure 4.9. ATRA supresses K1 and K10 mRNA expression while K2 mRNA expression is increased.** NHEK cells mixed with irradiated 3T3 feeder cells were grown in charcoal stripped FCS containing RM+ with or without PR. ATRA stock was made in DMSO and further diluted in Ethanol (EtOH). The cells were grown in three different ATRA concentrations of 1  $\mu$ M, 2  $\mu$ M, 3  $\mu$ M and DMSO/ETOH was used as a vehicle control (0.003%/0.03% maximum) for 24 h after which lysates were collected for qPCR mRNA expression analysis for *KRT1*, *KRT10* and *KRT2*. Data are shown as fold expression normalised to the expression of two housekeeping genes, *POL2A* and *YAP1*. STAT: n=3, Error bars=SEM, One-way ANOVA to measure the p values at different concentrations compared to the control (showed in figure) and between different concentrations of ATRA (ns). Two-way ANOVA was used to measure the statistical significance between PR+ and PR- groups for each keratin (K1\*, K10\*\*\*, K2\*\*\*\*), p-values (ns=p>0.05, \*=p<0.05, \*\*=p<0.01, \*\*\*=p<0.001 and \*\*\*\*=p<0.0001).

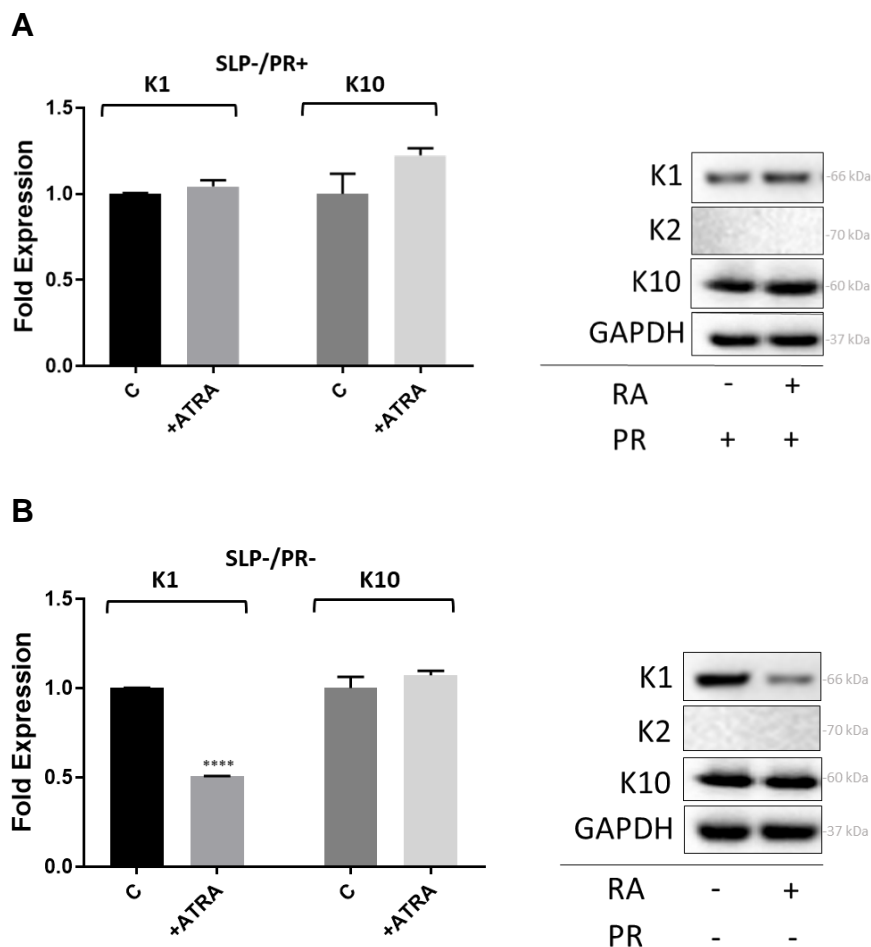


**Figure 4.10. ATRA reduces protein expression of K1 in NHEK.** NHEK cells mixed with irradiated 3T3 feeder cells were grown in charcoal stripped FCS RM+ medium with or without PR. ATRA stock made in DMSO and further diluted in EtOH. The cells were grown and treated next day with 1  $\mu$ M ATRA concentration for 24 h in PR containing medium (A) or PR free medium (B), DMSO/ETOH (0.001%/0.01%) mixture was used as a vehicle control after which lysates were collected for WB protein analysis. Keratins K1, K2 and K10 mAbs were used to detect the level of protein expression and GAPDH was used as a loading control. Data are shown as fold expression normalised to DMSO/EtOH control. STAT: n=3, Error bars= SEM, Student's t-test was performed, p-values (ns=p>0.05, \*=p<0.05, \*\*=p<0.01, \*\*\*=p<0.001 and \*\*\*\*=p<0.0001).

#### **4.8. PR downregulates *KRT1* and *KRT10* but not *KRT2* expression in NHEK.**

The role of ATRA on both mRNA and protein expression of K1, K10 and K2 was examined in our previous section 4.7. Based on the data shown from sections 4.5-4.7, a hypothesis that PR was playing a role in the regulation of genes for keratins K1, K2 and K10 was made, as ATRA was also showing stronger effect when PR is absent. To further study the role of PR on mRNA expression of *KRT1*, *KRT2* and *KRT10*, NHEK were grown with irradiated feeder fibroblasts in PR free RM<sup>+</sup> (charcoal stripped FCS) + 0.01 mg/ml of PR which is the concentration used in normal PR containing culture medium (Berthois et al., 1986) and (Sigma-Merck product information data sheet). Cells were grown in this medium for 3 days with or without 1  $\mu$ M of ATRA in the last 24 h before lysing the cells for qPCR analysis. The solvent DMSO/ETOH (0.001%/0.01%, v/v) treated cells were used as control for ATRA treated cells. Cells grown in charcoal stripped serum medium without PR were used as control for cells treated with PR, as both controls have the same values, only one control was used in this experiment. As shown in Figure 4.11, the expression of K1, K10 was reduced in PR treated cells significantly while K2 reduction was not significant. The addition of both PR and 1  $\mu$ M ATRA for 24 h reduced the expression by almost 1-fold for K1 and K10 with no significant change in K2 expression confirming data shown in Figure 4.9. This shows that PR treatment suppresses steady state level of *KRT1*, *KRT10* and *KRT2* mRNA which is further suppressed when ATRA is added in the case of *KRT1* and *KRT10* but no effect on *KRT2* expression which was shown in Figure 4.9 C when using PR containing medium plus ATRA treatment.

It was concluded, that ATRA is more potent and shows a stronger effect compared with PR even though they work synergistically. To make it easier to

correlates data of this experiment to the previous ones, abbreviations of treatments used in this experiment and the matching medium conditions used before were summarised as shown in the table below. Reference genes YAP1 and POL2 were not affected by these treatment as shown by their Cp values in Figure A.4 a (Appendix).

This experiment	Previous experiments
C	SLP-/PR-
PR+	SLP-/PR+
PR+/ATRA+	SLP-/PR+ (ATRA+)

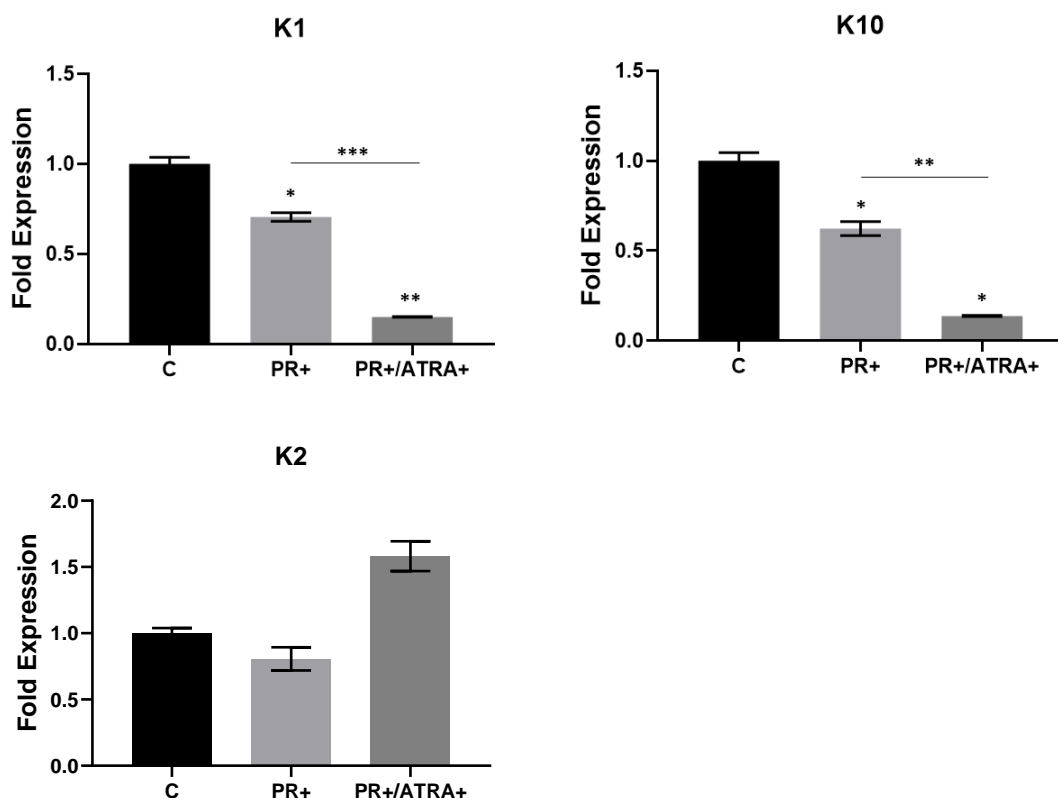


**Figure 4.11. PR supresses mRNA expression for K1 and K10 in NHEK.** NHEK cells were grown with irradiated 3T3 feeder in charcoal stripped FCS PR free RM<sup>+</sup> medium. PR was dissolved in this medium at a concentration similar to that used in normal culture medium (0.01 mg/ml). NHEK were cultured in this medium for 3 days either with or without 1  $\mu$ M ATRA in the last 24 h before collecting cell lysates for qPCR gene expression analysis for *KRT1*, *KRT10* and *KRT2*. Control cells treated with DMSO/EtOH (0.001%/0.01%). Data are shown as fold expression normalised to the expression of two housekeeping genes, POL2A and YAP1. STAT: n=3, Error bars=SEM, Student's t-test was performed, p-values (ns=p>0.05, \*=p<0.05, \*\*=p<0.01, \*\*\*=p<0.001 and \*\*\*\*=p<0.0001).

#### **4.9. $\beta$ -Estradiol has no effect on K1, K10 and K2 gene expression in NHEK.**

In the earlier experiments, it was observed that PR is having an effect on *KRT1* and *KRT10* expression in NHEK and due to the structural similarity between impurities in PR and  $\beta$ -estradiol (ED), a hypothesis that PR could be mimicking the effect of ED was made. Therefore, investigating the effect of ED on *KRT1*, *KRT2* and *KRT10* expression was done. NHEK were grown with irradiated feeder fibroblasts cells in PR free RM<sup>+</sup> medium with charcoal stripped FCS before ED was added at 10 nM, 50 nM, 100 nM, 500 nM and 1  $\mu$ M concentrations for 24 h before lysis and qPCR analysis. As shown in Figure 4.12 the expression of the three keratins did not show any significant change in the presence of ED compared with the control. This suggests that the effect of PR observed in Figures 4.6- 4.11 could not be due to the structural similarity to ED as has been proposed previously (Hofland et al., 1987, Berthois et al., 1986). Further investigations using higher  $\beta$ -estradiol concentrations or a different ED form are required to reach a definitive conclusion. Reference genes YAP1 and POL2 were not affected by ED treatment as shown by their Cp values in Figure A.4 b (Appendix).



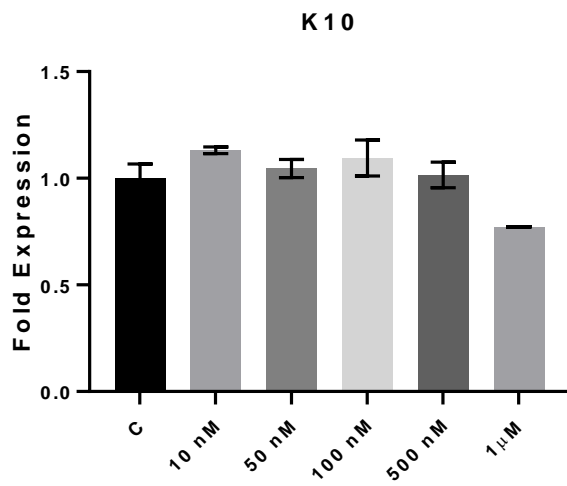
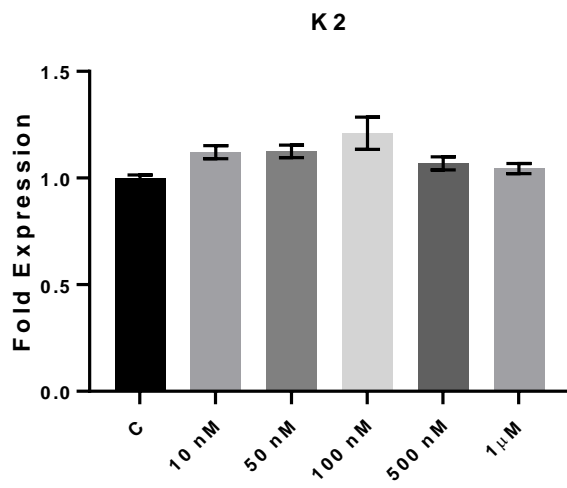
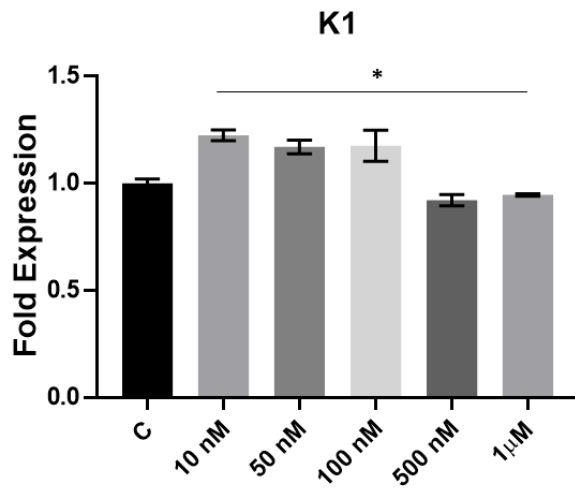


**Figure 4.12.  $\beta$ -Estradiol has no effect on the expression of *KRT1*, *KRT2* and *KRT10* genes in NHEK.** NHEK cells were grown with irradiated 3T3 feeder cells in charcoal stripped FCS PR free RM+ medium.  $\beta$ -Estradiol was dissolved in DMSO (0.001%). Concentrations of  $\beta$ -Estradiol in the range of 10 nM – 1  $\mu$ M were added in the culture medium and cells were treated for 24 h before collecting cell lysates for expression analysis for *KRT1*, *KRT10* and *KRT2* gene by qPCR. Control cells were treated only with DMSO (0.001%). Data are shown as fold expression normalised to the expression of two housekeeping genes, POL2A and YAP1. STAT: n=3, Error bars=SEM, One-way ANOVA was performed, p-values (ns=p>0.05, \*=p<0.05, \*\*=p<0.01, \*\*\*=p<0.001 and \*\*\*\*=p<0.0001).

## 4.10. Discussion and conclusion.

RA plays a fundamental role in maintaining the normal epidermal differentiation, it induces hyperproliferation and it is widely used as a therapeutic agent for treating many skin ailments (Virtanen et al., 2000, Torma, 2011). The effect of RA on cytokeratin expression is quite complex; high concentrations of RA ( $10^{-6}$ M) suppresses the expression of basal keratins K5 and K14 while K19 expression is enhanced (Crowe, 1993). For supra-basal keratins involved in terminal differentiation (K1, K2, K10), the expression is either downregulated or unaffected by topical RA treatment on normal skin of volunteers (Virtanen et al., 2000, Crowe, 1993, Kopan et al., 1987). The suppressive effect of RA on certain genes differs markedly *in vivo* and *in vitro* (Gendimenico and Mezick, 1993). Keratinocyte differentiation is retinoid sensitive, with nano-molar concentration required to keep the normal level of differentiation while excess or reduced RA concentrations could respectively reduce or amplifies the terminal differentiation (Randolph and Simon, 1997). RA binds to serum albumin and its concentration in FCS is around 2 mg/ml (Napoli, 1986). Stripped FCS in which most of the lipids have been removed by charcoal treatment including RA have been used and the cells were grown in this medium for studying the role of SLPs on the expression of late differentiation keratins in NHEK. FCS is widely used in tissue culture to maintain normal cellular growth and differentiation. It contains a wide range of vitamins, minerals, lipids and proteins as well as other molecules that are needed

by the cells such as hormones and growth factors (Gstraunthaler, 2003, Zheng et al., 2006). These molecules will have huge impact on cellular function and regulation, so charcoal stripping of serum would enable us to study the effect of serum lipid or hormones as studying the role of steroids and RA for example (Sorensen et al., 1997, Wille et al., 1984, Svendsen et al., 1997b, Sikora et al., 2016).

In this set of experiments, the role of RA and PR on the expression of K1, K2 and K10 in keratinocytes was investigated either by removing lipids from the serum or using PR free medium or both. The experiment started with two cell lines that were available in the lab and immortalised by the HPV16 method (Neb-1 and T103C), respectively derived from skin and oral tissues (Bryan et al., 1995, Dickson et al., 2000). Using these cell lines no induction of late differentiation keratins was detected as shown in Figure 4.3 when serum was stripped so these cell lines were removed from our next set of experiments and HaCaT and N/TERT were used which are immortalised differently (HaCaT is spontaneously transformed by prolonged cultivation at low  $\text{Ca}^{2+}$  concentration (0.2 mM) and moderately high temperature 38.5°C while N/TERT keratinocytes immortalised by ectopic expression of the telomerase catalytic subunit (hTERT) and subsequent spontaneous events leading to the loss of p16<sup>INK4a</sup> expression) (Smits et al., 2017, Fusenig and Boukamp, 1998).

As PR is known to have a weak estrogenic effect that could affect keratinocyte differentiation, this point of investigation was added into our study as well (Berthois et al., 1986, Welshons et al., 1988, Choi et al., 2000, Ramot et al., 2009). Keratinocytes cell lines and NHEK were grown in four different conditions of RM<sup>+</sup> medium as follows:

- SLP+/PR+ (lipid containing serum that contains PR).
- SLP-/PR+ (charcoal stripped serum containing PR).
- SLP+/PR- (lipid containing serum without PR).
- SLP-/PR- (charcoal stripped serum without PR).

Lipid removal from the serum did induce the expression of K1 and K10 in HaCaT with K10 being upregulated more when lipids and PR were removed from the medium (SLP-/PR-). N/TERT cell line data were different, in which removal of PR in the presence of SLP was the only condition showing upregulation of K1, K2 and K10 mRNA levels and K1 and K10 protein levels. This difference between HaCaT and N/TERT could be primarily due to their immortalisation method in which HaCaT is a cell line that is spontaneously immortalised while N/TERT is immortalised through hTERT component of the telomerase gene that maintains the telomerase end and repress replicative senescence (downregulation of p16) (Dickson et al., 2000). NHEK showed the same pattern as HaCaT with both K1 and K10 being more upregulated in SLP-/PR- condition, these changes have been shown at both mRNA and protein levels. Keratin K2 was showing a similar pattern in protein expression but no significant difference in mRNA levels. Other studies have shown an opposite effect when adding RA on skin or cultured keratinocytes in which K1 and K10 were either downregulated and in other studies unaffected and these findings strongly indicate that the effect that has been seen is primarily due to the presence of RA. Some reports have also shown that K2 mRNA levels were reduced and the protein levels were either unchanged or the protein became undetectable when skin tissue of volunteers were treated with RA (Torma, 2011, Rosenthal et al., 1992, Virtanen et al., 2000, Rosenthal et al., 1990). We have also added ATRA to charcoal stripped serum medium with

or without PR and the effect shown in other studies was able to be reproduced, where they have added RA directly on skin. Keratins 1 and 10 were downregulated on mRNA levels and protein which was more pronounced in PR free medium (Figure 4.9, 4.10).

Estrogen has also been shown to affect some keratin gene expression as upregulation of *KRT2*, *KRT14* and *KRT19* genes, this has been shown in human scalp skin after  $\beta$ -Estradiol treatment (Ramot et al., 2009). PR has been shown to bind to estrogen receptors at concentrations lower than 0.01 mg/ml and induces cell proliferation of MCF-7 cells (Berthois et al., 1986, Welshons et al., 1988), and reduced proliferation when only PR was removed from the medium. Based on these data, a hypothesis was made, that as PR is inducing proliferation it could be inhibiting differentiation, as part of normal cellular physiology in which factors that induce proliferation and cell cycle progression inhibit the cellular differentiation process (Suzan and Sander, 2016). A synergistic effect of removing PR with SLPs removal was observed that upregulated K1, K2 and K10 in NHEK while adding PR back did reduce the expression of *KRT1* and *KRT10* but not *KRT2* in NHEK. The estrogenic like effect of PR using  $\beta$ -estradiol addition to the culture medium has been also investigated. Although some studies have shown lower expression of differentiation-specific keratins when keratinocytes were treated with estrogen receptor ER- $\beta$  agonist, some genes that are not involved in terminal differentiation such as *KRT19* were induced by estrogen treatment (Choi et al., 2000), no effect on differentiation-specific keratin gene expression in NHEK by  $\beta$ -estradiol was shown (Figure 4.12). This indicates that PR effect that is shown in our experiments could be due to impurities other than its structural similarity with  $\beta$ -estradiol.

NHEK were used to rule out any effect of immortalisation that could disturb the normal process of keratinocyte differentiation and affect the expression of their genes.

**In conclusion:**

- In NHEK, the expression of K1 and K10 after lipid removal was significantly upregulated at both mRNA and protein levels while K2 only showed a non-significant reduction. At the protein level K2 was expressed slightly after lipids removal.
- Removing PR and lipids seem to work synergistically as when both were removed from growth medium the expression went more higher than removing either of them.
- K1 and K10 reacts in a similar way of response either to lipids removal or to ATRA and PR addition while K2 reacted in an opposite way.

Based on the data in this chapter, a hypothesis has been made that K1 and K10 are regulated in an inverse way compared to K2. Another hypothesis was made that ATRA is either activating K2 promotor and inducing more synthesis or it could be stabilising the mRNA after transcription. Our next set of experiments were planned to investigate these hypotheses.

# CHAPTER 5

## **5. Results III. mRNA stability of differentiation-specific keratins; effect of serum lipids and ATRA.**

### **5.1. Introduction.**

Gene regulation is a vital event for each living cell in all organisms. Genes are tightly regulated in mammalian cells at different levels from transcription down to protein synthesis and this regulation is controlled by a variety of pathways and regulatory factors that could affect the transcript pre- or post-transcriptionally. This controlled regulation results in a wide range of cellular proteins being synthesised in the correct time and location inside the cell giving a phenotypic diversity between different organisms (Newbury, 2006, Liu et al., 2014). The process of gene expression starts with DNA being transcribed to mRNA using the enzyme (RNA pol) inside the nucleus. The transcription process is divided into three stages (initiation, elongation and termination). In the initiation step, the enzyme RNA pol binds to the untranslated region (i.e. a promotor sequence at the start of the gene need to be transcribed) and start transcription by synthesising a DNA strand. This newly synthesised strand is complementary to one of the DNA strands (template) and this step starts at the DNAs 3'end. In elongation, the RNA starts to elongate as the RNA pol moves on until it hits transcriptional termination sequence that dissociates the polymerase and the transcription is terminated (Figure 5.1) (Taylor, 2006, Maraia and Arimbasseri, 2017). There are different types of RNA polymerases to transcribe different types of genes. For ribosomal RNA (rRNAs) genes, RNA pol I is required, for messenger RNAs (mRNAs) RNA polymerase II is required and for some small regulatory RNAs and other small RNAs such as transfer RNAs, RNA polymerase III is utilised (Carter and Drouin, 2009, Kwapisz et al., 2008).



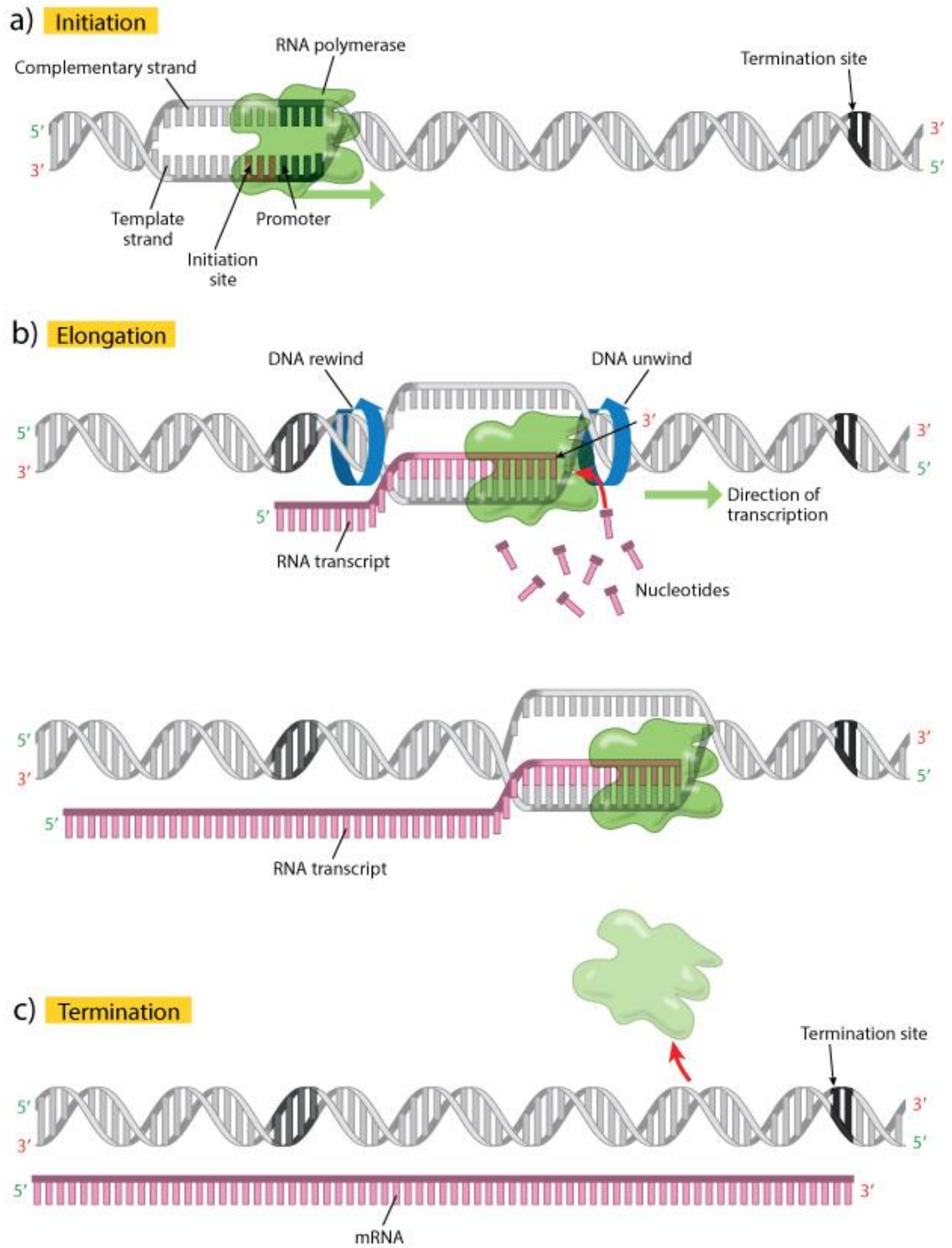


**Figure 5.1. Gene transcription steps.** A diagram showing gene transcription steps initiation (a) RNA pol bind to promotor at initiation site, elongation (b) RNA pol moves on copying template strand to form an RNA transcript .In termination (c) the RNA pol dissociates as it reaches the termination site (©2014 Nature Education).

The single strand RNA that has been synthesised is called a Transcript which undergoes a series of post-transcriptional modifications before the mature mRNA is ready to be exported to the cytoplasm. These modifications include RNA splicing in which sequences corresponding to introns are removed and sequences corresponding to exons are joined together, a cap at the 5' end and a poly-A tail at the 3' end is added. Later, the mature mRNA is exported into the cytoplasm. Only 10% of the synthesised RNA sequence is converted into the mature mRNA as around 90% are introns which are spliced out. Interestingly, around 70% of the nuclear transcripts are either un-polyadenylated or poorly spliced (defective post-transcriptional modifications) rendering them unable to be exported out of the nucleus (Liu et al., 2014). Once the mature mRNA is exported to the cytoplasm, some pre-translational changes are made before being translated into polypeptides that folds into structural and functional proteins (Figure 5.2).

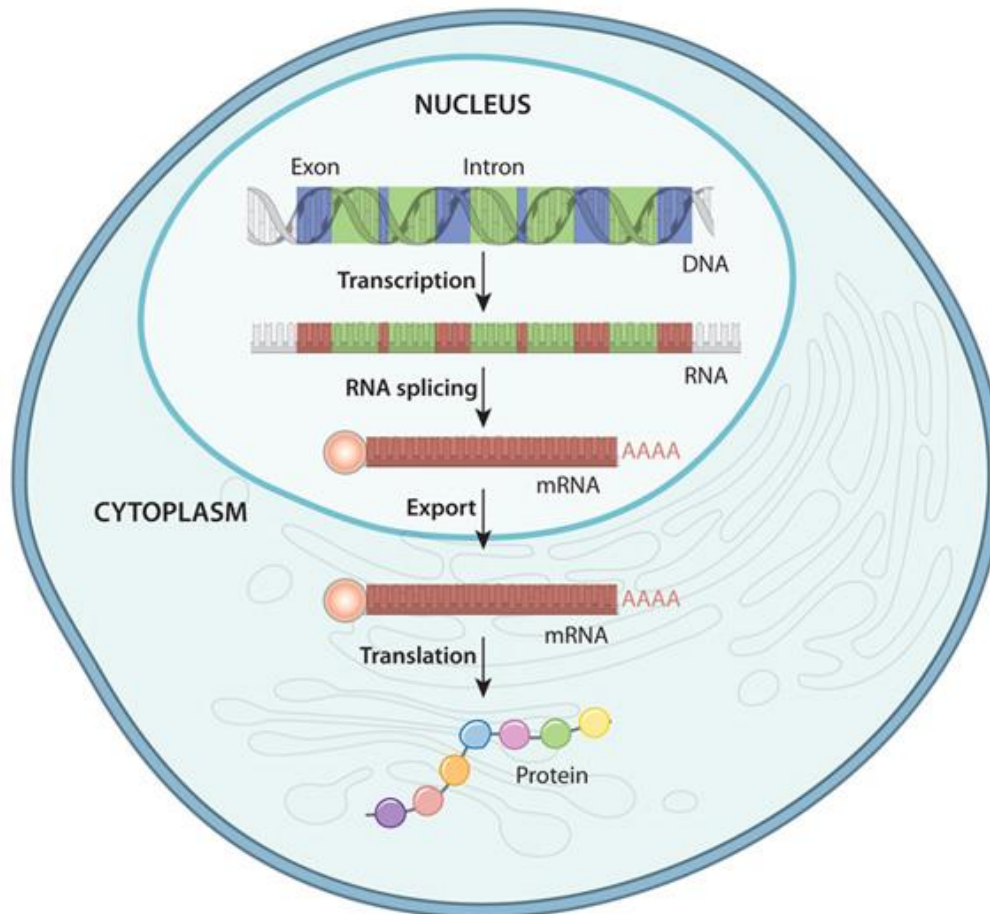


**Figure 5.2. RNA transcription and translation.** First, DNA is transcribed having both coding and noncoding regions, introns will be removed, and exons joined together. Spliced mRNA is prepared by adding a cap and a poly-A tail on the 5' and 3' respectively, before being exported out of the nucleus. In the cytoplasm, the mRNA is ready to be translated into protein. (©2010 Nature Education).

### 5.1.1. mRNA stability.

As part of the gene regulation process, the stability of the mRNA being transcribed is critical. Part of the transcript stability is controlled inside the nucleus in which faulty splicing or de-adenylation takes place using nuclease enzyme, this destabilises the transcript product and it is no longer functional although it has been transcribed. Part of these RNA degradation processes takes place in the cytoplasm in which some enzymes can de-cap or remove the poly-A tail of the transcript as the exosome enzyme for example. This mRNA decay or instability is a highly regulated cellular process. The mRNA decay happens in response to

different extrinsic or intrinsic stimuli allowing the cell to stop synthesising a certain protein that is no longer needed by the cell or its presence could affect other pathways that are needed under certain conditions. Those stimuli could be either a developmental stimulus such as proliferation and differentiation or a response to an environmental trigger such as temperature, hypoxia or viral infections. Certain nutrients, hormones or drug treatments could also affect mRNA stability (Guhaniyogi and Brewer, 2001). The decay response of the mRNA should be rapid, allowing the cell to keep the steady state level of the mRNA needed for normal cellular function. The differential stability of different mRNAs allows some to be highly stable while others degrade rapidly, c-fos and  $\beta$ -globin mRNAs are two examples of differential stability. The mRNA of c-fos is involved in cellular response to external stimuli so its half-life is no longer than 30 min while  $\beta$ -globin mRNA has a half-life greater than 24 h as it is required for the synthesis of red blood cells (Atwater et al., 1990). The mRNA level that scientists measure in cells using classical methods such as qPCR and northern hybridisation is the steady state level of this mRNA which represents the balance between production (transcription) and decay and this is usually measured using real time qPCR. In order to study the decay rate or the mRNA stability of a certain gene we need to measure the decay rate or the mRNA half-life and there are a wide variety of methods used in the literature that can be summarised into three main techniques as shown in Figure 5.3. (Wada and Becskei, 2017).

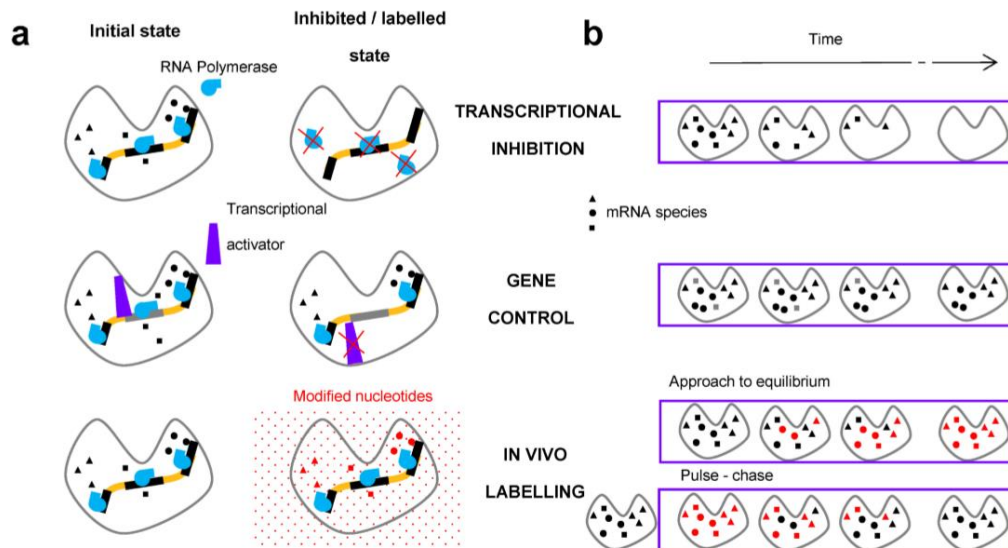


**Figure 5.3. Main classes of methods to study RNA stability.** In (a) the molecular mechanism affected by a specific method is shown. In transcriptional inhibition, the RNA pol is inactivated, and the expression of all genes is reduced. In the gene control method, a transcriptional activator dissociates from a specific promoter, shutting off the expression of that gene. In labelling, modified nucleotides introduced into the cell and incorporates into the RNA. In (b) the time course of the experiments is shown, for the first two methods time start at zero while in last method the increase of labelled mRNA is monitored after applying pulse to the nucleotides (Wada and Becskei, 2017).

The most commonly used method to measure mRNA turnover is transcriptional inhibition. When transcription is blocked, the transcription of all genes is reduced, RNA starts to decay, and the rate is measured overtime. Many drugs have been used to block transcription, Thiolutin,  $\alpha$ -Amantin, Triptolide and AD. Each drug has its advantages and limitations in which some drugs could have side effects other than transcriptional blockage such as thiolutin which can chelate  $Zn^{++}$  ions and inhibit metalloproteases that could affect other cellular functions. The most commonly used transcriptional inhibitor is AD which is an antibiotic isolated from *Streptomyces parvulus* and has been used as an anti-cancer drug as well. AD blocks the elongation step of mRNA synthesis in which RNA pol can no longer move on the DNA strand and continue the transcription. When elongation is blocked, RPB1 (subunit 1 of RNA polymerase II) is degraded which is mediated by the activation of p53, the major tumour suppressor gene. AD inhibits

transcription by all three RNA polymerases depending on the concentration of the drug used, low concentrations  $>0.01 \mu\text{g/ml}$  inhibits polymerase I while higher concentrations inhibit polymerase II. It has a fast rate of action (in minutes) with weak reversibility after being removed. Despite these advantages, it still has some limitations as it inhibits all genes non-specifically as well as its feedback loop in which some genes are enhanced after their initial inhibition, such as p53 gene, which affects a number of structural proteins and play a role in cellular apoptosis (Bensaude, 2011).

There are other methods to study mRNA decay such as gene control and *in vivo* labelling, but they are not commonly used. In the gene control method, transcription is also inhibited but in this technique the inhibition is specific to the gene of interest that its controlled by a promotor. Despite its low side effects, this method is not commonly used because each experiment ends by measuring only one mRNA half-life. In the metabolic labelling method, the half-life of the mRNA is measured by quantifying the rate at which the labelled mRNA increases or decreases after the labelled nucleotides is being introduced or removed. This could be measured using either the Approach to Equilibrium Method (AEM) or the Pulse-Chase Method (PCM). In the AEM, the rate of degradation is measured, and it corresponds with the increase in the labelled mRNA. On the other hand, in the PCM, the decline in the mRNA is measured that corresponds to the washout labelled nucleotides. In radioactive labelling of [ $^3\text{H}$ ]-adenine and [ $^{32}\text{P}$ ]-phosphate is no longer used as it induces cellular damage that affects mRNA stability (Atwater et al., 1990, Wada and Becskei, 2017).

Different mRNAs can be degraded through different pathways, but also the same mRNA can decay differently under different conditions. The structural key elements in the decay process are the 3'-poly-A tail, 3'-cap untranslated region

(UTR), the protein coding region, 5'-UTR and 5'-cap. The poly-A tail has an important role in nuclear processing of the mRNA and its export to the cytoplasm. Once the mRNA is in the cytoplasm its stability is affected and also its ability to translate into protein. There are three main pathways controlling mRNA degradation. The first pathway is the de-adenylation pathway, the poly-A tail interacts with the poly-A tail binding protein (Pab1p) and this binding protects the mRNA from rapid degradation. Under certain conditions, de-adenylase cleaves the poly-A tail rendering the mRNA to be degraded by exoribonuclease enzyme. The second pathway deals with the 5' cap and it's called de-capping. In this pathway de-capping proteins Dcp1p and Dcp2p form a complex that cleaves the mRNA at the 5'-end which allow it to be further degraded by Xrn1p exoribonuclease. This pathway could take place after or in conjunction with de-adenylation or could take place independently as well. The third pathway is called non-sense mediated decay pathway (NMD) in which endonuclease cleavage targets mRNA with non-sense codons or un-spliced introns. After cleavage, the 3'-end is degraded by exosomes and the 5'-end is degraded by Xrn1p (Figure 5.4). The eukaryotic exosome mentioned here is a ten subunit 3' exoribonuclease complex responsible for many RNA processing and degradation reactions, not to be mistaken with the exosomes that are secreted by the cells as vesicles used for intercellular communication (Simons and Raposo, 2009, Newbury, 2006, Kramer and McLennan, 2018, Chen et al., 2008, Guhaniyogi and Brewer, 2001, Wada and Becskei, 2017, Schaeffer et al., 2009, Qadir et al., 2018).

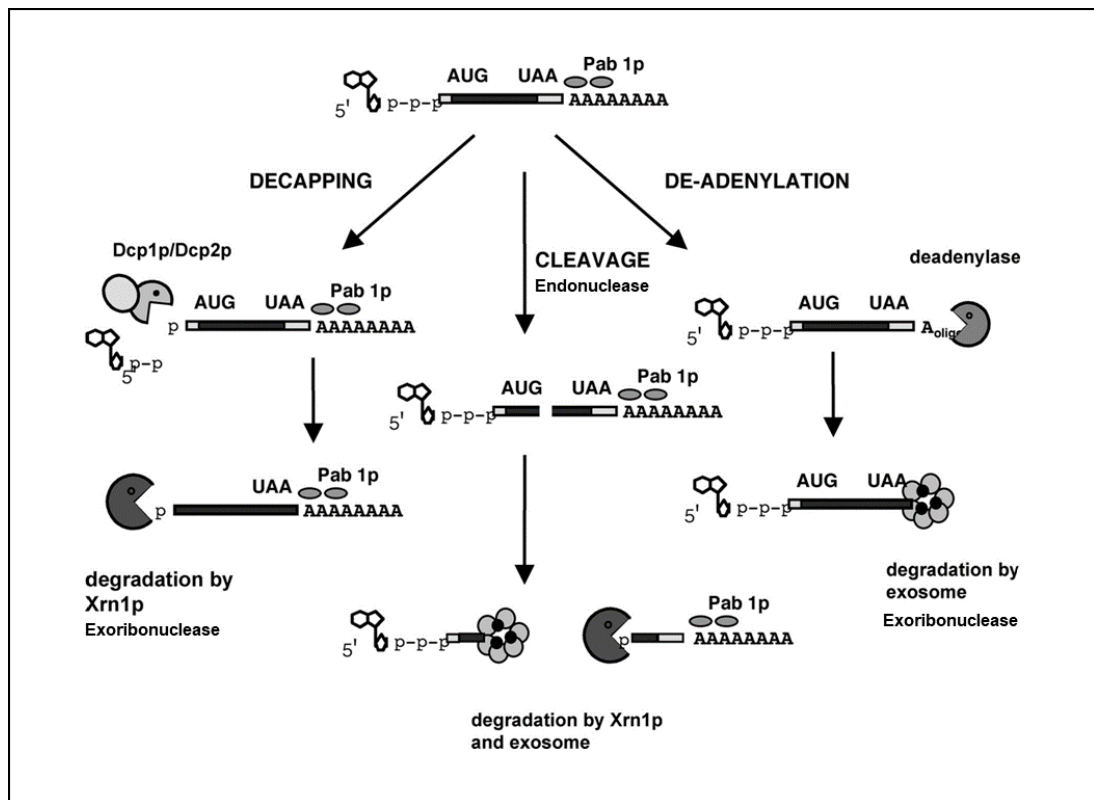


**Figure 5.4. Three main pathways controlling mRNA degradation in eukaryotes.** First pathway is de-adenylation in which poly-A tail is removed by deadenylase and mRNA is further degraded by exonome. Second pathway is de-capping at 5' end using de-capping proteins and the mRNA is further degraded using Xrn1p exonuclease. Third pathway endonuclease targets mRNA with non-sense codons or un-spliced introns and mRNA will be further degraded by Xrn1p exonuclease and exonome and this pathway is called non-sense mediated decay pathway (NMD). (Newbury, 2006).

The clinical significance of studying mRNA decay has been shown in a variety of human diseases such as cancer and Alzheimer's disease. In these conditions, certain stabilising mRNA proteins are affected either by allowing more decay or by stabilising mRNAs that encode unwanted proteins that leads to accumulation of these proteins inside the cell. The ability to study mutations of these stabilising components and the ability to regulate mRNA stability seems to be a promising novel therapeutic approach (Guhaniyogi and Brewer, 2001).

### 5.1.2. Promoter activity measurements.

Another important aspect of gene regulation is the promoter activity of a particular gene. It is vital to understand the molecular basis of underlying gene regulation



mechanisms at the transcription level. The promoter sequence is the DNA region that guides the initiation of RNA pol II transcription accurately. The RNA pol II will not be able to recognise the initiation site (promotor) without the aid of some additional transcription factors. Under certain defined conditions the transcription factors bind to a promotor region allowing RNA pol II to join and start transcription and could determine the strength of binding of pol II to the promotor region (Juven-Gershon and Kadonaga, 2010, Irie et al., 2011).

The activation of the promotor can be determined by measuring its gene products such as mRNA and proteins, but this method lacks the mechanism by which the promotor is activated. One of the most common methods to study promotor activity of a specific gene, is the use of a reporter gene linked to the promotor sequence of the gene of interest using transient transfection of a plasmid containing these genes. Later the expression of the reporter gene is measured and the most commonly used reporter genes are chloramphenicol acetyltransferase,  $\beta$ -galactosidase, firefly or renilla luciferase, alkaline phosphatase or green fluorescent protein (GFP) (Ducrest et al., 2002).

Luciferase reporter gene assays have been used to measure the promotor activities of functional gene and is considered one of the most commonly used reporter gene assays. It is highly sensitive compared to other reporter genes as well as it lacks any endogenous activities in eukaryotic cell. The firefly luciferase reporter gene is attached downstream to the promotor of interest, and when the promotor is activated, firefly gene will be transcribed and further translated into a luciferase protein that can be measured using a chemiluminescent detection system as shown in Figure 5.5 (Yun and Dasgupta, 2014).

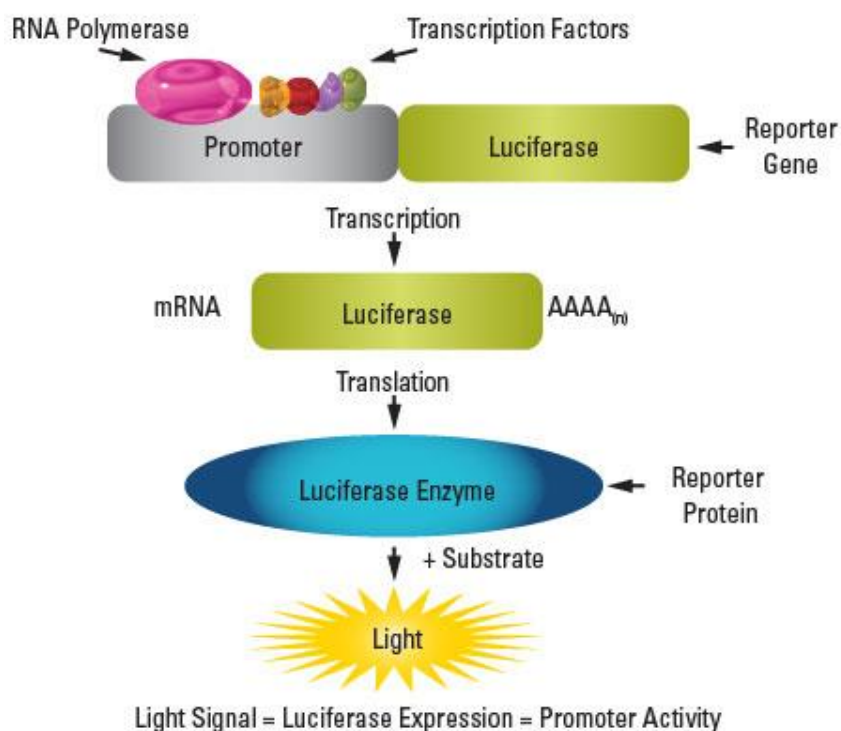


**Figure 5.5. The luciferase reporter assay.** Luciferase reporter gene attached downstream to promoter of interest. RNA pol and transcription factors transcribe DNA to mRNA. mRNA is translated into the luciferase enzyme (reporter protein) that will give a light signal when activated using a Substrate. Light signal is =Promoter activity. (Thermo-Fisher scientific.UK).

The method used to measure the stability of K1, K2 and K10 mRNAs in NHEK using AD will be described in this chapter. The role of ATRA on mRNA decay on these genes will also be investigated as well as the role of different growth conditions (SLP and PR) that were used in chapter 4 on the decay rate of these genes. To measure the promoter activity of K2 and K10 in keratinocytes, optimised keratinocytes transfection conditions in HaCaT were done using pLPC\_puro-AcGFP vector. Luciferases reporter pGL4.26 and pGL4.14 vectors were also used for measuring the activity of AP-1 and measure activities of K2 and K14 promoters using luciferase assay after PMA treatment or after using different growth conditions. Further details will be discussed in each section. Materials and Methods are described in chapter 2. For statistical analyses, n=3,

error bars represent SEM, p values are calculated using ANOVA or student t-test performed on raw data.

## **5.2. mRNA stability of late differentiation keratins.**

### **5.2.1. Measuring the stability of c-Myc mRNA and 18S rRNA after Actinomycin D treatment.**

To study the rate of mRNA decay of late differentiation keratin genes, the transcription inhibition method using AD was employed, the most commonly used drug to inhibit transcription. To determine whether the drug works in our hands and determine the optimal concentration to use for transcriptional inhibition, two genes were selected, c-Myc as a positive and 18S rRNA as a negative control for the decay process in which different concentrations of AD were used for 0-4h to study their decay. 18S rRNA is a ribosomal RNA that is present at high level in all eukaryotic cells (S represents Svedberg unit which is used to measure sedimentation rate of ribosomes). 18S rRNA is known to be a highly stable RNA that can be used as a reference gene as well (Gonzalez and Schmickel, 1986, Kuchipudi et al., 2012). On the other hand, c-Myc RNA is known to be highly unstable in mammalian cells with a half-life of 10-30 min in some cell lines after AD treatment. c-Myc gene is known to having a long UTR at the 3'-end that triggers de-adenylation (poly-A tail removal) and renders the transcript unstable (Atwater et al., 1990, Guhaniyogi and Brewer, 2001, Kuzyk and Mai, 2014, Miller et al., 2012). The concentration of AD was selected in our future experiments based on the AD concentration when c-Myc mRNA had completely decayed while 18S rRNA is still stable, the assumption being that our keratin mRNA stability will range somewhere in between the two extremes. As shown in Figure 5.6, AD

dissolved in distilled water at different concentrations was used, 0.25 µg/ml, 0.5 µg/ml, 1.0 µg/ml and 2.0 µg/ml for up to 4 h. 18S rRNA was decayed by around half after 1 h of AD treatment at all concentrations and stayed stable for up to 4 h. It could be that the very low concentration 0.25 µg/ml of AD started to become less effective after 2 h and transcription was induced again (blue line). For c-Myc, all four concentrations (0.25 µg/ml up to 2 µg/ml) showed similar complete decay after 2 h. Based on these observations, 2 µg/ml (the maximum concentration) were used for different time points for our experiments to ensure that transcription of our genes of interest will be completely inhibited. This AD concentration has also been used previously to study the mRNA stability of keratin K19 gene in keratinocytes (Crowe, 1993).

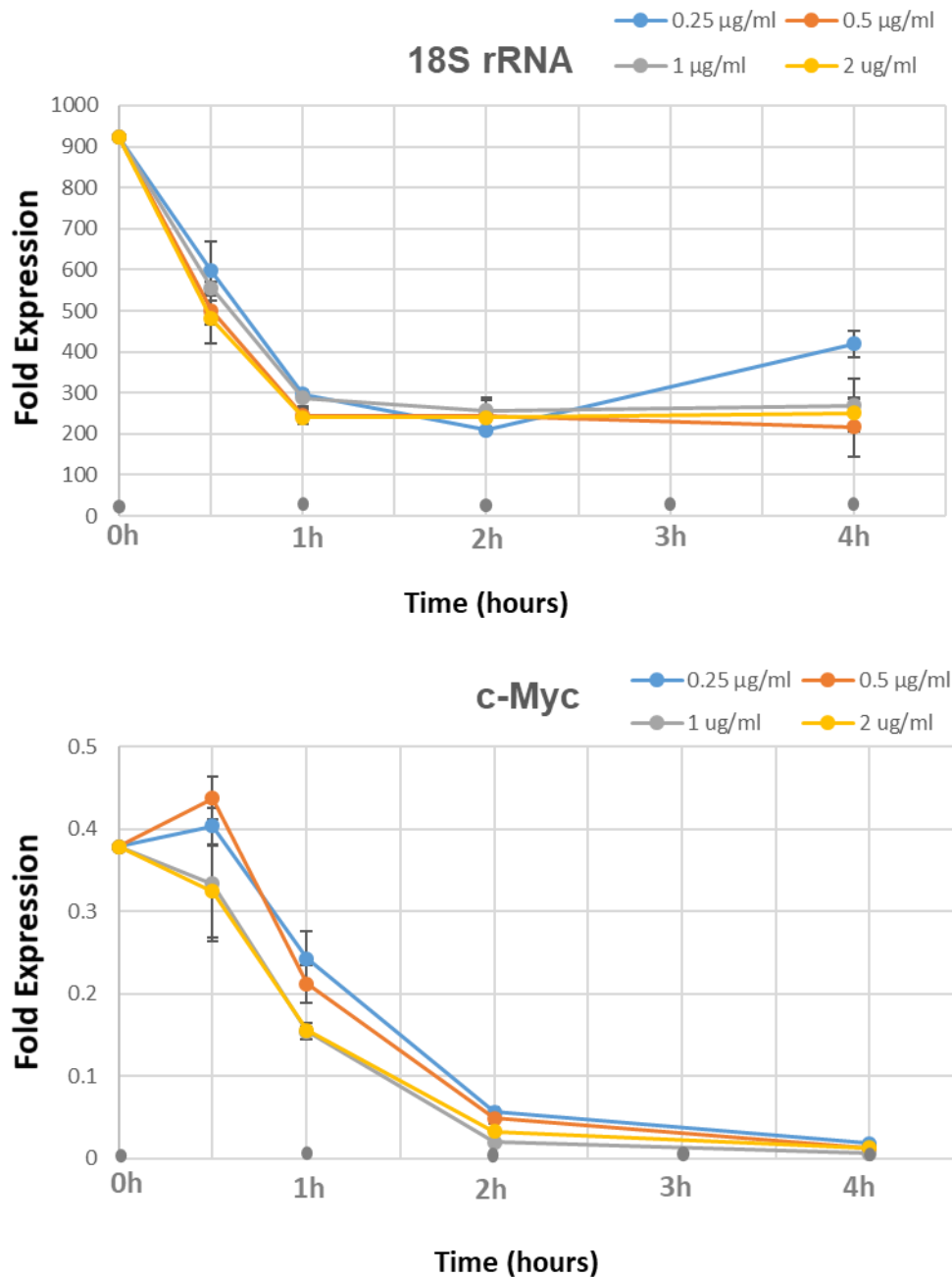


**Figure 5.6. mRNA decay of 18S rRNA and c-Myc mRNA in NHEK after AD treatment.** NHEK cells mixed with irradiated 3T3 feeder cells were grown in RM+ medium, starved overnight (4% v/v Hyclone II serum). Next day cells were treated with AD, dissolved in dd H<sub>2</sub>O, at different concentration (0.25, 0.5, 1.2 µg/ml) up to 4 h before lysates were collected for measuring remaining 18S rRNA and c-Myc mRNA by qPCR. All data shown as fold expression normalised to YAP-1 and POL2A, the housekeeping genes. Untreated cells were used as controls (0h). In this figure we are comparing a highly stable RNA (18SRNA) to an unstable RNA (c-Myc). STAT: n=3, Error bars= SEM, one-way ANOVA was used to measure p-values (ns=p>0.05, \*=p<0.05, \*\*=p<0.01 and \*\*\*\*=p<0.0001). In statistical analysis we are looking at relative mRNA expression for each concentration separately over treatment time as shown below.

Over time	18S rRNA	c-Myc
0.25 µg/ml	*	****
0.5 µg/ml	*	****
1 µg/ml	*	****
2 µg/ml	**	****

### 5.2.2. mRNA stability of differentiation-specific keratins in the presence of Actinomycin D.

Having determined the working concentration of AD from the two genes used as a positive (c-Myc) and a negative (18S rRNA) control, the mRNA decay of our genes of interest was investigated. NHEK growing with irradiated feeder fibroblasts in full RM+ medium (10% HyClone II serum) were starved in 4% HyClone II RM+ medium overnight and next day 2 µg/ml of AD was added into full RM+ medium for different time points up to 4 h. At each time point, cells were lysed for total RNA extraction, cDNA synthesis and qPCR analyses. YAP1 and POL2A were used as reference genes and their cp values are shown in Figure 5.7 B. As can be seen in Figure 5.7 A, *KRT1* and *KRT10* were having stable mRNAs up to 4 h in presence of AD. On the other hand, *KRT2* was less stable than c-Myc after 30 min which continue to decay overtime until it was completely degraded after 4 h. This suggested that the decay rate of *KRT2* was faster than *KRT1* and *KRT10* which were more stable over time. This fast decay rate could explain the low level of *KRT2* mRNA expression in keratinocytes under normal conditions seen in chapter 4 in which no K2 protein expression under normal growth conditions can be detected.

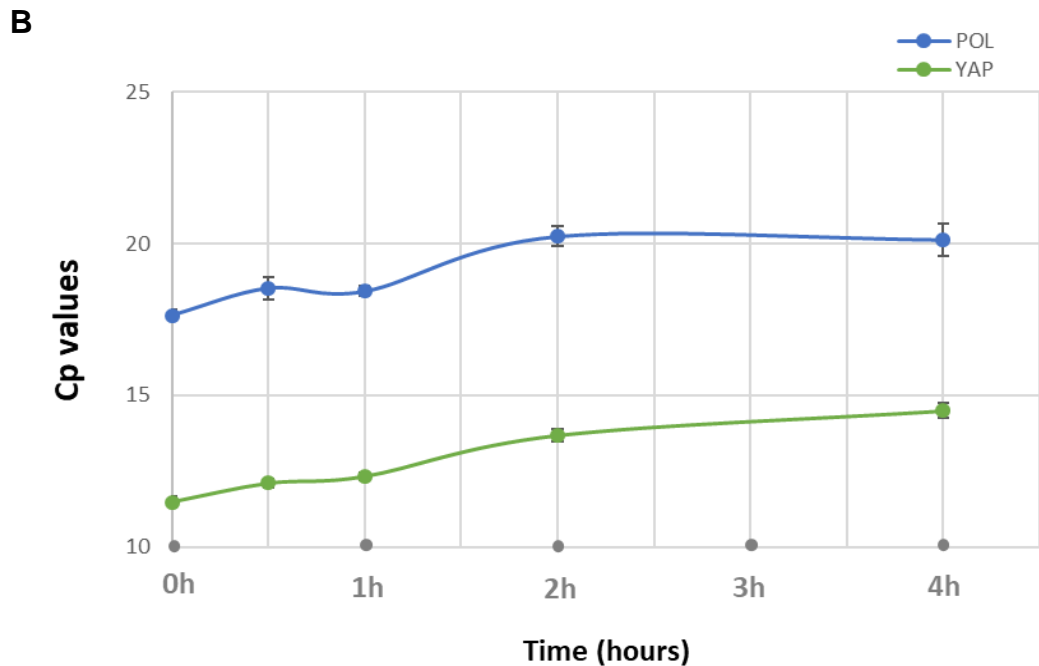
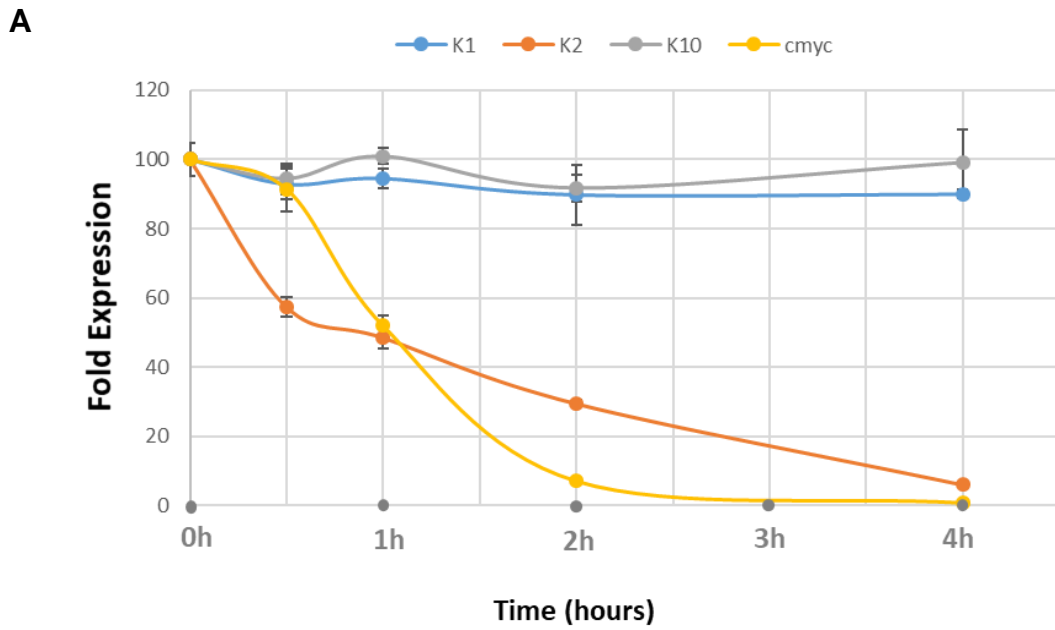


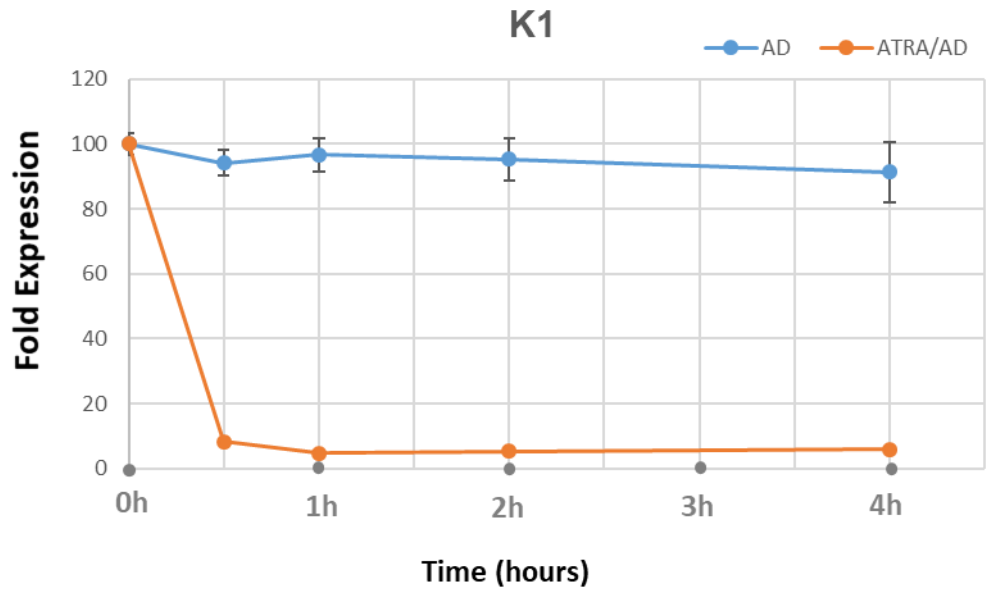
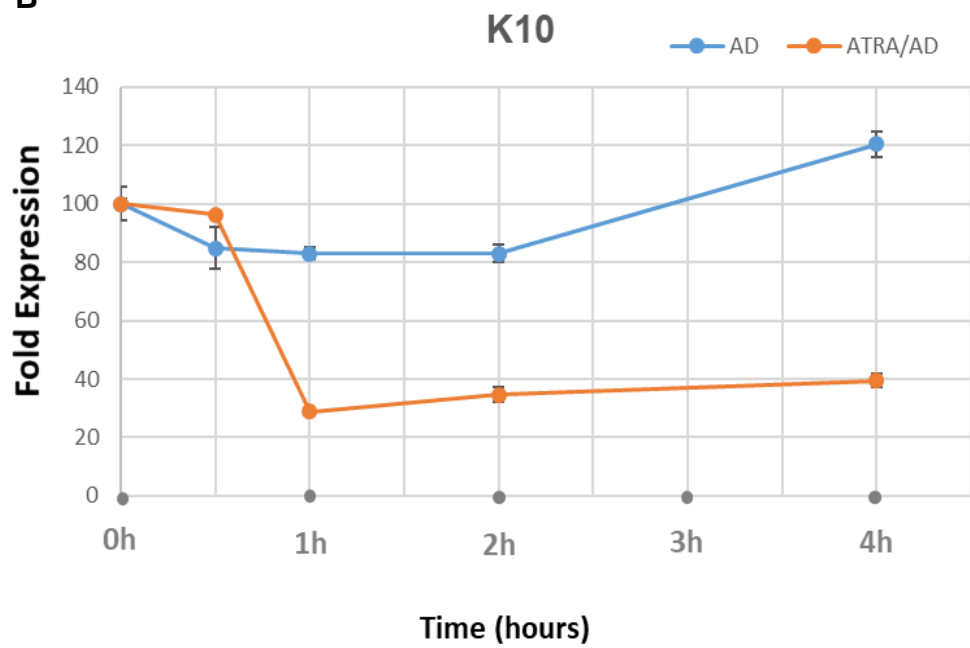
**Figure 5.7. Differential stability of K1, K10, K2 and c-Myc mRNAs in NHEK.** NHEK cells mixed with irradiated 3T3 feeder cells were grown in RM+ medium, containing PR. Cell were treated with AD, dissolved in dd H<sub>2</sub>O, at a concentration of 2 µg/ml for up to 4 h lysed for qPCR analysis of *KRT1*, *KRT10*, *KRT2* and c-Myc gene expression analysis. All data showed as fold expression normalised to YAP-1 and POL2A housekeeping genes, untreated cells were used as control (A). Cp values of YAP-1 and POL2A are shown overtime of AD treatment in (B). STAT: n=3, Error bars=SEM, P values calculated using One-way ANOVA, (ns=p>0.05, \*\*\*\*=p<0.0001).

K1	K2	K10	c-Myc	YAP Cp	POL Cp
ns	****	ns	****	****	****

### 5.2.3. ATRA stabilises *KRT2* but not *KRT1* and *KRT10* mRNAs.

In our previous experiments in chapter 4 (Figure 4.9) it has been shown that ATRA has reduced the expression of *KRT1* and *KRT10* in NHEK cells grown in RM+ medium containing lipid stripped serum with or without PR. *KRT2* on the other hand was showing upregulation of mRNA after ATRA treatment but only in PR free medium containing lipid stripped serum. To further investigate the role of ATRA on mRNA expression and to ask whether it's inducing mRNA synthesis or it's stabilising the mRNA that has already been synthesised in these cells, mRNA stability was measured in presence of ATRA. NHEK were grown with irradiated feeder fibroblasts in full RM+ (10% HyClone II serum), and then starved these cells overnight in RM+ (4% HyClone II serum). Next day the medium was changed to RM+ (charcoal stripped serum without PR) containing 2 µg/ml AD and incubated at 37°C for different time period. At each time point (30 min, 1h, 2h, 4h) cells were lysed, total RNA was extracted, cDNA synthesised, and mRNA expression was measured for each gene (*KRT1*, *KRT2*, *KRT10*) relative to two housekeeping genes YAP-1 and POL2A. In Figure 5.8, *KRT1* and *KRT10* are behaving in a similar fashion in which both genes were stable up to 4 h of AD treatment (blue line) while adding 1 µM of ATRA 24 h before the AD treatment (orange line) did cause mRNA decay for both genes. *K1* mRNA was completely decayed after 1 h while *K10* decay was about 80% at the same time point, suggesting that ATRA could be destabilising the mRNA of both *K1* and *K10* genes. *KRT2* mRNA was stabilised, and its decay was delayed around 40% in the presence of ATRA compared to the decay rate in the presence of AD only.



**A****B**

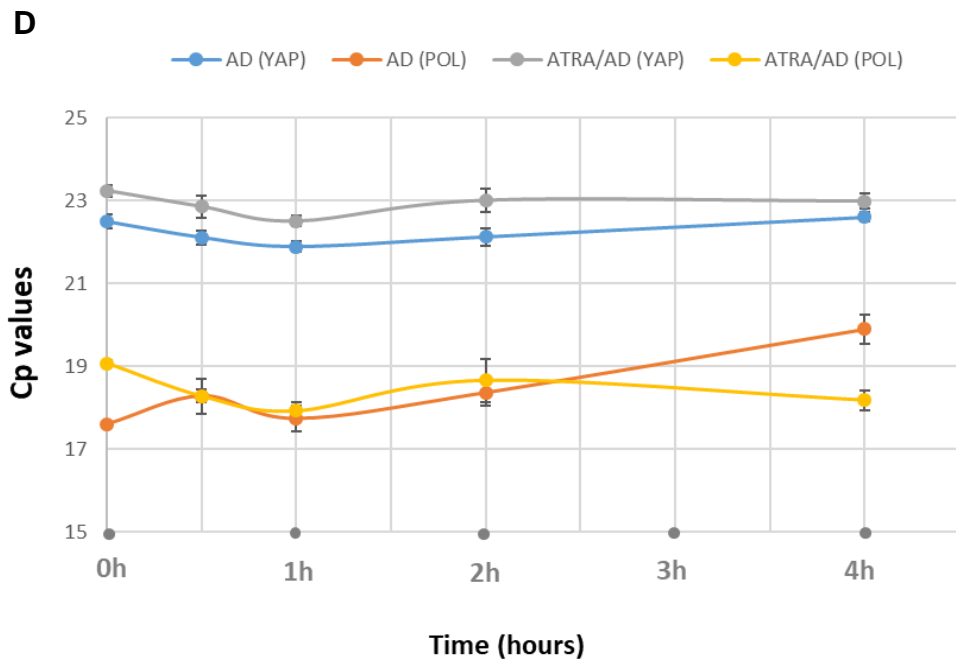
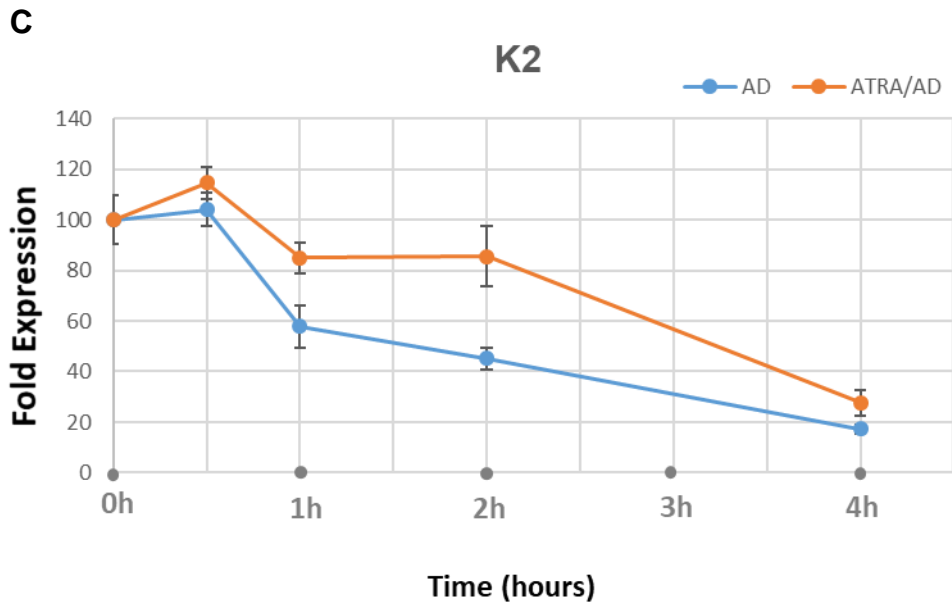


**Figure 5.8. ATRA destabilises K1 and K10 but stabilises K2 mRNAs.** NHEK cells mixed with irradiated 3T3 feeder cells were grown in charcoal stripped FCS RM+ medium in PR free medium. ATRA was added at 1  $\mu$ M for 24h prior to adding AD for up to 4 h before qPCR lysates were collected for *KRT1*, *KRT10* and *KRT2* gene expression analyses. DMSO/ETOH was used as a vehicle control (0.001%/0.01% mixture) for ATRA treated samples (A, B, C). In (D) Cp values of YAP-1 and POL2A is shown with and without AD treatment. All data shown as fold expression normalised to DMSO/ETOH control. STAT: n=3, Error bars =SEM, Two-way ANOVA (Time, Treatment) was calculated for P-values in (A, B, C), One-way ANOVA in (D), p-values (ns=p>0.05, \*=p<0.05, \*\*=p<0.01 and \*\*\*=p<0.001). In statistical analysis we are comparing the mRNA expression value either overtime in each treatment condition or the effect of treatment on the same time point as shown below.

Variable	K1	K2	K10
<i>Treatment</i>	*	*	***
<i>Time</i>	ns	**	ns

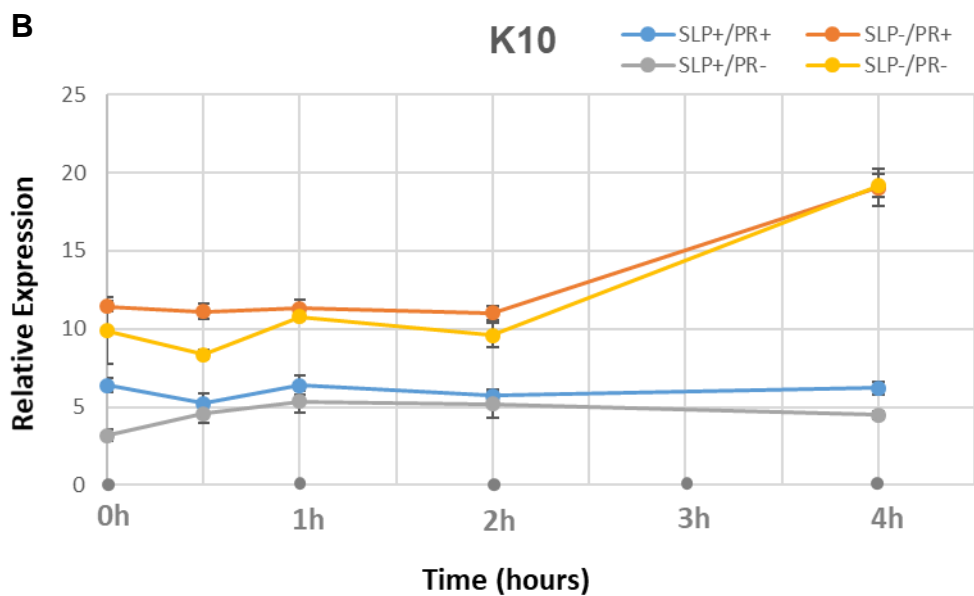
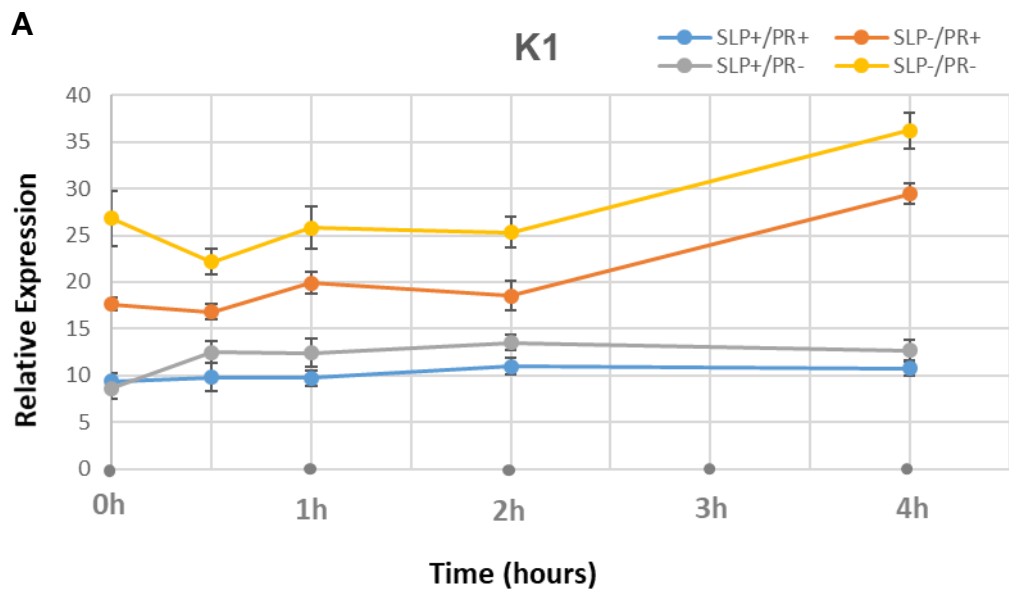
Variable	YAP(AD)	YAP(ATRA/AD)	POL(AD)	POL(ATRA/AD)
<i>Time</i>	*	ns	**	ns

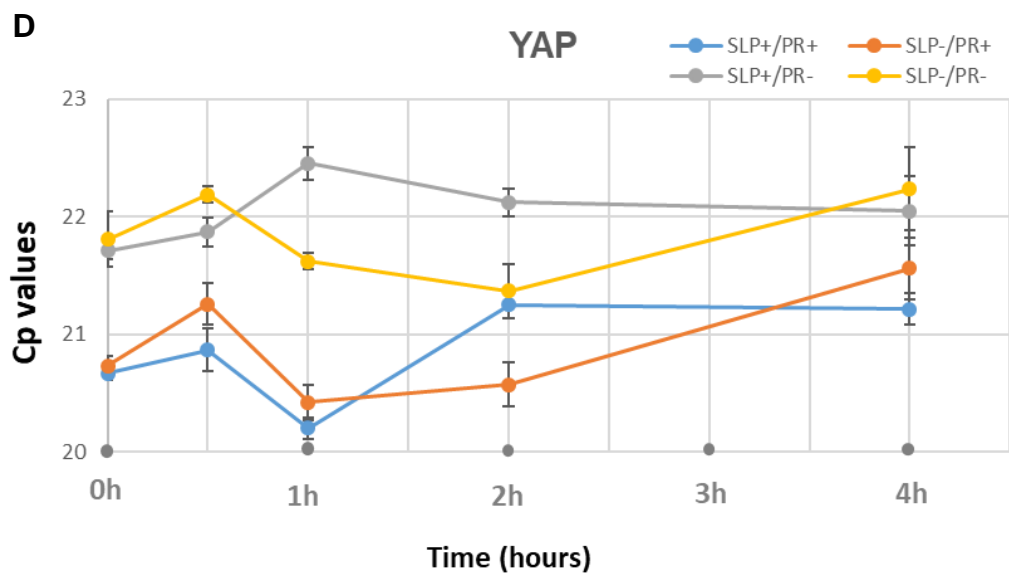
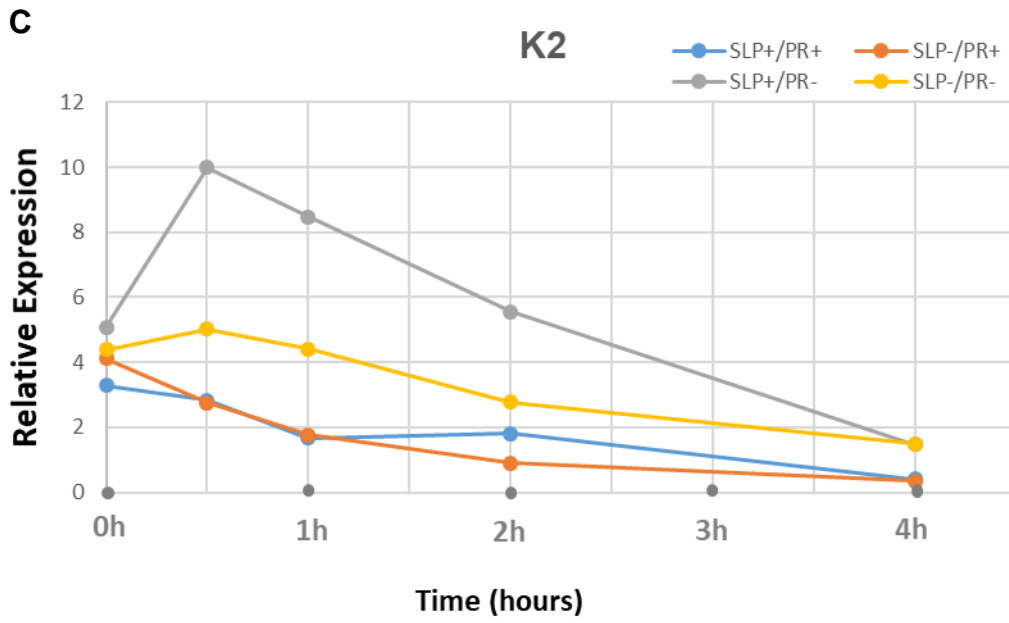
### 5.3. Role of serum lipids and PR on stability of K1, K2 and K10 mRNA in NHEK.

In our previous set of experiments in chapter 4, data was presented on the effect of SLPs and PR on the expression of 3 late differentiation markers K1, K10 and K2. A conclusion was made that lipid free serum did allow increased expression of K1 and K10 which was more pronounced if PR was absent. It has also been shown that K2 expression was unaffected under these conditions. Another observation that K1 and K10 mRNAs were downregulated while K2 expression was upregulated when ATRA was added to PR free RM+ (containing charcoal serum stripped) medium. Figure 5.8 C showed that the presence of ATRA (orange line) allowed stabilisation of K2 mRNA compared with control without ATRA (blue line). To further investigate the role of different serum growth conditions on the stability of K1, K2, K10 mRNAs, NHEK were grown with irradiated feeder cells under the same conditions mentioned in section 5.2.3. Next day, each group of cells were allowed to grow in four different conditions (same used in chapter 4) and AD at 2µg/ml was added for different time periods. Cells were lysed, total RNA was extracted, and stability was measured over time using mRNA expression by qPCR after AD treatment. As shown in Figure 5.9 A, B, K1 and K10 were behaving similarly with regard to their mRNA stability. In serum containing conditions (SLP+/PR+ and SLP+/PR-) there was no significant difference between mRNA expression overtime for both K1 and K10. Removal of SLPs did cause higher expression of K1, more significantly when PR is removed

(yellow line). A similar observation was made for K10 in which the use of stripped serum did allow higher expression of K10 mRNA with no significant difference between PR containing or PR free conditions (yellow and orange lines). From these observations it can be deduced that K1 and K10 mRNA is stable for up to 4 h in presence of AD under all conditions with different expression levels in each condition, which was shown before in chapter 4, Figure 4.6 A. After 4 h of AD in serum stripped conditions, a higher expression of K1 and K10 was seen, which could be due to inactivation of AD, no longer active under these two conditions (SLP-/PR+, SLP-/PR-) as shown in (Figure 5.9 A, B). Throughout our experiments, expression of *KRT2* was behaving differently compared to *KRT1* and *KRT10* in NHEK. In this experiment, this difference can be observed as well, in which the expression of *KRT2* is being more stable with higher expression in serum containing, PR free condition (gray line) but removing serum lipids (SLP-/PR-) showed less stable mRNA overtime with lower expression (yellow line). These data correlate with our previous data shown in Figure 5.8 C in which cells treated with ATRA/AD and cells grown in SLP+/PR- in Figure 5.9 C showed higher *KRT2* expression while cells treated with AD only in Figure 5.8 C showed less stable and lower expression of *KRT2* similar to cells grown in SLP-/PR- in Figure 5.9 C. On the other hand, in the presence of PR (with charcoal stripped serum vs unstripped serum), the decay rate and the mRNA expression of K2 is the same with lower expressions compared with PR free conditions (Figure 5.9 C). YAP-1 and POL2A were used as reference genes, so their cp values are shown in Figure 5.9 D in these four different conditions treated with AD overtime, YAP-1 and POL2A were showing a significant difference in their cp values between different growth conditions as well as overtime of AD treatment

indicating that these genes are not stable under these conditions and they are not the right genes to be used as references for these experiments.





**E**

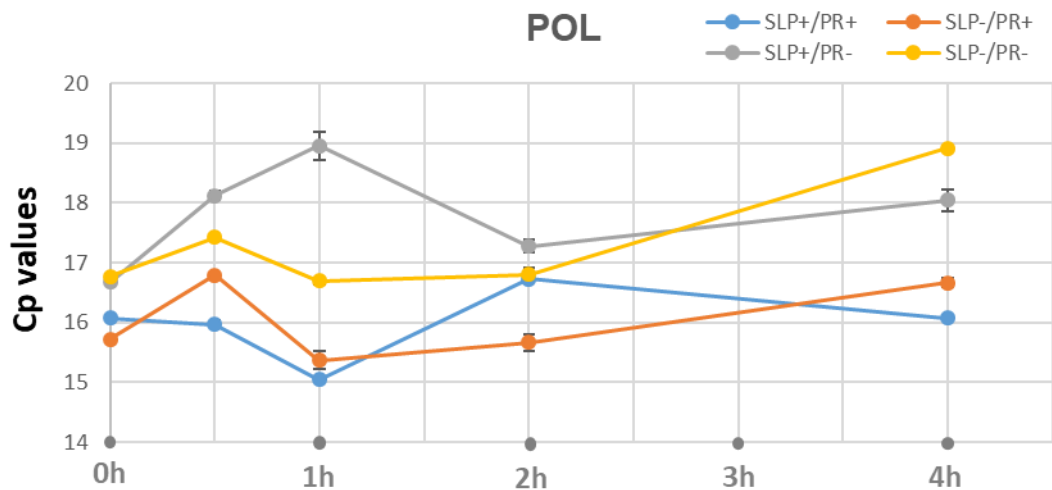


**Figure 5.9. Effect of serum lipids and PR on mRNA stability of K1, K2 and K10.** NHEK Cells were grown in four different conditions (SLP+/PR+, SLP-/PR+, SLP+/PR-, SLP-/PR-), next day 2 µg/ml AD was added for up to 4 h. At each time point qPCR lysates were collected for expression analyses of *KRT1*, *KRT10* and *KRT2* genes. Control was used as 0 h with no AD added (A, B, C). In D and E, cp values of housekeeping reference genes were shown under different conditions. STAT: n=3, error bars=SEM, P-values were calculated using One-way ANOVA as shown in the table below (ns=p>0.05, \*p<0.05, \*\*p<0.01 and \*\*\*p<0.001, \*\*\*\*p<0.0001). In statistical analysis we are comparing relative values of each mRNA in each growth condition overtime points or comparing relative values of each mRNA in every timepoint across each growth condition as shown below.

Condition overtime	K1	K10	K2	YAP	POL
SLP+/PR+	ns	ns	****	***	****
SLP-/PR+	***	****	****	**	****
SLP+/PR-	ns	ns	****	ns	****
SLP-/PR-	**	***	****	ns	****

Time points across conditions	K1	K10	K2
0h	****	****	ns
0.5h	***	****	**
1h	****	****	*
2h	****	****	*
4h	****	****	*

## **5.4. Investigating the promotor activity of *KRT1*, *KRT2* and *KRT10* in response to lipids and PR in culture medium.**

In this chapter, the results obtained using transfection of constructs containing promoters for *KRT1*, *KRT2*, *KRT10* and their deletion fragments will be described. These promoters (and their fragments) were PCR amplified using specific primers and cloned into pGL4.14 vector which was commercially obtained from Promega corporation (USA). This vector is a basal vector lacking either promoter or enhancer elements. One of advantages of using this vector is the ability to select the transfected cells using hygromycin as the vector contains hygromycin selection marker. The cloned inserts were sequenced through and through using the di-deoxy sequencing method and compared with the sequence entry in the Ensembl genome browser 95 databases. All PCR and cloning experiments described in this chapter were carried out by my supervisor, Professor Ahmad Waseem, before I started working on this project and were made available to me for this study. The cloning of AP-1 construct and its characterisation has been described previously (Brown et al 2014).

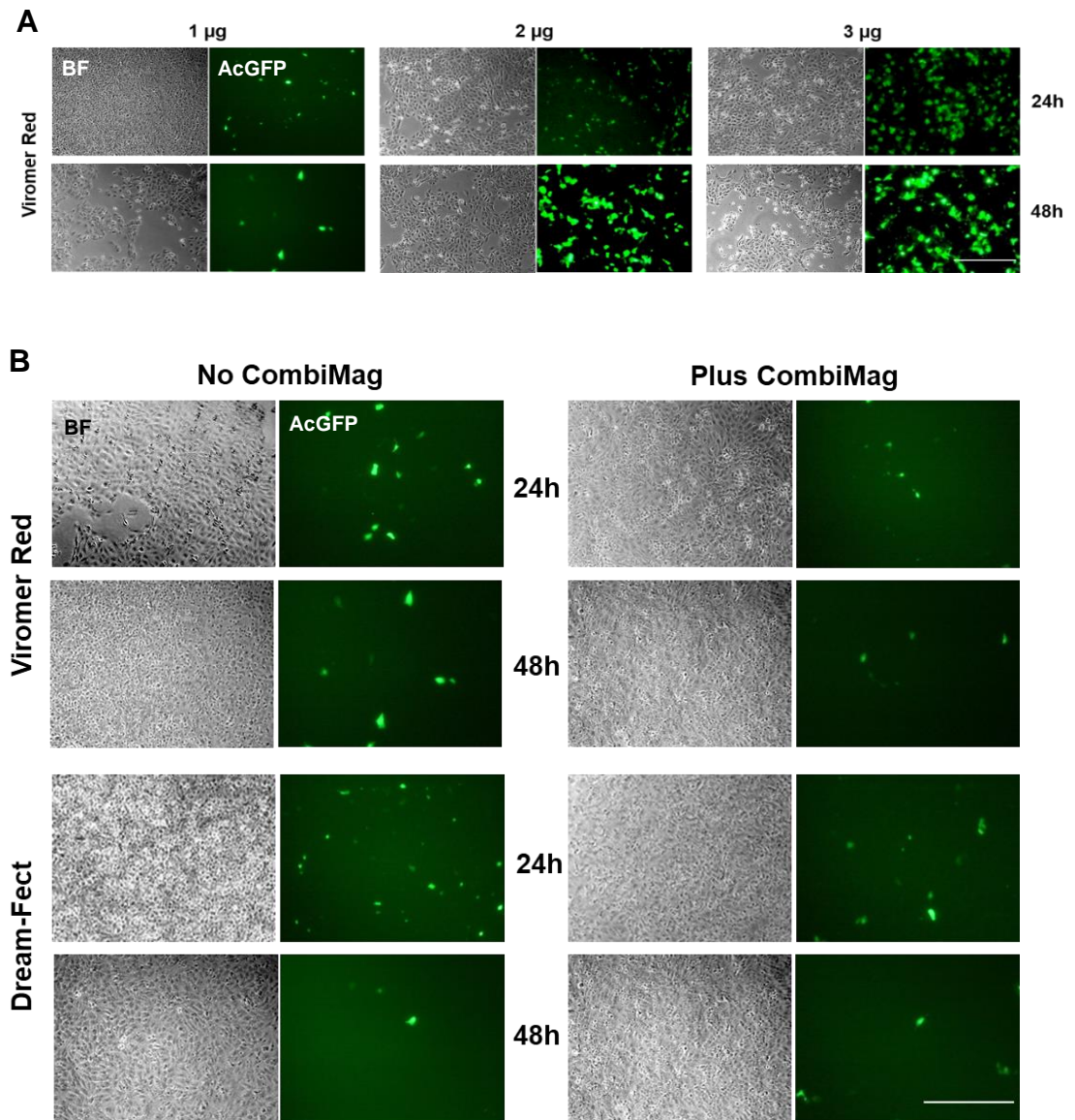
### **5.4.1. Optimisation of Keratinocytes transfection using AcGFP vector.**

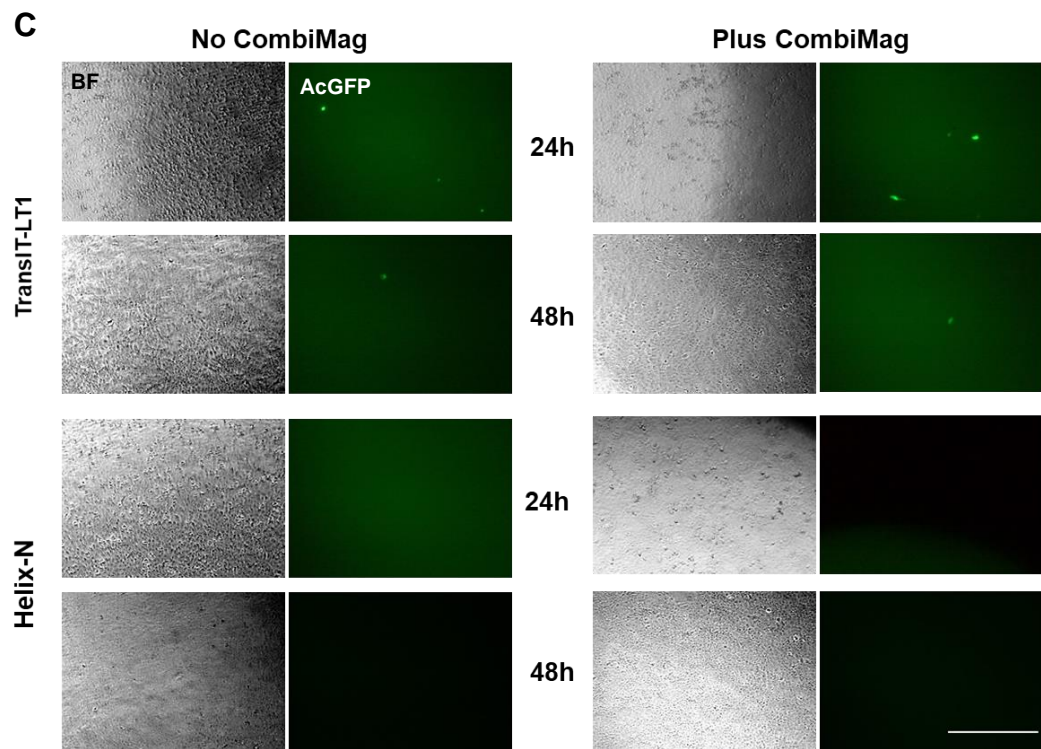
As keratinocytes are known to poorly transfect, HaCaT keratinocytes transfection efficiency was tested using different commercially available transfection reagents under different conditions with our plasmid DNA. In the optimisation set of experiments, HaCaT keratinocytes were grown in full DMEM medium with 10 %(v/v) FCS + 1% PS, once the cells were attached, transfection was started. To



quickly screen different conditions, pLPCpuro\_NAcGFP vector was used and transfection efficiency was monitored using the transfected cells under immunofluorescence microscope. First, different concentrations of the plasmid DNA in the range of 1 µg, to 3 µg were used with Viromer Red as a transfection reagent because it is based on endocytosis of the transfection complex so likely to be more efficient. With 1 µg, 2 µg and 3 µg of plasmid DNA, images were recorded after 24h and 48 hours post transfection (see Figure 5.10 A). Another transfection method was also used that is called CombiMag, which is based on the use of magnetic nanoparticles to pull the DNA complex into the cells. It has been designed for use with any transfection reagent to enhance its efficiency and required to be used with a strong magnetic plate. 1 µg of DNA (as recommended by the manufacturer) has been used in conjunction with four different commonly used transfection reagents, Viromer Red, Dream-Fect, X-Fect, *TransIT*<sup>TM</sup>-LT1 and Helix-N and the images were recorded 24 h and 48 h post transfection with and without the use of CombiMag magnetic plate. 2 µg and 3 µg of DNA for 48 h showed high transfection efficiency in Viromer Red compared to 1 µg of DNA for 24 h (Figure 5.10 A). The use of CombiMag did not improve transfection efficiency of HaCaT using 4 different transfection reagents for 48 h (Figure 5.10 B, C). The effect of calcium on the transfection efficiency was also compared. Cells were grown in a very low calcium containing medium (0.01-0.03mM) and compared the transfection efficiency with that in normal calcium containing medium (1.8 mM). It has been shown that transfection in normal calcium containing medium is more efficient than in low calcium medium for both reagents (Viromer Red and X-Fect) as shown in Figure 5.10 D, E. The use of *TransIT*<sup>TM</sup>-LT1 and Helix-N was not able to transfect HaCaT with 2 µg DNA up to 48 h with or without CombiMag

(Figure 5.10 C). The sources of all transfection reagents are described in the Materials and Methods section (Chapter 2).





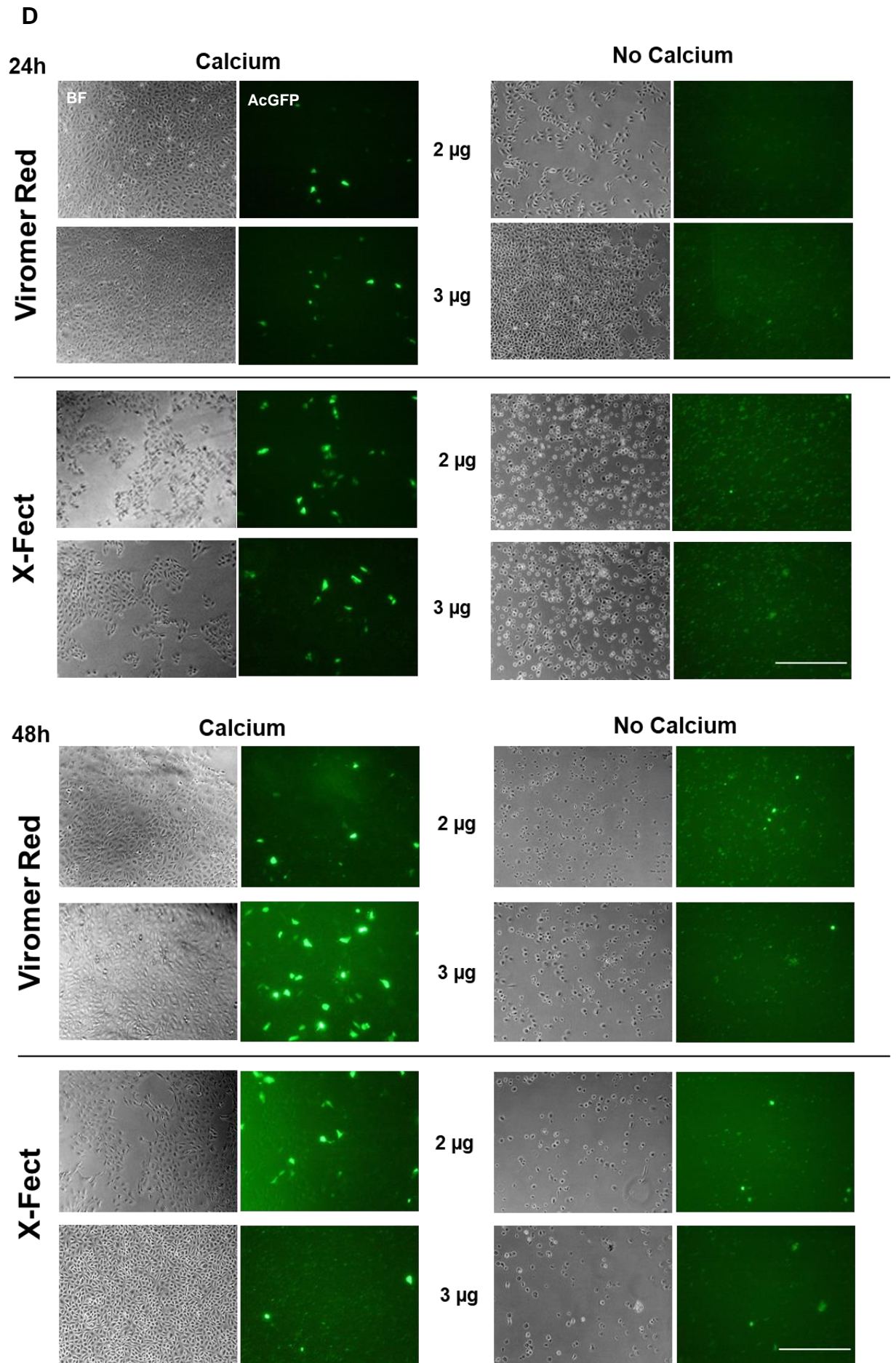


**Figure 5.10. Efficiency of HaCaT transfection as measured with pLPCpuro\_NAcGFP vector using different reagents.** HaCaT keratinocytes were grown in DMEM plus 10% (v/v) FCS and transfected with pLPCpuro\_NAcGFP at different DNA concentrations using different transfection reagents and conditions. (A) Viromer red is used with 1, 2, and 3 µg DNA for 24 h and 48 h. (B) Viromer red and Dream-Fect were used with and without Combi-Mag for 24 and 48 h (1 µg DNA). (C) Same as B but *TransIT-LT1* and *Helix-N* transfection reagents were used. (D) High and low calcium containing media were used to grow cells and transfect them with Viromer red and X-Fect for 24 and 48 h using 2 and 3 µg of DNA. Scale bar=100µm.

#### **5.4.2. Measuring AP-1, K2 and K14 promotor activities using Luciferase.**

To determine whether a reporter gene activity can be successfully measured in cells, the activity of AP-1 reporter construct in keratinocytes was compared to that in HEK293 cells. 2 µg of total DNA were used transfected into HaCaT and HEK293 cells using Viromer red for 48 h. In these experiments renilla CMV vector was used as an internal control for transfection efficiency co-transfecting it with firefly luciferase vector containing the AP-1 responsive element. The transfected cells were treated with PMA (10 nM) dissolved in DMSO or with DMSO (0.01%) only as a vehicle control for 8 h. As shown in Figure 5.11, in HaCaT there was no activation of AP-1 with PMA compared with DMSO control while in HEK293 cells there was more than 10-fold increase in luciferase activity compared with DMSO (all values have been normalised to the internal control renilla vector). AP-1 is known to be activated by PMA in keratinocytes and induces the expression of differentiation specific genes such as *KRT1* and *KRT10* (Karlsson et al., 2010, Briata et al., 1993, Eckert and Welter, 1996). HEK293 cells were then grown and used to show PMA dependent AP-1 activation under four different culture conditions that has been used in previous experiments described in chapter 4 (SLP+/PR+, SLP-/PR+, SLP+/PR-, SLP-/PR-) for 3 days, co- transfecting with AP-1 firefly plus renilla luciferase vectors. After 48 h post-transfection, cells were treated with (10 nM) PMA for 8 h and luciferase activity were measured. In Figure

5.12, there was no significant difference between luciferase activity along the four different conditions used. This may suggest that the changes in gene expression seen under different growth conditions in chapter 4 are unlikely to be through AP-1 activity and other pathways may need to be explored.

HaCaT were also transfected using Viromer red with 2 µg of K2 and K14 promotor sequences in firefly luciferase pGL4.14 vector. These cells were grown in the four different culture conditions that has been used in previous experiments (SLP+/PR+, SLP-/PR+, SLP+/PR-, SLP-/PR-). The promotor activity of K2 and K10 promoters measured by luciferase activity did not show any significant difference (Figure 5.13).

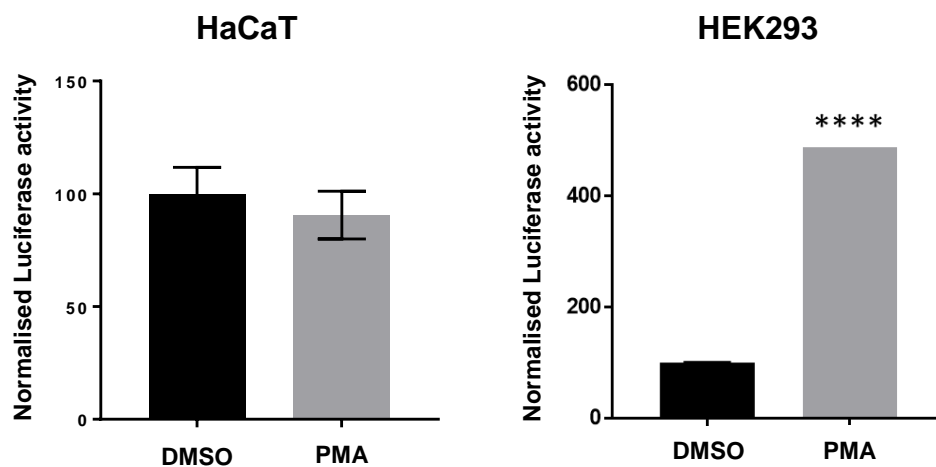


**Figure 5.11. Comparison of PMA inducible AP-1 activity in HaCaT and HEK293 cells.** HaCaT and HEK293 cells were grown in DMEM plus 10% (v/v) FCS, transfected with 2 µg of plasmid DNA (AP-1 firefly + renilla luciferase) for 48 h using Viromer red. Cells were treated with 10 nM PMA dissolved in DMSO for 8 h and DMSO alone treated cells were used as a vehicle control (0.01%). All values were normalised to the internal control, renilla luciferase, readings. STAT: n=3, Error bare=SEM, P-values were calculated using student t-test (ns=p>0.05 and \*\*\*\*=p<0.0001).

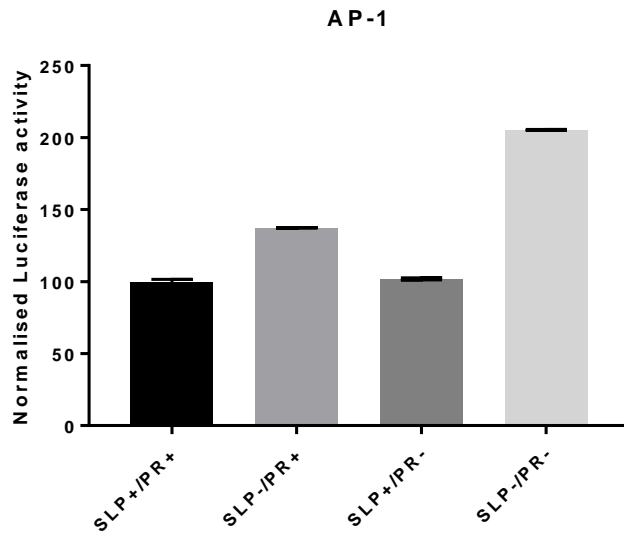


**Figure 5.12. Effect of serum lipids and PR on AP-1 reporter activity in HEK293 cells.** HEK293 cells were grown in four different culture conditions that has been used in previous experiments (SLP+/PR+, SLP-/PR+, SLP+/PR-, SLP-/PR-) for 3 days, co- transfected with AP-1 firefly plus renilla luciferase vector. After 48 h post-transfection, cells were treated with 10 nM PMA for 8 h and luciferase activity were measured. PMA dissolved in DMSO and DMSO treated cells were used as a vehicle control (0.01%) All values normalised to internal control renilla luciferase readings. STAT: n=3, Error bars=SEM, P-values were calculated using One-way Anova that showed ns difference between conditions (ns=p>0.05).

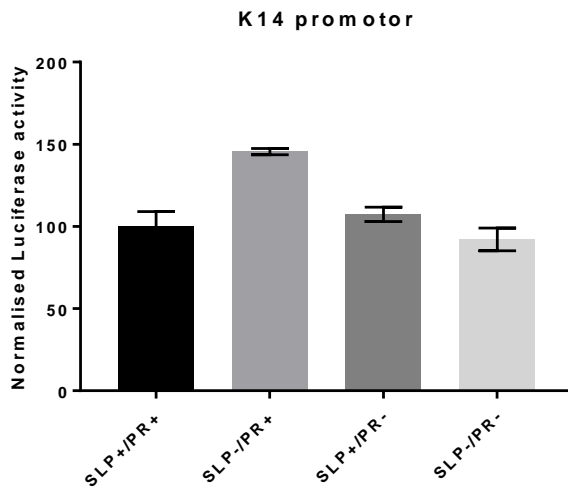
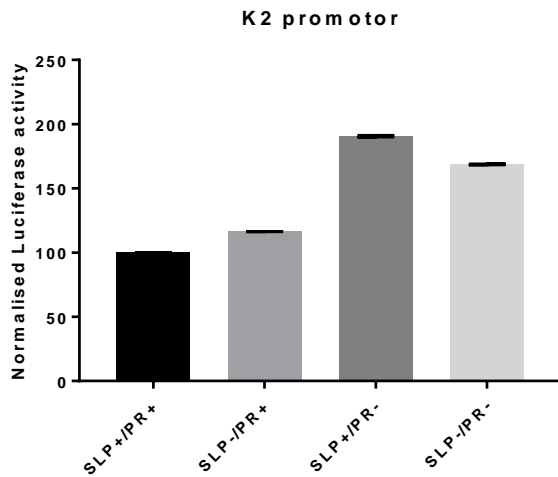


**Figure 5.13. Effect of serum lipids and PR on K2 and K14 promotor in HaCaT cell line.** HaCaT were grown in four different culture conditions that has been used in previous chapter 4 experiments (SLP+/PR+, SLP-/PR+, SLP+/PR-, SLP-/PR-) for 3 days, transfected with 2  $\mu$ g of plasmid DNA (K2 and K14 promotor firefly + Renilla luciferase) for 48 h using Viromer red transfection reagent. All values normalised to internal control, renilla luciferase, readings. STAT: n=3, Error bars=SEM, P-values were calculated using One-way Anova that showed ns difference between conditions (ns=p>0.05).



## 5.5. Discussion and conclusion.

The stability of mRNA is considered a fundamental process that affects protein expression and in fact many vital processes inside the cell. The mRNA decay process is highly selective, it differs widely from one mRNA to another. Studies have shown that this selectivity depends on certain sites on the mRNA sequence that are targets of factors responsible of this decay and degradation. In a previous study Shaw and Kamen (1986) have identified a non-coding region at the 3'end (5'-AUUUA-3') of a number of mRNAs that could be cleaved by a specific endonuclease (Shaw and Kamen, 1986). This region is called AU-rich elements (AREs), sequence elements rich in A and U nucleotides. Depending on the cellular condition and the presence of a certain stimulus, an ARE can also lead to the stabilisation of a mRNA and not only degradation (Barreau et al., 2005). It was found that using AD to measure mRNA decay of late differentiation keratins, that K2 mRNA is decaying about 50% within 30 min of AD treatment compared to K1 and K10 which were stable for up to 4 h (Figure 5.7 A). Ensembl genome browser 95 was used to find (5'-AUUUA-3') region in the mRNAs of *KRT1*, *KRT2* and *KRT10* sequences as shown in Figure 5.14. One AU-rich elements (5'-AUUUA-3') was found in *KRT2* but not in *KRT1* which implies that some ARE-binding proteins (ARE-BPs) could bind to K2 mRNA and activate endoribonuclease activity (Geissler and Grimson, 2016). This could explain the instability of *KRT2* and stability of *KRT1* mRNAs. As mentioned earlier the presence of AREs does not always contributes to degradation but could also lead to mRNA stability depending on the presence of other cellular factors, a certain stimulus and the cellular need. It was found that there are two (5'-AUUUA-3') elements in the *KRT10* sequence and it was stable enough to be translated into a protein that was detected using WB.

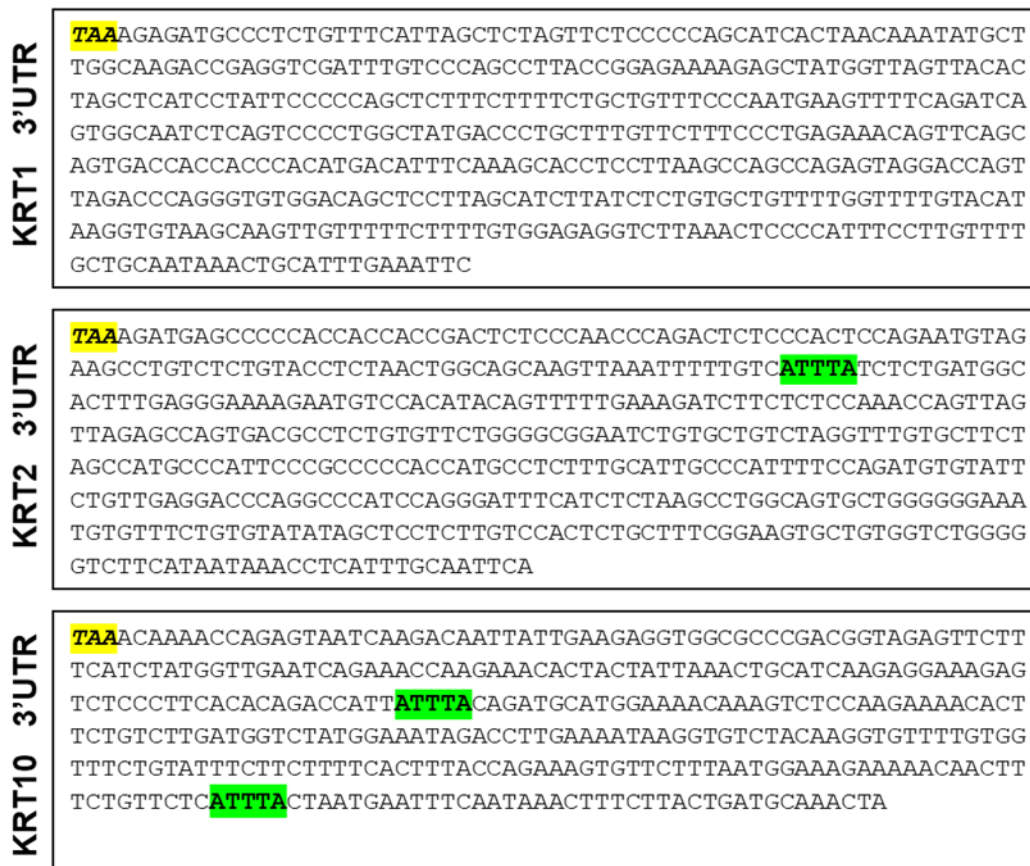


**Figure 5.14. 3' UTR of *KRT1*, *KRT2* and *KRT10* mRNA sequence using Ensembl genome browser 95 website.** mRNA sequences of *KRT1*, *KRT2* and *KRT10* showing the presence or absence of 3'end non-coding sequence (5'-AUUUA-3'). *KRT1* has none, *KRT2* has one while *KRT10* has two elements.

The steady state level of mRNA that was measured using qPCR is a balance between synthesis and decay. If the decay rate is high and transcription is blocked which means no more mRNA is synthesised and decreasing levels of *K2* was observed with time that means higher decay rate compared to *KRT1* and *KRT10*. As in the case of *KRT2*, it has been shown that human *K19* and prolactin mRNAs contains ARE in the 3'end non-coding sequence (5'-AUUUA-3') and their mRNA is more susceptible to degradation in the cytoplasm (Stasiak and Lane, 1987, Crowe, 1993).

Previous studies have shown that RA can suppress terminal differentiation in cultured keratinocytes as well in human skin (Fuchs and Green, 1981, Eichner et

al., 1992). This suppression of mRNA expression is not only due to transcriptional inhibition but could also involve mRNA stability. Other studies have shown mRNA stability of certain genes after RA treatment. It has been shown that there is a RA-dependant K19 mRNA stabilisation in the cytoplasm after AD treatment and this has been explained by the possibility of RA binding to some RA-binding proteins and these complexes perhaps directly or indirectly affect the endonuclease activity making the mRNA less vulnerable to degradation (Crowe, 1993). RA-dependant stabilisation of K2 mRNA was also shown in Figure 5.8.C and a thought that K2 could share the same control mechanism that explained the K19 mRNA stability was considered. It has been shown that after 4 h of AD treatment, K2 mRNA had decayed even in the presence of ATRA, this could be due to some other mRNA decay pathways that were taking over the RA stability effect or due to loss of ATRA effect that was added 24 h before the AD treatment (total of 28 h). It has been shown in a different study that ATRA stability is reduced in serum free medium after 24 h of treatment despite accurate handling during experimental procedures and that the stability of ATRA had been recovered when FCS was added back to the medium. As serum free medium and our charcoal stripped serum medium have no or extremely low quantities of lipids, this could explain the loss of RA-dependant mRNA stability of K2 shown in Figure 5.8 C in which ATRA stability could be lost after 24h. (Sharow et al., 2012, Kitano, 1985). Figure 4.9 C showed that ATRA increases the expression of K2 mRNA when added to charcoal stripped serum (SLP-/PR-). As there is no RA responsive element known in the K2 promoter, the role of ATRA could be either a post-transcriptional RA-dependant stabilisation or an indirect effect of RA on its promoter activity (Torma, 2011). Keratins K1 and K10 mRNAs are more stable and as the transcription is blocked and the decay is measured, it seems that the

mRNA that is in the cytoplasm is more compared to K2. This is understandable as K1 and K10 are expressed at far higher levels than K2. After up to 4 h of AD treatment, K1 and K10 mRNAs were stable which means very little or no degradation was taking place. This could be because K1 and K10 are expressed in differentiating keratinocytes all the time whereas K2 expression increases in response to certain normal or pathological triggers (Bloor et al., 2003). This could be further explained by the ARE region in *KRT2* that allows ARE-BPs to bind and degrade mRNA using endoribonuclease enzyme. The RA-dependent downregulation of K1 and K10 genes has been shown before to be due to binding of RA to RA-responsive elements that inhibits the expression of these genes either directly or indirectly through AP1 activity (Lefebvre et al., 2005, Briata et al., 1993).

In chapter 4 it has been shown that changing the growth conditions of NHEK did affect the expression of K1, K2 and K10 mRNA and protein. In order to investigate if this change in expression is regulated by transcription or by stability of mRNAs of these genes, NHEK cells were grown in the same four different conditions used in chapter 4 (SLP+/PR+, SLP-/PR+, SLP+/PR-, SLP-/PR-). Adding 2 µg/ml AD to study mRNA decay showed that K1 and K10 mRNAs have the same decay rate in all the conditions in which the stripped serum condition showed higher expression than other conditions and its more significant when PR is removed (Figure 5.9 A, B). These data suggest more synthesis of K1 and K10, is taking place under certain growth conditions before AD blocked the transcription (0 time). mRNA is stable in all conditions overtime when using AD except lipid free serum condition at 4 h, so changing the growth conditions did affect transcription levels of K1 and K10. As these conditions differ from each other's in the presence or absence of lipids mainly RA, the different levels of gene transcription per

condition could be explained by both genes having retinoic acid responsive elements through which their transcription is regulated (Torma, 2011). In K2 the regulatory control is different, the decay rate is much higher in stripped serum and the presence of lipids in PR free medium did slow the decay on in other words stabilised the mRNA compared to other conditions. Again, this could be due to the presence of lipids (mainly RA) in this condition plus being PR free.

To be able to study the promotor activity of K10 and K2 different segments of the promotor sequence were cloned into a pGL.4.14 vector with luciferase reporter activity to be able to measure the promotor activity through the luciferase enzymatic reaction. Although different transfection reagent were used on HaCaT keratinocyte using an AcGFP in pLPCpuro\_NAcGFP vector that has a CMV promotor and did show high transfection efficiency, transfection with our Luciferase vector didn't work. It was showing no difference in luciferase activity between AP-1 readings with and without PMA (Figure 5.11). To be able to measure the AP-1 construct activity another cell line HEK293 was tested, and it was showing more than 10-fold increase with PMA treatment compared with control (Figure 5.11). It is possible that our vector is not able to transfect keratinocytes so cloning AP-1 into another vector could allow better transfection and allow us to measure the AP-1 activity in HaCaT. As a transfection efficiency control, renilla internal control was used with CMV promotor and it was showing high readings each time. Full sequence promoters of K2 and K14 were also used to measure their activities under different growth conditions of HaCaT and showed no statistical difference in their luciferase readings (Figure 5.13). HEK293 cell line was transfected with AP-1 promotor vector and measured the activity under different growth conditions (same as used in K2 and K14 promotor experiments) and it did show no significant difference of luciferase activity

between the conditions indicating that the role of lipids on gene expression is a direct one and not through AP-1 transcription factor.

Activation protein-1 (AP-1) transcription factor is a family of JUN and FOS proteins that form dimers and bind to AP-1 binding site on genomic DNA. This binding affects many cellular processes such as proliferation, differentiation and apoptosis. Their role in skin is complicated due to being situation specific as well as having multiple family members that can make different combinations of protein complexes (Han et al., 2012). It is well known that binding of AP-1 to its DNA binding site, induces differentiation and gene expression of terminal differentiation markers. PMA treatment induces differentiation through activating AP-1 binding (Eckert and Welter, 1996, Briata et al., 1993, Karlsson et al., 2010). It was shown in chapter 4 that K1 and K10 mRNA and protein expression has been upregulated when serum lipid was removed from the growth medium. To be able to investigate the role of AP-1 in triggering this gene expression, it has been shown that using PMA did not activate AP-1 in our experimental growth conditions (Figure 5.12). The high level of gene expression that was observed before in certain growth conditions in chapter 4 could be through a direct role of SLPs on transcription and not through AP-1 activation. It could be that the non-significant difference in AP-1 activity shown in Figure 5.13 is due to low K2 and K14 promotor activity or a transfection efficiency issue.

**In conclusion**, the mRNA stability of late differentiation keratins was studied with main interest in K2 which was reacting differently in all our previous experiments. Since our interest was primarily K2, AD concentration was used that allow us to monitor the K2 decay until it reached full degradation after 4 h. It could be that this concentration or time points chosen was not enough to allow decay of K1 and K10 mRNAs, but these keratins were used as a control to K2 and to show that

they were much stable than K2 throughout this chapter. YAP-1 and POL2A, the two house-keeping genes used in this study, were stable under these conditions (section 5.2.3). In section 5.2.2, the Cp values of YAP-1 and POL2A were showing decay overtime but Cp values of keratins not normalised to YAP-1 and POL2A still showed the same stability pattern indicating that the normalisation to YAP-1 and POL2A did not affect their decay rate shown in Figure 5.7 A. Changing the growth conditions did affect YAP-1 and POL2A Cp values significantly that could give faulty reading of our genes relative to YAP-1 and POL2A so in this experiment YAP-1 and POL2A were not the correct reference genes to be used and absolute quantification would be a better way to measure the expression of these genes under these specific conditions.

# CHAPTER 6



## **6. General discussion, clinical significance and future directions.**

### **6.1. General discussion.**

#### **6.1.1. Keratin dynamics and phosphorylation.**

Keratins continuously undergo cycles of assembly and disassembly, being dynamic gives them the ability to perform a wide range of intra and intercellular functions. Keratins are the major stabilising protein of the cytoskeleton and they play a role in different cellular processes such as cell division, apoptosis, membrane trafficking, migration and wound healing (Strnad et al., 2001). As keratins are dynamic, the ability to allow new keratins to be introduced and integrate into the pre-existing network will be possible without affecting cellular functions and network stability (Windoffer et al., 2011). This is the case during epithelial differentiation in normal epidermis in which keratins K5/K14 in the basal proliferating layer are downregulated and they are replaced by a new set of keratins K1/K10 and K2 that integrate into the pre-existing network as cells move upward during stratification (Waseem et al., 1999). Studies have shown that microinjecting biotinylated type I keratins can be observed under confocal microscopy as spots containing both type I and type II keratins. This indicates that the endogenous type II keratins are dynamic and are able to change their endogenous structure to form complexes seen as spots with the injected type I keratins (Miller et al., 1993a). Once the keratins are integrated into the peripheral filaments network, they elongate and starts to bundle as they move toward the nucleus as a result of lateral compaction. This has been observed in a hepatocellular carcinoma cell line (PLC) containing K8/K18 after being stably expressing K18-YFP (K18 attached to a fluorescent tag) (Kolsch et al., 2010).

Keratin K2 (a late differentiation keratin marker) was used to be introduced into K8/K18/K19 filament network in MCF-7 (a breast carcinoma cell line) to study the dynamics of these keratins in a simple epithelial cell line model that is easy to visualise under a light microscope. Two tags differing in size (AcGFP 26 kDa vs 3x FLAG 3 kDa) were used attached to K2 and introduced them into MCF-7 cells using retroviral transduction to study its behaviour inside the cells. K2 is integrated into the pre-existing keratin network without affecting normal cell division or the known directionality of filaments equilibrium towards the nucleus as shown in (Figure 3.3, 3.4). This directionality of keratin integration has been shown when introducing K18-YFP into a hepatocellular carcinoma cell line as well as in primary human keratinocytes transduced with K14-YFP chimeras. These keratins were shown using live cell imaging where they start to join the existing network close to the cell membrane and later move toward the nucleus for bundling (Windoffer et al., 2004). On the other hand, filament stability was affected by introducing a new keratin into an existing network, but this was shown only when using AcGFP but not 3x FLAG as a tag on the head domain (N-terminus) of K2. This could indicate the role of the head domain in filament stability and not integration. Previous studies have shown that adding a big tag as EGFP on the tail-domain (C-terminus) did not interfere with K13 integration into the existing filament network in A-431 (vulvar carcinoma cell line), so blocking either domains (head or tail) with a large-sized tag does not appear to influence keratin protein integration (Windoffer and Leube, 1999). As keratin filaments stability observation was only seen when using AcGFP tag, but not FLAG, the conclusion was that using large-sized protein tag on the head domain could interfere with head domains folding back and their interaction with the rod domains, thus interfering with the tight packing of tetramers. Small tags such as

3x FLAG will be tolerated whereas large tags such as AcGFP will still be allowed to integrate into filaments, but they are likely to affect inter-rod domain interactions causing the filaments to destabilise which will be more obvious when filaments are hyperphosphorylated using OA or CL-A as shown in Figure 3.8-3.11 (Bray et al., 2015, Aziz et al., 2010). Other studies have shown that, when A-431 cells stably expressing K13 were treated with OA phosphatase inhibitor, filaments started to breakdown starting at the cell periphery with total filaments collapse after few hours of treatment without affecting the organisation of other cytofilaments (Strnad et al., 2001, Bray et al., 2015, Aziz et al., 2010). The process of assembly and disassembly of keratins has been known to be controlled primarily by phosphorylation, the key post-translational modification (Kim et al., 2015a). Phosphorylation could be induced as part of a normal cellular process such as during mitosis or by using phosphatase inhibitors. Phosphatase inhibitors such as OA and CL-A have been used to induce and study phosphorylation of different proteins (Paramio, 1999, Toivola et al., 1997). It has been shown that phosphorylation of keratins mainly Serine residue has been induced in mouse a keratinocyte cell line (BALB/MK-2) when treated with OA. This was identified using immunoblotting and immunoprecipitation with keratin specific antibodies and phosphorylation was located by autoradiography. The effect of hyperphosphorylation was shown as reorganisation of the filaments network that turn into perinuclear aggregates overtime with some rounding of the cell morphology (Kasahara et al., 1993).

It was shown using AcGFP-K2 in MCF-7 that during mitosis (physiologic phosphorylation inducer), filaments start to dis-assemble into small globules that allows the cell to be more flexible during division. After the cell divided, the globules start to join at the periphery of the cell forming short filaments that later

elongate while moving toward the nucleus forming a cage like structure (Figure 3.3 and 3.4) (Windoffer and Leube, 2004). K8 is well known to be phosphorylated on S73 during mitosis and K13 has been shown to form an elevated soluble pool during mitosis that was correlated to higher keratin phosphorylation levels (Liao et al., 1997, Windoffer and Leube, 2001).

Regulation of a protein activity requires a balance of kinases and phosphatases activities. Losing the balance between kinases and phosphatases activities could lead to different diseases such as cancer for example, in which cell migration, proliferation and differentiation are affected (Bononi et al., 2011). In toxic liver disease, Mallory bodies are seen due to hyperphosphorylation and this has been shown primarily due to p38 kinase (a class of MAPKs) pathway activation which also plays a role in other intermediate filaments aggregations that are seen in various diseases, including cardiac myopathy and numerous neurodegenerative disorders (Schutte et al., 2004, Woll et al., 2007). S73 in the head domain of K8 is a known major phosphorylation target for p38 kinase, and it could also be phosphorylated through JNKs. In K8, S23 and S431 are also well known phosphorylation sites that are activated under basal conditions or by SAPKs (JNKs and MAPK) respectively, while p38 phosphorylates only S73 (Woll et al., 2007). Phosphorylation of K8/S73 (on head domain) which is highly conserved among type II keratins and K8/S431 (on tail domain) as being well-known phosphorylation sites on K8 were investigated. The MCF-7 cell line (expresses K8 normally) was used, so antibodies against these well-known phospho-serine sites were used to study phosphorylation in our cell culture model (Toivola et al., 2002). To further investigate if the breakdown that was observed in AcGFP-K2 and not in FLAG-K2 was due to more phosphorylation being induced on S73 or S431 of K8, WB protein quantification was used. After inducing phosphorylation

with CL-A in MCF-7, the level of pK8/S73 or pK8/S431 were increasing with time, but there was no significant difference in the level of phosphorylation of S73 and S431 in K8 of AcGFP-K2 and FLAG-K2 as shown in Figure 3.9 and 3.10. This could rule out any role of phosphorylation in breaking down keratin filaments seen in our AcGFP-K2 expressing MCF-7 (see Figure 3.8). More likely this breakdown could be explained as mentioned earlier by the deleterious effect of the tag at the N-terminus of K2 on filament stability. In the filament assembly model, the rod domains of heterotypic keratins first associate as heterodimers followed by anti-parallel association into tetramers. In this model it has been shown that the head domains fold back and interact with the rod domains (Bray et al., 2015, Aziz et al., 2010).

As OA treatment and mitosis do induce phosphorylation of keratin filaments through MAPKs pathway (Liao et al., 1997), a different type of stress that is known to activate the same p38 kinase pathway (Rouse et al., 1994) was studied. A physical type of stress (heat shock) was used on our MCF-7 cell model. MCF-7 cells were subjected to a sub-lethal heat shock of 43°C for 30 min. This temperature was chosen based on previous studies that have shown the induction of MCF-7 apoptosis at 45°C for 45 min, HSPs are activated when temperature is above 42°C for 45 min and raising temperature 3-5°C is considered a mild heat shock (Fulda et al., 2010, Lee et al., 2019). It was shown using immunostaining and time-lapse confocal microscopy that keratin filaments start to reorganise and move toward the nucleus and condense around it in response to heat shock. This reorganisation requires phosphorylation of keratin filaments that is later balanced during recovery by phosphatases and the filaments started to spread back toward the cell periphery as shown in Figures 3.12, 3.14 and 3.15 (Shyy et al., 1989). In EBS, an inherited keratin mutation

disorder, keratins form aggregates when subjected to heat stress and it takes longer time to re-spread after removing the insult compared with normal keratinocytes. This delay in keratin remodelling gives enough time for cytolysis to take place if subjected to any other type of stress as rubbing or scratching during this time allowing the skin to become fragile and blisters easily (Morley et al., 1995). If MCF-7 cells were exposed to heat shock before inducing phosphorylation by phosphatase inhibitors (that induces p38 kinase pathway), breakdown of filaments is delayed or inhibited as shown in (Figures 3.13 and 3.17). This could be due to the effect of heat shock proteins (HSPs) that are activated after heat shock and act as inhibitors of the pro-apoptotic pathway regulated by MAPKs (Gabai et al., 1997). Leube and co-workers have shown that exposing A431 cells to light for (1-10 min) causes the keratin cytoskeleton to become resistant to the disruption caused by tyrosine phosphatase inhibitor OV that takes only few minutes to completely breakdown the filament network (Strnad et al., 2003). They have also shown that the pathway involved in this stability was p38 pathway as they have used the p38 kinase inhibitor SB203580 on these cells and showed the same result. The filaments were not stable when MAPK inhibitor PD98059 was used instead of p38 kinase inhibitor SB203580. These findings indicate a role of light in cytokeratin stability which is similar to our data using heat shock on MCF-7 cells, this finding might be helpful in treating some keratin disorders (Strnad et al., 2003). Using WB, the protein expression of HSP70 in transduced MCF-7 cells subjected to heat shock and recovery for different time intervals was measured. At the same time the level of pK8/S73 and pK8/S431 which are the main phosphorylation sites affected by p38 stress activated MAPK were also measured (Toivola et al., 2002). Phosphorylation levels were either stabilised or reduced after 2 h of recovery from heat shock while the level of

HSP70 was stabilised or increased overtime. This supports the hypothesis that HSP70 could be blocking or inhibiting the action of MAPK phosphorylating S73 and S431 on K8 (Gabai et al., 1997). This phenomenon is most likely explained by thermotolerance, in which the first heat shock given to the cells produces a cascades of events with the aim of protecting the cell from a second stress (which is the phosphatase inhibitor treatment in our case) that lasts for few days only (Landry et al., 1982, Dorion and Landry, 2002).

### **6.1.2. Keratinocyte differentiation and serum lipids.**

Keratin K2 ( $\approx 70$  kDa) is a known late differentiation marker in stratified epithelium. The significance of the epidermal K2 has been frequently questioned in the literature. K2 is found regularly in different body parts but at very low levels in foreskin and epithelial cancers as well as cultured cell lines derived from these cells (Collin et al., 1992). In cutaneous basal and squamous cell carcinomas, K2 was showing strong expression in the epidermis but was absent in tumour tissue islands. In oral epithelium there is no significant expression of K2 in both keratinised and non-keratinised epithelium. Interestingly, K2 is highly expressed in mild to moderate oral dysplasia with orthokeratinisation while in oral squamous cell carcinoma the expression is undetectable (Bloor et al., 2003). As K2 is undetectable after few passages of growing keratinocytes in culture, it will be almost impossible to study its role and importance in both skin and oral cavity. The influence of several factors in tissue culture that could affect the gene expression were studied, as well as trying to link these factors to the downregulation of K2. FCS is the main component of tissue culture medium that is commonly used, and it contains a wide range of vitamins, minerals, lipids, proteins and both free as well as bound carbohydrates that are needed by the cells to survive and grow. These components include cytokines, hormones and

growth factors (Gstraunthaler, 2003, Zheng et al., 2006). The role of SLPs on the expression of differentiation-specific keratin genes was studied using charcoal treated serum instead of using serum free medium as studies have shown that NHEK grown in serum free medium are unable to differentiate despite high levels of calcium in culture medium (Lamb and Ambler, 2013). As the presence of serum in culture medium is required for keratinocyte differentiation, the serum was kept and the role of lipids in this serum was studied. It has been shown that FCS used in cell culture medium contains enough vitamins that are able to affect cultured keratinocyte differentiation. Cellular properties have shown to be altered when vitamin A was removed from serum using de-lipidised serum. This removal allowed the expression of terminal differentiation keratins which was reversed by adding RA back into culture medium containing de-lipidised serum. The effect of vitamin A on keratin expression is cell type specific as well as concentration dependant (Fuchs and Green, 1981). Both systemic and topical vitamin A is widely used in dermato-pharmacology. There is a wide variety of vitamin A derivatives used for different skin conditions such as 13-cis retinoic acid, 9-cis retinoic acid and all-*trans* retinoic acid that is used topically to treat skin photoaging, post-inflammatory hyperpigmentation and acne. Retinoids are known to inhibit growth stimulating signals and induce apoptosis, growth arrest and cell differentiation. Due to their anti-cancer properties, they are used in dermato-oncology as a chemo-preventive agent through inducing differentiation and inhibiting proliferation. Retinoids are widely used as an anti-inflammatory agent that can accelerate healing and prevents aging (Beckenbach et al., 2015, Khalil et al., 2017). Whether RA induces or suppresses differentiation is still indeterminate. Many studies, as mentioned earlier, have been highlighting the anti-cancer property of RA as when used topically on skin or taken systemically



as an anti-cancer agent has been reducing the tumour size or spread therefore inducing differentiation. On the other hand, other studies have shown that RA suppresses epidermal differentiation and this has been measured by showing downregulation of differentiation markers as K1, K10 and loricrin (Rosenthal et al., 1992). Studies that have used RA as a cancer preventive agent relied on the fact that it reduces the size of the tumour (suppresses proliferation) so it should induce differentiation, but no study has measured the expression of differentiation markers after using RA for this purpose. This led to a big controversy on the effect of RA on keratinocyte differentiation, this could be explained by one or more of the following:

- Clinical studies using RA as a chemo preventive agent lack molecular level evidence of differentiation induction markers, this lack of evidence require more studies and further investigation to be done on cellular and subcellular levels.
- It is known that keratinocytes are RA sensitive and tiny variations in the drug concentration could bring some genes transcription levels up or down.
- It is possible that RA inhibit transcription of some differentiation-specific genes through receptor binding, so act as differentiation inhibitor while it does play a role in stabilising some other late differentiation mRNA as K2 or K19, inducing these genes could allow keratinocyte differentiation pathways to be activated in which could be inhibiting proliferation when used in a chemo-preventive dose.
- Previous data have shown using gel super-shift assays that the levels of endogenous RAR $\gamma$ /RXR $\alpha$  receptors are much lower in cultured

keratinocytes compared to their levels in skin *in vivo*. Using Ligand-binding assays, the levels of these receptors has been measured in which cultured keratinocytes showed only one-third of the level of (RAR) and one-eighth of the level of RXR found in skin. This could explain why different doses are needed to activate the same pathway and how the same dose could give different outcomes (Di et al., 1998).

To clarify the role of lipids and specifically ATRA's on keratinocyte differentiation different cell lines as well as NHEK were studied. The experiment started with 4 keratinocyte cell lines available in the lab and were grown in charcoal-treated serum (de-lipidised) containing RM+ medium and were compared to cells grown in RM+ medium with lipid containing serum. In NEB-1 (HPV16 immortalised skin keratinocytes) and T103C (HPV16 immortalised oral keratinocytes) cell lines, there was either a downregulation or no significant difference in the expression of K1, K2 and K10 (Figure 4.3) and this could be due to the way these cells were immortalised. These cell lines are immortalised by HPV16, which is known to alter RA (one of the main lipids in serum) response to terminal differentiation (Agarwal et al., 1991, Merrick et al., 1993). Two more cell lines were used HaCaT, a spontaneously immortalised cell line (Boukamp et al., 1988) and N/TERT, immortalised by overexpression of h-Tert and downregulation of p16 (Dickson et al., 2000), to study the role of SLPs and PR on keratinocyte differentiation (PR has an estrogenic-like effect that could affect cellular differentiation) (Berthois et al., 1986). Estrogen has been shown to affect some keratin gene expression as upregulation of *KRT2*, *KRT14* and *KRT19* genes and this has been shown in human scalp skin after  $\beta$ -Estradiol treatment (Ramot et al., 2009). AS shown in Figure 4.4 that removal of serum lipid by charcoal treatment did induce K1 and

K10 genes and proteins expression that became more significant in PR free medium in HaCaT. In N/TERT cells higher expression of K1 and K10 genes and proteins was only shown in PR free lipid containing serum condition (SLP+/PR-) in Figure 4.5 and this could be due to the method used to immortalise this cell line. The K2 gene on the other hand showed similar expression in both HaCaT and N/TERT cells in which the highest expression was seen in the presence of serum lipid but without PR (SLP+/PR-) with no protein detected in both cell lines. To rule out any effect of immortalisation techniques on keratin genes and protein expression, these experiments were repeated on NHEK. NHEK cells were cultured in different culture media conditions that was used for cell lines (SLP+/PR+, SLP-/PR+, SLP+/PR-, SLP-/PR-). The data in Figure 4.6 showed that NHEK were mimicking HaCaT in which K1 and K10 were showing higher expression of mRNAs and proteins when lipids were removed from the serum with more significant increases when PR was removed indicating a synergistic effect of removing both PR and lipids. Other studies in the literature have also shown that adding RA on normal skin of volunteered patients or cultured keratinocytes did downregulate K1 and K10 genes expression. The effect of RA on terminal differentiation markers was shown in some studies to be not only on keratins but also on other late differentiation markers such as cornifin, filaggrin and loricrin, these studies were done *in vitro* on NHEK (Marvin et al., 1992, Hohl et al., 1991), and these findings strongly suggest that the effect seen in our experiments was primarily due to the presence of RA in serum. Some reports have also shown that K2 mRNA levels were drastically reduced, and the K2 protein either unchanged or became undetectable when topical RA was applied on volunteers' skin (Torma, 2011, Rosenthal et al., 1990, Rosenthal et al., 1992, Virtanen et al., 2000). Keratinocyte differentiation is retinoid sensitive, with Nano-

molar concentration required to keep the normal level of differentiation, excess or reduced RA concentrations could, respectively, reduce or amplify the terminal differentiation process (Randolph and Simon 1997). To show that the effect of SLPs was primarily due to the RA present in the serum ATRA was added to charcoal stripped serum medium with or without PR, and interestingly the effect shown in other *in vivo* studies was reproduced where RA was directly applied on the skin. Keratins K1 and K10 were downregulated at both mRNA and protein levels, which was more pronounced in PR free medium (Figure 4.9 A, B and 4.10). ATRA increases the expression of K2 mRNA when added to charcoal stripped serum (SLP-/PR-) as shown in Figure 4.9 C. Studies have shown that *KRT2* is reduced in an *in vivo* human skin or *in vitro* organotypic skin models treated with RA, while cultured keratinocytes could show upregulation of *KRT2* when treated with RA. The fact that *KRT2* has no RA responsive elements known in the K2 promoter renders the role of ATRA to be either post-transcriptional RA-dependant stabilisation or an indirect effect of RA on its promotor activity. *KRT1* and *KRT10* are known to have RA responsive elements in which RAR/RXR receptors complexed with RA bind and inhibit the expression of these genes (Torma, 2011). Studies have shown that *KRT19* is upregulated by RA and this was explained not as being a result of transcription activation but is primarily due to enhanced mRNA stability (Crowe, 1993).

To study the influence of PR and its estrogenic-like effect on keratin gene expression, PR was added back to PR-free charcoal stripped serum containing RM+ medium. This addition did reduce the expression of *KRT1* and *KRT10* but not of *KRT2* in NHEK (Figure 4.11). The estrogenic-like effect of PR using  $\beta$ -estradiol addition to the culture medium (SLP-/PR-) was also investigated. Although some studies have shown lower expression of differentiation-specific

keratins when keratinocytes were treated with estrogen receptor ER- $\beta$  agonist, genes that are not involved in the terminal differentiation such as *KRT19* are induced by estrogen treatment (Choi et al. 2000). No effect was observed on differentiation-specific keratin gene expression in NHEK by  $\beta$ -estradiol treatment (Figure 4.11). This indicates that the effect of PR that is shown in our experiments could be due to impurities and not due to its structural similarity with  $\beta$ -estradiol.

### **6.1.3. mRNA stability.**

The role of ATRA and SLPs on differentiation-specific keratins could involve mRNA stability or promotor activity of these genes. As the abundance of mRNA in the cytoplasm is not only a result of its synthesis and rate of nuclear export but it is highly controlled by its decay rate. The stability of mRNAs is a vital process that affects protein expression and in fact many cellular processes (Wu and Brewer, 2012). The mRNA decay process is highly selective, as it differs widely from one mRNA to another. Studies have shown that some mRNA sequences contain a specific region on their 3' UTR named AREs (AU-rich elements). This region (5'-AUUUA-3') is known to be a binding site for some AREs binding proteins (AREs-BP) that can attract endonuclease enzyme and results in mRNA de-capping (Poly-A tail removal) (Shaw and Kamen, 1986). Depending on the cellular conditions and the presence of a certain trigger, AREs can either stabilise or degrade specific mRNAs (Barreau et al., 2005). The decay rate of K2 mRNA is around 50% within 30 min after AD treatment compared to K1 and K10 mRNAs which were stable up to 4 h (Figure 5.7 A). Ensembl Genome Browser 95 database was used to look for 5'-AUUUA-3' at the 3' UTR regions of *KRT1*, *KRT2* and *KRT10* genes as shown in (Figure 5.14). AU-rich elements (5'-AUUUA-3') were found in *KRT2* but not in *KRT1* allowing some proteins to bind (ARE-BPs) and activate endo-ribonuclease activity (Geissler and Grimson, 2016). This could

explain the instability of *KRT2* and stability of *KRT1* under certain growth conditions but as mentioned before the presence of AREs not always contributes to decay and could also lead to mRNA stability in some genes depending on the physiological stimulus and the cellular need. Two (5'-AUUUA-3') elements have been found in *KRT10* 3' UTR but the mRNA was stable enough to be translated into a protein as shown using WB. This perhaps suggests that the presence of AREs in a mRNA is not the only factor determining their stability. Other factors could be involved as well such as the cellular microenvironment and physiological conditions.

To study the role of ATRA on keratin mRNA stability, the rate of mRNA decay was measured using AD induced transcription blockage after ATRA treatment. *KRT1* and *KRT10* expression is shown to be downregulated by ATRA with increasing reduction over time due to transcription block with AD giving very low mRNA expression while K2 showed ATRA mediated stabilisation in cells treated with ATRA prior to AD-induced transcription inhibition. ATRA affects mRNA stability by delaying the breakdown in the cytoplasm through its role in mRNA degradations pathways. As seen in *KRT2*, it has been shown that human K19 and prolactin mRNAs contain the 3' end non-coding sequence (5'-AUUUA-3') and their mRNA is more susceptible to degradation in the cytoplasm (Stasiak and Lane, 1987, Crowe, 1993). But they become more stable when the cells are treated with RA indicating K19 mRNA stabilisation in the cytoplasm. RA binds to RA-binding proteins and these complexes perhaps directly or indirectly affect the endonuclease activity making the mRNA less vulnerable to degradation (Crowe, 1993). RA-dependant stabilisation of K2 mRNA is also shown in Figure 5.8.C after treating the cells with ATRA and AD, proposing that K2 could share the same control mechanism that has been used to explain K19 mRNA stability. The

K2 mRNA was stable for up to 3 h and became unstable after that despite the prior treatment with ATRA. This could be explained by the loss of ATRA activity, as some studies have shown that ATRA stability is reduced in serum free chemically defined medium (in which all of the chemical components are known) after 24 h of treatment despite accurate handling during experimental procedures. This medium lacks lipids and any undefined animal-derived products (Sharow et al., 2012, Kitano, 1985, Jayme and Smith, 2000). As this chemically defined serum free medium and our medium containing charcoal stripped serum contains no lipid, this could explain the loss of RA-dependant mRNA stability of K2 shown in Figure 5.8 C in which ATRA stability could be lost after 24 h. As discussed earlier changing the growth conditions of NHEK did affect the expression of K1, K2 and K10 mRNA and protein. In order to investigate if this change in expression has any transcription (synthesis) or post-transcription (stability) involvement, NHEK cells were grown in the same four different conditions used in chapter 4 (SLP+/PR+, SLP-/PR+, SLP+/PR-, SLP-/PR-). The decay rate of K1, K2 and K10 mRNA were then measured by blocking the transcription with AD. K1 and K10 mRNA were stable in all conditions, so changing the growth conditions (presence of SLPs and PR) did not affect the stability over time, but did affect transcription levels of *KRT1* and *KRT10* as shown in the mRNA level at 0 time point of AD treatment. K2 mRNA did not show any significant difference in expression when culture conditions were changed (comparing different conditions at 0 time). The decay rate of *KRT2* was highly significant over time of AD treatment for all conditions with more stability shown when using lipid containing PR free condition (SLP+/PR-), see Figure 5.9 C. This could be referred to the presence of lipid mainly RA that was shown previously to stabilise *KRT2* in the absence of PR (Figure 4.9 C).

As mentioned earlier, the differential regulation of late differentiation keratins observed in our experiments could also involve the promoter activity. The genes under study are involved in keratinocyte differentiation, these genes are known to be regulated through the activation of AP-1 (activation protein-1) transcription factor (Briata et al., 1993). AP-1 transcription factor is a family of JUN and FOS proteins that form dimers and bind to AP-1 responsive elements on the DNA. This binding induces expression of differentiation markers in keratinocytes. PMA treatment induces differentiation primarily through activating AP-1 binding (Eckert and Welter, 1996, Briata et al., 1993, Karlsson et al., 2010). To study the promoter activity of K10 and K2 using luciferase reporter assay, different fragments of the promoter sequence were cloned into a pGL4.14 vector. HaCaT and HEK293 (Human embryonic kidney epithelial) cells were transfected with pGL4.26\_AP-1, in which six copies of AP-1 responsive elements were cloned in pGL4.26 (Brown et al 2013), to measure AP-1 activity induced by PMA treatment of these cells. In HaCaT there is no difference in luciferase activity between the PMA treatment and control while in HEK293 cells there was more than 10-fold increase with PMA treatment compared with the control (Figure 5.11). The difference between the HEK293 and HaCaT could be due to our pGL4 construct is not able to transfect keratinocytes since Renilla vector that have been used for transfection efficiency internal control was giving consistently high readings which excludes a transfection problem. K2 and K14 promoters cloned in pGL4.14 vector were also used to measure their activity under different growth conditions in HaCaT cells. Data showed no statistical difference in their promoter activities using luciferase assay when cells were grown in different culture conditions (Figure 5.13). This could be due to low K2 and K14 promoter activity or low transfection efficiency of the constructs in HaCaT. Another experiment was done to investigate whether a



correlation existed between growing cells under different growth conditions (SLP+/PR+, SLP-/PR+, SLP+/PR-, SLP-/PR-) and the AP-1 activity measured. For this HEK293 cells were transfected with pGL4.26-AP-1 construct and the activity was measured under different growth conditions (same as used for K2 and K14 promotor experiment) and it did not show any significant difference of luciferase activity between the conditions indicating that the role of lipids on gene expression is a direct effect and not through AP-1 activity.

As housekeeping genes are also affected under growth conditions, the Cp values of YAP-1 and POL2A (housekeeping genes) were measured in this study. They were stable after ATRA, PR and  $\beta$ -estradiol treatments (Figure A.4). On the other hand, changing the growth conditions did affect YAP-1 and POL2A Cp values significantly when treated with AD and this could give faulty readings of our genes relative to YAP-1 and POL2A. This indicates that YAP-1 and POL2A were not the correct reference genes to be used in this set of experiments (effect of different serum conditions on stability of differentiation specific keratins using AD), and absolute quantification would be a more accurate measure of gene expression under specific growth conditions.

## **6.2. Clinical significance of this study.**

### **6.2.1. Keratin phosphorylation.**

Keratins are structural proteins that provide strength and integrity for epithelial cells and perform a wide variety of functions intra and extracellularly. Keratins undergo PTMs allowing them to reorganise inside the cell. The most common and well-studied PTM in keratins is phosphorylation. The majority of PTMs occur at the N or C-terminals of the keratin polypeptides suggesting the importance of

the head and tail domains in filaments stabilisation. All kind of stresses, apoptosis and mitosis are the main inducers of phosphorylation and they also cause keratin re-organisation (Hyder et al., 2008). Several studies have linked pathologies to the impairment in keratin phosphorylation. For example, in liver disease the presence of Serine 73 (S73) on the head domain of K8 acts as phosphate sponge (a cytoprotective buffer that absorbs phosphate) allowing phosphorylation to take place. Any impairment in this phosphorylation site causes liver injury in which the epithelial cells are not able to withstand different stresses (Ku and Omary, 2006). Furthermore, other studies have also proposed a role for keratins as a regulator of carcinogenesis (Karantza, 2011b). It has been shown that keratin phosphorylation is responsible for the viscoelasticity of the pancreatic cancer cells as some endogenous toxic compounds can induce phosphorylation and reorganisation of keratin network in cancer cells. Another example is that of human oral squamous cell carcinoma (OSCC) where loss of K8 S73 and S431 phosphorylation has been observed and dephosphorylation greatly associated with size, and progression of the tumour (Kim et al., 2015a) . The same players that allow phosphorylation and reorganisation of keratins are also responsible for EMT allowing cancer metastasis to take place, EGF, Interleukin-6 (IL-6) and PMA are few examples that could induces phosphorylation of keratins and enhances EMT (Kim et al., 2015a) .

In conclusion, keratin phosphorylation and its subsequent reorganisation is an emerging new method for controlling EMT and cancer metastasis. Kinase inhibitors could be used to reduce phosphorylation, keratin re-organisation and consequently suppress metastasis. The use of phosphatase inducers could also be another promising alternative for controlling keratin re-organisation by dephosphorylating either serine residue of keratins or through dephosphorylating

phosphorylated kinases (active kinases) that are involved in phosphorylation of keratins (Kim et al., 2015a, Beil et al., 2003).

The dynamics of keratins in a simple epithelial breast cancer cell line (MCF-7) was studied and showed that inducing phosphorylation using phosphatase inhibitors does allow re-organisation and breakdown of the filaments. AcGFP-tag on the head domain of K2 allowed more breakdown of filaments compared to a smaller tag indicating the role of head domain folding in filaments stabilisation. These data could lead to developing a novel strategy for studying cancer metastasis in which controlling keratin phosphorylation could be a promising target for controlling EMT.

### **6.2.2. Differentiation Therapy.**

The focus of this study was mainly on late differentiation keratins such as K1, K2 and K10, so the factors that could affect the process of keratinocyte differentiation could be of great importance in this case. Keratinocyte differentiation and proliferation has been widely studied in respect to SCC. Genetic alterations result in the loss of proliferative control of cells which is one of the hallmarks of cancer. Retinoids have been used in therapeutic doses in some types of SCCs to induce differentiation (Cheung et al., 2012). As cellular proliferation and differentiation have an inverse relationship (Suzan and Sander, 2016) and the level of differentiation is used in SCC staging, the ability to study the process of differentiation and factors affecting this process is of key importance. Using this phenomenon to force cancer cells to exit the cell cycle and stop proliferation to reduce tumor size and perhaps decrease the risk of cancer metastasis will be a promising approach in cancer therapy. Cancer remains a major medical problem as the most widely used therapeutic approaches are surgery, radiotherapy and chemotherapy. These treatment modalities are non-specific, highly toxic and can

lead to severe disfigurement. In order to reduce therapeutic complications, new treatment modalities have been introduced as adjuncts to conventional chemotherapy or radiotherapy such as differentiation therapy and angiogenesis inhibition as well as immunotherapy (Leszczyniecka et al., 2001). Studies have shown that cells with poorer differentiation ability are able to stimulate tissue renewal by cellular proliferation, which is of huge importance in increasing the rate of tumour growth and expansion. p53 is a gene that codes for the 53 kDa protein which regulates the cell cycle and therefore functions as a tumour suppressor, it also induces apoptosis and cell cycle arrest. It has been shown that p53 has the ability to induce terminal differentiation in keratinocytes with no effect on apoptosis (Guinea-Viniegra et al., 2012). It could be promising to use FOS/AP-1 inhibition, and p53 activation with TACE/NOTCH1-activating therapies in differentiation of skin SCCs. Similar approaches have been used in studies to modulate differentiation in breast cancer stem cells, so this strategy may hold great potential for future cancer treatment modalities (Guinea-Viniegra et al., 2012). ATRA did reduces the expression of *KRT1* and *KRT10* but not *KRT2* *in vitro* under certain growth conditions and drug concentrations. Other studies have shown that RA was used to treat SCC and induce differentiations as mentioned earlier (Beckenbach et al., 2015, Khalil et al., 2017). This indicates that cells are sensitive to RA concentrations and growth conditions and this play a very important role on keratinocyte differentiation.

### **6.2.3. mRNA stability.**

The regulation of mRNA stability and translation into protein are two essential processes that allow the cell to respond to changes in microenvironment as fast as possible. A stimulus or a trigger could either stabilise or de-stabilise the mRNA by either inhibiting or stimulating its degradation. The presence of AREs (AU-rich

elements) has been known to be the targets for different proteins that affects mRNA stability and they are named AREs-binding proteins. Under certain pathological conditions such as cancer or wound healing, deregulation of the mRNA stability takes place depending on the presence of these binding proteins (Barreau et al., 2005). For example, HuR (Human antigen R), also known as ELAV-like protein 1, in humans is encoded by the *ELAVL1*, contains 3 RNA-binding domains which bind cis-acting AU-rich elements to regulate mRNA stability. It is a member of the embryonic lethal abnormal vision family which has been involved in many biological events such as cell proliferation, differentiation, and carcinogenesis. When HuR was knocked down in oral cancer cells, ARE-mRNA stabilisations was inhibited. These cancer cells lost their ability to proliferate and invade indicating a potential ability of HuR to change the characteristics of oral cancer cells (Kakuguchi et al., 2010). Such a strategy can be employed to suppress not only oncogenesis but also metastasis. Another example emphasising the importance of mRNA stability and AREs-BP is their role in apoptosis. RNA binding protein, CELF1, can bind to mRNAs in pro-apoptotic oral cancer cells, de-stabilise them and prevent apoptosis. This indicates its role as a cancer maker and a future therapeutic target for oral cancer (Talwar et al., 2013).

The mRNA stability of three differentiation-specific keratins was studied showing that K2 was stabilised by ATRA treatment when K1 and K10 mRNAs were not. This was very interesting since the decay rate of K2 mRNA in the absence of ATRA was far higher compared with K1 and K10. This was explained by the presence of AREs in *KRT2* mRNA in which certain AREs-binding proteins can bind and destabilises the mRNA. The lower stability of K2 mRNA in the absence of ATRA could explain the undetectable K2 protein expression in cultured

keratinocytes. The importance of studying the mRNA stability of these keratins lies in the fact that they are differentiation markers and could play a significant role in the pathogenesis of SCCs. Targeting ARE-binding proteins to regulate mRNA stability and translation of oncogenic proteins is a potential therapeutic genetic approach in SCC treatment and management.

### **6.3. Future directions of this study.**

To broaden our findings, the following aspects could be investigated in future experiments:

1. Determining the role of head, tail and rod domains of the keratin polypeptide tagged and un-tagged in filament stability in phosphorylated and unphosphorylated states.
2. Further investigations of the role of heat shock proteins in keratin filament stability, which could be explored by using a p38 MAPK inhibitor such as SB203580 or/and using dominant negative or constitutively active p38 kinase.
3. Use FRET assay to measure the strength of binding of different pairs of keratins using SW13 (adrenal gland/cortex epithelial cell line which do not express any keratin). These data will determine *in vivo* binding characteristics and the role of head and tail in affecting the strength of binding of these keratins which has never been studied.
4. Role of RA on the expression of late differentiation keratins in an organotypic culture using skin and oral keratinocytes.

5. To further investigate the role of SLPs on keratin expression, absolute quantification of mRNA will give a better understating as the reference genes YAP1 and POL were affected by these conditions.
6. Further studies on mRNA stability of late differentiation keratins in NHEK using nuclear and cytoplasmic fractions of the RNA.
7. Characterisation of epigenetic regulation of K2 by studying promotor activity and DNA methylation.

## References.

- AGARWAL, C., RORKE, E. A., IRWIN, J. C. & ECKERT, R. L. 1991. Immortalization by human papillomavirus type 16 alters retinoid regulation of human ectocervical epithelial cell differentiation. *Cancer Res*, 51, 3982-9.
- ANG-TIU, C. U. & NICOLAS, M. E. 2012. Ichthyosis bullosa of Siemens. *J Dermatol Case Rep*, 6, 78-81.
- ANGEL, P., IMAGAWA, M., CHIU, R., STEIN, B., IMBRA, R. J., RAHMSDORF, H. J., JONAT, C., HERRLICH, P. & KARIN, M. 1987. Phorbol ester-inducible genes contain a common cis element recognized by a TPA-modulated trans-acting factor. *Cell*, 49, 729-39.
- ANSON, D. S. 2004. The use of retroviral vectors for gene therapy-what are the risks? A review of retroviral pathogenesis and its relevance to retroviral vector-mediated gene delivery. *Genet Vaccines Ther*, 2, 9.
- ARIN, M. J. 2009. The molecular basis of human keratin disorders. *Hum Genet*, 125, 355-73.
- ARSLAN, M., QIN, Z. & BUEHLER, M. J. 2011. Coiled-coil intermediate filament stutter instability and molecular unfolding. *Computer Methods in Biomechanics and Biomedical Engineering*, 14, 483-489.
- ATWATER, J. A., WISDOM, R. & VERMA, I. M. 1990. Regulated mRNA stability. *Annu Rev Genet*, 24, 519-41.
- AZIZ, A., HESS, J. F., BUDAMAGUNTA, M. S., VOSS, J. C. & FITZGERALD, P. G. 2010. Site-directed spin labeling and electron paramagnetic resonance determination of vimentin head domain structure. *J Biol Chem*, 285, 15278-85.
- BALMER, J. E. & BLOMHOFF, R. 2002. Gene expression regulation by retinoic acid. *J Lipid Res*, 43, 1773-808.
- BARREAU, C., PAILLARD, L. & OSBORNE, H. B. 2005. AU-rich elements and associated factors: are there unifying principles? *Nucleic Acids Research*, 33, 7138-7150.
- BECKENBACH, L., BARON, J. M., MERK, H. F., LOFFLER, H. & AMANN, P. M. 2015. Retinoid treatment of skin diseases. *European Journal of Dermatology*, 25, 384-391.
- BEERE, H. M. 2004. "The stress of dying": the role of heat shock proteins in the regulation of apoptosis. *J Cell Sci*, 117, 2641-51.
- BEIL, M., MICOULET, A., VON WICHERT, G., PASCHKE, S., WALTHER, P., OMARY, M. B., VAN VELDHOVEN, P. P., GERN, U., WOLFF-HIEBER, E., EGGERMANN, J., WALTENBERGER, J., ADLER, G., SPATZ, J. & SEUFFERLEIN, T. 2003. Sphingosylphosphorylcholine regulates keratin network architecture and visco-elastic properties of human cancer cells. *Nat Cell Biol*, 5, 803-11.
- BENKOUSSA, M., BRAND, C., DELMOTTE, M. H., FORMSTECHE, P. & LEFEBVRE, P. 2002. Retinoic acid receptors inhibit AP1 activation by regulating extracellular signal-regulated kinase and CBP recruitment to an AP1-responsive promoter. *Mol Cell Biol*, 22, 4522-34.
- BENSAUDE, O. 2011. Inhibiting eukaryotic transcription: Which compound to choose? How to evaluate its activity? *Transcription*, 2, 103-108.
- BERTHOIS, Y., KATZENELLENBOGEN, J. A. & KATZENELLENBOGEN, B. S. 1986. Phenol red in tissue culture media is a weak estrogen: implications



- concerning the study of estrogen-responsive cells in culture. *Proc Natl Acad Sci U S A*, 83, 2496-500.
- BIKLE, D. D. 2011. Vitamin D metabolism and function in the skin. *Mol Cell Endocrinol*, 347, 80-9.
- BIKLE, D. D. 2012. Vitamin D and the skin: Physiology and pathophysiology. *Rev Endocr Metab Disord*, 13, 3-19.
- BLOOR, B. K., SEDDON, S. V. & MORGAN, P. R. 2000. Gene expression of differentiation-specific keratins (K4, K13, K1 and K10) in oral non-dysplastic keratoses and lichen planus. *J Oral Pathol Med*, 29, 376-84.
- BLOOR, B. K., TIDMAN, N., LEIGH, I. M., ODELL, E., DOGAN, B., WOLLINA, U., GHALI, L. & WASEEM, A. 2003. Expression of keratin K2e in cutaneous and oral lesions: association with keratinocyte activation, proliferation, and keratinization. *Am J Pathol*, 162, 963-75.
- BOLLING, M. C., LEMMINK, H. H., JANSEN, G. H. L. & JONKMAN, M. F. 2011. Mutations in KRT5 and KRT14 cause epidermolysis bullosa simplex in 75% of the patients. *British Journal of Dermatology*, 164, 637-644.
- BONONI, A., AGNOLETTI, C., DE MARCHI, E., MARCHI, S., PATERGNANI, S., BONORA, M., GIORGI, C., MISSIROLI, S., POLETTI, F., RIMESSI, A. & PINTON, P. 2011. Protein kinases and phosphatases in the control of cell fate. *Enzyme Res*, 2011, 329098.
- BOSE, A., TEH, M. T., HUTCHISON, I. L., WAN, H., LEIGH, I. M. & WASEEM, A. 2012. Two Mechanisms Regulate Keratin K15 Expression In Keratinocytes: Role of PKC/AP-1 and FOXM1 Mediated Signalling. *Plos One*, 7.
- BOSE, A., TEH, M. T., MACKENZIE, I. C. & WASEEM, A. 2013. Keratin k15 as a biomarker of epidermal stem cells. *Int J Mol Sci*, 14, 19385-98.
- BOUKAMP, P., PETRUSSEVSKA, R. T., BREITKREUTZ, D., HORNUNG, J., MARKHAM, A. & FUSENIG, N. E. 1988. Normal keratinization in a spontaneously immortalized aneuploid human keratinocyte cell line. *J Cell Biol*, 106, 761-71.
- BOYCE, S. T. & HAM, R. G. 1983. Calcium-regulated differentiation of normal human epidermal keratinocytes in chemically defined clonal culture and serum-free serial culture. *J Invest Dermatol*, 81, 33s-40s.
- BRAGULLA, H. H. & HOMBERGER, D. G. 2009. Structure and functions of keratin proteins in simple, stratified, keratinized and cornified epithelia. *J Anat*, 214, 516-59.
- BRAY, D. J., WALSH, T. R., NORO, M. G. & NOTMAN, R. 2015. Complete Structure of an Epithelial Keratin Dimer: Implications for Intermediate Filament Assembly. *PLoS One*, 10, e0132706.
- BRIATA, P., D'ANNA, F., FRANZI, A. T. & GHERZI, R. 1993. AP-1 activity during normal human keratinocyte differentiation: evidence for a cytosolic modulator of AP-1/DNA binding. *Exp Cell Res*, 204, 136-46.
- BROWN, P. H., ALANI, R., PREIS, L. H., SZABO, E. & BIRRER, M. J. 1993. Suppression of oncogene-induced transformation by a deletion mutant of c-jun. *Oncogene*, 8, 877-86.
- BRYAN, D., SEXTON, C. J., WILLIAMS, D., LEIGH, I. M. & MCKAY, I. A. 1995. Oral keratinocytes immortalized with the early region of human papillomavirus type 16 show elevated expression of interleukin 6, which acts as an autocrine growth factor for the derived T103C cell line. *Cell Growth Differ*, 6, 1245-50.
- CANENE-ADAMS, K. 2013. Preparation of formalin-fixed paraffin-embedded tissue for immunohistochemistry. *Methods Enzymol*, 533, 225-33.

- CAO, Z., WEST, C., NORTON-WENZEL, C. S., REJ, R., DAVIS, F. B., DAVIS, P. J. & REJ, R. 2009. Effects of resin or charcoal treatment on fetal bovine serum and bovine calf serum. *Endocr Res*, 34, 101-8.
- CARTER, R. & DROUIN, G. 2009. Structural differentiation of the three eukaryotic RNA polymerases. *Genomics*, 94, 388-96.
- CASTAGNA, M., TAKAI, Y., KAIBUCHI, K., SANO, K., KIKKAWA, U. & NISHIZUKA, Y. 1982a. Direct activation of calcium-activated, phospholipid-dependent protein kinase by tumor-promoting phorbol esters. *J Biol Chem*, 257, 7847-51.
- CASTAGNA, M., TAKAI, Y., KAIBUCHI, K., SANO, K., KIKKAWA, U. & NISHIZUKA, Y. 1982b. Direct Activation of Calcium-Activated, Phospholipid-Dependent Protein-Kinase by Tumor-Promoting Phorbol Esters. *Journal of Biological Chemistry*, 257, 7847-7851.
- CAULIN, C., SALVESEN, G. & OSHIMA, R. G. 1997. Caspase cleavage of keratin 18 and reorganization of intermediate filaments during epithelial cell apoptosis. *Molecular Biology of the Cell*, 8, 367-367.
- CHAPMAN, S., LIU, X., MEYERS, C., SCHLEGEL, R. & MCBRIDE, A. A. 2010. Human keratinocytes are efficiently immortalized by a Rho kinase inhibitor. *J Clin Invest*, 120, 2619-26.
- CHEN, C. Y., EZZEDDINE, N. & SHYU, A. B. 2008. Messenger RNA half-life measurements in mammalian cells. *Methods Enzymol*, 448, 335-57.
- CHEN, J., CHENG, X., MERCHED-SAUVAGE, M., CAULIN, C., ROOP, D. R. & KOCH, P. J. 2006. An unexpected role for keratin 10 end domains in susceptibility to skin cancer. *J Cell Sci*, 119, 5067-76.
- CHEUNG, B. B., KOACH, J., TAN, O., KIM, P., BELL, J. L., D'ANDRETI, C., SUTTON, S., MALYUKOVA, A., SEKYERE, E., NORRIS, M., HABER, M., KAVALLARIS, M., CUNNINGHAM, A. M., PROBY, C., LEIGH, I., WILMOTT, J. S., COOPER, C. L., HALLIDAY, G. M., SCOLYER, R. A. & MARSHALL, G. M. 2012. The retinoid signalling molecule, TRIM16, is repressed during squamous cell carcinoma skin carcinogenesis in vivo and reduces skin cancer cell migration in vitro. *Journal of Pathology*, 226, 451-462.
- CHOI, I., GUDAS, L. J. & KATZENELLENBOGEN, B. S. 2000. Regulation of keratin 19 gene expression by estrogen in human breast cancer cells and identification of the estrogen responsive gene region. *Mol Cell Endocrinol*, 164, 225-37.
- COELHO, B. A., PETERLE, G. T., SANTOS, M., AGOSTINI, L. P., MAIA, L. L., STUR, E., SILVA, C. V. M., MENDES, S. O., ALMANCA, C. C. J., FREITAS, F. V., BORCOI, A. R., ARCHANJO, A. B., MERCANTE, A. M. C., NUNES, F. D., CARVALHO, M. B., TAJARA, E. H., LOURO, I. D. & SILVA-CONFORTI, A. M. A. 2015. Keratins 17 and 19 expression as prognostic markers in oral squamous cell carcinoma. *Genetics and Molecular Research*, 14, 15123-15132.
- COLLIN, C., MOLL, R., KUBICKA, S., OUHAYOUN, J. P. & FRANKE, W. W. 1992. Characterization of human cytokeratin 2, an epidermal cytoskeletal protein synthesized late during differentiation. *Exp Cell Res*, 202, 132-41.
- COLLINS, L. M. & DAWES, C. 1987. The surface area of the adult human mouth and thickness of the salivary film covering the teeth and oral mucosa. *J Dent Res*, 66, 1300-2.
- COULOMBE, P. A. & OMARY, M. B. 2002. 'Hard' and 'soft' principles defining the structure, function and regulation of keratin intermediate filaments. *Curr Opin Cell Biol*, 14, 110-22.

- CROWE, D. L. 1993. Retinoic acid mediates post-transcriptional regulation of keratin 19 mRNA levels. *J Cell Sci*, 106 ( Pt 1), 183-8.
- D'ALESSANDRO, M., COATS, S. E., JONKMANN, M. F., LEIGH, I. M. & LANE, E. B. 2011. Keratin 14-null cells as a model to test the efficacy of gene therapy approaches in epithelial cells. *J Invest Dermatol*, 131, 1412-9.
- DARLINGTON, G. J. 2008. Inoculation and passaging of Mammalian monolayer cell cultures. *CSH Protoc*, 2008, pdb prot4347.
- DAVIS, H. E., MORGAN, J. R. & YARMUSH, M. L. 2002. Polybrene increases retrovirus gene transfer efficiency by enhancing receptor-independent virus adsorption on target cell membranes. *Biophys Chem*, 97, 159-72.
- DEEK, J., HECHT, F., ROSSETTI, L., WISSMILLER, K. & BAUSCH, A. R. 2016. Mechanics of soft epithelial keratin networks depend on modular filament assembly kinetics. *Acta Biomater*, 43, 218-29.
- DEYRIEUX, A. F. & WILSON, V. G. 2007. In vitro culture conditions to study keratinocyte differentiation using the HaCaT cell line. *Cytotechnology*, 54, 77-83.
- DI, W., LI, X. Y., DATTA, S., ASTROM, A., FISHER, G. J., CHAMBON, P., VOORHEES, J. J. & XIAO, J. H. 1998. Keratinocyte-specific retinoid regulation of human cellular retinoic acid binding protein-II (hCRABPII) gene promoter requires an evolutionarily conserved DR1 retinoic acid-responsive element. *J Invest Dermatol*, 111, 1109-15.
- DICKSON, M. A., HAHN, W. C., INO, Y., RONFARD, V., WU, J. Y., WEINBERG, R. A., LOUIS, D. N., LI, F. P. & RHEINWALD, J. G. 2000. Human keratinocytes that express hTERT and also bypass a p16(INK4a)-enforced mechanism that limits life span become immortal yet retain normal growth and differentiation characteristics. *Mol Cell Biol*, 20, 1436-47.
- DLUGOSZ, A. A. & YUSPA, S. H. 1993a. Coordinate changes in gene expression which mark the spinous to granular cell transition in epidermis are regulated by protein kinase C. *J Cell Biol*, 120, 217-25.
- DLUGOSZ, A. A. & YUSPA, S. H. 1993b. Coordinate Changes in Gene-Expression Which Mark the Spinous to Granular-Cell Transition in Epidermis Are Regulated by Protein-Kinase-C. *Journal of Cell Biology*, 120, 217-225.
- DORION, S. & LANDRY, J. 2002. Activation of the mitogen-activated protein kinase pathways by heat shock. *Cell Stress Chaperones*, 7, 200-6.
- DOUNAY, A. B. & FORSYTH, C. J. 2002. Okadaic acid: the archetypal serine/threonine protein phosphatase inhibitor. *Curr Med Chem*, 9, 1939-80.
- DROZDOFF, V. & PLEDGER, W. J. 1993. Commitment to differentiation and expression of early differentiation markers in murine keratinocytes in vitro are regulated independently of extracellular calcium concentrations. *J Cell Biol*, 123, 909-19.
- DUCREST, A. L., AMACKER, M., LINGNER, J. & NABHOLZ, M. 2002. Detection of promoter activity by flow cytometric analysis of GFP reporter expression. *Nucleic Acids Res*, 30, e65.
- ECKERT, R. L., ADHIKARY, G., YOUNG, C. A., JANS, R., CRISH, J. F., XU, W. & RORKE, E. A. 2013. AP1 transcription factors in epidermal differentiation and skin cancer. *J Skin Cancer*, 2013, 537028.
- ECKERT, R. L., CRISH, J. F. & ROBINSON, N. A. 1997. The epidermal keratinocyte as a model for the study of gene regulation and cell differentiation. *Physiological Reviews*, 77, 397-424.

- ECKERT, R. L. & WELTER, J. F. 1996. Transcription factor regulation of epidermal keratinocyte gene expression. *Mol Biol Rep*, 23, 59-70.
- EICHNER, R., KAHN, M., CAPETOLA, R. J., GENDIMENICO, G. J. & MEZICK, J. A. 1992. Effects of topical retinoids on cytoskeletal proteins: implications for retinoid effects on epidermal differentiation. *J Invest Dermatol*, 98, 154-61.
- EICHNER, R., SUN, T. T. & AEBI, U. 1986. The role of keratin subfamilies and keratin pairs in the formation of human epidermal intermediate filaments. *J Cell Biol*, 102, 1767-77.
- ELSHOLZ, F., HARTENECK, C., MULLER, W. & FRIEDLAND, K. 2014. Calcium-a central regulator of keratinocyte differentiation in health and disease. *Eur J Dermatol*, 24, 650-61.
- ERDMANN, K., RINGEL, J., HAMPEL, S., WIRTH, M. P. & FUESSEL, S. 2017. Carbon nanomaterials sensitize prostate cancer cells to docetaxel and mitomycin C via induction of apoptosis and inhibition of proliferation. *Beilstein J Nanotechnol*, 8, 1307-1317.
- ETTINGER, A. & WITTMANN, T. 2014. Fluorescence live cell imaging. *Methods Cell Biol*, 123, 77-94.
- FELDMAN, A. T. & WOLFE, D. 2014. Tissue processing and hematoxylin and eosin staining. *Methods Mol Biol*, 1180, 31-43.
- FISCHER, H., LANGBEIN, L., REICHELT, J., BUCHBERGER, M., TSCHACHLER, E. & ECKHART, L. 2016. Keratins K2 and K10 are essential for the epidermal integrity of plantar skin. *J Dermatol Sci*, 81, 10-6.
- FISCHER, H., LANGBEIN, L., REICHELT, J., PRAETZEL-WUNDER, S., BUCHBERGER, M., GHANNADAN, M., TSCHACHLER, E. & ECKHART, L. 2014. Loss of keratin K2 expression causes aberrant aggregation of K10, hyperkeratosis, and inflammation. *J Invest Dermatol*, 134, 2579-88.
- FISHER, C., BLUMENBERG, M. & TOMIC-CANIC, M. 1995. Retinoid receptors and keratinocytes. *Crit Rev Oral Biol Med*, 6, 284-301.
- FUCHS, E. 1993. Epidermal differentiation and keratin gene expression. *J Cell Sci Suppl*, 17, 197-208.
- FUCHS, E. & GREEN, H. 1981. Regulation of terminal differentiation of cultured human keratinocytes by vitamin A. *Cell*, 25, 617-25.
- FULDA, S., GORMAN, A. M., HORI, O. & SAMALI, A. 2010. Cellular stress responses: cell survival and cell death. *Int J Cell Biol*, 2010, 214074.
- FUSENIG, N. E. & BOUKAMP, P. 1998. Multiple stages and genetic alterations in immortalization, malignant transformation, and tumor progression of human skin keratinocytes. *Mol Carcinog*, 23, 144-58.
- GABAI, V. L., MERIIN, A. B., MOSSER, D. D., CARON, A. W., RITS, S., SHIFRIN, V. I. & SHERMAN, M. Y. 1997. Hsp70 prevents activation of stress kinases. A novel pathway of cellular thermotolerance. *J Biol Chem*, 272, 18033-7.
- GEFEN, A. & WEIHS, D. 2015. Mechanical cytoprotection: A review of cytoskeleton-protection approaches for cells. *J Biomech*.
- GEISSLER, R. & GRIMSON, A. 2016. A position-specific 3'UTR sequence that accelerates mRNA decay. *Rna Biology*, 13, 1075-1077.
- GEMENETZIDIS, E., BOSE, A., RIAZ, A. M., CHAPLIN, T., YOUNG, B. D., ALI, M., SUGDEN, D., THURLOW, J. K., CHEONG, S. C., TEO, S. H., WAN, H., WASEEM, A., PARKINSON, E. K., FORTUNE, F. & TEH, M. T. 2009. FOXM1 Upregulation Is an Early Event in Human Squamous Cell

- Carcinoma and it Is Enhanced by Nicotine during Malignant Transformation. *Plos One*, 4.
- GENDIMENICO, G. J. & MEZICK, J. A. 1993. Pharmacological effects of retinoids on skin cells. *Skin Pharmacol*, 6 Suppl 1, 24-34.
- GIBSON, D. F. C., RATNAM, A. V. & BIKLE, D. D. 1996. Evidence for separate control mechanisms at the message, protein, and enzyme activation levels for transglutaminase during calcium-induced differentiation of normal and transformed human keratinocytes. *Journal of Investigative Dermatology*, 106, 154-161.
- GLOVER, J. F., IRWIN, J. T. & DARBRE, P. D. 1988. Interaction of phenol red with estrogenic and antiestrogenic action on growth of human breast cancer cells ZR-75-1 and T-47-D. *Cancer Res*, 48, 3693-7.
- GODFROID, E., GEUSKENS, M., DUPRESSOIR, T., PARENT, I. & SZPIRER, C. 1991. Cytokeratins are exposed on the outer surface of established human mammary carcinoma cells. *J Cell Sci*, 99 ( Pt 3), 595-607.
- GODSEL, L. M., HOBBS, R. P. & GREEN, K. J. 2008. Intermediate filament assembly: dynamics to disease. *Trends Cell Biol*, 18, 28-37.
- GONZALEZ, I. L. & SCHMICKEL, R. D. 1986. The human 18S ribosomal RNA gene: evolution and stability. *Am J Hum Genet*, 38, 419-27.
- GSTRAUNTHALER, G. 2003. Alternatives to the use of fetal bovine serum: Serum-free cell culture. *Altex-Alternativen Zu Tierexperimenten*, 20, 275-281.
- GU, L. H. & COULOMBE, P. A. 2007. Keratin function in skin epithelia: a broadening palette with surprising shades. *Curr Opin Cell Biol*, 19, 13-23.
- GUETTOUCHE, T., BOELLMANN, F., LANE, W. S. & VOELLMY, R. 2005. Analysis of phosphorylation of human heat shock factor 1 in cells experiencing a stress. *BMC Biochem*, 6, 4.
- GUHANIYOGI, J. & BREWER, G. 2001. Regulation of mRNA stability in mammalian cells. *Gene*, 265, 11-23.
- GUINEA-VINIEGRA, J., ZENZ, R., SCHEUCH, H., JIMENEZ, M., BAKIRI, L., PETZELBAUER, P. & WAGNER, E. F. 2012. Differentiation-induced skin cancer suppression by FOS, p53, and TACE/ADAM17. *J Clin Invest*, 122, 2898-910.
- GUO, J. 2014. Transcription: the epicenter of gene expression. *J Zhejiang Univ Sci B*, 15, 409-11.
- HAINES, R. L. & LANE, E. B. 2012. Keratins and disease at a glance. *J Cell Sci*, 125, 3923-8.
- HAN, B., RORKE, E. A., ADHIKARY, G., CHEW, Y. C., XU, W. & ECKERT, R. L. 2012. Suppression of AP1 transcription factor function in keratinocyte suppresses differentiation. *PLoS One*, 7, e36941.
- HANSSON, A., BLOOR, B. K., HAIG, Y., MORGAN, P. R., EKSTRAND, J. & GRAFSTROM, R. C. 2001. Expression of keratins in normal, immortalized and malignant oral epithelia in organotypic culture. *Oral Oncol*, 37, 419-30.
- HARBAUM, L., POLLHEIMER, M. J., KORNPRAT, P., LINDTNER, R. A., SCHLEMMER, A., REHAK, P. & LANGNER, C. 2012. Keratin 20 - A diagnostic and prognostic marker in colorectal cancer? *Histology and Histopathology*, 27, 347-356.
- HE, T., STEPULAK, A., HOLMSTROM, T. H., OMARY, M. B. & ERIKSSON, J. E. 2002. The intermediate filament protein keratin 8 is a novel cytoplasmic substrate for c-Jun N-terminal kinase. *J Biol Chem*, 277, 10767-74.

- HENNINGS, H. & HOLBROOK, K. A. 1983. Calcium regulation of cell-cell contact and differentiation of epidermal cells in culture. An ultrastructural study. *Exp Cell Res*, 143, 127-42.
- HENNINGS, H., MICHAEL, D., CHENG, C., STEINERT, P., HOLBROOK, K. & YUSPA, S. H. 1980. Calcium regulation of growth and differentiation of mouse epidermal cells in culture. *Cell*, 19, 245-54.
- HERRMANN, H. & AEBI, U. 2016. Intermediate Filaments: Structure and Assembly. *Cold Spring Harb Perspect Biol*, 8.
- HERRMANN, H., BAR, H., KREPLAK, L., STRELKOV, S. V. & AEBI, U. 2007. Intermediate filaments: from cell architecture to nanomechanics. *Nat Rev Mol Cell Biol*, 8, 562-73.
- HERRMANN, H., STRELKOV, S. V., FEJA, B., ROGERS, K. R., BRETTEL, M., LUSTIG, A., HANER, M., PARRY, D. A., STEINERT, P. M., BURKHARD, P. & AEBI, U. 2000. The intermediate filament protein consensus motif of helix 2B: its atomic structure and contribution to assembly. *J Mol Biol*, 298, 817-32.
- HESS, H. H., LEES, M. B. & DERR, J. E. 1978. A linear Lowry--Folin assay for both water-soluble and sodium dodecyl sulfate-solubilized proteins. *Anal Biochem*, 85, 295-300.
- HOFLAND, L. J., VAN KOETVELD, P., KOPER, J. W., DEN HOLDER, A. & LAMBERTS, S. W. 1987. Weak estrogenic activity of phenol red in the culture medium: its role in the study of the regulation of prolactin release in vitro. *Mol Cell Endocrinol*, 54, 43-50.
- HOHL, D., LICHTI, U., BREITKREUTZ, D., STEINERT, P. M. & ROOP, D. R. 1991. Transcription of the human loricrin gene in vitro is induced by calcium and cell density and suppressed by retinoic acid. *J Invest Dermatol*, 96, 414-8.
- HOLLE, A. W., KALAFAT, M., RAMOS, A. S., SEUFFERLEIN, T., KEMKEMER, R. & SPATZ, J. P. 2017. Intermediate filament reorganization dynamically influences cancer cell alignment and migration. *Sci Rep*, 7, 45152.
- HOMBERG, M., RAMMS, L., SCHWARZ, N., DREISSEN, G., LEUBE, R. E., MERKEL, R., HOFFMANN, B. & MAGIN, T. M. 2015. Distinct Impact of Two Keratin Mutations Causing Epidermolysis Bullosa Simplex on Keratinocyte Adhesion and Stiffness. *J Invest Dermatol*.
- HSIA, E., JOHNSTON, M. J., HOULDEN, R. J., CHERN, W. H. & HOFLAND, H. E. 2008. Effects of topically applied acitretin in reconstructed human epidermis and the rhino mouse. *J Invest Dermatol*, 128, 125-30.
- HUANG, Y. C., WANG, T. W., SUN, J. S. & LIN, F. H. 2006. Investigation of mitomycin-C-treated fibroblasts in 3-D collagen gel and conditioned medium for keratinocyte proliferation. *Artif Organs*, 30, 150-9.
- HYDER, C. L., PALLARI, H. M., KOCHIN, V. & ERIKSSON, J. E. 2008. Providing cellular signposts - Post-translational modifications of intermediate filaments. *Febs Letters*, 582, 2140-2148.
- INAGAKI, M., MATSUOKA, Y., TSUJIMURA, K., ANDO, S., TOKUI, T., TAKAHASHI, T. & INAGAKI, N. 1996. Dynamic property of intermediate filaments: Regulation by phosphorylation. *Bioessays*, 18, 481-487.
- IRIE, T., PARK, S. J., YAMASHITA, R., SEKI, M., YADA, T., SUGANO, S., NAKAI, K. & SUZUKI, Y. 2011. Predicting promoter activities of primary human DNA sequences. *Nucleic Acids Res*, 39, e75.
- JAYME, D. W. & SMITH, S. R. 2000. Media formulation options and manufacturing process controls to safeguard against introduction of

- animal origin contaminants in animal cell culture. *Cytotechnology*, 33, 27-36.
- JERABKOVA, B., MAREK, J., BUCKOVA, H., KOPECKOVA, L., VESELY, K., VALICKOVA, J., FAJKUS, J. & FAJKUSOVA, L. 2010. Keratin mutations in patients with epidermolysis bullosa simplex: correlations between phenotype severity and disturbance of intermediate filament molecular structure. *British Journal of Dermatology*, 162, 1004-1013.
- JHO, S. H., VOUTHOUNIS, C., LEE, B., STOJADINOVIC, O., IM, M. J., BREM, H., MERCHANT, A., CHAU, K. & TOMIC-CANIC, M. 2005. The book of opposites: the role of the nuclear receptor co-regulators in the suppression of epidermal genes by retinoic acid and thyroid hormone receptors. *J Invest Dermatol*, 124, 1034-43.
- JUVEN-GERSHON, T. & KADONAGA, J. T. 2010. Regulation of gene expression via the core promoter and the basal transcriptional machinery. *Dev Biol*, 339, 225-9.
- KAKUGUCHI, W., KITAMURA, T., KUROSHIMA, T., ISHIKAWA, M., KITAGAWA, Y., TOTSUKA, Y., SHINDOH, M. & HIGASHINO, F. 2010. HuR Knockdown Changes the Oncogenic Potential of Oral Cancer Cells. *Molecular Cancer Research*, 8, 520-528.
- KARANTZA, V. 2011a. Keratins in health and cancer: more than mere epithelial cell markers. *Oncogene*, 30, 127-138.
- KARANTZA, V. 2011b. Keratins in health and cancer: more than mere epithelial cell markers. *Oncogene*, 30, 127-38.
- KARLSSON, T., VAHLQUIST, A. & TORMA, H. 2010. Keratinocyte differentiation induced by calcium, phorbol ester or interferon-gamma elicits distinct changes in the retinoid signalling pathways. *J Dermatol Sci*, 57, 207-13.
- KARTASOVA, T., ROOP, D. R. & YUSPA, S. H. 1992. Relationship between the expression of differentiation-specific keratins 1 and 10 and cell proliferation in epidermal tumors. *Mol Carcinog*, 6, 18-25.
- KASAHARA, K., KARTASOVA, T., REN, X. Q., IKUTA, T., CHIDA, K. & KUROKI, T. 1993. Hyperphosphorylation of Keratins by Treatment with Okadaic Acid of Balb/Mk-2 Mouse Keratinocytes. *Journal of Biological Chemistry*, 268, 23531-23537.
- KHALIL, S., BARDAWIL, T., STEPHAN, C., DARWICHE, N., ABBAS, O., KIBBI, A. G., NEMER, G. & KURBAN, M. 2017. Retinoids: a journey from the molecular structures and mechanisms of action to clinical uses in dermatology and adverse effects. *J Dermatolog Treat*, 28, 684-696.
- KIM, H. J., CHOI, W. J. & LEE, C. H. 2015a. Phosphorylation and Reorganization of Keratin Networks: Implications for Carcinogenesis and Epithelial Mesenchymal Transition. *Biomol Ther (Seoul)*, 23, 301-12.
- KIM, K. H., CHUNG, W. S., KIM, Y., KIM, K. S., LEE, I. S., PARK, J. Y., JEONG, H. S., NA, Y. C., LEE, C. H. & JANG, H. J. 2015b. Transcriptomic Analysis Reveals Wound Healing of Morus alba Root Extract by Up-Regulating Keratin Filament and CXCL12/CXCR4 Signaling. *Phytother Res*, 29, 1251-8.
- KIM, S. & COULOMBE, P. A. 2007. Intermediate filament scaffolds fulfill mechanical, organizational, and signaling functions in the cytoplasm. *Genes Dev*, 21, 1581-97.
- KIM, S., WONG, P. & COULOMBE, P. A. 2006. A keratin cytoskeletal protein regulates protein synthesis and epithelial cell growth. *Nature*, 441, 362-5.

- KITANO, Y. 1985. Stability of retinoids in culture. All-trans-retinoic acid, 13-cis-retinoic acid and etretinate in the culture of human keratinocytes, B16 mouse melanoma cells and HeLa cells. *J Dermatol*, 12, 237-42.
- KOLLY, C., SUTER, M. M. & MULLER, E. J. 2005a. Proliferation, cell cycle exit, and onset of terminal differentiation in cultured keratinocytes: Pre-programmed pathways in control of c-Myc and Notch1 prevail over extracellular calcium signals. *Journal of Investigative Dermatology*, 124, 1014-1025.
- KOLLY, C., SUTER, M. M. & MÜLLER, E. J. 2005b. Proliferation, cell cycle exit, and onset of terminal differentiation in cultured keratinocytes: pre-programmed pathways in control of C-Myc and Notch1 prevail over extracellular calcium signals. *J Invest Dermatol*, 124, 1014-25.
- KOLSCH, A., WINDOFFER, R., WURFLINGER, T., AACH, T. & LEUBE, R. E. 2010. The keratin-filament cycle of assembly and disassembly. *J Cell Sci*, 123, 2266-72.
- KOPAN, R., TRASKA, G. & FUCHS, E. 1987. Retinoids as Important Regulators of Terminal Differentiation - Examining Keratin Expression in Individual Epidermal-Cells at Various Stages of Keratinization. *Journal of Cell Biology*, 105, 427-440.
- KOTANI, H., NEWTON, P. B., ZHANG, S., CHIANG, Y. L., OTTO, E., WEAVER, L., BLAESE, R. M., ANDERSON, W. F. & MCGARRITY, G. J. 1994. Improved methods of retroviral vector transduction and production for gene therapy. *Hum Gene Ther*, 5, 19-28.
- KRAMER, S. & MCLENNAN, A. G. 2018. The complex enzymology of mRNA decapping: Enzymes of four classes cleave pyrophosphate bonds. *Wiley Interdiscip Rev RNA*, e1511.
- KREGEL, K. C. 2002. Heat shock proteins: modifying factors in physiological stress responses and acquired thermotolerance. *J Appl Physiol (1985)*, 92, 2177-86.
- KU, N. O. & OMARY, M. B. 2006. A disease- and phosphorylation-related nonmechanical function for keratin 8. *J Cell Biol*, 174, 115-25.
- KUCHIPUDI, S. V., TELLABATI, M., NELLI, R. K., WHITE, G. A., PEREZ, B. B., SEBASTIAN, S., SLOMKA, M. J., BROOKES, S. M., BROWN, I. H., DUNHAM, S. P. & CHANG, K. C. 2012. 18S rRNA is a reliable normalisation gene for real time PCR based on influenza virus infected cells. *Virology Journal*, 9.
- KUZYK, A. & MAI, S. 2014. c-MYC-induced genomic instability. *Cold Spring Harb Perspect Med*, 4, a014373.
- KWAPISZ, M., BECKOUET, F. & THURIAUX, P. 2008. Early evolution of eukaryotic DNA-dependent RNA polymerases. *Trends in Genetics*, 24, 211-215.
- LAMB, R. & AMBLER, C. A. 2013. Keratinocytes Propagated in Serum-Free, Feeder-Free Culture Conditions Fail to Form Stratified Epidermis in a Reconstituted Skin Model. *Plos One*, 8.
- LAMERS, C. H., WILLEMSSEN, R. A., VAN ELZAKKER, P., VAN KRIMPEN, B. A., GRATAMA, J. W. & DEBETS, R. 2006. Phoenix-ampho outperforms PG13 as retroviral packaging cells to transduce human T cells with tumor-specific receptors: implications for clinical immunogene therapy of cancer. *Cancer Gene Ther*, 13, 503-9.
- LANDRY, J., BERNIER, D., CHRETIEN, P., NICOLE, L. M., TANGUAY, R. M. & MARCEAU, N. 1982. Synthesis and degradation of heat shock proteins



- during development and decay of thermotolerance. *Cancer Res*, 42, 2457-61.
- LANNEAU, D., BRUNET, M., FRISAN, E., SOLARY, E., FONTENAY, M. & GARRIDO, C. 2008. Heat shock proteins: essential proteins for apoptosis regulation. *J Cell Mol Med*, 12, 743-61.
- LEE, D. D., STOJADINOVIC, O., KRZYZANOWSKA, A., VOUTHOUNIS, C., BLUMENBERG, M. & TOMIC-CANIC, M. 2009. Retinoid-responsive transcriptional changes in epidermal keratinocytes. *J Cell Physiol*, 220, 427-39.
- LEE, D. D., ZAVADIL, J., TOMIC-CANIC, M. & BLUMENBERG, M. 2010. Comprehensive transcriptional profiling of human epidermis, reconstituted epidermal equivalents, and cultured keratinocytes using DNA microarray chips. *Methods Mol Biol*, 585, 193-223.
- LEE, T. H., BU, J., KIM, B. H., POELLMANN, M. J., HONG, S. & HYUN, S. H. 2019. Sub-lethal hyperthermia promotes epithelial-to-mesenchymal-like transition of breast cancer cells: implication of the synergy between hyperthermia and chemotherapy. *Rsc Advances*, 9, 52-57.
- LEE, Y. S., YUSPA, S. H. & DLUGOSZ, A. A. 1998a. Differentiation of cultured human epidermal keratinocytes at high cell densities is mediated by endogenous activation of the protein kinase C signaling pathway. *Journal of Investigative Dermatology*, 111, 762-766.
- LEE, Y. S., YUSPA, S. H. & DLUGOSZ, A. A. 1998b. Differentiation of cultured human epidermal keratinocytes at high cell densities is mediated by endogenous activation of the protein kinase C signaling pathway. *J Invest Dermatol*, 111, 762-6.
- LEFEBVRE, P., MARTIN, P. J., FLAJOLLET, S., DEDIEU, S., BILLAUT, X. & LEFEBVRE, B. 2005. Transcriptional activities of retinoic acid receptors. *Vitam Horm*, 70, 199-264.
- LESZCZYNIECKA, M., ROBERTS, T., DENT, P., GRANT, S. & FISHER, P. B. 2001. Differentiation therapy of human cancer: basic science and clinical applications. *Pharmacol Ther*, 90, 105-56.
- LETAI, A., COULOMBE, P. A., MCCORMICK, M. B., YU, Q. C., HUTTON, E. & FUCHS, E. 1993. Disease Severity Correlates with Position of Keratin Point Mutations in Patients with Epidermolysis-Bullosa Simplex. *Proceedings of the National Academy of Sciences of the United States of America*, 90, 3197-3201.
- LEUBE, R. E., MOCH, M., KOLSCH, A. & WINDOFFER, R. 2011. "Panta rhei": Perpetual cycling of the keratin cytoskeleton. *Bioarchitecture*, 1, 39-44.
- LIAO, J., KU, N. O. & OMARY, M. B. 1997. Stress, apoptosis, and mitosis induce phosphorylation of human keratin 8 at Ser-73 in tissues and cultured cells. *J Biol Chem*, 272, 17565-73.
- LICHTI, U. & YUSPA, S. H. 1988a. Modulation of tissue and epidermal transglutaminases in mouse epidermal cells after treatment with 12-O-tetradecanoylphorbol-13-acetate and/or retinoic acid in vivo and in culture. *Cancer Res*, 48, 74-81.
- LICHTI, U. & YUSPA, S. H. 1988b. Modulation of Tissue and Epidermal Transglutaminases in Mouse Epidermal-Cells after Treatment with 12-O-Tetradecanoylphorbol-13-Acetate and or Retinoic Acid Invivo and in Culture. *Cancer Research*, 48, 74-81.
- LIU, H., LUO, M. & WEN, J. K. 2014. mRNA stability in the nucleus. *J Zhejiang Univ Sci B*, 15, 444-54.

- LIU, X., ORY, V., CHAPMAN, S., YUAN, H., ALBANESE, C., KALLAKURY, B., TIMOFEEVA, O. A., NEALON, C., DAKIC, A., SIMIC, V., HADDAD, B. R., RHIM, J. S., DRITSCHILO, A., RIEGEL, A., MCBRIDE, A. & SCHLEGEL, R. 2012. ROCK inhibitor and feeder cells induce the conditional reprogramming of epithelial cells. *Am J Pathol*, 180, 599-607.
- LOWRY, O. H., ROSENBROUGH, N. J., FARR, A. L. & RANDALL, R. J. 1951. Protein measurement with the Folin phenol reagent. *J Biol Chem*, 193, 265-75.
- MACHESNEY, M., TIDMAN, N., WASEEM, A., KIRBY, L. & LEIGH, I. 1998. Activated keratinocytes in the epidermis of hypertrophic scars. *Am J Pathol*, 152, 1133-41.
- MACKINDER, M. A., EVANS, C. A., CHOWDRY, J., STATON, C. A. & CORFE, B. M. 2012. Alteration in composition of keratin intermediate filaments in a model of breast cancer progression and the potential to reverse hallmarks of metastasis. *Cancer Biomark*, 12, 49-64.
- MADISON, K. C. 2003. Barrier function of the skin: "la raison d'etre" of the epidermis. *J Invest Dermatol*, 121, 231-41.
- MAGIN, T. M., VIJAYARAJ, P. & LEUBE, R. E. 2007. Structural and regulatory functions of keratins. *Exp Cell Res*, 313, 2021-32.
- MARAIA, R. J. & ARIMBASSERI, A. G. 2017. Factors That Shape Eukaryotic tRNAomes: Processing, Modification and Anticodon-Codon Use. *Biomolecules*, 7.
- MARGOLIS, S. S., PERRY, J. A., FORESTER, C. M., NUTT, L. K., GUO, Y., JARDIM, M. J., THOMENIUS, M. J., FREEL, C. D., DARBANDI, R., AHN, J. H., ARROYO, J. D., WANG, X. F., SHENOLIKAR, S., NAIRN, A. C., DUNPHY, W. G., HAHN, W. C., VIRSHUP, D. M. & KORNBLUTH, S. 2006. Role for the PP2A/B56delta phosphatase in regulating 14-3-3 release from Cdc25 to control mitosis. *Cell*, 127, 759-73.
- MARGULIS, A., ZHANG, W. & GARLICK, J. A. 2005. In vitro fabrication of engineered human skin. *Methods Mol Biol*, 289, 61-70.
- MARVIN, K. W., GEORGE, M. D., FUJIMOTO, W., SAUNDERS, N. A., BERNACKI, S. H. & JETTEN, A. M. 1992. Cornifin, a Cross-Linked Envelope Precursor in Keratinocytes That Is down-Regulated by Retinoids. *Proceedings of the National Academy of Sciences of the United States of America*, 89, 11026-11030.
- MASTERS, J. R. & STACEY, G. N. 2007. Changing medium and passaging cell lines. *Nat Protoc*, 2, 2276-84.
- MATSUI, M. S., CHEW, S. L. & DELEO, V. A. 1992. Protein kinase C in normal human epidermal keratinocytes during proliferation and calcium-induced differentiation. *J Invest Dermatol*, 99, 565-71.
- MCLEAN, W. H. & MOORE, C. B. 2011. Keratin disorders: from gene to therapy. *Hum Mol Genet*, 20, R189-97.
- MERLO, S., FRASCA, G., CANONICO, P. L. & SORTINO, M. A. 2009. Differential involvement of estrogen receptor alpha and estrogen receptor beta in the healing promoting effect of estrogen in human keratinocytes. *J Endocrinol*, 200, 189-97.
- MERRICK, D. T., GOWN, A. M., HALBERT, C. L., BLANTON, R. A. & MCDUGALL, J. K. 1993. Human papillomavirus-immortalized keratinocytes are resistant to the effects of retinoic acid on terminal differentiation. *Cell Growth Differ*, 4, 831-40.
- MILLER, D. M., THOMAS, S. D., ISLAM, A., MUENCH, D. & SEDORIS, K. 2012. c-Myc and cancer metabolism. *Clin Cancer Res*, 18, 5546-53.

- MILLER, R. K., KHUON, S. & GOLDMAN, R. D. 1993a. Dynamics of Keratin Assembly - Exogenous Type-I Keratin Rapidly Associates with Type-II Keratin in-Vivo. *Journal of Cell Biology*, 122, 123-135.
- MILLER, R. K., KHUON, S. & GOLDMAN, R. D. 1993b. Dynamics of keratin assembly: exogenous type I keratin rapidly associates with type II keratin in vivo. *J Cell Biol*, 122, 123-35.
- MILLER, R. K., VIKSTROM, K. & GOLDMAN, R. D. 1991. Keratin Incorporation into Intermediate Filament Networks Is a Rapid Process. *Journal of Cell Biology*, 113, 843-855.
- MIZZEN, L. A. & WELCH, W. J. 1988. Characterization of the thermotolerant cell. I. Effects on protein synthesis activity and the regulation of heat-shock protein 70 expression. *J Cell Biol*, 106, 1105-16.
- MOLL, R., DIVO, M. & LANGBEIN, L. 2008. The human keratins: biology and pathology. *Histochem Cell Biol*, 129, 705-33.
- MOLL, R., FRANKE, W. W., SCHILLER, D. L., GEIGER, B. & KREPLER, R. 1982. The Catalog of Human Cytokeratins - Patterns of Expression in Normal Epithelia, Tumors and Cultured-Cells. *Cell*, 31, 11-24.
- MORIMOTO, R. I. 1993. Cells in stress: transcriptional activation of heat shock genes. *Science*, 259, 1409-10.
- MORLEY, S. M., D'ALESSANDRO, M., SEXTON, C., RUGG, E. L., NAVSARIA, H., SHEMANKO, C. S., HUBER, M., HOHL, D., HEAGERTY, A. I., LEIGH, I. M. & LANE, E. B. 2003. Generation and characterization of epidermolysis bullosa simplex cell lines: scratch assays show faster migration with disruptive keratin mutations. *Br J Dermatol*, 149, 46-58.
- MORLEY, S. M., DUNDAS, S. R., JAMES, J. L., GUPTA, T., BROWN, R. A., SEXTON, C. J., NAVSARIA, H. A., LEIGH, I. M. & LANE, E. B. 1995. Temperature sensitivity of the keratin cytoskeleton and delayed spreading of keratinocyte lines derived from EBS patients. *J Cell Sci*, 108 ( Pt 11), 3463-71.
- NAPOLI, J. L. 1986. Quantification of physiological levels of retinoic acid. *Methods Enzymol*, 123, 112-24.
- NEWBURY, S. F. 2006. Control of mRNA stability in eukaryotes. *Biochem Soc Trans*, 34, 30-4.
- NEWTON, A. C. 2010a. Protein kinase C: poised to signal. *American Journal of Physiology-Endocrinology and Metabolism*, 298, E395-E402.
- NEWTON, A. C. 2010b. Protein kinase C: poised to signal. *Am J Physiol Endocrinol Metab*, 298, E395-402.
- OH, J. W., HSI, T. C., GUERRERO-JUAREZ, C. F., RAMOS, R. & PLIKUS, M. V. 2013. Organotypic skin culture. *J Invest Dermatol*, 133, 1-4.
- OKAZAKI, M., YOSHIMURA, K., SUZUKI, Y. & HARII, K. 2003. Effects of subepithelial fibroblasts on epithelial differentiation in human skin and oral mucosa: heterotypically recombined organotypic culture model. *Plast Reconstr Surg*, 112, 784-92.
- OMARY, M. B. 2009. "IF-pathies": a broad spectrum of intermediate filament-associated diseases. *J Clin Invest*, 119, 1756-62.
- OMARY, M. B., KU, N. O., LIAO, J. & PRICE, D. 1998. Keratin modifications and solubility properties in epithelial cells and in vitro. *Subcell Biochem*, 31, 105-40.
- OMARY, M. B., KU, N. O., TAO, G. Z., TOIVOLA, D. M. & LIAO, J. 2006. "Heads and tails" of intermediate filament phosphorylation: multiple sites and functional insights. *Trends Biochem Sci*, 31, 383-94.

- OWENS, D. W. & LANE, E. B. 2004. Keratin mutations and intestinal pathology. *Journal of Pathology*, 204, 377-385.
- PALAZZO, E., KELLETT, M. D., CATAISSON, C., BIBLE, P. W., BHATTACHARYA, S., SUN, H. W., GORMLEY, A. C., YUSPA, S. H. & MORASSO, M. I. 2017. A novel DLX3-PKC integrated signaling network drives keratinocyte differentiation. *Cell Death Differ*, 24, 717-730.
- PAN, X., HOBBS, R. P. & COULOMBE, P. A. 2013. The expanding significance of keratin intermediate filaments in normal and diseased epithelia. *Curr Opin Cell Biol*, 25, 47-56.
- PAPP, H., CZIFRA, G., LAZAR, J., GONCZI, M., CSERNOCH, L., KOVACS, L. & BIRO, T. 2003. Protein kinase C isozymes regulate proliferation and high cell density-mediated differentiation in HaCaT keratinocytes. *Exp Dermatol*, 12, 811-24.
- PARAMIO, J. M. 1999. A role for phosphorylation in the dynamics of keratin intermediate filaments. *Eur J Cell Biol*, 78, 33-43.
- PARENTEAU, N. L., BILBO, P., NOLTE, C. J., MASON, V. S. & ROSENBERG, M. 1992. The organotypic culture of human skin keratinocytes and fibroblasts to achieve form and function. *Cytotechnology*, 9, 163-71.
- PARK, K. 2015. Role of micronutrients in skin health and function. *Biomol Ther (Seoul)*, 23, 207-17.
- PAUL, A., WILSON, S., BELHAM, C. M., ROBINSON, C. J., SCOTT, P. H., GOULD, G. W. & PLEVIN, R. 1997. Stress-activated protein kinases: activation, regulation and function. *Cell Signal*, 9, 403-10.
- PEKNY, M. & LANE, E. B. 2007. Intermediate filaments and stress. *Exp Cell Res*, 313, 2244-54.
- PERZELOVA, V., SABOL, F., VASILENKO, T., NOVOTNY, M., KOVAC, I., SLEZAK, M., DURKAC, J., HOLLY, M., PILATOVA, M., SZABO, P., VARINSKA, L., CRIEPOKOVA, Z., KUCERA, T., KALTNER, H., ANDRE, S., GABIUS, H. J., MUCAJI, P., SMETANA, K., JR. & GAL, P. 2016. Pharmacological activation of estrogen receptors-alpha and -beta differentially modulates keratinocyte differentiation with functional impact on wound healing. *Int J Mol Med*, 37, 21-8.
- PILLAI, S., BIKLE, D. D., MANCIANTI, M. L., CLINE, P. & HINCENBERGS, M. 1990. Calcium regulation of growth and differentiation of normal human keratinocytes: modulation of differentiation competence by stages of growth and extracellular calcium. *J Cell Physiol*, 143, 294-302.
- PITTENGER, J. T., HESS, J. F. & FITZGERALD, P. G. 2007. Identifying the role of specific motifs in the lens fiber cell specific intermediate filament phakosin. *Invest Ophthalmol Vis Sci*, 48, 5132-41.
- POUMAY, Y. & PITTELKOW, M. R. 1995. Cell density and culture factors regulate keratinocyte commitment to differentiation and expression of suprabasal K1/K10 keratins. *J Invest Dermatol*, 104, 271-6.
- PRESLAND, R. B. & DALE, B. A. 2000. Epithelial structural proteins of the skin and oral cavity: function in health and disease. *Crit Rev Oral Biol Med*, 11, 383-408.
- PRESLAND, R. B. & JUREVIC, R. J. 2002. Making sense of the epithelial barrier: what molecular biology and genetics tell us about the functions of oral mucosal and epidermal tissues. *J Dent Educ*, 66, 564-74.
- QADIR, F., AZIZ, M. A., SARI, C. P., MA, H., DAI, H., WANG, X., RAITHATHA, D., DA SILVA, L. G. L., HUSSAIN, M., POORKASREIY, S. P., HUTCHISON, I. L., WASEEM, A. & TEH, M.-T. 2018. Transcriptome

- reprogramming by cancer exosomes: identification of novel molecular targets in matrix and immune modulation. *Molecular Cancer*, 17, 97.
- RAMOT, Y., PAUS, R., TIEDE, S. & ZLOTOGORSKI, A. 2009. Endocrine controls of keratin expression. *Bioessays*, 31, 389-99.
- RANDOLPH, R. K. & SIMON, M. 1997. Metabolism of all-trans-retinoic acid by cultured human epidermal keratinocytes. *J Lipid Res*, 38, 1374-83.
- RAO, R. S., PATIL, S. & GANAVI, B. S. 2014. Oral cytokeratins in health and disease. *J Contemp Dent Pract*, 15, 127-36.
- RHEINWALD, J. G. & GREEN, H. 1975. Serial cultivation of strains of human epidermal keratinocytes: the formation of keratinizing colonies from single cells. *Cell*, 6, 331-43.
- RHEINWALD, J. G. & GREEN, H. 1977. Epidermal growth factor and the multiplication of cultured human epidermal keratinocytes. *Nature*, 265, 421-4.
- ROSENTHAL, D. S., GRIFFITHS, C. E., YUSPA, S. H., ROOP, D. R. & VOORHEES, J. J. 1992. Acute or chronic topical retinoic acid treatment of human skin in vivo alters the expression of epidermal transglutaminase, loricrin, involucrin, filaggrin, and keratins 6 and 13 but not keratins 1, 10, and 14. *J Invest Dermatol*, 98, 343-50.
- ROSENTHAL, D. S., ROOP, D. R., HUFF, C. A., WEISS, J. S., ELLIS, C. N., HAMILTON, T., VOORHEES, J. J. & YUSPA, S. H. 1990. Changes in photo-aged human skin following topical application of all-trans retinoic acid. *J Invest Dermatol*, 95, 510-5.
- ROTHNAGEL, J. A., FISHER, M. P., AXTELL, S. M., PITTELKOW, M. R., ANTON-LAMPRECHT, I., HUBER, M., HOHL, D. & ROOP, D. R. 1993. A mutational hot spot in keratin 10 (KRT 10) in patients with epidermolytic hyperkeratosis. *Hum Mol Genet*, 2, 2147-50.
- ROUSE, J., COHEN, P., TRIGON, S., MORANGE, M., ALONSO-LLAMAZARES, A., ZAMANILLO, D., HUNT, T. & NEBREDA, A. R. 1994. A novel kinase cascade triggered by stress and heat shock that stimulates MAPKAP kinase-2 and phosphorylation of the small heat shock proteins. *Cell*, 78, 1027-37.
- SANTOS, M., PARAMIO, J. M., BRAVO, A., RAMIREZ, A. & JORCANO, J. L. 2002. The expression of keratin k10 in the basal layer of the epidermis inhibits cell proliferation and prevents skin tumorigenesis. *J Biol Chem*, 277, 19122-30.
- SCHAEFFER, D., TSANOVA, B., BARBAS, A., REIS, F. P., DASTIDAR, E. G., SANCHEZ-ROTUNNO, M., ARRAIANO, C. M. & VAN HOOFF, A. 2009. The exosome contains domains with specific endoribonuclease, exoribonuclease and cytoplasmic mRNA decay activities. *Febs Journal*, 276, 218-219.
- SCHULE, R., RANGARAJAN, P., YANG, N., KLIEWER, S., RANSONE, L. J., BOLADO, J., VERMA, I. M. & EVANS, R. M. 1991. Retinoic Acid Is a Negative Regulator of Ap-1-Responsive Genes. *Proceedings of the National Academy of Sciences of the United States of America*, 88, 6092-6096.
- SCHUTTE, B., HENFLING, M., KOLGEN, W., BOUMAN, M., MEEX, S., LEERS, M. P., NAP, M., BJORKLUND, V., BJORKLUND, P., BJORKLUND, B., LANE, E. B., OMARY, M. B., JORNVALL, H. & RAMAEKERS, F. C. 2004. Keratin 8/18 breakdown and reorganization during apoptosis. *Exp Cell Res*, 297, 11-26.

- SCHWEIZER, J., BOWDEN, P. E., COULOMBE, P. A., LANGBEIN, L., LANE, E. B., MAGIN, T. M., MALTAIS, L., OMARY, M. B., PARRY, D. A., ROGERS, M. A. & WRIGHT, M. W. 2006. New consensus nomenclature for mammalian keratins. *J Cell Biol*, 174, 169-74.
- SEFTON, B. M. & SHENOLIKAR, S. 2001. Overview of protein phosphorylation. *Curr Protoc Protein Sci*, Chapter 13, Unit13 1.
- SEXTON, C. J., PROBY, C. M., BANKS, L., STABLES, J. N., POWELL, K., NAVSARIA, H. & LEIGH, I. M. 1993. Characterization of factors involved in human papillomavirus type 16-mediated immortalization of oral keratinocytes. *J Gen Virol*, 74 ( Pt 4), 755-61.
- SHAROW, K. A., TEMKIN, B. & ASSON-BATRES, M. A. 2012. Retinoic acid stability in stem cell cultures. *International Journal of Developmental Biology*, 56, 273-278.
- SHAW, G. & KAMEN, R. 1986. A Conserved Au Sequence from the 3' Untranslated Region of Gm-Csf Messenger-Rna Mediates Selective Messenger-Rna Degradation. *Cell*, 46, 659-667.
- SHENG, S., BARNETT, D. H. & KATZENELLENBOGEN, B. S. 2008. Differential estradiol and selective estrogen receptor modulator (SERM) regulation of Keratin 13 gene expression and its underlying mechanism in breast cancer cells. *Mol Cell Endocrinol*, 296, 1-9.
- SHETTY, S. & GOKUL, S. 2012. Keratinization and its disorders. *Oman Med J*, 27, 348-57.
- SHYY, T. T., ASCH, B. B. & ASCH, H. L. 1989. Concurrent collapse of keratin filaments, aggregation of organelles, and inhibition of protein synthesis during the heat shock response in mammary epithelial cells. *J Cell Biol*, 108, 997-1008.
- SIKORA, M. J., JOHNSON, M. D., LEE, A. V. & OESTERREICH, S. 2016. Endocrine Response Phenotypes Are Altered by Charcoal-Stripped Serum Variability. *Endocrinology*, 157, 3760-3766.
- SIMONS, M. & RAPOSO, G. 2009. Exosomes - vesicular carriers for intercellular communication. *Current Opinion in Cell Biology*, 21, 575-581.
- SMITS, J. P. H., NIEHUES, H., RIKKEN, G., VAN VLIJMEN-WILLEMS, I., VAN DE ZANDE, G., ZEEUWEN, P., SCHALKWIJK, J. & VAN DEN BOGAARD, E. H. 2017. Immortalized N/TERT keratinocytes as an alternative cell source in 3D human epidermal models. *Sci Rep*, 7, 11838.
- SNIDER, N. T. & OMARY, M. B. 2014. Post-translational modifications of intermediate filament proteins: mechanisms and functions. *Nat Rev Mol Cell Biol*, 15, 163-77.
- SNIDER, N. T. & OMARY, M. B. 2016. Assays for Posttranslational Modifications of Intermediate Filament Proteins. *Methods Enzymol*, 568, 113-38.
- SORENSEN, S., SOLVSTEN, H., POLITI, Y. & KRAGBALLE, K. 1997. Effects of vitamin D3 on keratinocyte proliferation and differentiation in vitro: modulation by ligands for retinoic acid and retinoid X receptors. *Skin Pharmacol*, 10, 144-52.
- SQUIER, C. A. & KREMER, M. J. 2001. Biology of oral mucosa and esophagus. *J Natl Cancer Inst Monogr*, 7-15.
- STASIAK, P. C. & LANE, E. B. 1987. Sequence of Cdna Coding for Human Keratin-19. *Nucleic Acids Research*, 15, 10058-10058.
- STRELKOV, S. V., HERRMANN, H., GEISLER, N., WEDIG, T., ZIMBELMANN, R., AEBI, U. & BURKHARD, P. 2002. Conserved segments 1A and 2B of the intermediate filament dimer: their atomic structures and role in filament assembly. *Embo Journal*, 21, 1255-1266.

- STRNAD, P., STUMPTNER, C., ZATLOUKAL, K. & DENK, H. 2008. Intermediate filament cytoskeleton of the liver in health and disease. *Histochemistry and Cell Biology*, 129, 735-749.
- STRNAD, P., WINDOFFER, R. & LEUBE, R. E. 2001. In vivo detection of cytokeratin filament network breakdown in cells treated with the phosphatase inhibitor okadaic acid. *Cell Tissue Res*, 306, 277-93.
- STRNAD, P., WINDOFFER, R. & LEUBE, R. E. 2003. Light-induced resistance of the keratin network to the filament-disrupting tyrosine phosphatase inhibitor orthovanadate. *J Invest Dermatol*, 120, 198-203.
- SUZAN, R. & SANDER, V. D. H. 2016. Coordinating cell proliferation and differentiation: Antagonism between cell cycle regulators and cell type-specific gene expression.
- SVENDSEN, M. L., DANEELS, G., GEYSEN, J., BINDERUP, L. & KRAGBALLE, K. 1997a. Proliferation and differentiation of cultured human keratinocytes is modulated by 1,25(OH)2D3 and synthetic vitamin D3 analogues in a cell density-, calcium- and serum-dependent manner. *Pharmacol Toxicol*, 80, 49-56.
- SVENDSEN, M. L., DANEELS, G., GEYSEN, J., BINDERUP, L. & KRAGBALLE, K. 1997b. Proliferation and differentiation of cultured human keratinocytes is modulated by 1,25(OH)(2)D-3 and synthetic vitamin D-3 analogues in a cell density-, calcium- and serum-dependent manner. *Pharmacology & Toxicology*, 80, 49-56.
- SWIFT, S., LORENS, J., ACHACOSO, P. & NOLAN, G. P. 2001. Rapid production of retroviruses for efficient gene delivery to mammalian cells using 293T cell-based systems. *Curr Protoc Immunol*, Chapter 10, Unit 10 17C.
- TAKUMA, T., ICHIDA, T., OKUMURA, K. & KANAZAWA, M. 1993. Protein phosphatase inhibitor calyculin A induces hyperphosphorylation of cytokeratins and inhibits amylase exocytosis in the rat parotid acini. *FEBS Lett*, 323, 145-50.
- TALWAR, S., BALASUBRAMANIAN, S., SUNDARAMURTHY, S., HOUSE, R., WILUSZ, C. J., KUPPUSWAMY, D., D'SILVA, N., GILLESPIE, M. B., HILL, E. G. & PALANISAMY, V. 2013. Overexpression of RNA-binding protein CELF1 prevents apoptosis and destabilizes pro-apoptotic mRNAs in oral cancer cells. *Rna Biology*, 10, 277-286.
- TAYLOR, W. R. 2006. Transcription and translation in an RNA world. *Philos Trans R Soc Lond B Biol Sci*, 361, 1751-60.
- TAYLOR-PAPADIMITRIOU, J., STAMPFER, M., BARTEK, J., LEWIS, A., BOSHELL, M., LANE, E. B. & LEIGH, I. M. 1989. Keratin expression in human mammary epithelial cells cultured from normal and malignant tissue: relation to in vivo phenotypes and influence of medium. *J Cell Sci*, 94 ( Pt 3), 403-13.
- TELLMANN, G. 2006. The E-Method: a highly accurate technique for gene-expression analysis. *Nature Methods*, 3.
- TOIVOLA, D. M., GOLDMAN, R. D., GARROD, D. R. & ERIKSSON, J. E. 1997. Protein phosphatases maintain the organization and structural interactions of hepatic keratin intermediate filaments. *Journal of Cell Science*, 110, 23-33.
- TOIVOLA, D. M., STRNAD, P., HABTEZION, A. & OMARY, M. B. 2010. Intermediate filaments take the heat as stress proteins. *Trends in Cell Biology*, 20, 79-91.

- TOIVOLA, D. M., ZHOU, Q., ENGLISH, L. S. & OMARY, M. B. 2002. Type II keratins are phosphorylated on a unique motif during stress and mitosis in tissues and cultured cells. *Mol Biol Cell*, 13, 1857-70.
- TORMA, H. 2011. Regulation of keratin expression by retinoids. *Dermatoendocrinol*, 3, 136-40.
- TRASK, D. K., BAND, V., ZAJCHOWSKI, D. A., YASWEN, P., SUH, T. & SAGER, R. 1990. Keratins as Markers That Distinguish Normal and Tumor-Derived Mammary Epithelial-Cells. *Proceedings of the National Academy of Sciences of the United States of America*, 87, 2319-2323.
- VAN DRONGELEN, V., DANSO, M. O., MULDER, A., MIEREMET, A., VAN SMEDEN, J., BOUWSTRA, J. A. & EL GHALBZOURI, A. 2014. Barrier properties of an N/TERT-based human skin equivalent. *Tissue Eng Part A*, 20, 3041-9.
- VIRTANEN, M., TORMA, H. & VAHLQUIST, A. 2000. Keratin 4 upregulation by retinoic acid in vivo: a sensitive marker for retinoid bioactivity in human epidermis. *J Invest Dermatol*, 114, 487-93.
- WADA, T. & BECSKEI, A. 2017. Impact of Methods on the Measurement of mRNA Turnover. *Int J Mol Sci*, 18.
- WADE, E. J., KLUCHER, K. M. & SPECTOR, D. H. 1992. An AP-1 binding site is the predominant cis-acting regulatory element in the 1.2-kilobase early RNA promoter of human cytomegalovirus. *J Virol*, 66, 2407-17.
- WANG, F., ZIEMAN, A. & COULOMBE, P. A. 2016. Skin Keratins. *Methods Enzymol*, 568, 303-50.
- WASEEM, A., DOGAN, B., TIDMAN, N., ALAM, Y., PURKIS, P., JACKSON, S., LALLI, A., MACHESNEY, M. & LEIGH, I. M. 1999. Keratin 15 expression in stratified epithelia: downregulation in activated keratinocytes. *J Invest Dermatol*, 112, 362-9.
- WASEEM, A., GOUGH, A. C., SPURR, N. K. & LANE, E. B. 1990. Localization of the gene for human simple epithelial keratin 18 to chromosome 12 using polymerase chain reaction. *Genomics*, 7, 188-94.
- WASEEM, A., WHITE, K. & WASEEM, N. H. 1997. Identification of a novel keratin epitope: evidence for association between non-helical sub-domains L12 during filament assembly. *Int J Biochem Cell Biol*, 29, 971-83.
- WAUTERS, C. C. A. P., SMEDTS, F., GERRITS, L. G. M., BOSMAN, F. T. & RAMAEKERS, F. C. S. 1995. Keratin-7 and Keratin-20 as Diagnostic Markers of Carcinomas Metastatic to the Ovary. *Human Pathology*, 26, 852-855.
- WELCH, W. J. & MIZZEN, L. A. 1988. Characterization of the Thermotolerant Cell .2. Effects on the Intracellular-Distribution of Heat-Shock Protein-70, Intermediate Filaments, and Small Nuclear Ribonucleoprotein Complexes. *Journal of Cell Biology*, 106, 1117-1130.
- WELSHONS, W. V., WOLF, M. F., MURPHY, C. S. & JORDAN, V. C. 1988. Estrogenic activity of phenol red. *Mol Cell Endocrinol*, 57, 169-78.
- WILLE, J. J., JR., PITTELKOW, M. R., SHIPLEY, G. D. & SCOTT, R. E. 1984. Integrated control of growth and differentiation of normal human prokeratinocytes cultured in serum-free medium: clonal analyses, growth kinetics, and cell cycle studies. *J Cell Physiol*, 121, 31-44.
- WILSON, A. K., COULOMBE, P. A. & FUCHS, E. 1992. The roles of K5 and K14 head, tail, and R/K L L E G E domains in keratin filament assembly in vitro. *J Cell Biol*, 119, 401-14.
- WILSON, V. G. 2014. Growth and differentiation of HaCaT keratinocytes. *Methods Mol Biol*, 1195, 33-41.



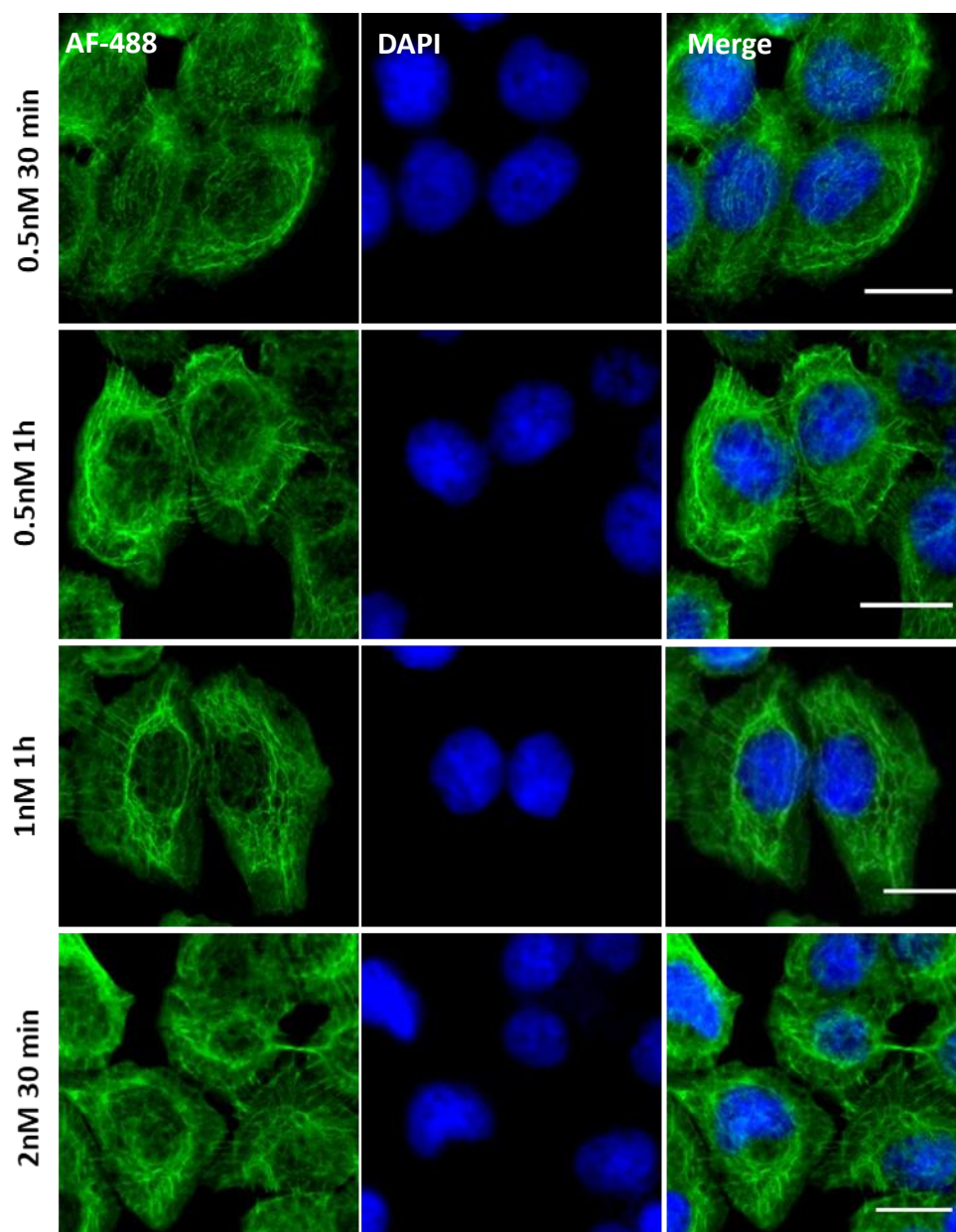
- WINDOFFER, R., BEIL, M., MAGIN, T. M. & LEUBE, R. E. 2011. Cytoskeleton in motion: the dynamics of keratin intermediate filaments in epithelia. *J Cell Biol*, 194, 669-78.
- WINDOFFER, R. & LEUBE, R. E. 1999. Detection of cytokeratin dynamics by time-lapse fluorescence microscopy in living cells. *J Cell Sci*, 112 ( Pt 24), 4521-34.
- WINDOFFER, R. & LEUBE, R. E. 2001. De novo formation of cytokeratin filament networks originates from the cell cortex in A-431 cells. *Cell Motil Cytoskeleton*, 50, 33-44.
- WINDOFFER, R. & LEUBE, R. E. 2004. Imaging of keratin dynamics during the cell cycle and in response to phosphatase inhibition. *Methods Cell Biol*, 78, 321-52.
- WINDOFFER, R., WOLL, S., STRNAD, P. & LEUBE, R. E. 2004. Identification of novel principles of keratin filament network turnover in living cells. *Mol Biol Cell*, 15, 2436-48.
- WOLL, S., WINDOFFER, R. & LEUBE, R. E. 2007. p38 MAPK-dependent shaping of the keratin cytoskeleton in cultured cells. *J Cell Biol*, 177, 795-807.
- WU, K. C., BRYAN, J. T., MORASSO, M. I., JANG, S. I., LEE, J. H., YANG, J. M., MAREKOV, L. N., PARRY, D. A. D. & STEINERT, P. M. 2000. Coiled-coil trigger motifs in the 1B and 2B rod domain segments are required for the stability of keratin intermediate filaments. *Molecular Biology of the Cell*, 11, 3539-3558.
- WU, X. & BREWER, G. 2012. The regulation of mRNA stability in mammalian cells: 2.0. *Gene*, 500, 10-21.
- YAMAGUCHI, H., WYCKOFF, J. & CONDEELIS, J. 2005. Cell migration in tumors. *Curr Opin Cell Biol*, 17, 559-64.
- YATSUNAMI, J., KOMORI, A., OHTA, T., SUGANUMA, M., YUSPA, S. H. & FUJIKI, H. 1993. Hyperphosphorylation of cytokeratins by okadaic acid class tumor promoters in primary human keratinocytes. *Cancer Res*, 53, 992-6.
- YUN, C. & DASGUPTA, R. 2014. Luciferase reporter assay in *Drosophila* and mammalian tissue culture cells. *Curr Protoc Chem Biol*, 6, 7-23.
- YUSPA, S. H., KILKENNY, A. E., STEINERT, P. M. & ROOP, D. R. 1989. Expression of murine epidermal differentiation markers is tightly regulated by restricted extracellular calcium concentrations in vitro. *J Cell Biol*, 109, 1207-17.
- ZHENG, X., BAKER, H., HANCOCK, W. S., FAWAZ, F., MCCAMAN, M. & PUNGOR, E., JR. 2006. Proteomic analysis for the assessment of different lots of fetal bovine serum as a raw material for cell culture. Part IV. Application of proteomics to the manufacture of biological drugs. *Biotechnol Prog*, 22, 1294-300.

## Appendix

### A.1. Supplementary results.

Supplementary Figures for results in chapter 3 and chapter 4 are shown in section

A.1 supplementary results.



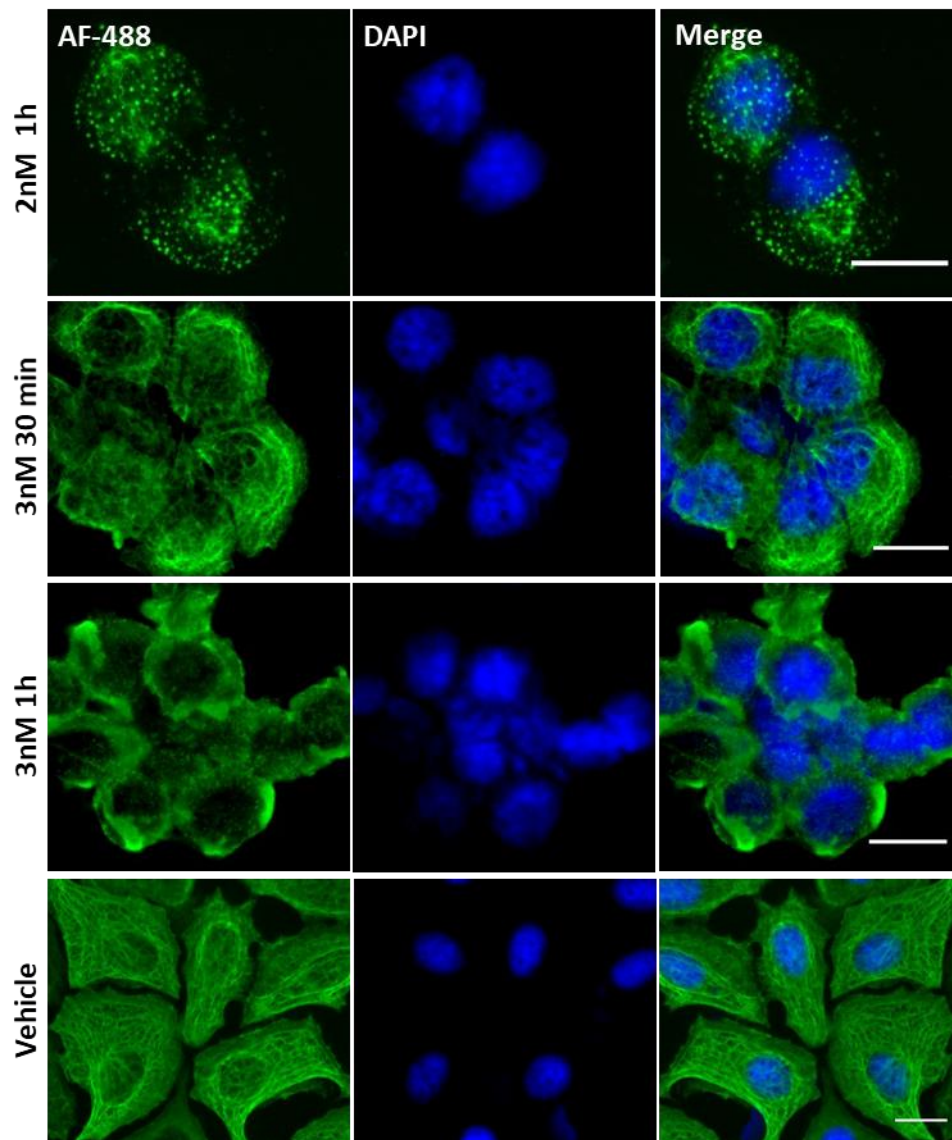


**Figure A. 1. Optimisations of CL-A treatment concentrations in MCF-7 cells.** Cells were grown in full DMEM (10% FCS and 1% PS), next day treated with different concentrations of CL-A for different time points to optimise the concentration and time point at which filaments breakdown into globules while cells are still intact. 2nM for 1 hour was the optimum concentration that was used in later experiments. DMF treated cells for up to 1 hour are shown as a vehicle control. All cells were immunostained with LE65 and Alexa Flour® 488-labelled anti-mouse secondary antibody. Cells counter stained with DAPI in blue and overlapping of immunostaining with DAPI is shown as Merge. Leica Epi-fluorescence microscope model DM5000 and DFC350 camera were used for recording pictures. (Scale bar=20  $\mu$ m)

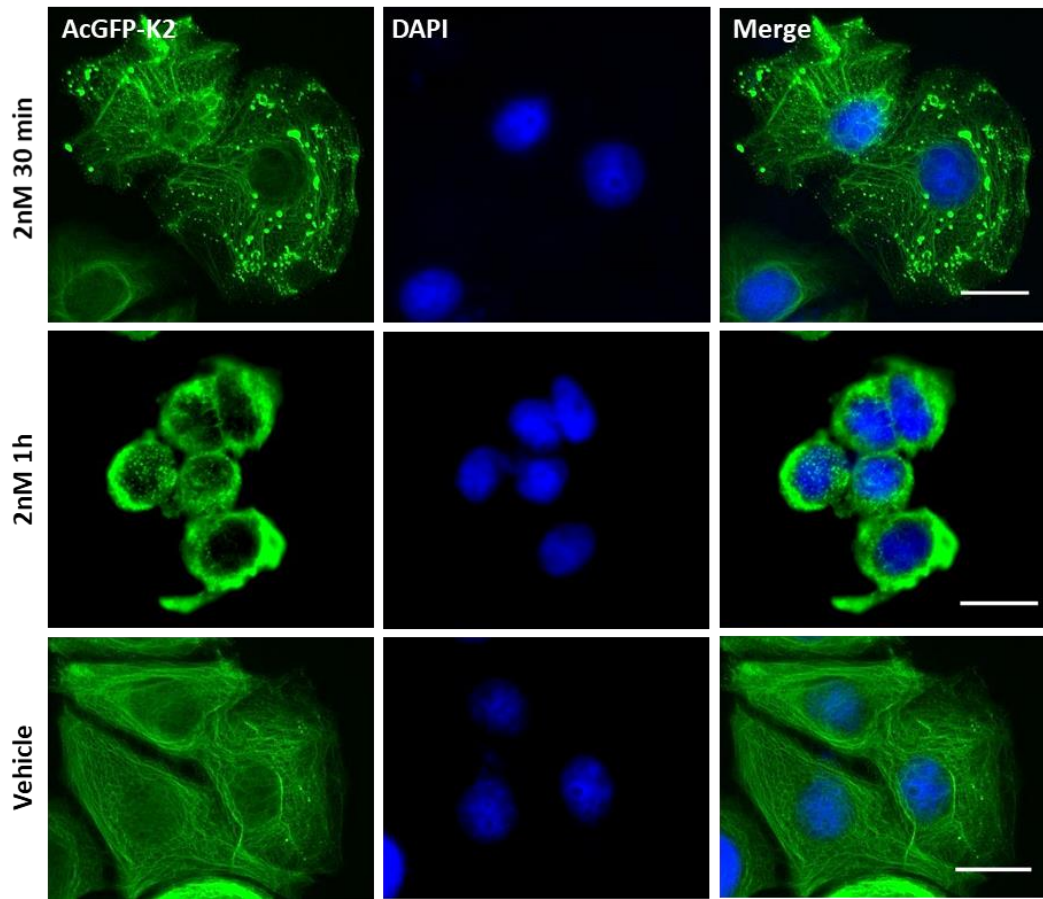
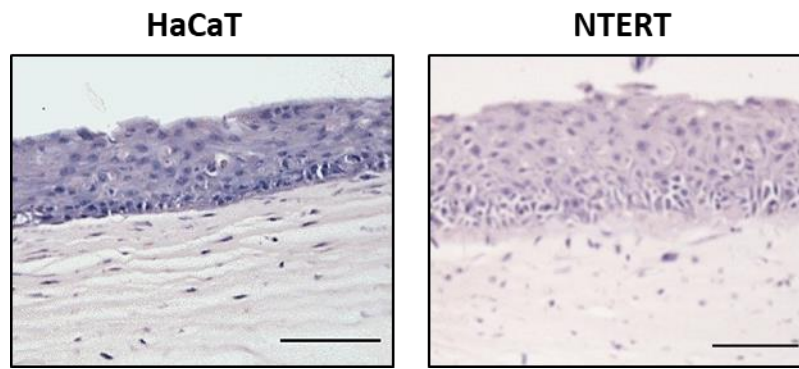
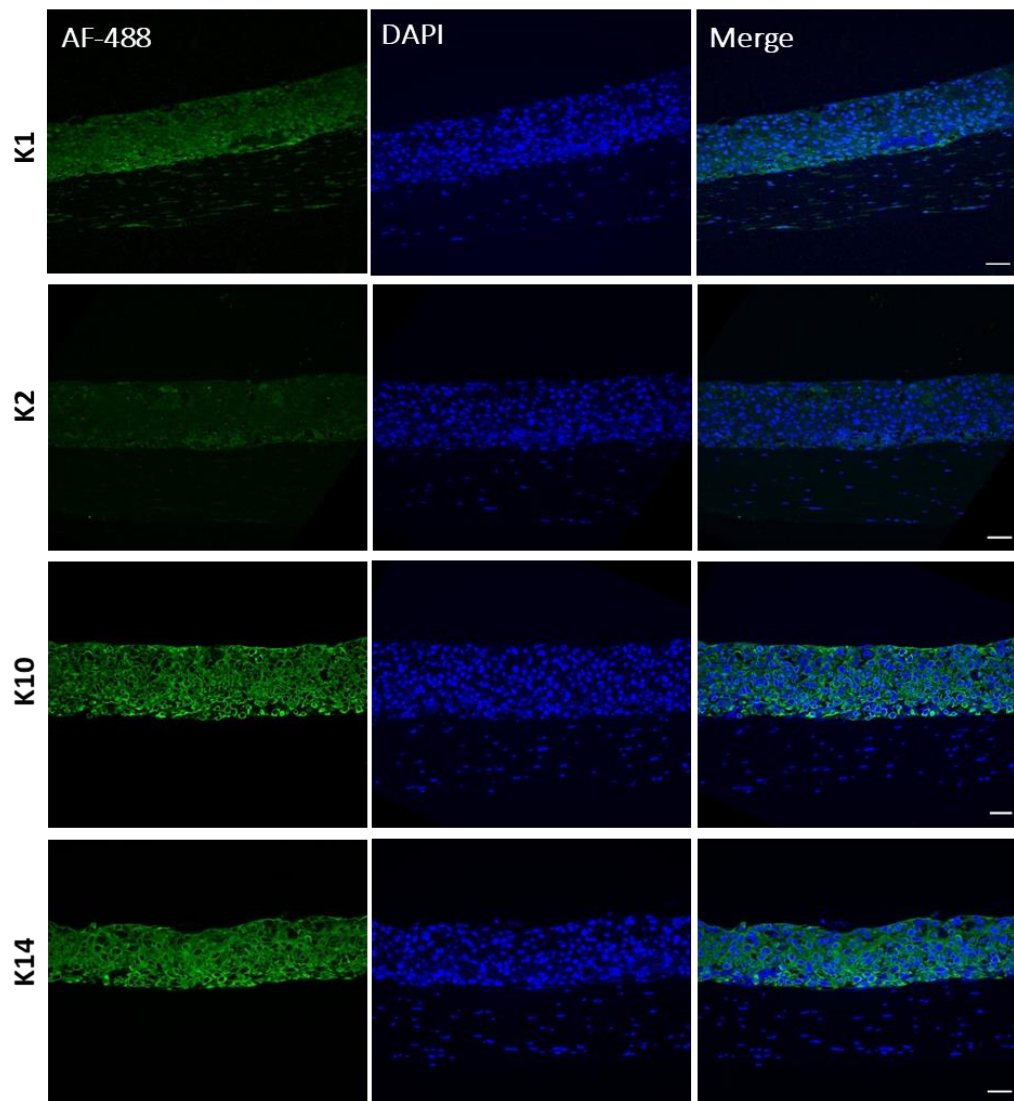


**Figure A. 2. Optimisations of CL-A treatment time points in AcGFP-K2/MCF-7 cells.** Cells were grown in full DMEM (10% FCS and 1% PS), next day treated with 2nM CL-A for different time points to optimise the time point based on data from untransduced MCF-7. 2nM for 30 min was the optimum concentration that was used in later experiments while 2nM for 1h was showing cells rounding up and lysed. DMF treated cells for up to 1 hour are shown as a vehicle control. Cells counter stained with DAPI in blue and overlapping of immunostaining with DAPI is shown as Merge. Leica Epi-fluorescence microscope model DM5000 and DFC350 camera were used for recording pictures. (Scale bar=20 µm)

**A**



**B**



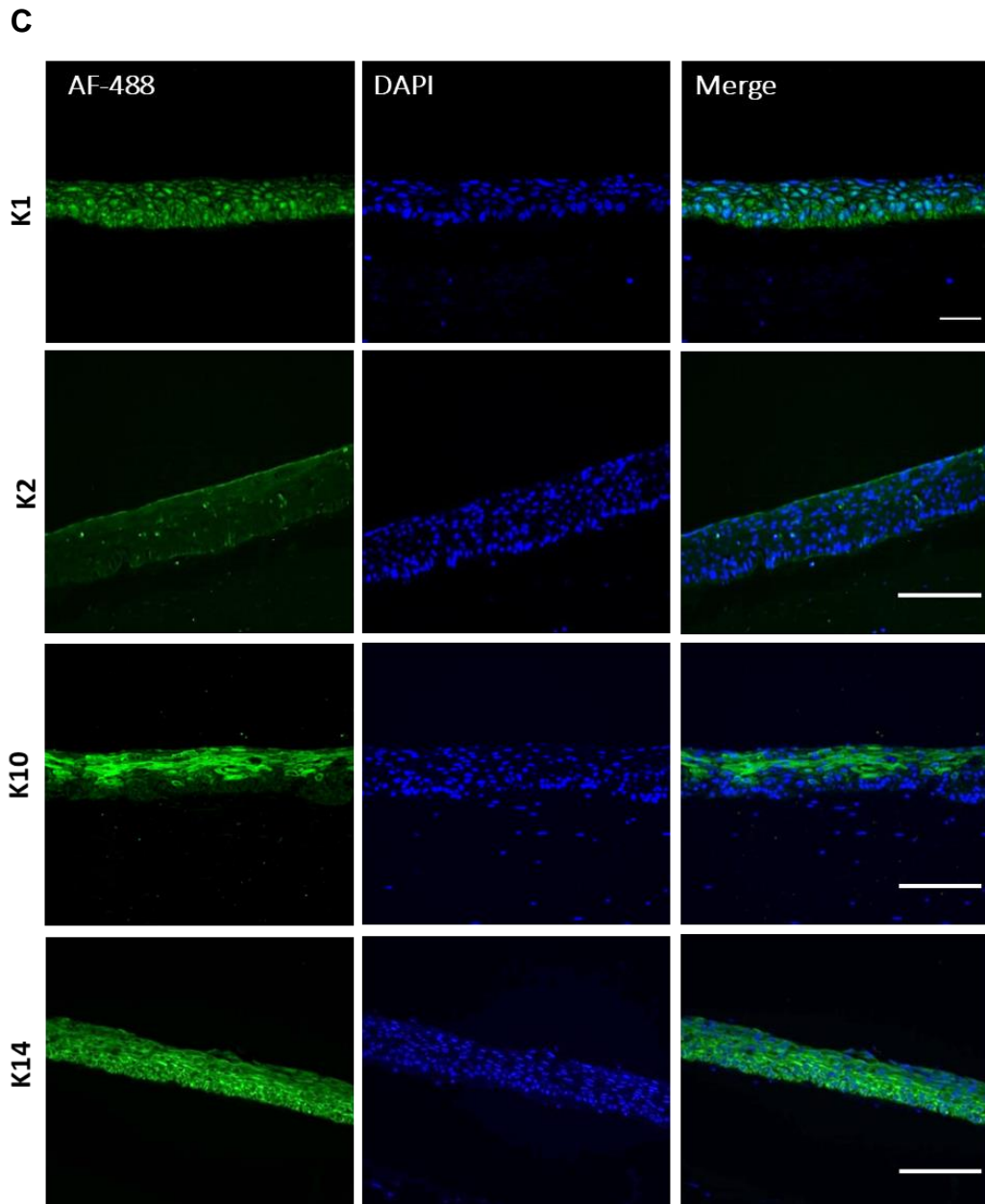
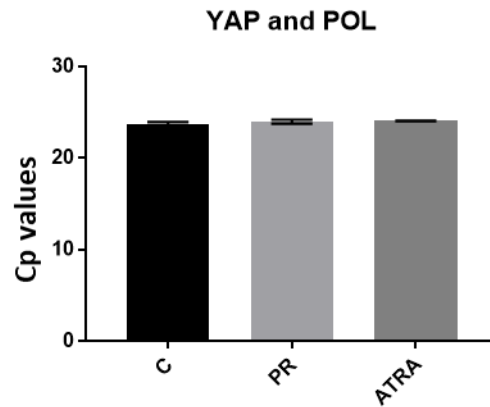


**Figure A. 3. Optimisation of organotypic growth conditions.** Haematoxylin and Eosin staining shown in (A), scale bar =100  $\mu\text{m}$ ). In (B) HaCaT and N/TERT (C) keratinocytes cell lines were grown in OTCs in an insert (pore size 0.4  $\mu\text{m}$ ) based method. Primary dermal fibroblasts were used in collagen matrix to support the growth of keratinocytes. The cells were grown at air-liquid interface for 10 days in RM+ medium, fixed in 4% (w/v) paraformaldehyde/PBS and paraffin embedded. Sections of 5 $\mu\text{m}$  thickness were cut, antigen retrieved, followed by immunostaining with antibodies against K1, K2, K10 and K14, the nuclei were counterstained with DAPI, overlap of green fluorescence with DAPI (Blue) is shown as merge image. The Leica DM4000B Epi-fluorescence microscope was used to record Images (scale bar = 40  $\mu\text{m}$ ).

**A**



**B**

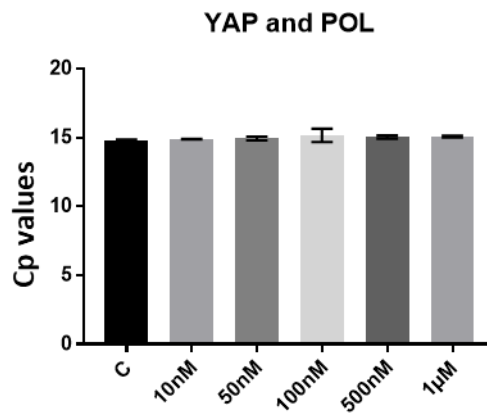


**Figure A. 4. Cp values of YAP and POL.** NHEK cells mixed with irradiated 3T3 feeder cells were grown in charcoal stripped FCS containing RM+ with or without PR. In (A), for ATRA cells were grown in 1  $\mu$ M ATRA concentrations for 24 h, for PR 0.01 mg/ml was used in PR free culture medium and control cells treated with DMSO/EtOH (0.001%/0.01%) for 24h. In (B),  $\beta$ -Estradiol was dissolved in DMSO (0.001%). Concentrations of  $\beta$ -Estradiol in the range of 10nM- 1 $\mu$ M were added in the culture medium and cells were treated for 24 h. Later lysates were collected for qPCR mRNA expression analysis for KRT1, KRT10 and KRT2. Data shown in this figure represent fold expression of Cp values of two housekeeping genes, POL2A and YAP1. For statistical analysis we have used One-way ANOVA to measure the p values. mean  $\pm$  SEM, n=3, ns=p>0.05, \*=p<0.05, \*\*=p<0.01 and \*\*\*=p<0.001 calculated using ANOVA test. One-way ANOVA showed no significant difference in both A and B.

## A.2. Maps and vectors used in this study.

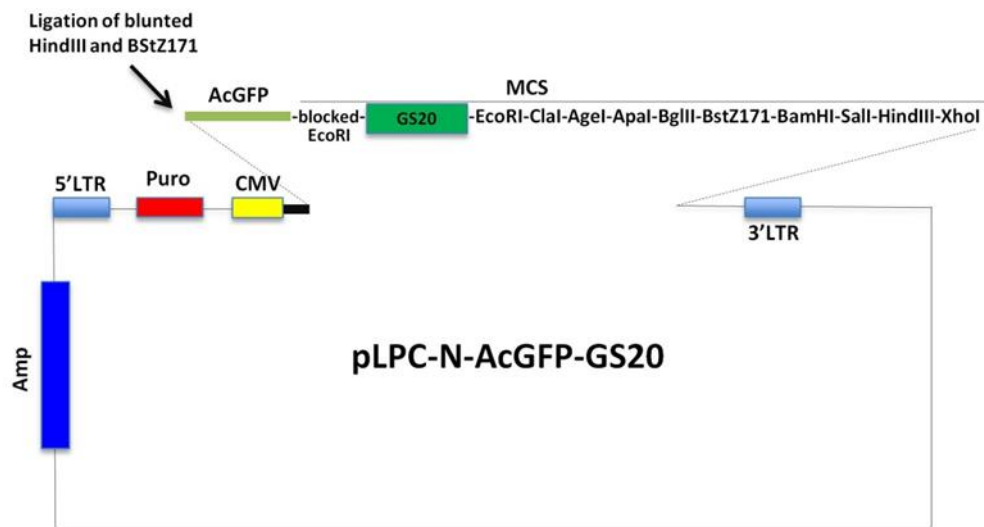


**Figure A. 5. Map of pLPC-N-AcGFP-GS20 vector.** This vector was used for K2 genome cloning. Amp – ampicillin resistance gene; 5'/3' LTR – 5'/3' long terminal repeat; Puro – puromycin resistance gene; CMV - human cytomegalovirus promoter; AcGFP – *Aequorea coerulea* GFP; GS20 – 20 amino acid insert; MCS – multiple cloning site. The vector as well as the vector map was kindly provided by my supervisor, Prof. Ahmad Waseem.



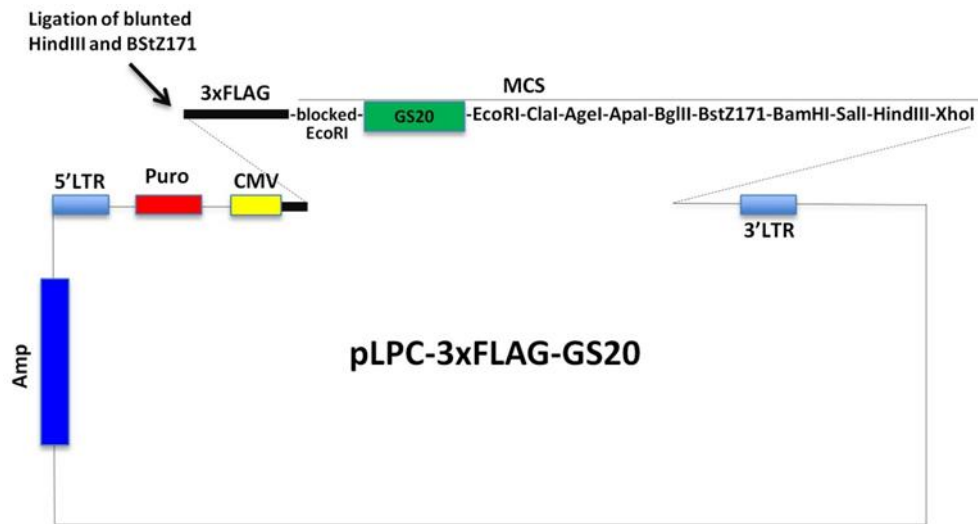


**Figure A. 6. Map of pLPC-3xFLAG-GS20 vector.** This vector was used for K2 cloning. Amp – ampicillin resistance gene; 5'/3' LTR – 5'/3' long terminal repeat; Puro – puromycin resistance gene, CMV – human cytomegalovirus promoter; AcGFP – *Aequorea coerulescens* GFP; MCS – multiple cloning site; GS20 – 20 amino acid insert. The vector as well as the vector map was kindly provided by my supervisor, Prof. Ahmad Waseem

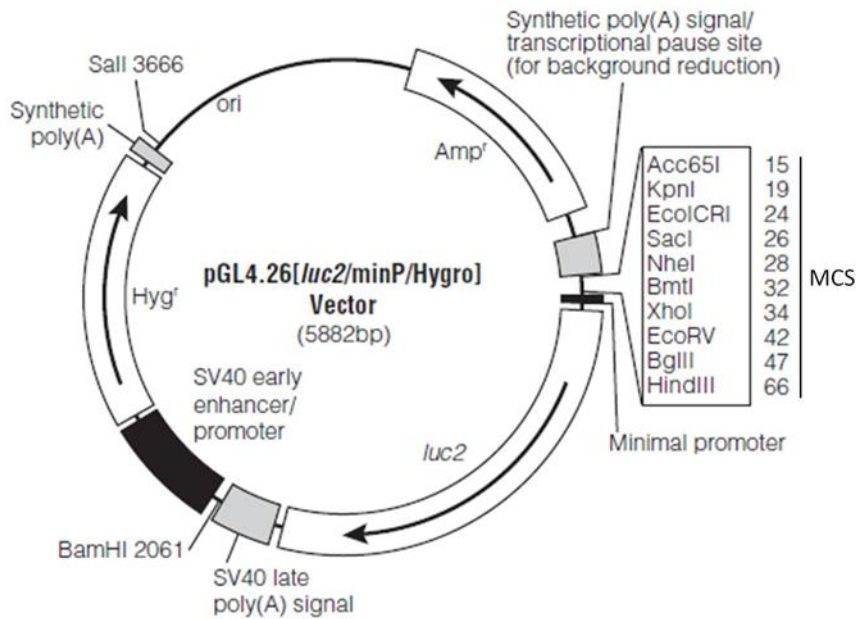


**Figure A. 7. Map of pGL4.26 vector.** pGL4.26 vector was used in luciferase assays for examination of AP-1 activity. Six copies of AP-1 responsive elements were previously cloned into this vector by Prof. A. Waseem. Hyg<sup>r</sup> – hygromycin resistance gene; ori – ColE1-derived plasmid replication origin; Amp<sup>r</sup> – ampicillin resistance gene; MCS – multiple cloning site; luc2 – luciferase reporter gene (*Photinus pyralis*). This figure was adapted from Promega, literature file # 9PIE844.

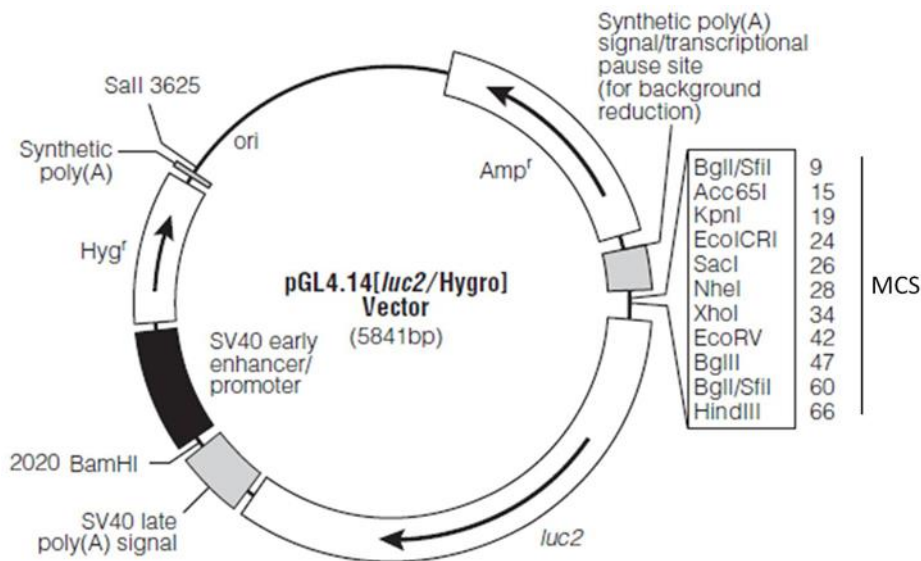


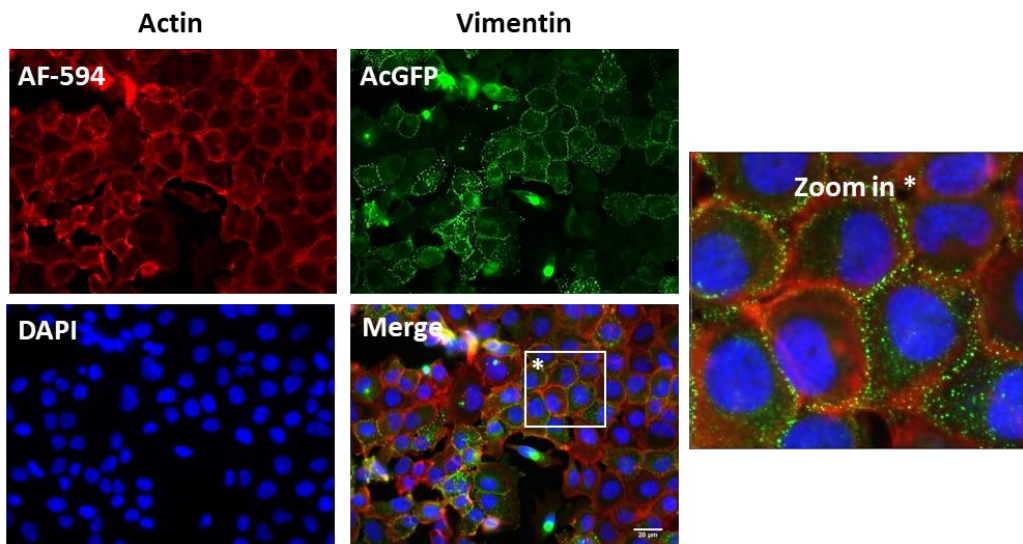
**Figure A. 8. Map of pGL4.14 vector.** pGL4.14 vector was used in luciferase assays for examination of K2, K14 promoter activity. K15 promoter (and its fragments F1 – F7) was previously cloned into this vector by Prof. A. Waseem. Hyg<sup>r</sup> – hygromycin resistance gene; ori – ColE1-derived plasmid replication origin; Amp<sup>r</sup> – ampicillin resistance gene; MCS – multiple cloning site; luc2 – luciferase reporter gene (*Photinus pyralis*). The figure was adapted from Promega, literature file # 9PIE669.

### A.3. Additional work.

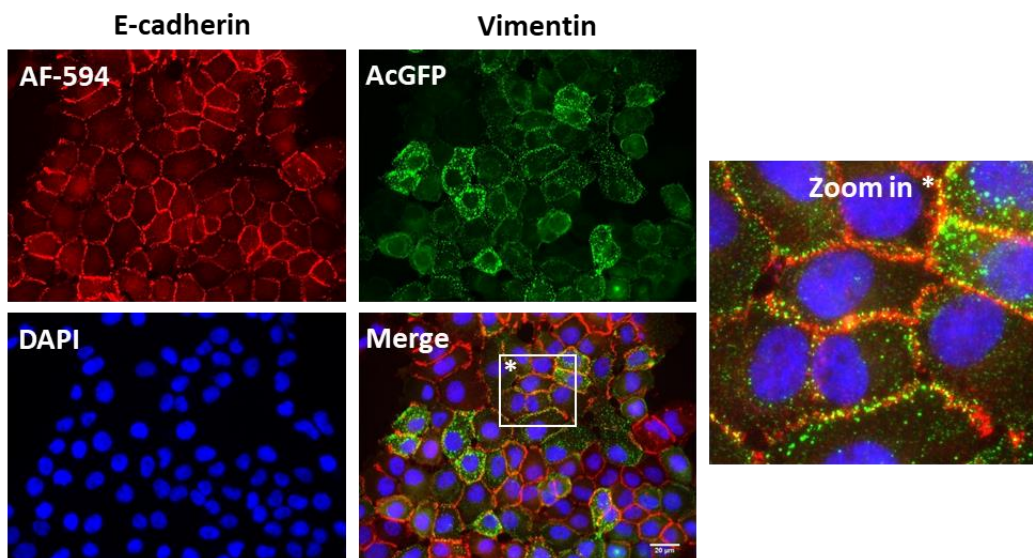
#### A.3.1. Vimentin co-localisation with other cell adhesion proteins

(as part of my supervisor's ongoing research).

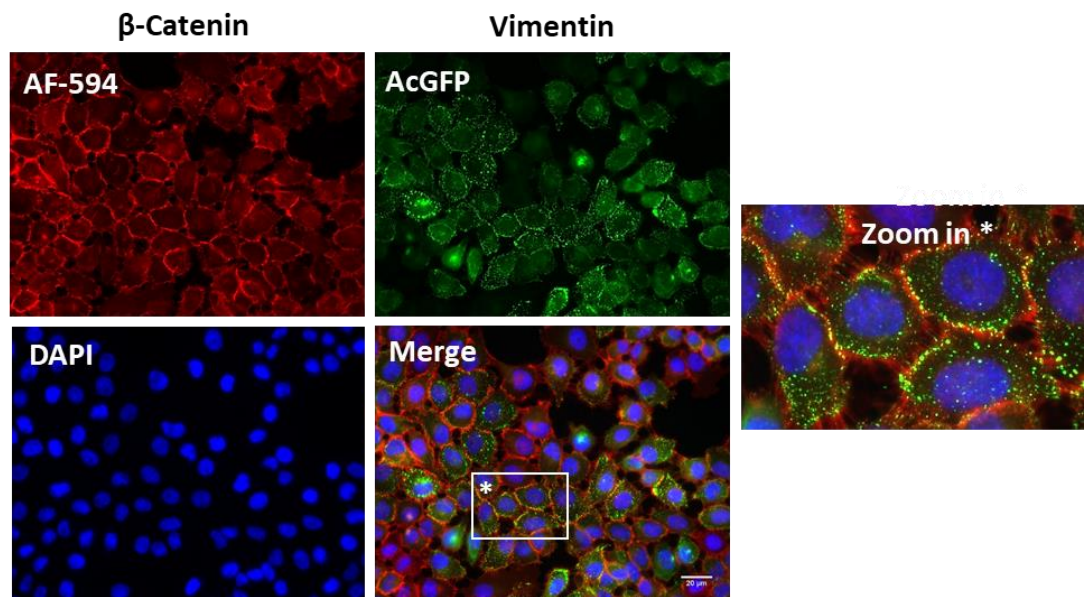
**A**



**B**



C



D

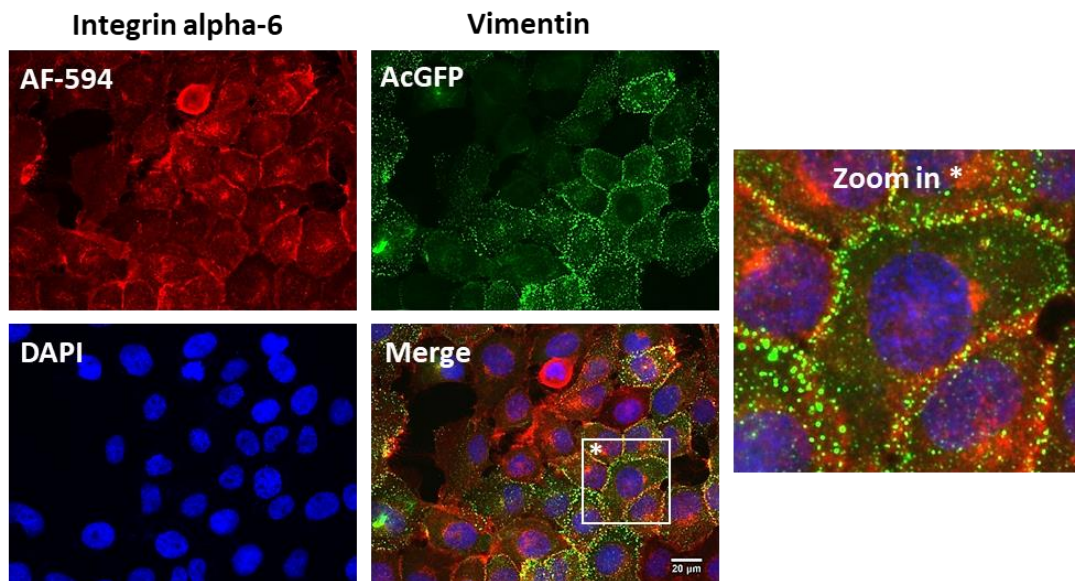


**Figure A. 9. Colocalisation of Vimentin with other proteins.** MCF-7 cells transduced with AcGFP-Vimentin were grown in full DMEM (10% FCS,1% PS), fixed using acetone/methanol (1:1). Cells were stained using primary antibodies for (Actin, A), (E-Cadherin, B), ( $\beta$ -Catenin, C), (Integrin alpha-6, D). Secondary antibodies were used (AF-594) for co-localisation proteins only. Vimentin was tagged to AcGFP. Cells were visualised using Leica DM4000 Epi-fluorescence microscope model and DFC350 camera. (Scale bar=20  $\mu$ m).

# SCIENTIFIC REPORTS

OPEN

## The monoclonal antibody EPR1614Y against the stem cell biomarker keratin K15 lacks specificity and reacts with other keratins

Received: 26 October 2018  
Accepted: 20 December 2018  
Published online: 13 February 2019

Hebah Aldehlawi, Katarzyna A. Niemiec, Deepa R. Avisetti, Anand Lalli, Muy-Teck Teh & Ahmad Waseem

Keratin 15 (K15), a type I keratin, which pairs with K5 in epidermis, has been used extensively as a biomarker for stem cells. Two commercial antibodies, LHK15, a mouse monoclonal and EPR1614Y, a rabbit monoclonal, have been widely employed to study K15 expression. Here we report differential reactivity of these antibodies on epithelial cells and tissue sections. Although the two antibodies specifically recognised K15 on western blot, they reacted differently on skin sections and cell lines. LHK15 reacted in patches, whereas EPR1614Y reacted homogenously with the basal keratinocytes in skin sections. In cultured cells, LHK15 did not react with K15 deficient NEB-1, KEB-11, MCF-7 and SW13 cells expressing only exogenous K8 and K18 but reacted when these cells were transfected with K15. On the other hand, EPR1614Y reacted with these cells even though they were devoid of K15. Taken together these results suggest that EPR1614Y recognises a conformational epitope on keratin filaments which can be reconstituted by other keratins as well as by K15. In conclusion, this report highlights that all commercially available antibodies may not be equally specific in identifying the K15 positive stem cell.

The epidermis is a multilayered stratified epithelium designed to provide a protective barrier throughout the life of an individual. It is made up of two compartments, a basal cell compartment where cells are attached to the basal lamina and are mostly proliferating, and the suprabasal compartment where the progenies of the basal layer undergo differentiation. Epidermal basal keratinocytes predominantly express keratin 14 (K14), a type I keratin, which together with keratin 5 (K5), a type II keratin, assemble into intermediate filaments (IFs)<sup>1,2</sup>. In addition to K5/K14, the basal keratinocytes also express K15, which does not have a defined type II keratin partner and pairs with K5<sup>3,4</sup>. Synthesis of K5/K14 ceases when the committed cells in the basal layer move into the suprabasal layers but their expression continues in keratinocytes of the spinous layers<sup>5-7</sup>. The synthesis of K15 (mRNA and protein) on the other hand is confined only in the epidermal basal layer<sup>8,9</sup>. The downregulation of K5/K14/K15 synthesis in the spinous layer is accompanied by upregulation of differentiation-specific keratins K1 and K10. As the cells move further up into the stratum granulosum another type II keratin, K2, is induced<sup>10,11</sup>. This programme produces several layers of keratinocytes at different stages of differentiation until the cells are terminally differentiated and sloughed from the skin surface.

The balance between the proliferation and differentiation is important to establish the tissue homeostasis essential for the protective function of the epidermis. The epidermis is regenerated and maintained by stem cells present in the basal layer. Earlier reports had suggested that less than 10% of basal cells were stem cells in murine skin<sup>12-15</sup>, however, more recently this number has been revised to about 1 stem cell per 10,000 (0.01%) basal keratinocytes in interfollicular epidermis<sup>16</sup>. These stem cells can divide either symmetrically to produce two stem cells<sup>17-19</sup>, one of them later becomes a transit-amplifying (TA) cell, or divide asymmetrically (laterally or

Centre for Immunobiology and Regenerative Medicine, Institute of Dentistry, Barts and The London School of Medicine and Dentistry, Turner Street, London, E1 2AD, United Kingdom. Hebah Aldehlawi and Katarzyna A. Niemiec contributed equally. Correspondence and requests for materials should be addressed to A.W. (email: [a.waseem@qmul.ac.uk](mailto:a.waseem@qmul.ac.uk))

perpendicularly) to produce two different stem cells, one of them remains in the basal layer and the other is committed to undergo differentiation<sup>20,21</sup>. The TA cells in the symmetrical model divide rapidly only a few times to produce a population of “committed cells”, which become less adhesive due to down-regulation of integrin extracellular matrix receptors (reviewed in<sup>18,22</sup>) and leave the basal layer to move up into the spinous layer to begin the programme of differentiation. This can be followed precisely by expression of different keratins.

As stem cells in the basal layer play a key role in tissue regeneration and homeostasis, their precise identification and characterisation is important. Earlier studies exploited the slow cycling nature of these cells to develop label-retaining assays for their identification. In this assay all the S-phase cycling cells of the skin are first labelled with 5-bromo-2'-deoxyuridine (BrdU) or <sup>3</sup>[H]-thymidine and the label is then chased for several weeks or months, the differentiating cells are lost from the skin surface, and the more proliferative cells dilute their label as they divide, leaving behind the slow cycling label-retaining cells (LRCs) as stem cells<sup>13,14,23,24</sup>. However, the cumbersome and time-consuming nature of these assays encouraged researchers to identify biomarkers which would specifically target stem cells. One of them, keratin K15, has received considerable attention as a biomarker of stem cells in stratified epithelia for the following reasons: first, localisation of K15+ cells in the murine and human hair follicle bulge region considered rich in multipotent stem cells<sup>8,25</sup>; second, K15 promoter was able to target  $\beta$ -galactosidase to the bulge region in murine epidermis<sup>26</sup>; third, K15 expressing murine bulge cells were able to reconstitute the entire epidermis and had higher proliferation potential than other keratinocytes<sup>27</sup>; fourth, K15+ epidermal cells were able to form fewer but larger colonies<sup>28</sup>; fifth, K15+ progenitor cells contribute towards homeostasis and regeneration in oesophagus<sup>29</sup>; and sixth, K15+ intestinal crypt cells were radio resistant and tumour initiating<sup>30</sup>. Any conclusion correlating the number or stemness of stem cell population in a tissue or in cultured cells with K15 expression is highly dependent on the specificity of the reagent used to detect the K15 polypeptide.

A number of mono- and polyclonal antibodies have been developed for detection of K15 in cultured cells and tissues using immunochemistry. The first monospecific K15 antibody was a polyclonal antibody reported by Lloyd and co-workers in 1995 against the last 12 residues of the K15 polypeptide<sup>3</sup>. Later, a mouse monoclonal antibody, LHK15, raised against the last 17 residues of K15 polypeptide had been published<sup>8</sup> and is now commercially available. Two more mouse monoclonal against K15, clones 6B4F8 and 6E7, are commercially available but they have not been cited so far in any published study. In addition, two cross reacting mouse monoclonals, one against the C-terminal cytoplasmic domain of the cluster of differentiation 8 (CD8) polypeptide (C8/144B), and another against the N-terminal K18 peptide (LC18N) have been published<sup>3,25</sup>. More recently a rabbit monoclonal antibody, EPR1614Y, against a much longer epitope on K15, raised using a patented technology has been marketed by Abcam UK.

In this study we have systematically compared the specificities of two of the most widely used monoclonal antibodies, LHK15 and EPR1614Y, to detect K15 in cells and tissues. Although both antibodies recognise denatured K15, they react differently with the protein in tissues and cell lines. While LHK15 reacted specifically with keratin cytoskeleton containing K15, EPR1614Y recognised IFs completely devoid of K15. Our data suggests that EPR1614Y epitope may acquire a conformation that can also be mimicked by keratins other than K15.

## Results

The epitope locations of 4 different K15 antibodies on the K15 polypeptide are shown in Fig. 1A. Two of them, LHK15 and EPR1614Y, are monoclonal and both are commercially available. The EPR1614Y epitope is located between 400–456 residues on K15 polypeptide (Abcam, UK; [www.abcam.com/cytokeratin-15-antibody-epr1614y-ab52816.html](http://www.abcam.com/cytokeratin-15-antibody-epr1614y-ab52816.html)) and therefore could overlap with the last 13 residues of the rod domain, on the other hand LHK15 has its epitope located in the last 17 residues of the tail domain<sup>8</sup>. We designed a series of experiments to compare the reactivities of EPR1614Y and LHK15 on cells and tissue sections. On western blotting using lysates derived from N/Tert-1, a K15+ cell line<sup>31</sup> and MCF-7, a K15- human breast carcinoma cell line<sup>32</sup>, grown in 2-dimensional (2-D) cultures, both antibodies recognised a single 50 kDa band only in N/Tert-1 but not in MCF-7 cells (Fig. 1B). This set of experiments established that on western blot both antibodies were specifically reacting with the K15 polypeptide.

**Immunoreactivity of LHK15 and EPR1614Y with basal keratinocytes in skin.** To compare the reactivity of the two antibodies in skin tissues, sections of freshly frozen human foreskin and abdominal skin were immunostained with LHK15 and EPR1614Y. As shown in Fig. 2 both antibodies specifically reacted with the basal layer; EPR1614Y displayed homogenous reactivity with the basal keratinocytes whereas LHK15 showed interrupted staining in sections of both foreskin and abdominal skin. We also compared the K15 staining with K14, a known basal cell specific marker, using anti-K14 LLOO1 antibody, which reacted with basal and some suprabasal keratinocytes in both types of skin samples (Fig. 2A,B).

**Reactivity of LHK15 and EPR1614Y with keratin cytoskeleton in 2-D cultures.** To further compare the specificity of the two antibodies, we investigated the specificity of LHK15 and EPR1614Y in K15+ and K15- epithelial cells including HaCaT (low level of K15)<sup>3</sup>, N/Tert-1 (K15+)<sup>31</sup>, NEB-1 (K15-)<sup>33</sup>, KEB-11 (K15-)<sup>33</sup> and MCF-7 (K15-)<sup>32</sup>, grown in 2-D cultures by immunostaining and western blotting. As shown in Fig. 3A, we observed strong reactivity of EPR1614Y with keratin cytoskeleton present in all 5 cell lines tested (HaCaT, N/Tert-1, NEB-1, KEB-11 and MCF-7). However, on western blot EPR1614Y recognised the K15 band only in HaCaT and N/Tert-1 but not in NEB-1, KEB-11 or MCF-7 (Figs 1Bi and 3C). As a control the anti-K14 LLOO1 reacted with HaCaT, N/Tert-1, NEB-1 but not with KEB-11 as it was derived from a patient suffering from a recessive form of epidermolysis bullosa simplex (EBS) with a premature termination codon in the K14 gene (Fig. 3C).

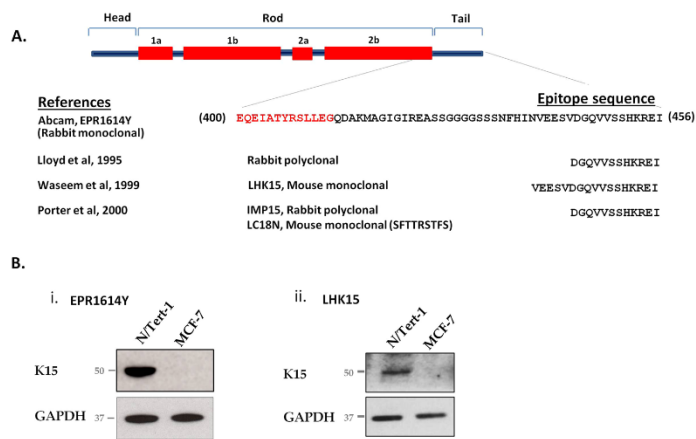


**Figure 1.** Location of antibody epitopes on K15 polypeptide. (A) The domain structure of an intermediate filament polypeptide is shown at the top. The sequence from 400–456 residues, which included the peptide used to raise EPR1614Y, including the end of rod (shown in red) and the entire tail domain of K15 is shown. The peptide sequences used to raise different antibodies along with published references are also listed. A keratin K18 peptide from the N-terminus used to raise LC18N antibody which cross reacts with K15 is also shown. (B) Western blotting of keratins present in N/Tert-1 and MCF-7 lysates using EPR1614Y (i) and LHK15 (ii). GAPDH was used as loading control. Relevant bands were cropped from different blots and grouped together. Original blots are shown in supplementary Fig. S1.

We also tested the reactivity of LHK15 with all 5 cell lines and observed weak reactivity with HaCaT and strong reactivity with N/Tert-1 but no reactivity with NEB-1, KEB-11 or MCF-7 cells (Fig. 3B). On western blot LHK15 showed reactivity only with HaCaT and N/Tert-1 but not with NEB-1, KEB-11 or MCF-7 (Figs 1Bii and 3D).

**LHK15 and EPR1614Y immunoreactivity with differentiating keratinocytes in organotypic cultures (OTCs).** To compare reactivity of the two antibodies in differentiating keratinocytes we prepared OTCs from HaCaT, N/Tert-1, KEB-11 and NEB-1. As shown in Fig. 4, only 3 cell lines HaCaT, N/Tert-1 and NEB-1 produced stratified epithelium, which as expected, was thicker after 9 days of culturing compared with that obtained after 7 days. KEB-11 cells did not produce a stratified epithelium under these conditions (Fig. 4).

To characterise the OTCs we immunostained the cryofixed sections of 3-D cultures for K14, a marker of basal keratinocytes<sup>1</sup>, and K10, a marker of suprabasal layers<sup>32</sup>. The expression of K14 was more or less homogenous in the stratified layers of OTCs from HaCaT and N/Tert-1. In NEB-1 cultures, K14 was expressed in patches of cells located near the junction of epithelium and the collagen base (Fig. 5A), whereas K10 expression was primarily located towards the suprabasal layers in OTCs from all 3 cell lines (Fig. 5B). In OTCs of HaCaT only few cells located at the top showed K10 expression whereas in N/Tert-1 and NEB-1 strong expression was seen in all suprabasal layers (Fig. 5B).

We then investigated the reactivity of EPR1614Y and LHK15 with cryofixed sections of OTCs derived from HaCaT, N/Tert-1 and NEB-1. EPR1614Y reacted strongly with all layers of OTCs derived from the 3 different cell lines (Fig. 5C). LHK15 on the other hand reacted weakly with HaCaT OTCs but it reacted strongly with N/Tert-1 OTCs (Fig. 5D). The most significant difference was the strong reactivity of EPR1614Y with NEB-1 derived OTCs, whereas LHK15 showed no reactivity with these OTCs (Fig. 5C,D).

**K15 add back experiments to restore antibody reactivity.** To further investigate the specificity, we tested reactivity of these antibodies after overexpressing K15 in cells devoid of this polypeptide. As K15 is absent in NEB-1 cells (Fig. 3B–D), we ectopically expressed K15 in these cells using retroviral transduction and immunostained the cells with LHK15 and EPR1614Y. As shown in Fig. 6A the NEB-1 cells transduced with the vector control virus immunoreacted with anti-K14 LLOO1 but did not stain with LHK15 (Fig. 6B) whereas the K15 transduced cells stained strongly with this antibody (Fig. 6C). EPR1614Y antibody on the other hand reacted strongly with NEB-1 in the absence as well as in the presence of K15 (Fig. 6D,E). These observations suggest that EPR1614Y may be reacting non-specifically with keratin filaments in the absence of K15.

We then did a similar experiment using MCF-7 cells, which express only K8, K18 and K19<sup>1,32</sup>. Vector control MCF-7 cells reacted with K8 antibody A45-B/B3 (Fig. 6F), they did not react with LHK15 (Fig. 6G) but the reactivity was induced when K15 was added into MCF-7 cells (Fig. 6H). On the other hand, EPR1614Y reacted

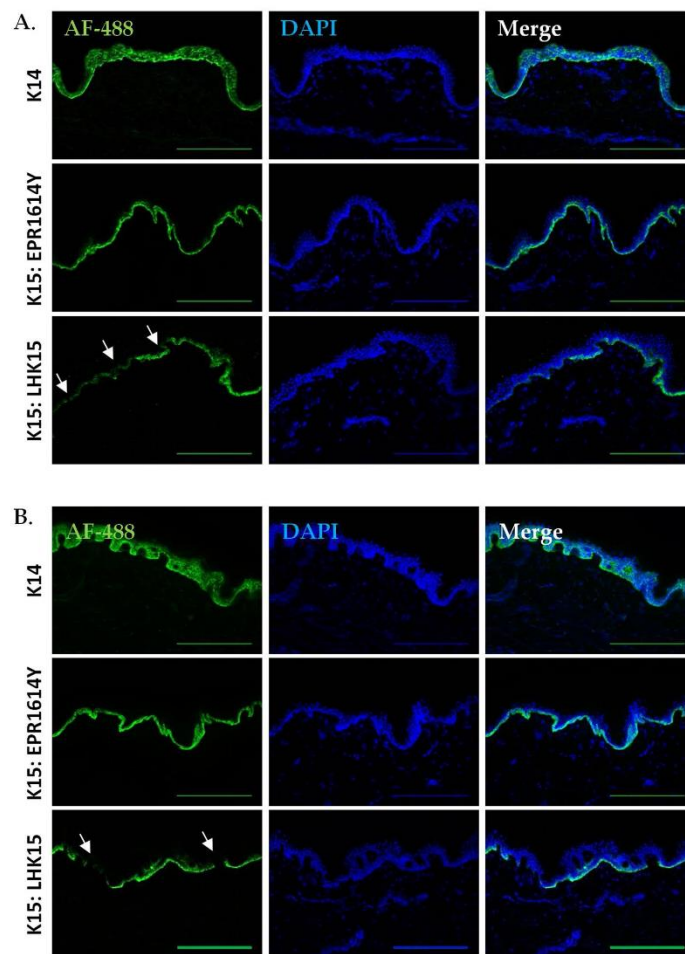


**Figure 2.** Specificity of anti-K15 antibodies on skin sections. Frozen human foreskin (A) and abdominal skin (B) sections were immunostained for K14 (LLOO1) and K15 (LHK15 and EPR1614Y) and the nuclei were counterstained with DAPI. Arrows indicate interruption in basal staining. Images were acquired using the Leica DM5000B epi-fluorescence microscope; scale bar = 250  $\mu$ m.

strongly with MCF-7 vector control cells (Fig. 6I) which did not change when K15 was added into these cells (Fig. 6J).

To substantiate the above observations, we transduced SW13, a cell line which does not express keratin filaments, with recombinant retroviruses expressing K8 and K18 and applied double selection with G418 and hygromycin. K8 and K18 formed IFs in SW13 cells as shown by A45-B/B3 immunostaining (Fig. 6K), these IFs did not react with LHK15 (Fig. 6L). SW13 cells expressing K8 + K18 [SW13(K8 + K18)] showed weak but detectable reactivity with EPR1614Y (Fig. 6N). The SW13(K8 + K18) cells were further transduced with K15 containing retroviruses and they were subjected to triple selection with G418, hygromycin and puromycin. As expected, the immunoreactivity of LHK15 with SW13(K8 + K18) was induced when K15 was added into these cells (Fig. 6M) and the reactivity of EPR1614Y with these cells became stronger and more filamentous in the presence of K15



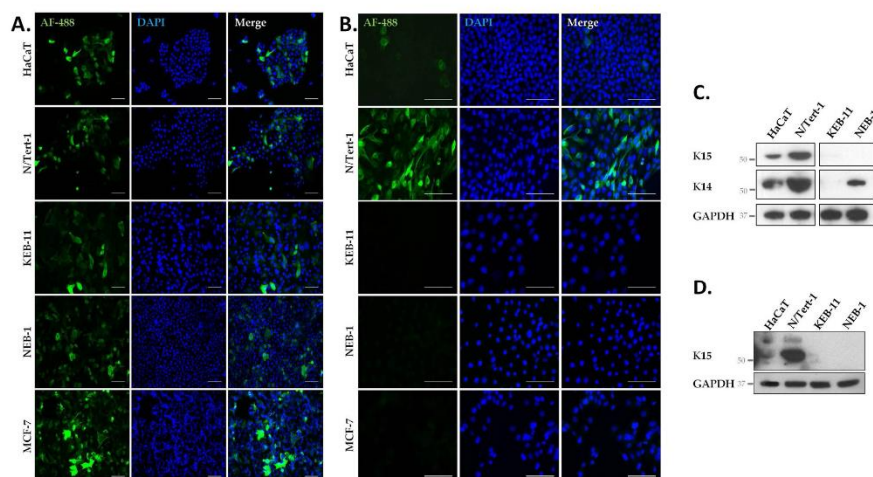


**Figure 3.** Immunoreactivity of EPR1614Y and LHK15 with keratins in epithelial cell lines. Cultured cells (HaCaT, N/Tert-1, KEB-11, NEB-1 and MCF-7) were fixed and stained for K15 (EPR1614Y) (A), K15 (LHK15) (B) and counterstained with DAPI. All slides were photographed at the same magnification using the Leica Epi DM5000B microscope (scale bar = 100  $\mu$ m). Western blotting of keratins present in HaCaT, N/Tert-1, KEB-11 and NEB-1 cell lysates using anti-K14 L1.OO1 and EPR1614Y for K15 (C) and LHK15 antibodies (D). GAPDH was used as loading control. Relevant bands were cropped from different blots and grouped together. Original blots are shown in supplementary Figs S2 and S3.

(Fig. 6O). Taken together these results suggest that the reactivity of LHK15 is specific to K15 whereas EPR1614Y will react non-specifically with other keratins in the absence of K15 polypeptide.

## Discussion

Immunocytochemistry, flow cytometry, enzyme-linked immunosorbent assays (ELISAs) and western blotting provide some of the most valuable, powerful, research as well as diagnostic tools in the field of biomedical sciences. However, it is well-known that the choice of the most specific and reliable antibody is of critical importance, as it determines the validity and credibility of the scientific data. Use of a non-specific antibody could lead to false results and conclusions<sup>34</sup>. As an example, a 2009 editorial by Michel and co-workers demonstrated that lack of selectivity appears to be the rule rather than the exception for antibodies against G-protein-coupled receptors (49 antibodies against 19 subtypes of the receptors have been tested in those studies and none of them was found to be selective)<sup>35</sup>. Other authors had to withdraw their publications because the antibodies they used against novel markers were later found to react in tissues from knock-out mice that lacked the markers<sup>36</sup>. Hence, determining the specificity of antibodies is extremely important especially when the antigen, K15, is widely used as a biomarker for adult stem cells<sup>37–42</sup>.

Before the use of synthetic peptides for monospecific antibody production became common, most of the antibodies raised were against keratin complexes derived from cytoskeletal extracts or using purified peptides from SDS gels. Some of these antibodies recognised keratin filaments only under certain physiological conditions. For example, AE1 and COU-1 react only with tumour cells<sup>43,44</sup> and K<sub>8</sub>,8.13 reacts with cells undergoing mitosis<sup>45</sup>. A number of monoclonal antibodies such as K<sub>18</sub>,18, LE61 and LE65 do not react with individual polypeptide but instead their epitopes are reconstituted only when complementary keratins associate into heterotypic complexes<sup>46–48</sup>. Other antibodies, such as A45-B/B3, are able to recognise conformational changes associated with heterotypic association of keratin pairs<sup>49</sup>. On the other hand, most antibodies raised using synthetic peptides reacted strongly with specific keratins on western blots as well as immunocytochemistry which increased their usefulness in keratin expression studies. Here we have compared the reactivity of two of the most widely used monoclonal antibodies, LHK15 and EPR1614Y, for the stem cell biomarker K15 by western blotting and immunocytochemistry in 2-D and 3-D cultures.

The choice of K15 antibody to address a particular set of research questions should be decided primarily by the techniques to be employed. On western blotting both antibodies, LHK15 and EPR1614Y, reacted strongly with K15 polypeptides in N/Tert-1 but no reactivity was observed with any protein band in MCF-7 cells suggesting they both specifically recognise a linear or denatured epitope. Therefore, if western blotting assay for K15 expression is to be used then either of the antibodies could be employed. However, if the expression of K15 polypeptide is to be investigated in cells and tissues by immunocytochemistry then significant differences in the ability of LHK15

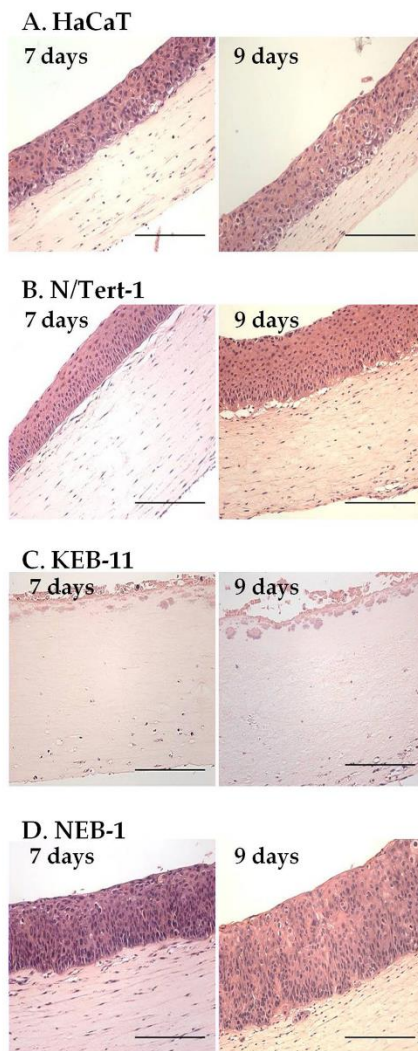


**Figure 4.** Organotypic cultures (OTCs) of keratinocyte cell lines. HaCaT (A), N/Tert-1 (B), KEB-11 (C) and NEB-1 (D) cells were co-cultured with primary dermal fibroblasts in OTCs for 7 and 9 days, followed by paraffin embedding and sectioning. Images of I&E-stained specimens were acquired using Leica Epi DM5000B or Nikon Eclipse 80i microscopes; scale bar = 200  $\mu$ m.

and EPR1614Y to recognise K15 were observed. In the epidermis both LHK15 and EPR1614Y reacted with the basal keratinocytes, however LHK15 gave discontinuous reactivity which was consistent with the data reported previously<sup>8,9</sup>, EPR1614Y on the other hand gave a homogenous reactivity with both foreskin as well as abdominal skin. This is in variance with a recent report where EPR1614Y was shown to recognise patches of basal keratinocytes in human breast skin<sup>50</sup>. It is therefore conceivable that patchy vs continuous staining of K15 depends on the body site where skin was taken for immunohistochemistry. Although the molecular basis for the discontinuous

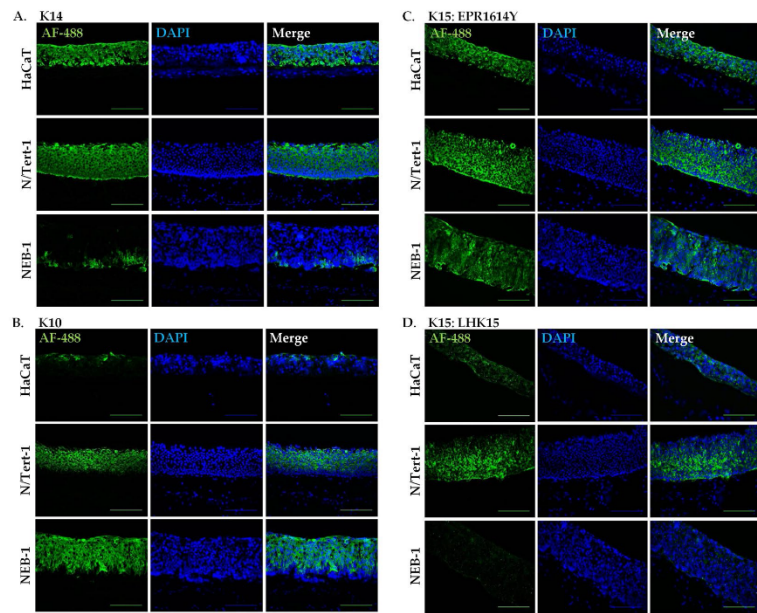


**Figure 5.** Immunoreactivity of OTCs with different antibodies. After 9 days of culturing HaCaT, N/Tert-1 and NEB-1 OTCs were cryofixed, sectioned and stained for K14 (A), K10 (B); K15 (EPR1614Y) (C); and K15 (LHK15) (D). The nuclei were counterstained with DAPI. Images were acquired using the Leica DM5000B epifluorescence microscope (scale bar = 200  $\mu$ m).

staining of adult skin section by LHK15 is not clear, it could be due to the heterogeneity in the basal keratinocytes reported previously<sup>51–53</sup>. This antibody has been shown to give a continuous staining in foetal skin as well as internal epithelia such as oral and oesophageal epithelia<sup>8,9</sup>.

On immunocytochemistry the IFs in the human epidermal keratinocyte cell lines, NEB-1, KEB-11 and N/Tert-1, reacted very differently with LHK15 and EPR1614Y. On western blotting, both LHK15 and EPR1614Y did not react with any protein band in lysates of NEB-1 and KEB-11 suggesting they did not express K15 (Fig. 3C,D). The absence of K15 in NEB-1 and KEB-11 could be due to HPV16 induced immortalisation, perhaps involving post-transcriptional mechanisms<sup>33</sup>. Absence of K15 in KEB-11, which already does not express K14, would leave no type I basal keratin which explains why this cell line does not form stratified epithelia in OTCs (Fig. 4C). Surprisingly, EPR1614Y gave positive reactivity with all epithelial cell lines used in this study whereas LHK15 reacted only with HaCaT and N/Tert-1 (Figs 3, 5 and 6). Absence of immunofluorescence reactivity of LHK15 with KEB-11, NEB-1 and MCF-7 suggests that presence of K15 is an absolute requirement for this antibody to show reactivity. EPR1614Y on the other hand reacted with keratin cytoskeleton even in the absence of K15, which implies that the three-dimensional reconstitution of EPR1614Y epitope may not require presence of K15.

The epitope of LHK15 is derived from the last 17 residues of K15 polypeptide which is the end of the tail domain (Fig. 1A), a region which can vary strongly in size and sequence amongst keratins<sup>54,55</sup>. Therefore, an antibody raised against this region is most likely to be specific towards its target. The epitope for EPR1614Y is poorly defined. This antibody was generated by Abcam UK using their own patented technology and their website claimed the epitope was between residues 400–500, however, as there are only 456 residues in K15 polypeptide, the epitope must be between 400–456 residues. Assuming the epitope begins from residue 400 in K15 polypeptide, the peptide used to raise this antibody would contain the last 13 residues of the rod domain. This region is part of the Helix Termination Peptide (HTP), which is highly conserved and it is a high affinity association site for stabilisation of heterotypic complexes between type I and type II keratins<sup>56</sup>. Mutations in this region are known to destabilise the cytoskeleton and are associated with a large number of blistering syndromes<sup>57–59</sup>. The high degree of sequence conservation in this region amongst different keratins<sup>56</sup> suggests that heterotypic keratin complexes could assemble into a very similar three-dimensional epitope even in the absence of K15. This hypothesis is supported by the data presented in Fig. 6 which shows that EPR1614Y reactivity in the absence of K15 seems to depend on the number of polypeptides present in the cytoskeleton, with low reactivity when K8 + K18 were present and increasing strongly in MCF-7, with additional keratin K19, and in NEB-1 which would express other

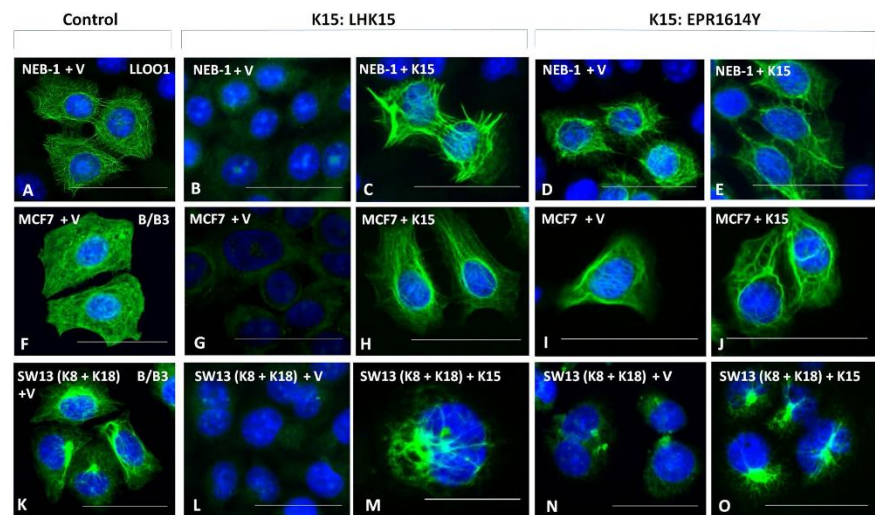


**Figure 6.** Immunostaining of epithelial cells with LHK15 and EPR1614Y in the presence and absence of K15 polypeptide. NEB-1 and MCF-7 cells were transfected with vector control and K15 recombinant retroviruses, after puromycin selection they were immunostained with LHK15 and EPR1614Y. NEB-1 vector control cells stained for K14 (LLOO1) (A), K15 (LHK15) (B), and K15 (EPR1614Y) (D), NEB-1 cells transfected with K15 virus were stained for K15 (LHK15) (C) and K15 (EPR1614Y) (E). MCF-7 vector control cells stained for K8 (A45-B/B3) (F), K15 (LHK15) (G) and K15 (EPR1614Y) (I), MCF-7 cells transfected with K15 virus were stained for K15 (LHK15) (H) and K15 (EPR1614Y) (J). SW13 cells which do not express any keratin were transfected with K8 and K18 retroviruses and selected with G418 and hygromycin. SW13 (K8 + K18) cells were transfected with vector control virus and after selection with puromycin stained for K8 (A45-B/B3) (K), K15 (LHK15) (L) and K15 (EPR1614Y) (N), SW13 (K8 + K18) cells transfected with K15 virus were stained for K15 (LHK15) (M) and K15 (EPR1614Y) (O). All images were acquired at the same gain and exposure using the Leica DM4000B epi-fluorescence microscope (scale bar = 50  $\mu$ m).

keratins such as K5, K14, K1 and K10. This explains why EPR1614Y reacts with keratin cytoskeleton devoid of K15 in immunocytochemistry but will not react on western blot if K15 was absent. There are other reports in the literature where cytoskeleton formed from different IF polypeptides are recognised by the same antibody. The well-documented example is that of anti-IFA antibody which recognises intermediate filaments formed from almost all IF polypeptides including keratins, vimentin, desmin, neurofilaments and glial fibrillary acidic protein<sup>60</sup>. Interestingly the epitope of this antibody is also located in the highly conserved HTP region<sup>60,61,62</sup>.

The antibody LHK15 reacts with K15 from human, rat, cow and mouse ([www.abcam.com/cytokeratin-15-antibody-lhk15-ab80522.html](http://www.abcam.com/cytokeratin-15-antibody-lhk15-ab80522.html)) whereas EPR1614Y reacts only with mouse and human ([www.abcam.com/cytokeratin-15-antibody-cpr1614y-ab52816.html](http://www.abcam.com/cytokeratin-15-antibody-cpr1614y-ab52816.html)) but both reagents react strongly with keratin filaments fixed with either acetone/methanol or with formalin. As the epitope for EPR1614Y is not defined, it is conceivable that the epitope does not involve HTP and it is derived entirely from the tail domain. In that case it is possible that during heterotypic dimerisation the tail domains of type I and type II keratins associate such that they form a 3-D structure mimicking the EPR1614Y epitope.

The EPR1614Y antibody has been widely used to study K15 expression as a biomarker of epidermal stem cells in scar formation<sup>63</sup>, differentiation of human hair follicle cells into neurons<sup>64</sup>, psoriatic skin lesions<sup>50</sup>, ameloblastoma<sup>65</sup>, mammary epithelium<sup>66</sup>, developing ureters<sup>67</sup> and human cornea<sup>37</sup>. In view of our data that EPR1614Y would react with cell cytoskeleton even when K15 is absent, some of the published work in which this antibody has been used may require reinterpretation. Furthermore, as our understanding of the clinical relevance of K15 positive cells in cancer, tissue homeostasis and other pathology develops, it is fundamental that only highly specific antibodies are employed to correctly identify these important cells *in vivo*.

In conclusion, we show that both antibodies, LHK15 and EPR1614Y, recognise K15 on western blotting. However, in immunocytochemistry LHK15 showed reactivity only when K15 was present whereas EPR1614Y showed strong reactivity even when there was no K15 polypeptide. The study highlights the extreme care one should exercise in choosing and validating the specificity of an antibody for their studies.

## Methods and Materials

**Materials.** The cell lines and antibodies used along with their sources in parenthesis were as follows: HaCaT, KEB-11 and NEB-1 (Cancer Research United Kingdom Laboratories, CRUK), MCF-7 (in house), N/Tert-1 (James Rheinwald, Harvard Medical School, Boston, USA), Phoenix E (Gary Nolan, Stanford University), PT67 (Dusty Miller, Fred Hutchinson Cancer Research Centre, University of Washington, USA), A45-B/B3, a gift from Uwe Karsten (Max Delbrück Centre for Molecular Medicine, Berlin-Buch, Germany) and anti-K14 LLOO1 (CRUK laboratories). DMEM (Lonza), FCS (First Link UK Ltd), penicillin and streptomycin (Gibco<sup>®</sup>, Life technologies Ltd) and components of the FAD medium were all obtained from Sigma-Aldrich apart from Ham's F12, which was obtained from Lonza. The commercially available primary antibodies used in this study were as follows: anti-GAPDH (ab9485), mouse anti-K15 clone LHK15 (ab80522), rabbit anti-K15 clone EPR1614Y (ab52816) and anti-K10 clone RKSE60 (ab902) from Abcam, UK. The secondary antibodies used were as follows: peroxidase goat anti-mouse (AP124P) and goat anti-rabbit (AP132P) IgGs (Millipore, UK) and Alexa Fluor 488-labeled goat anti-mouse IgG (H + L) (A11029) and F(ab')<sub>2</sub> goat anti-rabbit IgG (H + L) (A11070) from Life Technologies, UK. Retroviral vector pLPC-N MYC was a gift from Professor Titia de Lange (Addgene plasmid # 12540). Informed consents were obtained from all patients for collection of skin samples which was reviewed and approved by the NRES Committee London- City and East (REC ref. 09/H0704/69) and all methods were performed in accordance with the relevant guidelines and regulations.

**Molecular cloning.** All molecular cloning experiments were performed using standard cloning techniques<sup>68</sup>. The retroviral expression vector pLPC\_NMyC was re-engineered to remove N-MyC tag and replaced by K15 cDNA allowing its expression to be driven by CMV promoter. Total mRNA was isolated from K15 + N/Tert-1 cells using the Dynabeads<sup>®</sup> mRNA DIRECT<sup>™</sup> Purification Kit (Ambion<sup>®</sup>, Paisley, UK) and transcribed into cDNA by a mixture of poly A and random hexamer using the qPCR BIO cDNA Synthesis Kit (PCRBIOSYSTEMS, PB30.11-10) according to the manufacturer's instructions. K15 cDNA was amplified using Q5 DNA polymerase (New England Biolabs, UK) and ligated into *Eco*RI and *Bam*HI sites of pLPCpuro. Keratin K18 cDNA was ligated in *Eco*RI and *Hind*III sites of pLPCneo and K8 cDNA was ligated in *Eco*RI and *Bam*HI sites of pLPCchgro vectors.

**Cell culture.** Phoenix E (ecotropic), PT67 (amphotropic) retroviral packaging cell lines and HaCaT, a spontaneously immortalised normal epidermal keratinocytes<sup>69</sup>, were cultured in DMEM with 10% (v/v) FCS with 100 units/ml penicillin and 100 µg/ml streptomycin (1 x Pen/Strep). N/Tert-1, normal epidermal keratinocytes immortalised by overexpression of h-Tert and downregulation of p16<sup>70</sup>, KEB-11, K14 deficient keratinocytes derived from an EBS patient<sup>71,72</sup> and NEB-1, derived from an unaffected relative of the EBS patient used as a control for KEB-11, both immortalised by HPV16<sup>73</sup> were cultured in FAD medium consisting DMEM and Ham's F12 in 3:1 ratio containing 10% FCS, 1 X Pen/Strep, adenine (24 µg/ml), cholera toxin (8.4 ng/ml), epidermal growth factor (10 ng/ml), hydrocortisone (0.4 µg/ml), insulin (5 µg/ml), liothyronine ( $2 \times 10^{-11}$  M) and transferrin (5 µg/ml)<sup>74</sup>. All cells were cultured at 37 °C in a humidified atmosphere of 5–10% CO<sub>2</sub>.

**Retroviral packaging, viral transduction using spinfection.** Phoenix E cells were transfected with the constructs pLPCneo, pLPCchgro and pLPCpuro (control vectors) and pLPCneo\_K18, pLPCchgro\_K8 and pLPCpuro\_K15 using *TransIT<sup>®</sup>-LTI* transfection reagent (Cambridge Biosciences, UK). After 48 h culture supernatants containing ecotropic viruses were used to transduce PT67 cells in presence of 5 µg/ml polybrene (1,5-dimethyl-1,5-diazaundecamethylene polymethobromide) using the spinning method as described previously<sup>34,75</sup>. Briefly, the viral supernatant was treated with 5 µg/ml polybrene and the growth medium was replaced with the prepared viral supernatant. Plates were centrifuged at 1000 rpm at 32 °C for 1 h and then incubated for 24 h at 32 °C in a humidified atmosphere of 10% CO<sub>2</sub>. Cells were cultured in fresh complete growth medium at 37 °C for 48 h to ensure viral integration and protein expression followed by appropriate drug selection (1 mg/ml G418; 400 µg/ml hygromycin and 1–1.5 µg/ml puromycin) for several days. Amphotropic retroviral supernatants were collected from PT67 cells three times every 24 h and snap frozen and stored at –80 °C. SW13 cells were transduced with K18 followed by K8 amphotropic retrovirus and selected with a combination of G418 and hygromycin. MCF-7, SW13 (K8 + K18) and NEB-1 cell lines were transduced with K15 (or control) amphotropic retroviral supernatant using the spinfection method as described above and selected with puromycin.

**3-dimensional tissue culture model of keratinocyte differentiation.** HaCaT, N/Tert-1, KEB-11 and NEB-1 keratinocytes were seeded on a human primary dermal fibroblast containing disc of rat-tail collagen type I (Corning, UK) in a Millipore<sup>®</sup> Millicell<sup>®</sup> (Sigma-Aldrich, UK). The cells were cultured for 24 h at 37 °C in a humidified atmosphere of 10% CO<sub>2</sub> and maintained in FAD medium. After 24 h the collagen disc was raised to the air-liquid interphase to induce keratinocyte differentiation. The cells were cultured for 7 or 9 more days after which they were either fixed with 4% (w/v) paraformaldehyde, embedded in paraffin or cryofixed and sectioned for immunostaining.

**SDS electrophoresis and western blotting.** Cultured cells were lysed in lysis buffer (4% (w/v) SDS, 20% (v/v) glycerol in 0.125 M Tris HCl, pH 6.8), heated to 95 °C for 5 min and the protein concentration was measured with *DC<sup>™</sup> Protein Assay* (Bio-Rad, Hemel Hempstead, UK). Just before electrophoresis, 10% (v/v) 2-mercaptoethanol and 0.004% (w/v) bromophenol blue were added and the lysate was separated by SDS-PAGE (NuPAGE<sup>®</sup> Novex<sup>®</sup> 10% Bis-Tris Protein Gels) with NuPAGE<sup>®</sup> MOPS SDS Running Buffer (Novex<sup>®</sup>, Paisley, UK). The proteins in the gel were transferred onto 0.45 µm nitrocellulose membranes (Sigma-Aldrich, Gillingham, UK) in transfer buffer (20 mM Tris base, 190 mM glycine, 20% (v/v) methanol). The membranes were blocked with 5% (w/v) non-fat dry milk for 30 min and washed with TBS-T buffer (20 mM Tris base, 150 mM NaCl, 1% (v/v) Tween<sup>®</sup>20). Membranes were probed with primary antibodies overnight at 4 °C and incubated with the secondary antibody for 1 h at room temperature (RT). The target proteins were detected using

Amersham ECL Prime Western Blotting Detection Reagent (GE Healthcare, Little Chalfont, UK). Peroxidase activity was detected with Amersham Hyperfilm<sup>TM</sup> ECL autoradiography film (GE Healthcare).

**Immuno-cytochemistry and –histochemistry.** Cells were cultured on collagen-coated coverslips for 24 h, fixed in a mixture of ice-cold acetone and methanol (1:1) for 10 min and dried in air. After blocking the non-specific antibody reactivity with 10% (v/v) normal goat serum, the coverslips were incubated with primary antibody for 2 h at RT. After washing with phosphate-buffered saline (PBS) the coverslips were incubated with Alexa Fluor<sup>®</sup> 488-labelled anti-mouse or anti-rabbit secondary antibodies in the dark for 1 h at RT. The coverslips were washed again and mounted on glass slides using VECTASHIELD HardSet Antifade Mounting Medium with DAPI (Vector Laboratories, UK) and visualised with a Leica Epi DM5000B or DM4000B microscope equipped with a DFC350 FX digital camera and 20x/0.5 NA and 40x/0.75 NA objective lenses.

The 3-D reconstructed plugs or human tissues were cryo-sectioned and attached to glass slides, fixed in ice-cold methanol for 15 min and washed with PBS. The sections were treated with primary antibodies at 4 °C overnight, washed, stained with secondary antibody and mounted in DAPI containing mounting medium as described above for cultured cells.

#### Data Availability

Any supporting data not included in this manuscript or reagents used in this study, which are not commercially available, will be provided to readers following a written request to the corresponding author.

#### References

- Moll, R., Franke, W. W., Schiller, D. L., Geiger, B. & Krepler, R. The catalog of human cytokeratins: patterns of expression in normal epithelia, tumors and cultured cells. *Cell* **31**, 11–24 (1982).
- Kirfel, J., Magin, T. M. & Reichelt, J. Keratins: a structural scaffold with emerging functions. *Cell Mol Life Sci* **60**, 56–71 (2003).
- Lloyd, C. *et al.* The basal keratin network of stratified squamous epithelia: defining K15 function in the absence of K14. *J Cell Biol* **129**, 1329–1344 (1995).
- Jonkman, M. F. *et al.* Effects of keratin 14 ablation on the clinical and cellular phenotype in a kindred with recessive epidermolysis bullosa simplex. *J Invest Dermatol* **107**, 764–769 (1996).
- Fuchs, E. & Green, H. Changes in keratin gene expression during terminal differentiation of the keratinocyte. *Cell* **19**, 1033–1042 (1980).
- Stoler, A., Kopan, R., Duvic, M. & Fuchs, E. Use of monospecific antisera and cRNA probes to localize the major changes in keratin expression during normal and abnormal epidermal differentiation. *J Cell Biol* **107**, 427–446 (1988).
- Purkis, P. E. *et al.* Antibody markers of basal cells in complex epithelia. *J Cell Sci* **97**(Pt 1), 39–50 (1990).
- Waseem, A. *et al.* Keratin 15 expression in stratified epithelia: downregulation in activated keratinocytes. *J Invest Dermatol* **112**, 362–369. <https://doi.org/10.1046/j.1523-1747.1999.00535.x> (1999).
- Porter, R. M. *et al.* K15 expression implies lateral differentiation within stratified epithelial basal cells. *Lab Invest* **80**, 1701–1710 (2000).
- Bloor, B. K. *et al.* Expression of keratin K2e in cutaneous and oral lesions: association with keratinocyte activation, proliferation, and keratinization. *Am J Pathol* **162**, 963–975. [https://doi.org/10.1016/S0002-9440\(10\)63891-6](https://doi.org/10.1016/S0002-9440(10)63891-6) (2003).
- Collin, C., Moll, R., Kubicka, S., Ouhayoun, J. P. & Franke, W. W. Characterization of human cytokeratin 2, an epidermal cytoskeletal protein synthesized late during differentiation. *Exp Cell Res* **202**, 132–141 (1992).
- Mackenzie, I. C. & Bickenbach, J. R. Label-retaining keratinocytes and Langerhans cells in mouse epithelia. *Cell Tissue Res* **242**, 551–556 (1985).
- Bickenbach, J. R., McCutcheon, J. & Mackenzie, I. C. Rate of loss of tritiated thymidine label in basal cells in mouse epithelial tissues. *Cell Tissue Kinet* **19**, 325–333 (1986).
- Morris, R. J. & Potten, C. S. Slowly cycling (label-retaining) epidermal cells behave like clonogenic stem cells *in vitro*. *Cell Prolif* **27**, 279–289 (1994).
- Heenen, M. & Galand, P. The growth fraction of normal human epidermis. *Dermatology* **194**, 313–317. <https://doi.org/10.1159/000246122> (1997).
- Schneider, T. E. *et al.* Measuring stem cell frequency in epidermis: a quantitative *in vivo* functional assay for long-term repopulating cells. *Proc Natl Acad Sci USA* **100**, 11412–11417. <https://doi.org/10.1073/pnas.2034935100> (2003).
- Watt, F. M. & Hogan, B. L. Out of Eden: stem cells and their niches. *Science* **287**, 1427–1430 (2000).
- Janes, S. M., Lowell, S. & Hutter, C. Epidermal stem cells. *J Pathol* **197**, 479–491. <https://doi.org/10.1002/path.1156> (2002).
- Jensen, U. B., Lowell, S. & Watt, F. M. The spatial relationship between stem cells and their progeny in the basal layer of human epidermis: a new view based on whole-mount labelling and lineage analysis. *Development* **126**, 2409–2418 (1999).
- Lechler, T. & Fuchs, E. Asymmetric cell divisions promote stratification and differentiation of mammalian skin. *Nature* **437**, 275–280. <https://doi.org/10.1038/nature03922> (2005).
- Clayton, E. *et al.* A single type of progenitor cell maintains normal epidermis. *Nature* **446**, 185–189. <https://doi.org/10.1038/nature05574> (2007).
- Watt, F. M. Role of integrins in regulating epidermal adhesion, growth and differentiation. *EMBO J* **21**, 3919–3926. <https://doi.org/10.1093/emboj/cdf399> (2002).
- Bickenbach, J. R. Identification and behavior of label-retaining cells in oral mucosa and skin. *J Dent Res* **60** Spec No C, 1611–1620 (1981).
- Bickenbach, J. R. & Chism, E. Selection and extended growth of murine epidermal stem cells in culture. *Exp Cell Res* **244**, 184–195. <https://doi.org/10.1006/excr.1998.4163> (1998).
- Lyle, S. *et al.* The C8/144B monoclonal antibody recognizes cytokeratin 15 and defines the location of human hair follicle stem cells. *J Cell Sci* **111**(Pt 21), 3179–3188 (1998).
- Liu, Y., Lyle, S., Yang, Z. & Cotsarelis, G. Keratin 15 promoter targets putative epithelial stem cells in the hair follicle bulge. *J Invest Dermatol* **121**, 963–968. <https://doi.org/10.1046/j.1523-1747.2003.12600.x> (2003).
- Morris, R. J. *et al.* Capturing and profiling adult hair follicle stem cells. *Nat Biotechnol* **22**, 411–417. <https://doi.org/10.1038/nbt950> (2004).
- Inoue, K. *et al.* Differential expression of stem-cell-associated markers in human hair follicle epithelial cells. *Lab Invest* **89**, 844–856. <https://doi.org/10.1038/labinvest.2009.48> (2009).
- Giroux, V. *et al.* Long-lived keratin 15+ esophageal progenitor cells contribute to homeostasis and regeneration. *J Clin Invest* **127**, 2378–2391. <https://doi.org/10.1172/JCI88941> (2017).
- Giroux, V. *et al.* Mouse Intestinal Krt15+ Crypt Cells Are Radio-Resistant and Tumor Initiating. *Stem Cell Reports* **10**, 1947–1958. <https://doi.org/10.1016/j.stemcr.2018.04.022> (2018).

31. Bose, A. *et al.* Two mechanisms regulate keratin K15 expression in keratinocytes: role of PKC/AP-1 and FOXM1 mediated signalling. *PLoS One* **7**, e38599, <https://doi.org/10.1371/journal.pone.0038599> (2012).
32. Quinlan, R. A. *et al.* Patterns of expression and organisation of cyokeratin intermediate filaments. *Ann. N. Y. Acad. Sci.* **455**, 282–306 (1985).
33. Niemiec, K. A. *An investigation on the effects of HPV16-induced immortalisation and POU2F3 regulation in keratinocytes*, (Queen Mary University of London, (2017).
34. Kalyuzhny, A. E. The dark side of the immunohistochemical moon: industry. *J Histochem Cytochem* **57**, 1099–1101, <https://doi.org/10.1369/jhc.2009.954867> (2009).
35. Michel, M. C., Wieland, T. & Tsujimoto, G. How reliable are G-protein-coupled receptor antibodies? *Naunyn-Schmiedeberg Arch Pharmacol* **379**, 385–388, <https://doi.org/10.1007/s00210-009-0395-y> (2009).
36. Jensen, B. C., Swigart, P. M. & Simpson, P. C. Ten commercial antibodies for alpha-1-adrenergic receptor subtypes are nonspecific. *Naunyn-Schmiedeberg Arch Pharmacol* **379**, 409–412, <https://doi.org/10.1007/s00210-008-0368-6> (2009).
37. Hanson, C. *et al.* Transplantation of human embryonic stem cells onto a partially wounded human cornea *in vitro*. *Acta Ophthalmol* **91**, 127–130, <https://doi.org/10.1111/j.1755-3768.2011.02358.x> (2013).
38. Ocampo, A. *et al.* *In Vivo* Amelioration of Age-Associated Hallmarks by Partial Reprogramming. *Cell* **167**, 1719–1733 e1712, <https://doi.org/10.1016/j.cell.2016.11.052> (2016).
39. Achilleos, C., Michael, S. & Strati, K. Terc is dispensable for most of the short-term HPV16 oncogene-mediated phenotypes in mice. *PLoS One* **13**, e0196604, <https://doi.org/10.1371/journal.pone.0196604> (2018).
40. Higa, K. *et al.* Aquaporin-1-positive stromal niche-like cells directly interact with N-cadherin-positive clusters in the basal limbal epithelium. *Stem Cell Res* **10**, 147–155, <https://doi.org/10.1016/j.scr.2012.11.001> (2013).
41. Nagao, K. *et al.* Stress-induced production of chemokines by hair follicles regulates the trafficking of dendritic cells in skin. *Nat Immunol* **13**, 744–752, <https://doi.org/10.1038/ni.2353> (2012).
42. Fridriksson, A. J. *et al.* Propagation of oestrogen receptor-positive and oestrogen-responsive normal human breast cells in culture. *Nat Commun* **6**, 8786, <https://doi.org/10.1038/ncomms9786> (2015).
43. Asch, B. B. & Asch, H. L. A keratin epitope that is exposed in a subpopulation of preneoplastic and neoplastic mouse mammary epithelial cells but not in normal cells. *Cancer Res* **46**, 1255–1262 (1986).
44. Ditzel, H. J. *et al.* Cancer-associated cleavage of cytokeratin 8/18 heterotypic complexes exposes a neoepitope in human adenocarcinomas. *J Biol Chem* **277**, 21712–21722, <https://doi.org/10.1074/jbc.M202140200> (2002).
45. Franke, W. W. *et al.* Change of cytokeratin filament organization during the cell cycle: selective masking of an immunological determinant in interphase PKC2 cells. *J Cell Biol* **97**, 1255–1260 (1983).
46. Waseem, A., Lane, E. B., Harrison, D. & Waseem, N. A keratin antibody recognizing a heterotypic complex: epitope mapping to complementary locations on both components of the complex. *Exp Cell Res* **223**, 203–214, <https://doi.org/10.1006/excr.1996.0074> (1996).
47. Waseem, A., White, K. & Waseem, N. H. Identification of a novel keratin epitope: evidence for association between non-helical subdomains L12 during filament assembly. *Int J Biochem Cell Biol* **29**, 971–983 (1997).
48. Franke, W. W. *et al.* Monoclonal cytokeratin antibody recognizing a heterotypic complex: immunological probing of conformational states of cytoskeletal proteins in filaments and in solution. *Exp Cell Res* **173**, 17–37 (1987).
49. Waseem, A. *et al.* Conformational changes in the rod domain of human keratin 8 following heterotypic association with keratin 18 and its implication for filament stability. *Biochemistry* **43**, 1283–1295, <https://doi.org/10.1021/bi035072s> (2004).
50. Jia, H. Y. *et al.* Asymmetric stem-cell division ensures sustained keratinocyte hyperproliferation in psoriatic skin lesions. *Int J Mol Med* **37**, 359–368, <https://doi.org/10.3892/ijmm.2015.2445> (2016).
51. Cotsarells, G., Cheng, S. Z., Dong, G., Sun, T. T. & Lavker, R. M. Existence of slow-cycling limbal epithelial basal cells that can be preferentially stimulated to proliferate: Implications on epithelial stem cells. *Cell* **57**, 201–209 (1989).
52. Lavker, R. M. & Sun, T. T. Heterogeneity in epidermal basal keratinocytes: morphological and functional correlations. *Science* **215**, 1239–1241 (1982).
53. Lavker, R. M. & Sun, T. T. Epidermal stem cells. *J Invest Dermatol* **81**, 121s–127s (1983).
54. Steinert, P. M., Rice, R. H., Roop, D. R., Trus, B. L. & Steven, A. C. Complete amino acid sequence of a mouse epidermal keratin subunit and implications for the structure of intermediate filaments. *Nature* **302**, 794–800 (1983).
55. Hanukoglu, I. & Fuchs, E. The cDNA sequence of a Type II cytoskeletal keratin reveals constant and variable structural domains among keratins. *Cell* **33**, 915–924 (1983).
56. Hatzfeld, M. & Weber, K. A synthetic peptide representing the consensus sequence motif at the carboxy-terminal end of the rod domain inhibits intermediate filament assembly and disassembles preformed filaments. *J Cell Biol* **116**, 157–166 (1992).
57. Lane, E. B. *et al.* A mutation in the conserved helix termination peptide of keratin 5 in hereditary skin blistering. *Nature* **356**, 244–246, <https://doi.org/10.1038/356244a0> (1992).
58. Irvine, A. D., McKenna, K. E., Bingham, A., Nevin, N. C. & Hughes, A. E. A novel mutation in the helix termination peptide of keratin 5 causing epidermolysis bullosa simplex Dowling-Meara. *J Invest Dermatol* **109**, 815–816, <https://doi.org/10.1111/1523-1747.ep12341024> (1997).
59. Rugg, E. L. *et al.* Epidermolysis bullosa simplex in Scotland caused by a spectrum of keratin mutations. *J Invest Dermatol* **127**, 574–580, <https://doi.org/10.1038/sj.jid.5700571> (2007).
60. Pruss, R. M. *et al.* All classes of intermediate filaments share a common antigenic determinant defined by a monoclonal antibody. *Cell* **27**, 419–428 (1981).
61. Geisler, N., Kaufmann, E., Fischer, S., Plessmann, U. & Weber, K. Neurofilament architecture combines structural principles of intermediate filaments with carboxy-terminal extensions increasing in size between triplet proteins. *EMBO J* **2**, 1295–1302 (1983).
62. Magin, T. M., Hatzfeld, M. & Franke, W. W. Analysis of cytokeratin domains by cloning and expression of intact and deleted polypeptides in *Escherichia coli*. *EMBO J* **6**, 2607–2615 (1987).
63. Wang, P. *et al.* Basic fibroblast growth factor reduces scar by inhibiting the differentiation of epidermal stem cells to myofibroblasts via the Notch1/Jagged1 pathway. *Stem Cell Res Ther* **8**, 114, <https://doi.org/10.1186/s13287-017-0549-7> (2017).
64. Wu, W., Wu, X. L., Ji, Y. Q. & Gao, Z. Differentiation of nestin-negative human hair follicle outer root sheath cells into neurons *in vitro*. *Mol Med Rep* **16**, 95–100, <https://doi.org/10.3892/mmr.2017.6585> (2017).
65. Pal, S. K., Sakamoto, K., Aragaki, T., Akashi, T. & Yamaguchi, A. The expression profiles of acidic epithelial keratins in ameloblastoma. *Oral Surg Oral Med Oral Pathol Oral Radiol* **115**, 523–531, <https://doi.org/10.1016/j.oooo.2013.01.017> (2013).
66. Meier-Abt, E., Brinkhaus, H. & Bentes-Alj, M. Early but not late pregnancy induces lifelong reductions in the proportion of mammary progesterone sensing cells and epithelial Wnt signaling. *Breast Cancer Res* **16**, 402 (2014).
67. Tai, G. *et al.* Cytokeratin 15 marks basal epithelia in developing ureters and is upregulated in a subset of urothelial cell carcinomas. *PLoS One* **8**, e81167, <https://doi.org/10.1371/journal.pone.0081167> (2013).
68. Sambrook, J. F. & Russell, D. W. *Molecular Cloning: A Laboratory Manual*, 3rd ed., (Cold Spring Harbor Laboratory Press 2001).
69. Boukamp, P. *et al.* Normal keratinization in a spontaneously immortalized aneuploid human keratinocyte cell line. *J Cell Biol* **106**, 761–771 (1988).
70. Dickson, M. A. *et al.* Human keratinocytes that express hTERT and also bypass ap16(INK4a)-enforced mechanism that limits life span become immortal yet retain normal growth and differentiation characteristics. *Mol Cell Biol* **20**, 1436–1447 (2000).
71. Rugg, E. L. *et al.* A functional “knockout” of human keratin 14. *Genes Dev* **8**, 2563–2573 (1994).

72. D'Alessandro, M., Coats, S. E., Jonkmann, M. E., Leigh, I. M. & Lane, E. B. Keratin 14-null cells as a model to test the efficacy of gene therapy approaches in epithelial cells. *J Invest Dermatol* **131**, 1412–1419. <https://doi.org/10.1038/jid.2011.19> (2011).
73. Morley, S. M. *et al.* Generation and characterization of epidermolysis bullosa simplex cell lines: scratch assays show faster migration with disruptive keratin mutations. *Br J Dermatol* **149**, 46–58 (2003).
74. Rheinwald, J. G. & Green, H. Serial cultivation of strains of human epidermal keratinocytes: the formation of keratinizing colonies from single cells. *Cell* **6**, 331–343 (1975).
75. Gemenetzidis, E. *et al.* FOXM1 upregulation is an early event in human squamous cell carcinoma and it is enhanced by nicotine during malignant transformation. *PLoS One* **4**, e4849. <https://doi.org/10.1371/journal.pone.0004849> (2009).

#### Acknowledgements

The authors acknowledge the support from the Rosetrees Trust, Queen Mary Innovations and from The Facial Surgery Research Foundation-Saving Faces (to AW). We thank Professor Mike Philpott for providing normal skin sections used in this study. We are also thankful to Professors Ian Mackenzie and Iain Hutchison for suggestions and comments on this manuscript.

#### Author Contributions


(K.A.N., H.A.D., D.A.) performed most of the experiments, (D.A., H.A.D., A.L.) produced recombinant retroviruses and transduced cells, (A.W., A.L., M.T.T.) got the funding and wrote the manuscript.

#### Additional Information

**Supplementary information** accompanies this paper at <https://doi.org/10.1038/s41598-018-38163-5>.

**Competing Interests:** The authors declare no competing interests.

**Publisher's note:** Springer Nature remains neutral with regard to jurisdictional claims in published maps and institutional affiliations.

 **Open Access** This article is licensed under a Creative Commons Attribution 4.0 International License, which permits use, sharing, adaptation, distribution and reproduction in any medium or format, as long as you give appropriate credit to the original author(s) and the source, provide a link to the Creative Commons license, and indicate if changes were made. The images or other third party material in this article are included in the article's Creative Commons license, unless indicated otherwise in a credit line to the material. If material is not included in the article's Creative Commons license and your intended use is not permitted by statutory regulation or exceeds the permitted use, you will need to obtain permission directly from the copyright holder. To view a copy of this license, visit <http://creativecommons.org/licenses/by/4.0/>.

© The Author(s) 2019



#### **A.4. Research Presentation of this thesis.**

- Institute of Dentistry PhD Day 2016 (QMUL, London, UK; April 26th).  
***Keratin filament dynamics in live cells***  
(poster presentation).
- Institute of Dentistry PhD Day 2017 (QMUL, London, UK; April 26th).  
***Keratin filaments dynamics in live cells: Role of N-terminus in filaments stabilisation***  
(PowerPoint presentation).
- Institute of Dentistry PhD Day 2018 (QMUL, London, UK; May 11th).  
***In vitro analysis of Keratin K2 function in protecting against carcinogenesis.***  
(poster presentation).
- Institute of Dentistry PhD Day 2019 (QMUL, London, UK; June 11th).  
***Effect of lipids on keratinocyte differentiation***  
(PowerPoint presentation).
- BSODR conference (2017 Plymouth, UK).  
***In vitro analysis of Keratin K2 function in protecting against carcinogenesis.***  
(poster presentation).  
Award winning: Oral Medicine and Pathology Group Prize

## A.5. Manuscripts communicated.

### 1. Communicated to BMC Cancer

**Title:** Clinical correlation of opposing molecular signatures in head and neck squamous cell carcinoma.

Authors: Fatima Qadir; Anand Lalli; Huma Habib Dar; Sungjae Hwang; **Hebah Aldehlawi**; Hong Ma; Haiyan Dai; Ahmad Waseem; Muy-Teck The.

### 2. To be communicated to PLoS Genetics

**Title:** Mutations in *SPATA13/ASEF2* cause primary angle closure glaucoma.

Authors: Naushin H Waseem, Sancy Low, Amna Z Shah, Deepa Avisetti, Pia Ostergaard, Michael Simpson, Katarzyna A Niemiec, Belen Martin-Martin, **Hebah Aldehlawi**, Saima Usman, Pak Sang Lee, Anthony P Khawaja, Jonathan B Ruddle, Ameet Shah, Ege Sackey, Alexander Day, Sanny Jiang, Geoff Swinfield, Ananth Viswanathan, Giovanna Alfano, Christina Chakarova, Heather J Cordell, David F Garway-Heath, Peng T Khaw, Shomi S Bhattacharya, Ahmad Waseem, Paul J Foster.

### 3. Communicated to BJOMP

**Title:** Screening for oral cancer utilising risk-factor analysis is ineffective in high-risk populations.

Authors: Anand Lalli; **Hebah Aldehlawi**; John Buchanan; Noha Seoudi; Farida Fortune; Ahmad Waseem.